Faculty of Science and Engineering

A Numerical and Experimental Investigation of the Effects of Cutting Fluid on Machining Performance

Sayem Ahmed Chowdhury

This thesis is presented for the Degree of
Doctor of Philosophy
Curtin University

August 2016

STATEMENT

To the best of my knowledge and belief this thesis contains no material previously published by any other person except where due acknowledgment has been made.

This thesis contains no material which has been accepted for the award of any other degree or diploma in any university.

Sayem Chowdhury

Date
29/08/2016

ABSTRACT

Cutting fluids play an important role in improving machining performance. However, cutting fluids have adverse effects on health and environment. It is revealed that a large quantity of liquid cutting fluid is used during the machining operations without knowing the accurate amount required for the machining operations. Therefore, additional knowledge is essential regarding the effects of cutting fluid on machining performance to justify the usage of the cutting fluid during the machining operations.

This research work represents a detailed study to identify the effects of the cutting fluid on tool temperature distributions and machining performance. A new methodology has been developed for the prediction of tool temperature distributions during turning operations. The proposed methodology was developed with the help of computational fluid dynamics based commercial modelling software, ANSYS CFX® and validated by experimental method. By applying the proposed methodology, it has been identified that turning operations can be performed with reduced amount of the cutting fluid. Followed by, experiments were conducted with reduced amount of cutting fluid to investigate the machining performance. The study presented in this thesis has the following unique characteristics:

- Developed a new methodology for determining the effect of the cutting fluid on the tool temperature distributions. This development process demonstrated the application of the computational fluid dynamics to predict the effect of the cutting fluid on tool temperatures for varying cutting parameters and cutting environments.
- Employed thermocouples inside the tungsten carbide cutting tools by creating holes applying spark eroding technique for the experimental validation of the proposed methodology. The results obtained from these tests proved that the developed model was capable of capturing the effects of cutting conditions on the tool temperatures and the prediction of tool temperatures were in agreement with the measured results.
- Applied the newly developed computational fluid dynamics based methodology to demonstrate the effects of the amount of cutting fluid on tool temperature distributions for flood turning operations. The proposed methodology was used as an effective tool for identifying the optimal flow rate for flood machining. Based on the identified flow rate, experiments were conducted to investigate the machining performance characteristics such as tool wear, surface finish, cutting force etc. The results revealed that the reduce amount of cutting fluid is sufficient to obtain acceptable machining performance. In addition, the proposed methodology was applied for the MQL cooling environment and obtained numerical results were compared to show the effectiveness of the MQL and conventional flood cooling processes.

ACKNOWLEDGEMENTS

The author gratefully acknowledges the assistance of following people:

Dr Nazrul Islam, Senior Lecturer, Curtin University, for his supervision, motivation and sharing knowledge of during the research period. Dr Brian Boswell, Lecturer, Curtin University, for his co-supervision and advice during the course of study.

Dr Ramesh Narayanaswamy, Associate Professor, Curtin University, for his advice as a Chair of the thesis committee.

Professor Tilak Chandratilleke, Head of Department, Curtin University, for the approvals and support regarding the research.

Dr Kian Teh and Dr Jonathan Dong, Senior Lecturers, Curtin University, for sharing knowledge of the Finite Element Analysis.

Dr Rebecca Hartman-Baker, Supercomputing Specialist, iVEC, for her instruction regarding Supercomputing.

Mr John Murray and Mr Ashley Hughes, Curtin University, for scheduling and allocation of the time for the experiments in the laboratory. Mr David Collier, Mr Graeme Watson and Mr Aaron Bell, Curtin University, for allowing me to enter in the lab regarding the experiment.

Ms Margaret Brown and Mr Frankie Sia, Curtin University, for their administrative support.

TABLE OF CONTENTS

LIST OF FIGURES

LIST OF TABLES

NOMENCLATURE

V_c	Cutting velocity
P_{total}	Total heat generation
F_c	Cutting force
F_t	Trust force,
F_n	Normal force
F_s	Shearing force
τ_y	Shear strength of the work material
t_1	Before cut chip thickness
b_c	Chip width
A_c	Chip cross-sectional area
K_s	Specific cutting force
d	Depth of cut
f	Feed rate
C_F	Coolant flow rate
v	Flow velocity
ρ	Density of the fluid
p	Pressure of the fluid
T	Total stress of the fluid
f	force of the fluid
∇	del operator
μ	Dynamic viscosity
R_a	Arithmetic average roughness
Y	Vertical deviation
L	Measured distance
F_{total}	Total Cutting Force
Fr	Radial force

Chapter 1

Introduction

1.1 Background of the Research

Historically, cutting fluids have been used during machining operations over the last 200 years [1]. In 1894, Taylor highlighted that higher cutting speed can be achieved by using fluid during metal cutting without decreasing the tool life [2]. Initially, oils were used as the cutting fluids, but nowadays, the formulations of modern cutting fluids are more sophisticated. The role of cutting fluid is significant for the machining processes and manufacturing industry is dependent on the machining processes. The small parts and tools are vital to keep running the manufacturing industry. In 2006, about 12.2% of the total US GDP or $1.6 trillion was contributed from manufacturing sector [3]. Therefore, manufacturing is considered as the backbone of the industrial countries. Annually, metal part finishing processes, such as turning and milling, cost over US$ 100 billion around the world [4]. Thus, machining industry is a significant part of the manufacturing industry. It is noteworthy that the cost of cutting fluid used during the machining is 15% of the total machining costs [5]. The distribution of cost for flood turning operations is shown in Figure 1.1. The schematic diagram of metal cutting operations is shown in Figure 1.2.

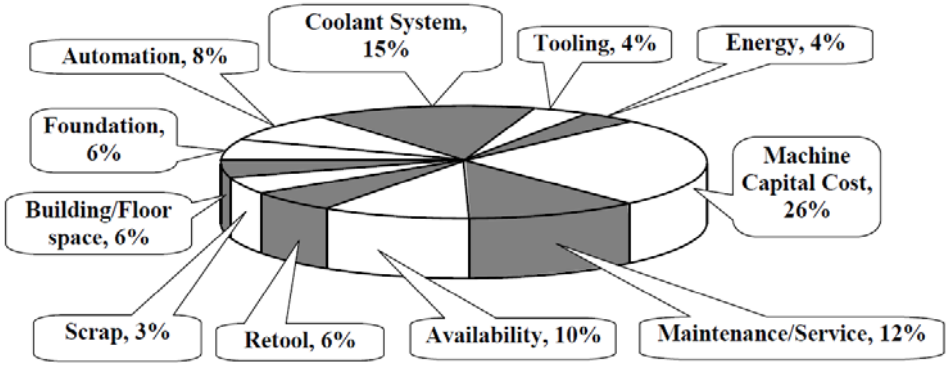

Figure 1.1: The distribution of cost for flood turning operations [6]

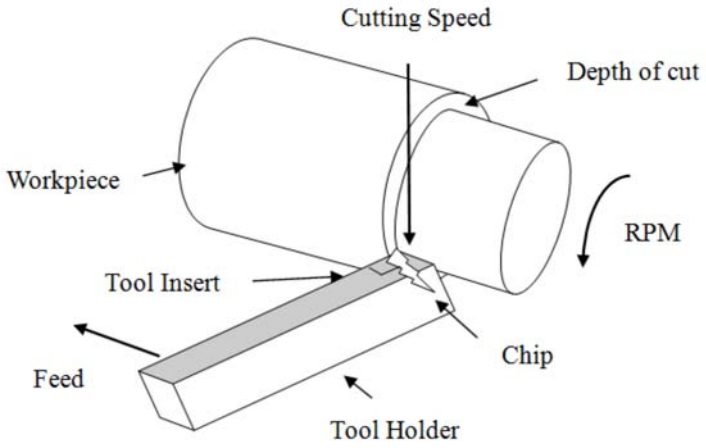

Figure 1.2: Typical turning operation showing machining parameters

The disposal cost of cutting fluids can be up to four times of the purchasing price, as the most of the cutting fluids are not biodegradable and should be disposed according to environmental regulations [7]. It is estimated that annually 155 million litres of oily, bacteria and fungus-laden potentially hazardous effluent should be treated prior to discharge to the environment [8]. The schematic of the application of the flood cutting fluid is shown in Figure 1.3.

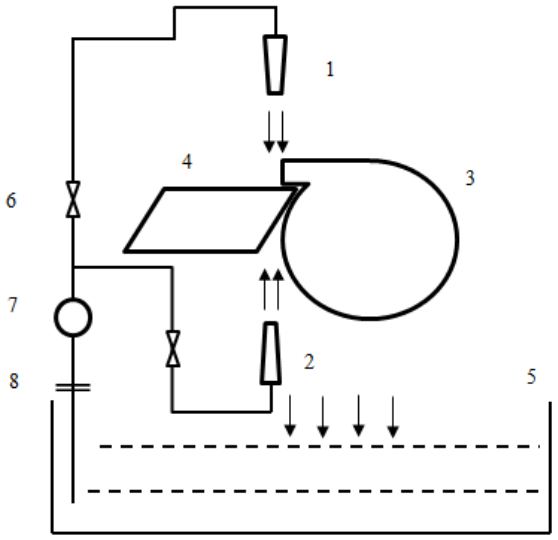

Figure 1.3: The schematic of the application of the flood cutting fluid on the rake face and flank side (1) nozzle toward rake face (2) nozzle toward flank side (3) workpiece (4) tool insert (5) cutting fluid tank (6) control valve (7) pump and (8) filter

Recently, cutting fluids have given rise to great concern to the metal cutting industry due to the undesirable environmental effects. The disposal cost and new environmental protection legislation have initiated cutting fluid related research [9]. In other words, researchers around the world are trying to reduce the amount of cutting fluid for machining [10]. Regardless of the research efforts, the problem related to the cutting fluid still exists. Coolants are commonly used during machining processes in order to achieve some advantages over dry cutting condition. The main advantage of using the cutting fluid is removing the elevated heat from the cutting tool and the workpiece. It is anticipated that cutting fluid can provide less tool wear, better surface finish and dimensional accuracy. Tool wear reduces the tool life, minimises the surface finish and reduces dimensional accuracy. For the acceptance of manufactured parts, size tolerance is an essential criterion [11], [12], [13]. One of the ways to achieve improved sustainability is optimal management of metalworking fluids [14]. It is expected that the machining processes will remain as a significant part for the economy of world. Therefore, any additional knowledge regarding the tool cooling process and reduction of the usage of the cutting fluid will contribute significantly to the world economy. In the present study, the cutting tool cooling process during the turning operations with flood cooling method will be analysed.

1.2 Effect of Cutting Fluids

Although cutting fluid is essential for some machining operations, but literature review identifies that there are adverse health effects of cutting fluid [15] and also causing pollution [16]. The machine tool users should be careful during selecting the cutting fluid [17]. Most of the cutting fluids available in the market are mineral oil based. The dependency on the petroleum related product is making the beaches, highways and landfills contaminated [18].

Sayuti et al. [19] emphasised that cutting fluids are hazard for the ecology and health of machinists. The machinists are the main concern of the effect of contact of cutting fluid as they work near the machine tool. The cutting fluid primarily goes to the machine shop floor by (a) splashing (b) spinning-off and (c) evaporation [20]. The odours, smoke fumes and bacteria are effecting the people as well [21].

Michalek et al. [22] investigated the mist formation process of the cutting fluids. The authors experimentally and analytically characterised the mist formation and behaviour of cutting fluid during machining operations. The authors developed a

model to predict quantity of mist for flood turning operations. The authors also analysed the atomisation and vaporisation including condensation and droplet settling. The mist formation and atomisation process of cutting fluid in turning operations are shown in Figure 1.4 and Figure 1.5.

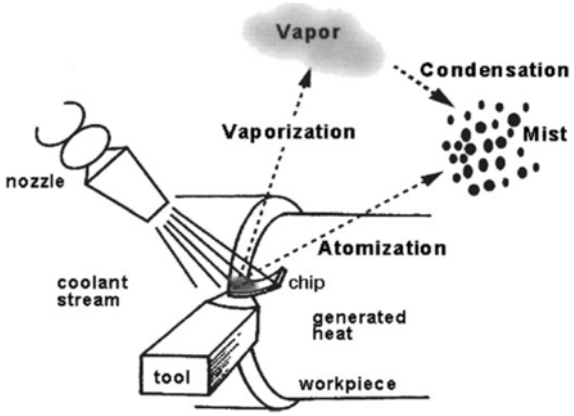

Figure 1.4: The mist formation process from cutting fluid during turning operations [22]

(a) (b) (c)

Figure 1.5: The modes of atomisation: (a) formation of drop (b) formation of ligament and (c) formation of film [22]

The USA Occupational Safety and Health Administration (OSHA) [23] emphasised that metalworking cutting fluids are the reason of causing adverse health issues when coming in the skin contact. People may inhale the mist or aerosol as well. The health problems are (a) skin disorders, (b) respiratory diseases and (c) cancer. The cutting fluid can cause several health problems if it comes in skin contact or is inhaled. Skin irritation and asthma may be common problems. It is noteworthy that an increased level of DNA damage was found in metal workers depending on the concentration in the air of the work places [24].

Foulds [25] emphasised that cutting fluids are causing oil-induced acne, boils and allergic contact dermatitis. Health and safety of the workers, even the environment, are the major concern during machining with cutting fluid. These issues arise from: (a) toxic ingredients added to the cutting fluid (b) flammable nature of the cutting fluid and (c) disposal problem with the cutting fluid [23]. As shown in Figure 1.6, atomisation and drop formation is common during machining operations.

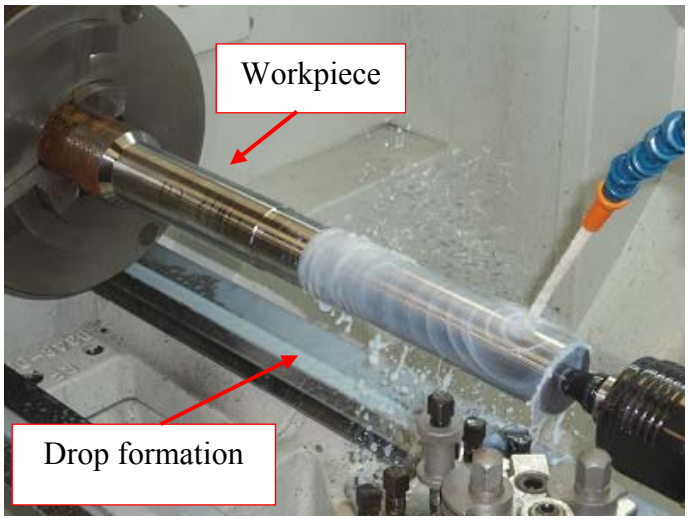

Figure 1.6: Drop formation of cutting fluid during turning operations

Cutting fluids contain additives such as biocides, chlorine, oxazolines, sulphur, phosphorus etc. [26]. The biocides, used to control the bacteria of the coolant, are harmful additives [27]. Due to the presence of these toxic additives, cutting fluids are environmental pollutants and health hazards as well [28]. The cutting fluid used in the present study was consist of mineral oil between 10-30%, chlorinated wax between 10-30%, potash soaps less than 10%, biocide less than 10% and petroleum sulfonates less than 10%. The p^H level of the fluid is 9.7 at 15:1. Due to the presence of these chemicals and high p^H level safety precautions are necessary during the use of the cutting fluid. The recommendations regarding cutting fluid from the Chemwatch Material Safety Data Sheet are as following [29]:

- Do not inhale
- Avoid skin contact
- Wear suitable protection equipment
- Rinse eyes with plenty of water in case of contact and inform doctor

Although, it is recommended to avoid breathing the cutting fluid as gas, Adler et al. [30] found that the mist produced during machining operations can be inhaled by the machining technicians. This mist can be a risk for the health and safety of the machining technicians [31], [32].

1.3 Problem Statement

In the machining industry, some machine tool operators apply a large amount of cutting fluid for the turning operations without knowing the optimal flow rate. The amount of cutting fluid used in the turning operations often does not have any scientific base. However, it is believed that, with the help of numerical method, additional knowledge regarding the tool cooling process can be acquired and the effect of the cutting fluid on the tool temperature can be identified. The obtained knowledge will be helpful to identify the amount of cutting fluid necessary for the tool cooling and thus overuse of the cutting fluid can be reduced.

The flood cooling process is the most traditional tool cooling method and also the most widely used in the machining industry. As there is an impact on the health and environment due to the application of cutting fluid, any reduction of the amount of the cutting fluid during turning operations will be beneficial for a large number of stakeholders of the manufacturing industry. In order to maximise the value of products, the 6Rs should be considered which are Reduce, Reuse, Redesign, Recover, Recycle and Remanufacturing [33]. The aim of the present study is analysing the effect of the cutting fluid on the tool temperature and thus identifying the opportunity to reduce the amount of cutting fluid usage during the turning operations. By reducing the amount of cutting fluid, financial benefit can be achieved and the adverse effects of cutting fluid on the environment can be minimised. The present research is important from economic and environmental points of view as the manufacturing industry contributes significantly to the economy of world. To achieve the aim of the study, the following research questions are addressed in this thesis:

(1) How a computational fluid dynamics based methodology can be developed to predict the cutting tool temperature?
(2) How the validation of the developed methodology can be performed by experimental method?
(3) How the reduced amount of cutting fluid effects the machining performance?

In other word, the present study is involved to determine the potential of using computational fluid dynamic (CFD) modelling technique to predict the cutting tool temperature. In addition, the feasibility of validating the proposed model by experimental method will be investigated. Finally, initiative will be taken to identify the effects of reduced amount of cutting fluid on machining performance.

1.4 Scope of the Project

The scope of the research is conducting numerical and experimental analysis of the tool cooling process with cutting fluid during the turning operations and identifying the effect of cutting fluid on the machining performance. In the present study, a methodology will be developed to obtain the tool temperature distributions for variety of cutting conditions. A number of numerical experiments will be conducted to understand the effect of the cutting fluid on the cutting tool temperature. In addition, experimental investigation will be conducted to understand the effects of cutting fluid on cutting force, tool wear, surface finish etc. Therefore, the scope of the research is limited and no other aspect or parameter of the machining process is included in the present study except the above mentioned issues due to constraint of time.

1.5 Objective of the Thesis

One of the main objectives of the present study is to predict the tool temperatures for variety of cutting parameters and identify the effects of the cutting fluid on tool temperature during turning operations by developing a computational fluid dynamics based three dimensional (3D) model. To achieve the goal, a numerical model will be developed and tool temperatures for varying cutting fluid flow rates will be obtained. The proposed methodology will be validated against data available from the literature and subsequently by experimental method.

After completion of the validation process, a series of numerical experiments will be conducted to analyse the influence of the cutting fluid on the tool temperatures. Further experimental investigations will be conducted to analyse the machining performance. Finally, the application of the proposed methodology will be presented to compare the tool temperatures under different types of tool cooling environments.

1.6 Layout of the Thesis

To fulfil the objective of the present study, the thesis has been divided into several chapters. Each chapter of this thesis has its individual objectives which are presented below:

Chapter 1: This chapter provides the background of the research and clarify the scope of the study. The problem statement is declared in this chapter. The individual objectives of each chapter of the thesis are presented in a synchronised way. This chapter also describes the interaction and relevance of the elements of the study. The proposed research strategy is also presented in this chapter.

Chapter 2: The objective of this chapter is to present the reviews of the literature for the study. The literature reviews, presented in this chapter, will be related to the role of the cutting fluid in the machining operations, the methods of obtaining cutting tool temperature and the numerical methodology to simulate the tool temperature distributions.

Chapter 3: The objective of this chapter is to present a computational fluid dynamics based methodology to analyse the tool cooling process. The development process of the methodology will be described in a systematic way by means of five steps. Each of the five steps will be explained in details. Finally, the validation of the proposed methodology will be presented against experimental results available from literature.

Chapter 4: The objective of this chapter is experimental validation of the proposed methodology by obtaining the tool temperature with embedded thermocouple method. The experimental procedure will be described in details. The tool insert temperatures will be obtained for variety of cutting parameters. Comparisons will be presented between the experimental and numerical tool temperatures.

Chapter 5: The objective of this chapter is to demonstrate the application of the proposed methodology to identify the effects of the amount of cutting fluid on the tool temperature distributions for turning operations. To capture the effect of the cutting fluid on the tool insert, a line will be assigned along the cutting edge and temperature will be obtained from this line. A number of numerical experiments will be conducted to understand the effect of the cutting fluid along this line by varying the cutting fluid flow rates. Any opportunity to reduce the amount of cutting fluid will be identified as well.

Chapter 6: The objective of this chapter is to identify the effects of reduced amount of cutting fluid on the machining performance. An experimental investigation will be presented to identify the effects of the reduced amount cutting fluid on tool wear, surface finish, cutting forces, cutting power etc. The procedure of the experiment will be described in details. Finally, this chapter will be concluded by highlighting the significant findings.

Chapter 7: The objective of this chapter is to demonstrate the application of the proposed methodology to predict the tool temperatures under different types of cooling environments. The proposed methodology will be applied for the three machining environments (a) dry or no additional cutting fluid (b) flood with liquid cutting fluid and (c) combination of clod air with minimal quantity lubrication. The influence of cooling environments on the tool temperatures will be identified and presented accordingly.

Chapter 8 The objectives of this chapter are further clarifications of the achievement of the present study, providing conclusions of the research project and recommendations for future research interests.

To achieve of the objectives the study and present the findings in a synchronised way, the thesis is divided into several chapters. The elements of the research are presented in Figure 1.7, showing the chapters of the thesis and the interaction between the chapters.

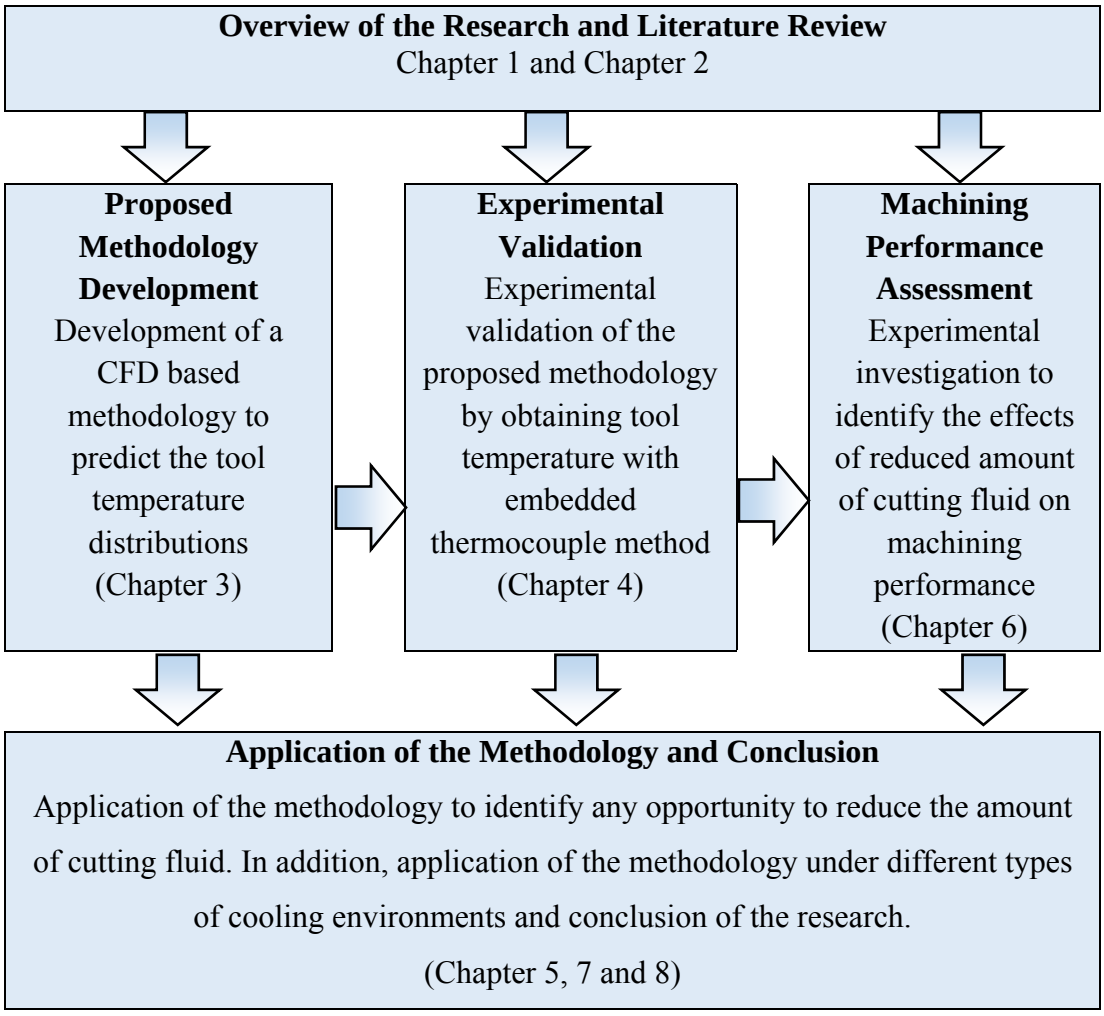

Figure 1.7: The interaction and relevance of the chapters of the thesis

1.7 Present Research Approach

The main focus of the present study is to develop a computational fluid dynamics based methodology for flood turning operations. The study will be also involved in identifying the effects of cutting fluid on the machining performance. The present study will be divided into a number of parts. Literature review will be conducted at the beginning of the research. The next part of the study will be the development of a methodology to obtain tool temperatures. The methodology development process will

be divided into a number of sections. The heat generation and distributions during the turning operations will be analysed at the beginning of the development process. After the development process, the numerical results will be validated against experimental results from literature. Further the experimental investigations will be conducted to validate the numerical model against the experimental results. For the validation of the proposed methodology, the cutting tool temperature will be obtained by varying the flow rate of the cutting fluid. Alloy steel AISI 4140 will be used as the work material for the experiment.

After experimental validation, a number of numerical experiments will be conducted. A reference line will be assigned along the cutting edge and temperature of the reference line will be obtained. The flow rate of the cutting fluid will be varied to understand the effect of cutting fluid on the tool temperature. The amount of cutting fluid sufficient to reduce the temperature to an acceptable level will be identified.

By controlling the cutting fluid supply according to the obtained tool temperatures, it will be possible to optimise the amount of cutting fluid during the turning operations. In other words, if the temperature of the tool is high, more cutting fluid will be supplied to reduce the tool temperature. Afterwards, when the temperature of the tool is low enough, the cutting fluid flow rate will not be increased further. The numerically obtained results will be examined by Pareto ANOVA and Taguchi's signal-to-noise ratio (S/N) analysis to identify the contribution of cutting fluid. The details of these methods can be found in [34, 35]. Finally, the effects of the reduced amount of cutting fluid on the machining performance will be identified by metal cutting experiments. Machining performance parameters, such as surface finish, dimensional accuracy, tool wear and cutting force, will be measured with reduced amount of cutting fluid.

Chapter 2

Literature Review

2.1 Introduction

The objective of the literature review is to identify the state of art and apply the knowledge to fulfil the aim of the present study. The literature reviews presented in the thesis are the established research previously performed by the related researchers. For each part of the research related literature was reviewed. Therefore, the literature review for the present study was divided into three strategic streams which are (a) application of cutting fluids and its effect (b) tool temperature measurement methods and (c) numerical methods and model development processes. The research area and literature, as presented in Table 2.1, establish that the area for the research is numerical analysis and experimental investigation of tool temperature during turning operations with cutting fluid.

Table 2.1: Summary of Literature Survey

Group No	Research Area	Number of references used in the present study
1	Cutting fluids and its effect	[39-45], [49-55], [57-88]
2	Methods of obtaining tool temperature	[89-90], [95-115], [117-130], [133-139]
3	Numerical methods and model development	[147-148], [151], [153 -155], [161-163], [165], [169], [174], [176-185], [188-190]

At the beginning of the present study, the significance of the cutting fluid during machining operations was reviewed. The various factors related to the cutting fluids were analysed. In addition, as a part of the study a computational fluid dynamics based 3D model was developed. Therefore, the numerical method related literature was reviewed to understand the numerical investigation process. In the present study, experimental investigations were performed to obtain tool temperatures and identify

the effects of cutting fluid on tool insert temperature distributions. Therefore, literature related to the experimental methods to obtain tool temperature was reviewed as well.

2.2 Cutting Fluids and its Effect

The reduction of elevated tool temperature during the machining operations is one of the purposes of using the cutting fluids. Although, the three functions of cutting fluids are cooling [36], lubrication [37] and chip transport [38] from the cutting zone, but cooling, i.e. removing the elevated heat during machining, is the most significant one as Choudhury and Srinivas [39] highlighted that the cutting tools may fail due to the rise in the interface temperatures. Martin [40] conducted extensive research on heat transfer of impinging jet with solid surface. The author investigated the hydrodynamics of impinging flow emphasising the heat and mass transfer variables for nozzle and the influence of outlet flow conditions. The author also emphasised on impinging flow on concave surfaces and the angle of impact.

Viskanta [41] evaluated the flow regions of an impinging free surface jet. The flow structure of impinging axisymmetric jet can be subdivided in several characteristic regions as shown in Figure 2.1. Based on the Reynolds number, the impinging jet is defined as whether it is laminar or not. The number of characteristic regions in the circular free jets are: (a) the dissipated laminar jet, where the Reynolds number, Re is less than 300; (b) the fully laminar jet, where the Reynolds number, Re is between 300 and 1000; (c) transition or semi-turbulent jet, where the Reynolds number, Re is between 1000 and 3000; and (d) A fully turbulent jet, where the Reynolds number, Re is more than 3000.

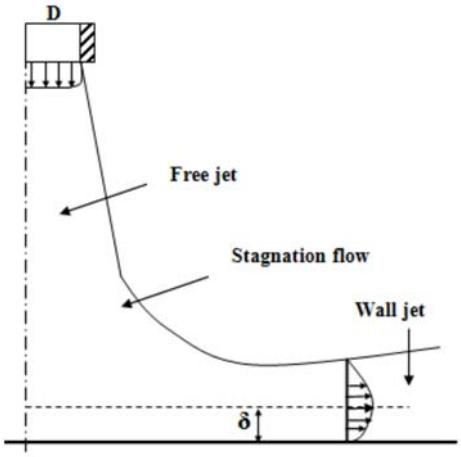

Figure 2.1: Flow regions of an impinging free surface jet, adopted from [41]

The influence of the cutting fluid during turning operations was investigated by many researchers. Li [42] theoretically analysed the role of cutting fluid for heat removing during machining operations and numerically simulated the temperature distribution. The author found that heat-transfer coefficient was higher, if the amount of fluid was increased, but a large increase of the amount of fluid flow contributed a little increase of the heat-transfer coefficient.

Li [43] experimentally concluded that the effectiveness of cooling process is governed by the properties of the cutting fluid and the amount of heat comes to exposed surface from the high heat area. The author expressed the overall cooling effect by the following Equation 2.1:

$$q = h.\ A.\ (T_w - T_f) \tag{2.1}$$

where, heat transfer rate is q due to temperature difference of the surface, T_w, and temperature of the coolant, T_f. Cooled surface area is A and heat-transfer coefficient is h.

The forced-convection heat transfer can be expressed by the following equation:

$$N_u = f\ (Re,\ Pr,\ generic\ shape) \tag{2.2}$$

where, Nusselt number can be expressed by *Nu, and*

$$N_u = h\ D\ /\ k \tag{2.3}$$

Reynolds number is expressed by *Re,* and

$$Re = \rho\ v\ D\ /\ k \tag{2.4}$$

Prandtl number is expressed by *Pr,* and

$$Pr = \mu\ C_p\ /\ k \tag{2.5}$$

where D is the characteristic length, v is the velocity, K is the conductivity, ρ is the density, μ is the viscosity and C_p is the specific heat of the coolant properties respectively.

Li [42] found that, as shown in Figure 2.2, the heat transfer coefficient, h, of a jet impinging on a surface, is governed by an additional parameters, where L/D is the normalised jet nozzle-to-plane spacing; α is jet inclination angle; E is the stagnation point displacement from jet geometric centre on impingement surface; r/D is the normalised distance from stagnation point to a point considered on impingement surface. The jet Reynolds number is Re_j and can be expressed as following:

$$Re_j = \rho U_j D/\mu \tag{2.6}$$

where D is the nozzle diameter and U_j is the velocity of the jet when it exits the nozzle.

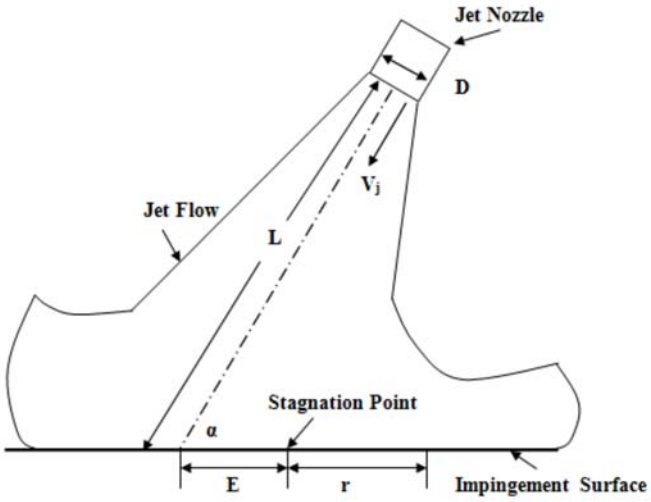

Figure 2.2: Schematic of the impinging jet on a flat surface, adopted from [42]

Daniel et al. [44] identified that the transverse Reynolds number varies with the fluid velocity. Application of cutting fluid as jet on the workpiece is shown in Figure 2.3. Based on the assumptions that forced convection is predominant and the natural convection is negligible, the Nusselt number can be expressed as Equation 2.7:

$$N_u = 0.1075\, Pr^{0.35} [0.5\, Re_r^{\,2} + Re_t^{\,2}]^{0.35} \qquad (2.7)$$

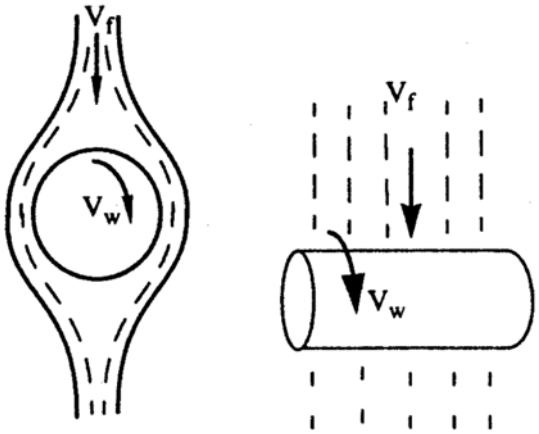

Figure 2.3: Velocity vectors during machining with flood application of cutting fluid [44]

In a turning operations, applying Equation 2.7, the heat transfer coefficient, with pure water jet, is found between 9,000–12,000 W/m^{2}K depending on cutting velocity

and the jet velocity. Daniel et al. [44] also presented that, an appropriate correlation for Nusselt number can be expressed as following:

$$N_u / Pr^{0.42} = 2G\, R^{0.5} (l + 0.005\, Re^{0.55})^{0.5} \quad (2.8)$$

where,

$$G = D_n /R ((1\text{-}1.1\, D_n /R) / (1 + 0.1(H/D_n - 6)D_n /R)) \quad (2.9)$$

In a turning operations, applying Equation 2.8, the heat transfer coefficient, with pure water jet, is found between 12,000–20,000 W/m^{2}K depending on cutting velocity.

Lawal et al. [45] stressed that the machining cost is heavily dependent on the metal removal rate, but higher removal rate can be a reason for short tool life due to the increase in friction and additional heat generation. During the machining, cutting tool suffers thermal stresses which is the reason for fatigue and fracture. Beyond the critical temperature cutting tools become soften and cutting fluid helps the tool to not exceed this temperature range. Rapid tool wear occurs if the temperature exceeds crystal binding limits [46]. Cutting fluid is used to remove the heat from the tool, at the same time it removes the chips away as well [47]. It is noteworthy that aggressive adhesion wear is caused by the high temperature during machining operations [48]. The other functions of cutting fluid are providing temporary protection against oxidation, corrosion and reducing the occurrence of built-up edge [22].

Bachraty et al. [49] highlighted the influence of cutting fluids on power consumption during turning operations. The authors monitored the output parameters of the machining processes and found that cutting fluids reduce the energy consumption and proper section of the cutting fluids can increase the profitability.

Debnath et al. [50] emphasised that the flow rate of the cutting fluid has significant contribution on the surface roughness. By varying both the flow rate and velocity, the authors investigated the role of the cutting fluids on surface roughness and tool wear during turning operations. To minimise the total number of experiments, they employed the Taguchi orthogonal array and found that flow rate of the cutting fluid is more important than the fluid velocity.

Brinksmeier et al. [51] highlighted that during machining operations, a large quantity of liquid cutting fluid is used (a) to reduce the cutting temperature (b) to lengthen the life of the tools (c) to produce a better surface finish; (d) to improve dimensional accuracy and (e) to facilitate chip disposal.

Hodowany et al. [52] emphasised that a rapid and highly localised plastic deformation of metal can generate a significant amount of heat as there is less time for

heat conduction. The mechanical energy that is consumed during the machining process is converted into thermal energy. There are a number of heat sources during the machining operations, for example (a) heat converted from plastic work and (b) heat transformed by viscous dissipation from viscoplastic material.

Al-Odat [53] emphasised that the power consumed during machining operations is mostly converted into heat. The heat conversion particularly happens around the edge of the cutting tool mainly through plastic deformation during the formation of chip. The author also described that high temperatures is the reason for the tool softening which causes tool wear.

2.2.1 Categorisation of Cutting Fluids

The cutting fluids can be classified in multiple sections. National Institute for Occupational Safety and Health [54] classified the metalworking fluids into four types: (a) straight oils (b) soluble oils (c) synthetics and (d) semi-synthetics. The straight oils are basically refined petroleum products, or these are animal fat, marine oils or vegetable oils. El baradie [55] categorised the cutting fluids which is shown in Figure 2.4, although other classifications exist in the literature [56].

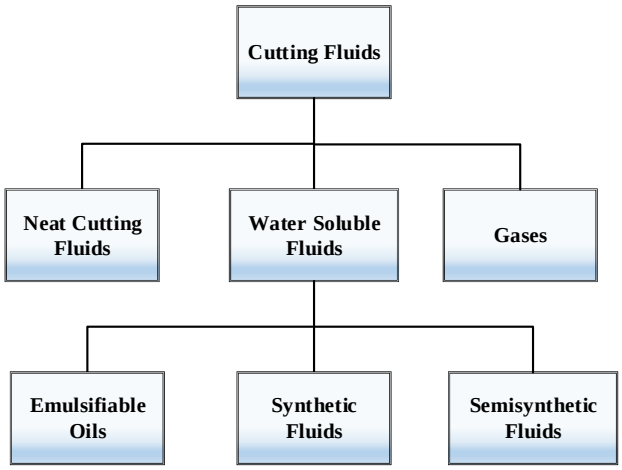

Figure 2.4: Classification of cutting fluids, adopted from [55]

Debnath et al. [57] emphasised that, around the world, 85% of the total cutting fluids are mineral-based cutting fluids. Water-based cutting fluids provide better cooling properties, on the other hand, mineral oils provide better lubrication [58]. Water based cutting fluids can reduce the tool failure due to temperature. After tool wear experiment, Ozcelik et al. [59] found that life of the tools with dry cutting, semi-

synthetic and mineral based cutting fluids were 200, 1000 and 2000 seconds respectively under the same machining conditions.

Irani et al. [60] asserted that the oils that are used in these fluid basically refined from crude oil such as naphthenic and paraffinic hydrocarbons. There is no water in the straight oils or not diluted with water. Some metalworking fluids are water diluted solutions. The soluble oils and semi-synthetic fluids contain oil but the synthetic fluids are completely water based liquid. Metalworking fluids contain additives which are biocides, metal fines, tramp oils etc. [54]. The advantages and disadvantages of cutting fluids are presented in Table 2.2.

Table 2.2: Advantages and Disadvantages of Cutting Fluids, adopted from [61]

	Straight oils	Soluble oils	Semi-synthetics	Synthetics
Advantages	Excellent lubricity Excellent rust control	Good lubricity Good cooling	Good cooling Good rust control Excellent microbial control	Excellent cooling Good microbial control Nonflammable, nonsmoking Good corrosion control Reduced misting and foaming problems
Disadvantages	Low cooling Fire hazard Create a mist or smoke Limited to low-speed and heavy cutting operations	Rust control Problems Bacterial growth Evaporation losses	Foam easily Stability is affected by water hardness Easily contaminated by other machine fluids	Poor lubricity Easily contaminated by other machine fluids

Eppert et al. [62] affirmed that thermo-physical properties influence the capacity of cooling of a cutting fluid. The wettability of the fluid depends on the surface tension and a low film coefficient ensures that the fluid maintains contact with the tool and workpiece. A high specific heat of fluid allows to reduce a large amount of heat. Water can be considered as good cutting fluid, but cutting fluids should not react or cause corrosion of the machine tool or workpiece. The oxidation protection and corrosion resistance characteristics are achieved with the help of additives [63].

Vieira et al. [64] accentuated that synthetic and semi-synthetic cutting fluids possess significant wetting and lubrication quality, low corrosion, less bacteria growth, low skin irritation and negligible odour. The water-based cutting fluids are composed of dissolved chemicals such as (a) sulphur, (b) chlorine, and (c) phosphorous [65].

Chiffre and Belluco [66] emphasised on the characteristic of the cutting fluid tests that there is no absolute value from the performance test of the cutting fluid, rather the test results are stated as the efficiency of the test fluid relatively to the performance of a reference fluid. Therefore, reproducibility of test results are achieved by comparing the relative efficiency.

Rao [67] concluded that the selection of cutting fluids mainly depends on the process of machining, material of the workpiece and material of the cutting tool. The other factors are economy, performance requirements and interaction of operators. As the cutting fluid has adverse effects on health and the environment, the environment friendliness should be given priority. Similarly, Sales et al. [68] emphasised that cutting fluids should have good cooling properties in addition to environmental friendly disposal after the treatment. The quality cutting fluids starts to degrade with the use; and disposal is mandatory after the fluids lose the quality [69].

Dhar et al. [70] highlighted that cutting fluids can cause damage to the soil and water resources if the fluids are inappropriately disposed to the environment. The environmental protection law and regulations should be followed during the handling and disposal of cutting fluids. In other words, the life cycle of the cutting fluids should be properly maintained [71]. In addition to the cost of fluid purchase [72], system maintenance and discarded fluid treatment are major contributors to the total cost [73]. The cost of fluid supply system installation is also included in the cutting fluid related expenses. Sometimes large manufacturing factories use multiple large reservoirs for the cutting fluid which result higher fluid related costs. Therefore, cost savings and waste reduction can be achieved by minimising the use of cutting fluid during

machining operations. Even an well organised manufacturer concerns about cutting fluid related environmental effects [30].

Devillez et al. [74] emphasised that efforts should be taken to reduce the impact of on the health and environment. There is a potential risk to the employees regarding bacterial growth in cutting fluids. The existence of bacteria and yeast in the cutting fluid is a potential hazard [69]. Literature review [75] revealed that the presence of bacteria in the cutting fluid can be tested by a simple dip-slide analysis. The water-based cutting fluid is more vulnerable to the bacterial growth which can be hazardous to machine shop workers; and can cause bio-deterioration and bio-corrosion to the equipment [76].

2.2.2 Tool Cooling Approaches

In addition to the flood cooling, there are several other cooling approaches. Sharma et al. [77] considered different tool cooling approaches in turning operations as presented in Figure 2.5.

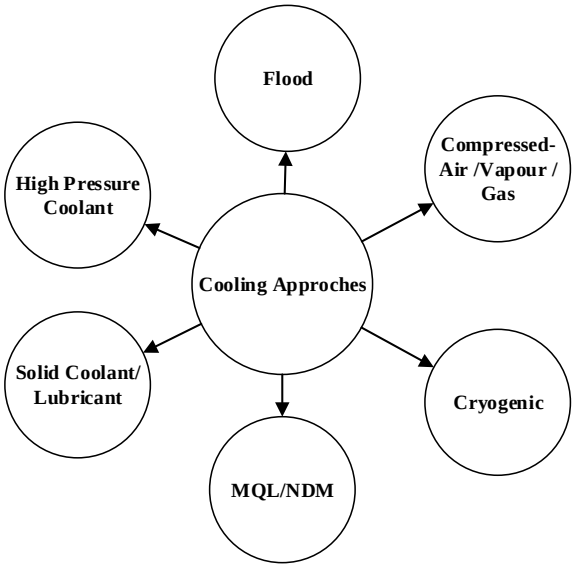

Figure 2.5: Tool cooling approaches in turning operations, adapted from [77]

As an alternative of flood cooling, a process known as minimum quantity of lubricant (MQL) can be used. However, this method have undesirable effects on air quality, although the machining cost can be minimised by reducing the volume of coolant needed in traditional machining methods [78]. A mixture with pressurised air is delivered through a nozzle to the machining tool and the air quality in the machine shop is found worse than that of flood machining [79]. Therefore, mist collection or

filtering equipment is necessary for controlling this fine mist [80]. Without the mist collection equipment, the MQL approach does not provide the breathing comfort, even though vegetable oil is used.

To find an alternative to flood cooling, Rahman et al. [81] investigated the performance of the different types of cooling environments and observed that flank land wear was higher in the MQL than flood machining. Comparison of the flank wear and the surface roughness in dry, flood and MQL are shown in Figure 2.6. By experimental investigation, Rahman et al. [82] identified that the MQL method is only effective when the cutting speed is low, the feed rate is low and the depth of cut is low compared to flood machining. At higher speed, flank wear is higher in the MQL than flood cooling method.

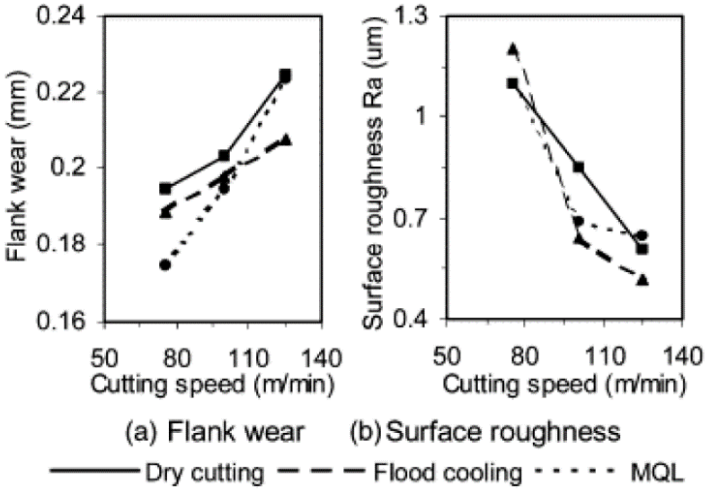

Figure 2.6: Comparison of (a) the flank wear and (b) the surface roughness in dry condition, flood cooling and the MQL [82]

Boswell and Chandratilleke [83] found that the tool temperature starts to build up after several minutes of machining with cold air cooling method. In other words, compressed air cooling is not an effective alternative of flood as cooling limitation identified during machining with the air cooling method. The flood cooling method reduces the heat build-up as a liquid coolant removes the heat better than air cooling method. On the other hand, air has poor cooling capability. Flood cooling method also has an advantage over the dry and minimum quantity of lubrication method which is that the flood coolant flushes the chips away.

Khan and Ahmed [84] investigated tool life improvement using cryogenic cooling and found that the application of cryogenic coolant was more effective at a higher

cutting speed. As at a higher cutting speed, cooling rate of the conventional coolant cannot cope with the heat generation on the tool insert. The authors also highlighted that at a higher feed rate chip thickness is higher and plastic deformation at the shear zone takes place at a faster rate generating more heat. As a result they found cryogenic cooling more effective at a higher feed rate rather than at a higher depth of cut.

Dhananchezian and Kumar [85] investigated the effect of cryogenic machining with liquid nitrogen. The authors compared the cryogenic results of the cutting temperature, cutting forces, surface roughness and tool wear with those of flood turning operations. The authors supplied liquid nitrogen to the flank surface and auxiliary flank surface through the holes made in the cutting tool insert. The authors found relatively better results because of the modified cutting tool insert.

Paul et al. [86] investigated the role of cryogenic cooling by liquid nitrogen jet on tool wear and surface finish in plain turning. The authors compared the cryogenic results against the dry and flood with soluble oil machining results; and found substantial benefit of cryogenic cooling on tool life and surface finish. The authors concluded that cryogenic cooling by liquid nitrogen jets provided reduced tool wear, improved tool life and surface finish as compared to dry and wet machining.

About High Pressure Cooling, Ezugwu [4] recommended that sealing of the machine tool is necessary to prevent leaking and spillage; and thus to reduce the health hazard to the machinists form coolant. In addition, sufficient ventilation and air extractors are also required. Therefore, implementation of High Pressure Cooling in the machining shop is not a simple process.

Upadhyay [87] found that researchers developed vegetable oil based cutting fluids to diminish the negative effects of the cutting fluids. It is notable that the biodegradable flood cooling method can be a better option as this process leaves less mist in the air [88]. However, Pusavec et al. [14] found that limited success is detected with the biodegradable cutting fluids because of higher cost and low performance. Kuram et al. [61] emphasised that, in order to replace the hazardous coolant with environmentally friendly one, the new coolants should have the equivalent properties and provide equivalent machining performance and productivity.

Therefore, the other cooling approaches have some limitations and not as popular as flood cooling method in the industry. The use of flood cooling process is essential for some machining operations. As long as the application of cutting fluid exists, the related problems with the cutting fluid will effect mankind and environment.

2.3 Methods of Obtaining Tool Temperature

One of the essential parts of achieving the research goal is to obtain the tool temperature for turning operations. Several techniques can be found in the literature to measure the temperature of chip-tool interface. The method used during an investigation is so crucial that the obtained temperature can be changed based on the method used for the same cutting parameters. Researchers categorised the cutting tool temperature obtaining methods in several ways. Arndt and Brown [89] pointed out analogue computation as a method of the measurement of metal cutting temperature distribution. The authors categorised analytical method and experimental methods as two main methods.

The use of computer to obtain the machining temperature is in practice for a period of time. Tay et al. [90] categorised the main methods of calculating machining temperature as: (1) the heat source moving method (2) image sources method (3) finite difference (4) finite element and (5) semi-analytical methods.

In summary, the methods reported in the literature to determine the chip-tool interface temperature can be divided into following major categories: (i) Analytical analysis (ii) Experimental analysis and (iii) Numerical analysis. Further subdivisions of these methods can be as following:

1. Analytical analysis can be further divided into several subcategories, out of these the following two are frequently used by researchers which are (a) Shear plane model and (b) Slip-line field model.
2. Experiment method can be subdivided into (a) Tool-workpiece thermocouple technique (b) Embedded thermocouple method (c) Infrared radiation method (d) Metal microstructure method and microhardness variation method (e) Thermosensitive painting method and (f) Temper colour method.
3. Numerical analysis can be mainly subdivided into (a) Finite difference method (b) Finite element method and (c) Boundary element method.

In addition, researchers also applied semi-analytical or hybrid method to obtain the tool temperature which is based on the combination of two methods. In general, one of the methods is applied to obtain the tool temperature and another method is used to compare to the results.

2.3.1 Analytical Methods

Analytical methods are based on the law of physics where theoretical analysis is applied for the interface temperature distributions. Analytical methods provide better physical understanding of the thermal process. In analytical approach, it is assumed that the chip is formed instantaneously by a shearing action and heat is generated due to friction [91]. The early analytical solutions are based on moving heat source method or image heat source method [92]. In moving heat source approach, it is assumed that temperature distribution along the shear plane is a uniform band source of heat which moves obliquely through the workpiece. On the other hand, in image heat source method, a grid of real and imaginary point heat sources are considered [90].

Few research groups applied the theoretical analysis to obtain the tool-chip interface temperature distributions. In early analytical methods, some simplified assumptions were made. For example, the non-sensible heat generated due to the deformation was not considered and it was assumed that the heat sources were uniformly distributed at the shear plane and the tool-chip interface [93]. The uniformly distributed assumption logically resulted to no temperature distribution [89]. Chao and Trigger [94] enhanced the analytical method and predicted the distribution of temperature both at the tool-chip and tool-work interfaces.

Moufki et al. [95] presented a thermomechanical model of the primary shear zone including the friction law to estimate the temperature. The authors considered the effects of cutting conditions and material behaviour on the temperature, mean friction and global cutting force.

By applying analytical method, Komanduri and Hou [96], [97], [98] presented a new analytical model for chip-tool interface distribution in a three-part series on the thermal modelling of the metal cutting process. In the first part of the research, Komanduri and Hou [96] determined the temperature rise distribution due to shear plane heat source. In the second part, Komanduri and Hou [97] determined the temperature rise distribution due to frictional heat source at the tool–chip interface. Finally, in the third part, Komanduri and Hou [98] presented a model combining the two to calculate metal cutting temperature due to frictional heat and shear plane heat. The authors claimed that their analytical approach was easier, faster, and more accurate to use than the numerical methods available at the time. Komanduri and Hou [98] also used computer program to obtain the analytical solutions.

Karas et al. [99] simplified the model developed by Komanduri and Hou and obtained the temperature distributions for tool-chip-workpiece individually from their own axes system. Figure 2.7 shows isothermal contours of the temperature of the tool and the workpiece due to the shear plane and frictional heat.

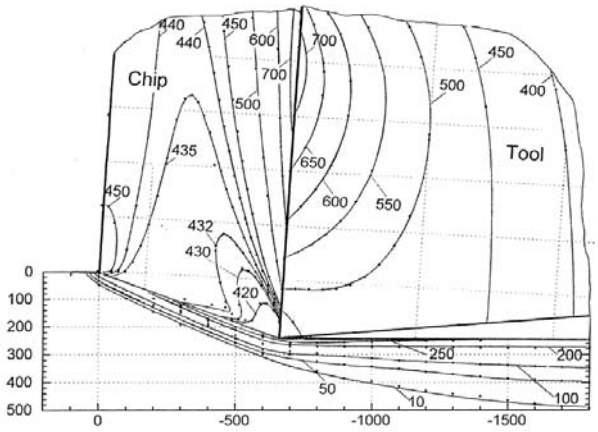

Figure 2.7: Isothermal contours due to frictional heat and shear plane heat [98]

Huang and Yang [100] noted the Komanduri and Hou's thermal model has no the cooling process for the workpiece. The authors improved the model by introducing a heating time for the workpiece. The authors also validated the result by comparing against numerical and experimental methods.

Karpat and Özel [101] developed thermal model by analytically combining modified Oxley's parallel shear zone theory with the oblique moving band heat source theory. In the second part of the analytical thermal modelling, Karpat and Özel [102] considered the effect of the tool wear on the force, stress and temperature. The authors obtained the metal cutting temperature distributions as shown in Figure 2.8.

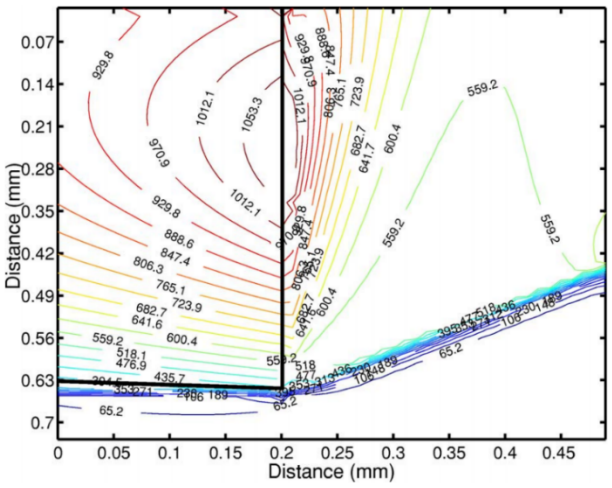

Figure 2.8: Metal cutting temperature distributions [101]

Radulescu and Kapoor [103] developed an enhanced analytical model for prediction of tool temperature fields which can be applied to a continuous or interrupted three-dimensional cutting process.

Tool temperature was obtained by the slip-line based model in several study. Dewhurst [104] developed the slip-line model for machining which provides curled chip effects as shown in Figure 2.9.

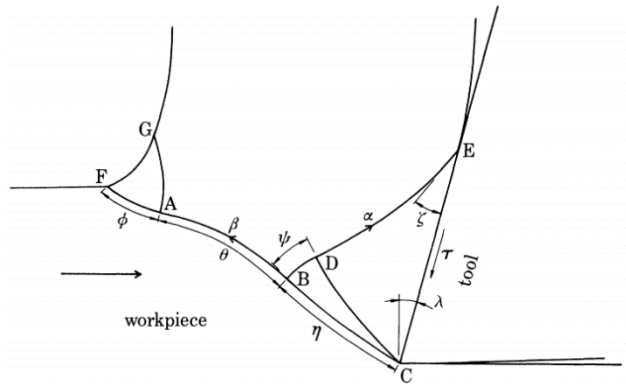

Figure 2.9: Slip-line model with curl chip effects [104]

The slip-line based analytical model by Kudo [105] also provided curled chip effect. In addition, the slip-line based analytical model by Shi and Ramalingam [106] provided curled chip effects with the grooved cutting tool, as shown in Figure 2.10. Fang et al. [107] proposed slip-line analytical model with chip curl and chip back flow; also studied built-up-edge. Finally, Fang et al. [108] predicted temperature by the slip-line based model. Similarly, Karpat and Ozel [109] applied the analytical slip-line approach to investigate the friction factor at the tool-chip interface and dead metal zone phenomenon for machining temperature.

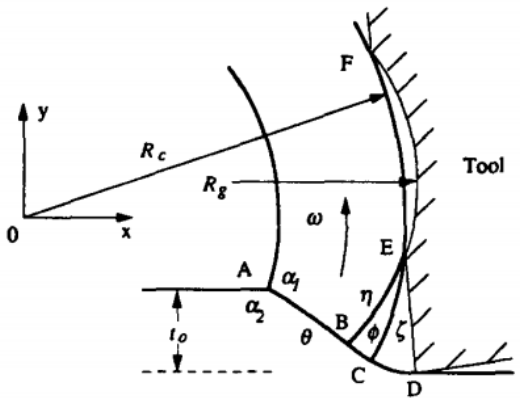

Figure 2.10: Slip-line model with grooved tool [106]

2.3.2 Experimental Methods

Even after simplified assumptions, obtaining the temperature at chip-tool interface by analytical methods was found to be difficult which has led to the development of experimental methods [110]. Over the years, a number of methods were used to obtain the tool temperature and the experimental methods are frequently used by the researchers. Arndt and Brown [89] subdivided the experimental methods as following: (a) embedded thermocouples (b) thermo-colours (c) analogue computation (d) radiation measurement and (e) crater wear.

Astakhov [110] divided experimental methods into following two categories as non-contact and contact methods. In further details, non-contact method is subdivided into (1) microstructural method (2) infrared thermography method. Contact method is basically thermocouple method which can be further subdivided into (1) embedded thermocouple method (2) running thermocouple method and (3) tool-work thermocouple method.

Amritkar et al. [111] categorised the experimental tool temperature measurement methods as shown in Figure 2.11. The authors used the tool-work thermocouple method to obtain the tool temperature. The authors performed the calibration process with an electric heater, as calibration is necessary for the tool-work method.

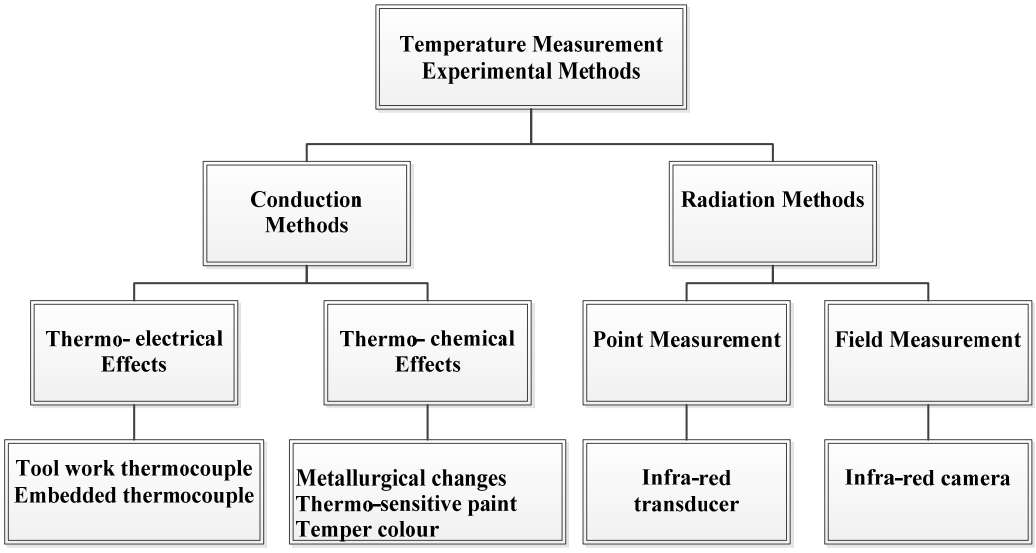

Figure 2.11: Categories of the experimental tool interface temperature measurement methods, adopted from [111]

The tool-work thermocouple method, embedded thermocouple method and thermal radiation method are widely used methods to measure the tool chip temperature for turning operations. In addition, the thin film thermocouples are also used by the researchers for turning temperature measurement. However, it is a challenge to place a standard thermocouple in the tool chip interface due to the moving tool-chip contact area.

Boothroyd [112, 113] used a photographic plate which is infra-red sensitive for photographing the chip, tool and workpiece. With the help of a microdensitometer, the author determined the optical density. The work material was carbon steel and the cutting speed was 11 feet per min, 0.0119 inch depth of cut. Figure 2.12 shows the isothermal temperature contours of the tool and chip for turning operations.

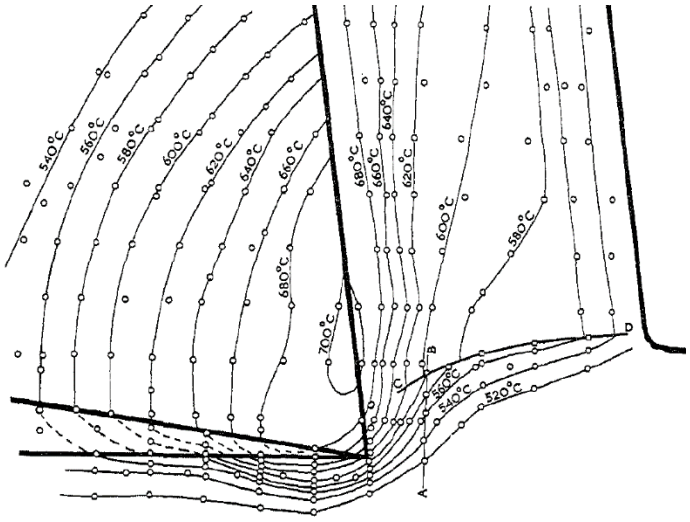

Figure 2.12: Isothermal temperature distribution of chip and tool during orthogonal machining [112]

Applying a thermal imaging camera, Abukhshim et al. [114] obtained interface temperature considering that the radiation technique provided some benefit against thermo-electric procedure such as rapid response and easy to implement without any physical contact and without effecting the temperatures and materials.

Sutter et al. [115] used the radiation pyrometer technique based on the principle of pyrometry which uses an intensified charge-coupled device (CCD) camera with very short exposure time. As there is no physical contact, the temperatures and materials are not influenced. In addition, the technique has fast response time and it is

easy to implement. The radiation pyrometer technique of temperature measurement was successfully used by other researchers as well, such as [116].

Kikuchi [117] estimated the cutting temperature by measuring the electromotive force (EMF) from tool–workpiece thermocouple for machining operations. Similarly, Stephenson [118] concluded that the tool-work thermocouple temperature measurement method is most promising as this method able to provide repeatable result that correlates with tool wear mechanism for many materials. The author used the idealised tool-work thermocouple circuit with insulated tool subject to a distributed interfacial emf as shown in Figure 2.13.

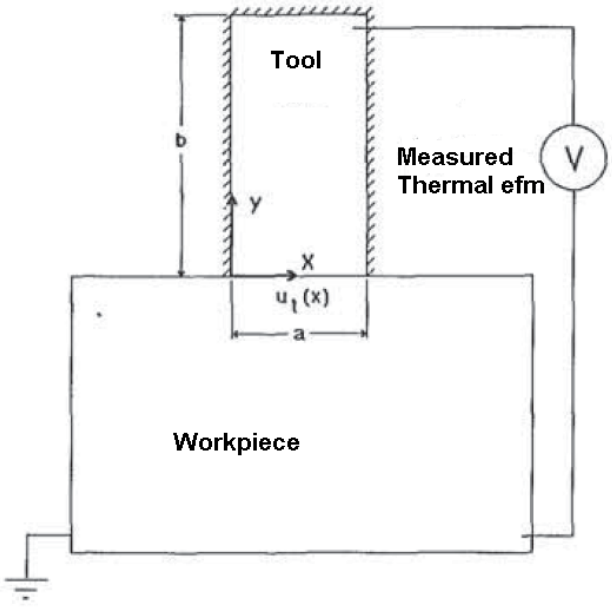

Figure 2.13: Idealised tool work thermocouple circuit with insulated tool [118]

Leshock and Shin [119] identified the problems associated with the tool-work thermocouple method of measuring tool-interface temperature which are as following: (a) the parasitic e.m.f.'s created by secondary junctions (b) calibration of the experimental setup is necessary (c) the experimental setup should be insulated from the environment and (d) e.m.f. measured by the thermocouple is the correct one. The set up for tool-work thermocouple calibration conducted by them is shown in Figure 2.14.

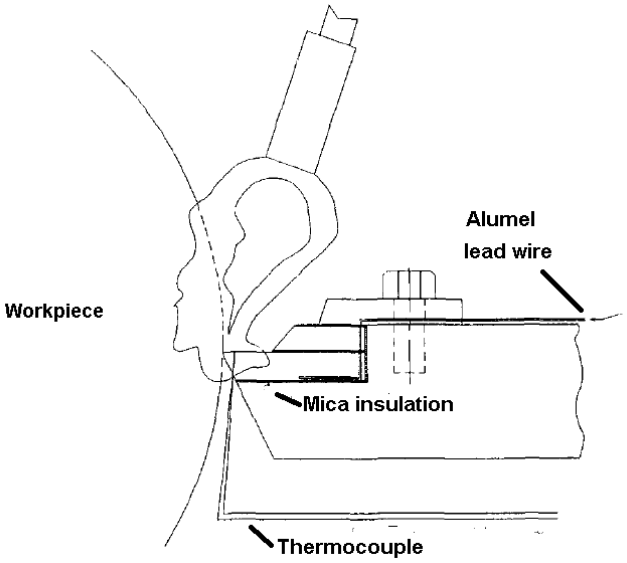

Figure 2.14: The set up for tool work thermocouple calibration [119]

Abhang and Hameedullah [120] measured the tool temperature experimentally by using the tool-work thermocouple technique for turning steel alloy using tool inserts made of tungsten carbide. Based on the experimental results, the authors developed model based on first order and second order of mathematics with cutting parameters. Figure 2.15 shows the setup for experiment to measure average temperature for chip-tool interface.

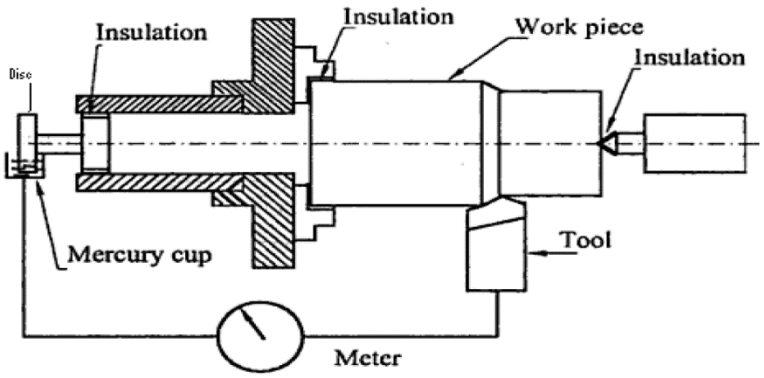

Figure 2.15: Experimental setup to measure the tool temperature by the tool-work thermocouple method [120]

One of the challenges of the embedded thermocouple method is that it requires drilling hole in the tool to place the thermocouple. This challenge can be resolved by selecting suitable tool insert that provide sufficient tensile strength to cut the metal after drilling the hole. Another option is the reduction of the number of holes as low

as possible. Materials such as tungsten carbide inserts are strong enough to provide the sufficient tensile strength for this purpose. Nowadays, it is possible to make the hole with small diameter in the tool by electrical discharge machine. But during selecting the position of the hole, attention should be given so that the location of the hole does not alter the heat flow.

Li et al. [121] measured the tool interface temperature by implanted workpiece thermocouple technique. The authors obtained the temperature of the cutting zone consist of workpiece and implanted thin flat constantan wire. Similarly, O'Sullivan and Cotterell [122] placed the a thermocouples inside the workpiece and compared the results by using infrared camera. The authors taped thermocouples at the inside of the tube and inserted a plug into the open end of the tube for support and damp out any unnecessary vibrations. They made up another plug to hold the tube and to mount the electrical slip ring in order to measure the temperature.

In contrast, Kishawy [123] inserted a K-type thermocouple in a recess of the carbide tool and grooved on chip breaker. The experimental results showed that higher cutting speed and feed rate increased the cutting temperature. Korkut et al. [124] investigated chip temperature developed in machining process by inserting thermocouple inside of a tool. The authors used thermal camera for their investigation and concluded that the result of increasing cutting speed or depth of cut or feed rate was increased the tool temperature but the cutting speed has the most influence on the tool temperature. Figure 2.16a and Figure 2.16b show the experimental setup with the thermocouple and the thermal camera view.

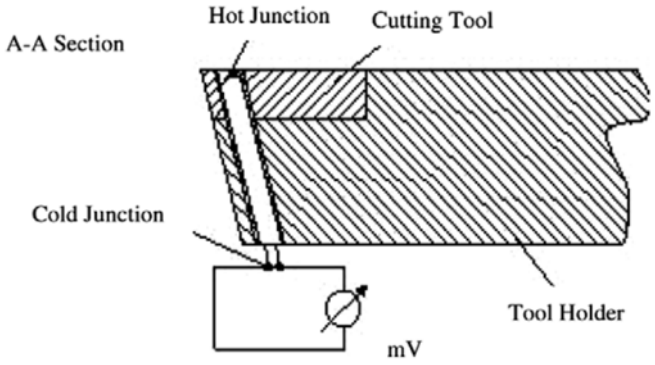

(a)

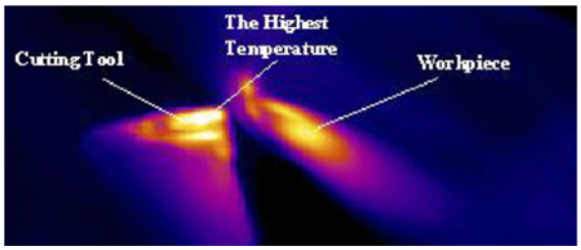

(b)

Figure 2.16: Turning temperature investigation (a) experimental setup with the thermocouple and (b) thermal camera view [124]

Haddag and Nouari [125] conducted experimental measurements of the heat transfer into the cutting tool and compared with finite element calculations. The authors used two thermocouples with different distance from the rake face. As shown in Figure 2.17, the obtained temperatures were different based on the distance from the rake face and the locations, where d_{x1} is 1.6 mm and d_{y1} is 0.5 mm for TC_1; and d_{x2} is 2.4 mm and d_{y2} is 1.0 mm for TC_2. The velocity is 250 m/min, feed is 0.1 mm and depth of cut is 1.1 mm. Therefore, based on their experiment, it is established that the location of the embedded thermocouple is important for obtaining the tool temperature.

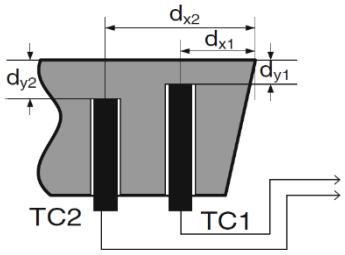

(a)

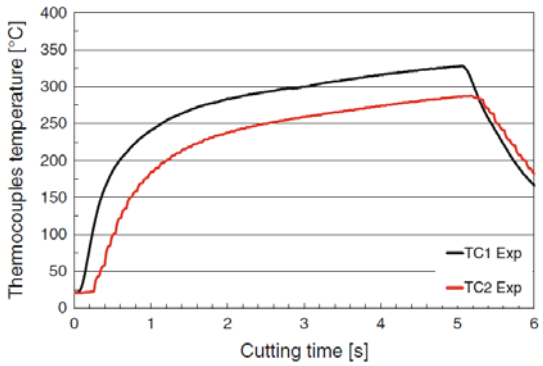

(b)

Figure 2.17: Experimental tool temperature measurement (a) insert with location of the holes for the thermocouples and (b) difference of the temperature due to the distance [125]

Some group of researchers identified the effectiveness of different tool temperature measurement methods. Filice et al. [126] compared the thermocouple based approach, thermographic approach and numerical method. As shown in Figure 2.18b and Figure 2.19b, the obtained temperature with thermocouple based approach was higher than that of thermographic approach for the same cutting parameters, where velocity was 200 m/min and feed rate was 0.2 mm/rev.

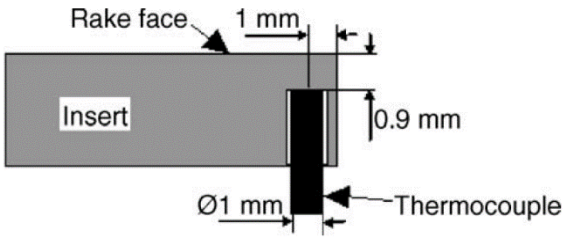

(a)

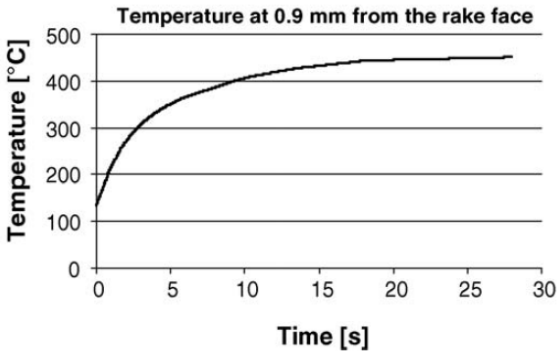

Velocity = 200 m/min, feed = 0.2 mm/rev

(b)

Figure 2.18: Tool temperature measurement with thermocouple (a) experimental location of the thermocouple and (b) obtained temperature with the thermocouple [126]

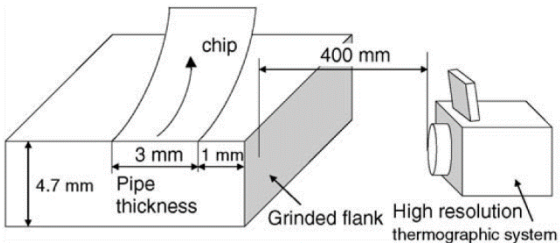

(a)

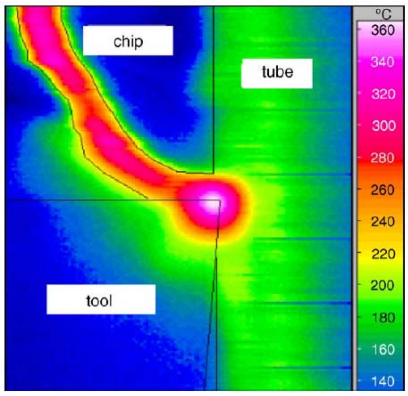

Velocity = 200 m/min, feed = 0.2 mm/rev

(b)

Figure 2.19: Thermographic temperature investigation (a) experimental setup for thermal camera and (b) thermal camera view [126]

By using fibre-optic sensor with two colour pyrometer, Tapetado et al. [127] measured tool temperature during turning operation. The fibre-optic sensor was embedded on a standard tool holder. The damage at the end of the optical fibre was a major limitation of their experiment which could lead to the spectral loss attenuation and responsivity. Figure 2.20 illustrates the fibre-optic sensor for two colour pyrometer during turning temperature investigation.

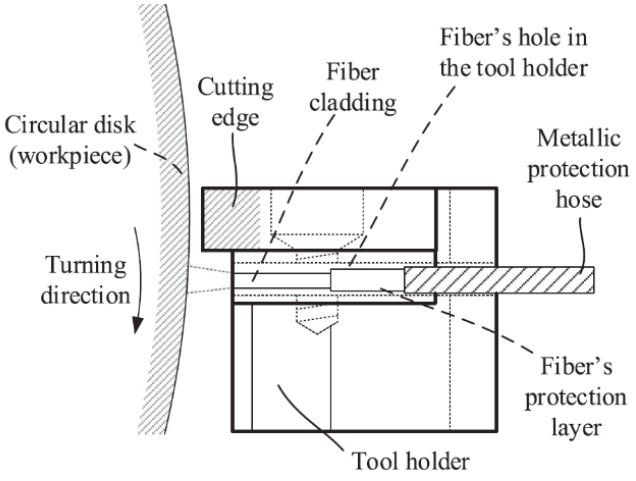

Figure 2.20: Fibre-optic sensor for two-colour pyrometer during turning temperature investigation [127]

But Huda et al. [128] overcame the limitation of damaged end of the optical fibre by using a translucent alumina (Al2O3) tool and fibre coupler with a two-colour pyrometer to measure tool temperature. The authors were able to measure the

temperature both in dry and flood machining operations. However, this method is not suitable for regular tool inserts as the regular tool inserts are not translucent.

Abang Kamaruddin et al. [129] used the chalcogenide glass fibre with two colour pyrometer by making a narrow hole up to the inner surface of the cylindrical workpiece. The fibre captured the ray and transmitted the pyrometer when the cutting tool was passing over the hole during machining operations.

Hautamaki [130] measured the tool temperature by the microelectromechanical systems. The micro thin film thermocouples can be created by adapted semiconductor microfabrication methods to measure the tool internal temperatures which are embedded in the cutting tool insert, as shown in Figure 2.21 [131]. In ceramic material, the thin film sensor can be placed by diffusion bonding technique [132].

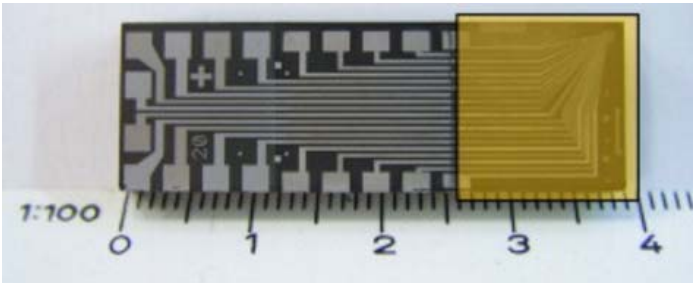

Figure 2.21: The micro thin film thermocouples [131]

Basti et al. [133] observed the thermal impact and thermal activation on the cutting tools in real time by thin film thermocouples which were formed on cutting tools. The authors confirmed that the main limitation of the thin film thermocouples method was that the thermal sensors should have the ability to bear high stress and the high temperature of machining operations. The authors recorded the melting temperature of A6061 aluminium alloy 876K although no trace of melted chip found. The authors explained that it was possible that the chip transformed after leaving the high cutting temperature. Figure 2.22 shows the turning experiment by thin film thermocouples.

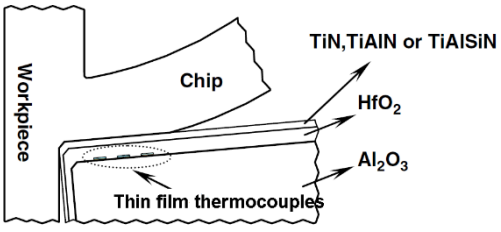

(a)

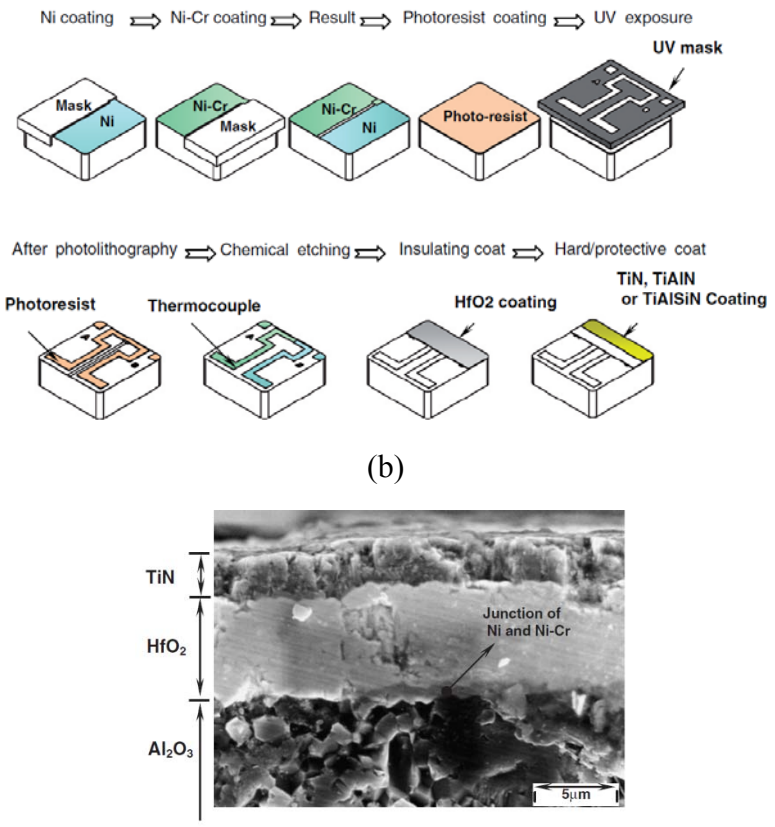

(b)

(c)

Figure 2.22: Thin film thermocouples (a) The location of the built in thin film thermocouple in tool (b) The thin film thermocouple fabrication sequence and (c) Backscattered electron structure image [133]

Shinozuka and Jaharadak [134] highlighted that the strength of thin film thermocouples against the friction of the chips was low. The authors overcame the limitations of the thin film thermocouples by the introducing an indexable tool insert. Near the cutting edge on the rake face, the authors embedded seven pairs of micro Cu/Ni thermocouples to obtain the tool temperature distributions more accurately.

Smart and Trent [135] measured the temperature gradients in high speed steel tools for turning iron, titanium and nickel; by using metal microstructure and microhardness variation measurement method. The authors found that temperature distributions on the tool were different for each of the three metals. In addition, Kato et al. [136] applied thermo-sensitive painting technique method to measure tool temperature distribution. The authors used fine powders that have a constant melting point and observed the boundary line which was formed by melted and unmelted powder scattered on the tool surface.

Yeo and Ong [137] applied the temper colour technique to study the thermal effect. By applying the chip-colour approach, the authors obtained a chart for chip colours where lightness is the function of the temperature. The authors assessed the temperature for varying cutting conditions to establish the relation of the lightness and the chip colour. Figure 2.23 shows the lightness and the colour of the chip against the temperature of the tool or chip.

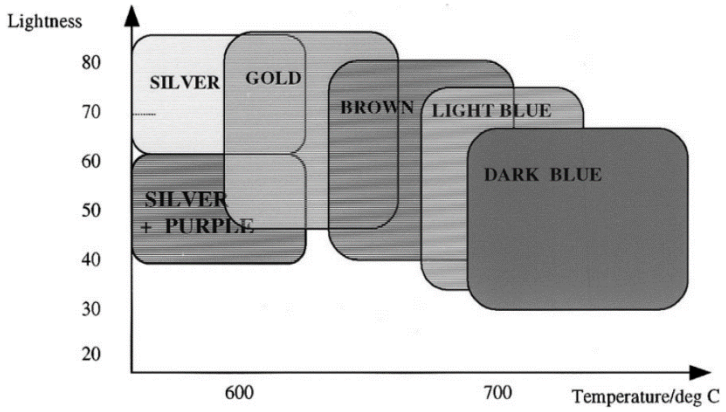

Figure 2.23: Lightness and the colour of the chip against the temperature of the tool or chip [137]

Davoodi and Tazehkandi [69] glued a thermocouple to the tool by covering with insulation to measure the temperature. The insulation was heat-resistance up to 1400°C. The thermocouple was attached only 0.5 mm distance from the tool tip. Tazehkandi et al. [138, 139] measured the tool temperature by similar approach, gluing a thermocouple on the cutting tool. In addition, the authors used a thermal imager to record the machining temperature and verified the temperature obtained by thermocouple.

2.3.3 Numerical Methods

Numerical methods have been applied for modelling machining operations by several researchers. The researchers used the numerical methods to simulate the metal cutting process and predicted the stress or temperature distribution [140]. The currently available numerical models can be divided into two main sections (a) machining variables models and (b) machining performance models [141]. Numerical methods can be applied in calculating the temperature distribution and thermal deformation in the tool, chip, and workpiece. The results from some simulations are close to the experimental results which confirms the practical applicability of the experimental–

theoretical simulation approach [142], [143]. Numerical methods can be divided into: (a) Finite Difference Method (FDM), (b) Finite Element Method (FEM), and (c) Boundary Element Method (BEM). In addition, there are other numerical methods such as the Finite Difference Element Method (FDEM) which is a simulation approach that combines the advantages of FDM and FEM [144]. The Finite Element Method can provide the tool temperature distribution during machining operations [145], [146].

Mackerle [147] presented a bibliography of simulation of machining by finite element methods, including general solution techniques; and divided into following main concerns: (a) material removal or cutting process and chip formation mechanism (b) effects of geometric and process parameters, (c) thermal analysis of machining, (d) tool wear (e) residual stresses in machining and (f) dynamic analysis of machine tools.

To assess the success of different numerical methods, Cheng and Cheng [148] performed the keyword search on a scientific index and summarised that the finite element method is the most popular method, the finite difference method is a distant second, less than one third of the finite element method. The boundary element method ranks third with less than one sixth of the finite element method.

Based on finite difference method, one of the early applications of the numerical methods was performed by Dutt and Brewer [93]. The authors established generalised equations for chip, workpiece and tool. Figure 2.24 shows the isothermals obtained from numerical solution by them. A number of publications based on finite difference method support the importance of this method [149-152].

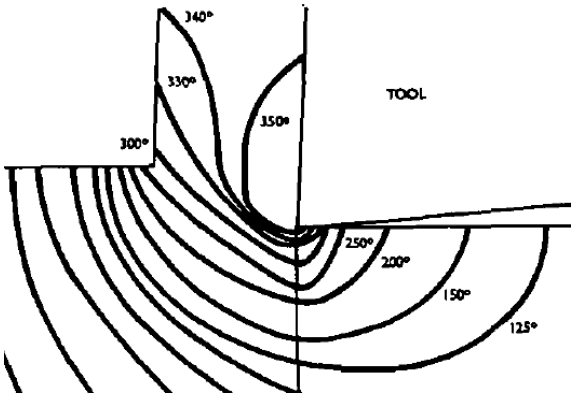

Figure 2.24: Isothermals derived from theoretical solution [93]

Islam et al. [151] used finite difference technique with implicit time discretization to solve the partial differential equations and obtain the machining temperature. Their

model was applicable for both continuous machining processes i.e. turning and interrupted processes i.e. milling.

Tay et al. [153] applied finite element technique for calculating tool temperatures during orthogonal machining. But the authors used only 255 numbers of elements and 308 numbers of nodes for the analysis. In numerical analysis, the number of elements plays an important role on the outputs of the analysis. The analysis can generate different results based on the number of elements. Numerical method is applied in the present study to determine the effects of cutting fluid on machining temperature, but the numbers of elements and nodes are much higher than those of Tay et al. [153]. With the help of a computer model, it is possible to capture the effects of varying machining parameters on the tool-chip interface temperature and the best cooling technique for particular cutting parameters can be obtained. Figure 2.25 and Figure 2.26 show the typical mesh and temperature contours of the FEM analysis.

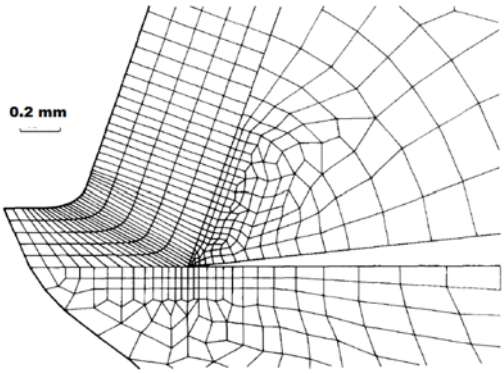

Figure 2.25: Mesh used for the FEM analysis [90]

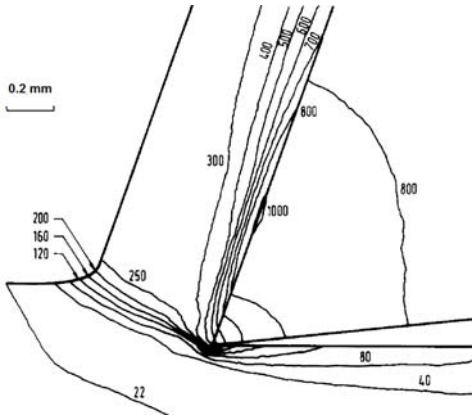

Figure 2.26: Isothermal contours in chip, tool and workpiece [90]

Chan and Chandra [154] applied boundary element method formulation for the determination of design sensitivities of temperature and flux distributions for machining operations. First, the authors calculated heat transfer and its sensitivities in

tool, chip, and workpiece independently. Then, the authors developed a complete model by matching the boundary conditions across the interfaces.

As semi-analysis method, Muraka et al. [155] numerically obtained the temperature distribution for orthogonal machining by applying the Galerkin approach. The authors conducted the experiment with a Piezo- electric dynamometer. Figure 2.27 shows the isothermal contours in workpiece, tool and chip which were predicted by the finite element method.

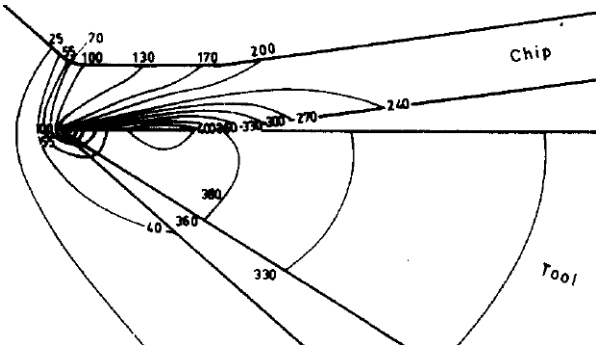

Figure 2.27: Isothermals obtained using the finite element method [155]

In some finite element analysis, experimental investigations were performed to compare experimental results against the numerical results [156, 157]. Some group of researchers, experimentally calculated heat flux or heat transfer coefficient for their analysis [158-160].

Majumdar et al. [161] deployed the finite element code ANSYS® to compute two-dimensional heat conduction. The authors observed the effect of cutting fluids on the tools and noticed that the temperature decreased by 9.3% if the boiling heat transfer coefficient was increased from 13,000W/m^{2}K to 25,000W/m^{2}K. Figure 2.28 shows the temperature contours for the machining.

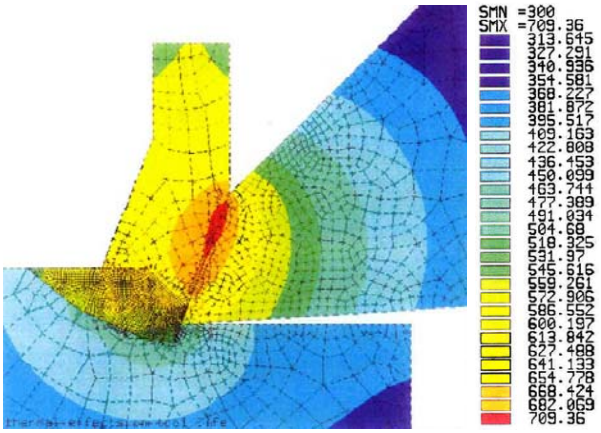

Figure 2.28: Temperature distribution for cutting zone [161]

Carvalho et al. [162, 163] estimated the temperature and heat flux by the inverse method. The authors considered both the tool holder and the tool for the numerical analysis. Figure 2.29a and 2.29b show the simulated temperature distributions. In some research, finite element methods used with tool-work temperature measurement for validation purpose [164]. Chen et al. [165] developed three-dimensional model by the boundary element method. In addition, the application of inverse heat transfer technique is noticeable by some group of researchers [166, 167].

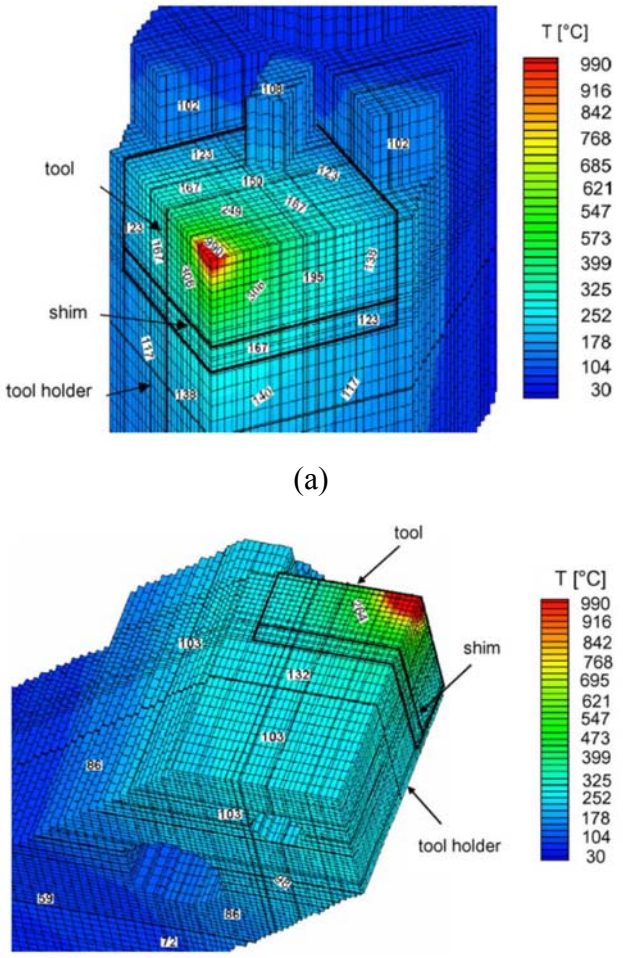

Figure 2.29: Tool temperature distributions of the cutting tool including the tool holder (a) Front view and (b) Side view [162]

Bagheri and Mottaghizadeh [168] applied two different approaches (a) with embedded thermocouple technique and (b) with infrared camera for tool-chip interface temperature measurement. The authors compared experimental results against the data obtained from the MSC.SuperForm® and ANSYS FLUENT®. Their numerical simulations of the machining operations are shown in Figure 2.30. One of the

advantage of the infrared method is that it does not affect the heat transfer process of the tool [169]. The deployments of machining simulation software such as NASTRAN [164], Abaqus [170], AdvantEdge [171] and Deform 3D [172, 173] are also noticeable for the finite element modelling.

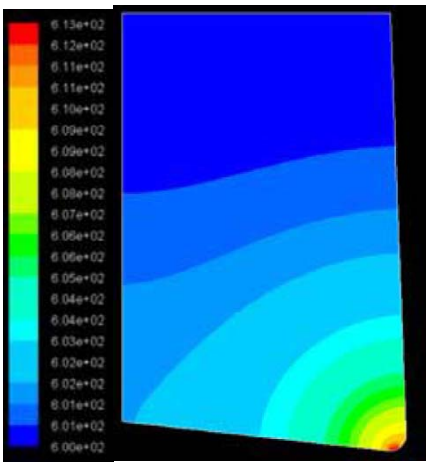

(a)

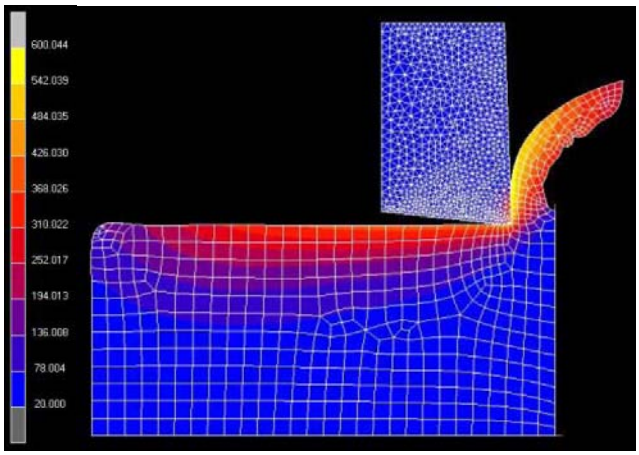

(b)

Figure 2.30: Temperature distributions for turning (a) Cutting tool temperature distribution and (b) Temperature distribution during chip formation process [168]

Li et al. [174] estimated the tool-chip temperatures by remote thermocouple method for the turning operations. The authors also obtained the temperature of tool–chip interface by using Groover's model [175] and validated the results against the experimental results. The authors demonstrated that it was possible to obtain the interface temperature by their model without the requirement of force during cutting or any heat partition.

Kagnaya et al. [176] measured temperature at two points of tool insert by using the embedded thermocouple method. In addition, the authors conducted numerical experiments to compare the results. The thermal simulations were based on calculated heat flux from measured cutting forces. Figure 2.31 shows the numerical temperature distributions and rake face temperatures based on their numerical analysis.

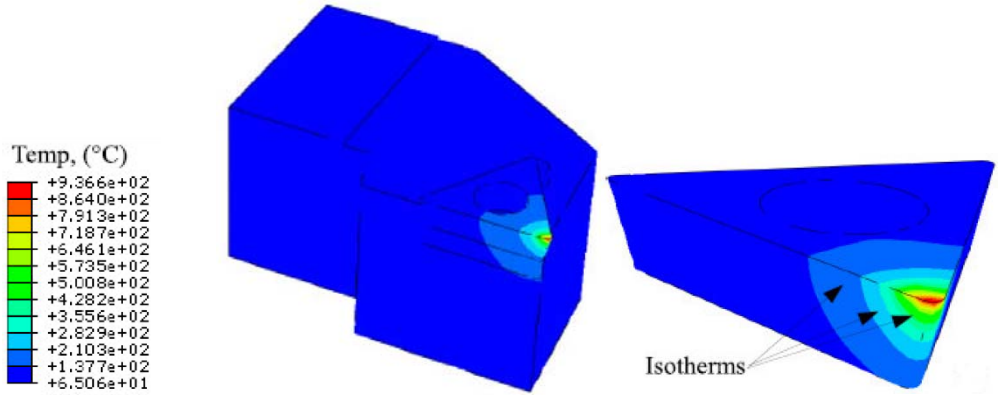

(a)

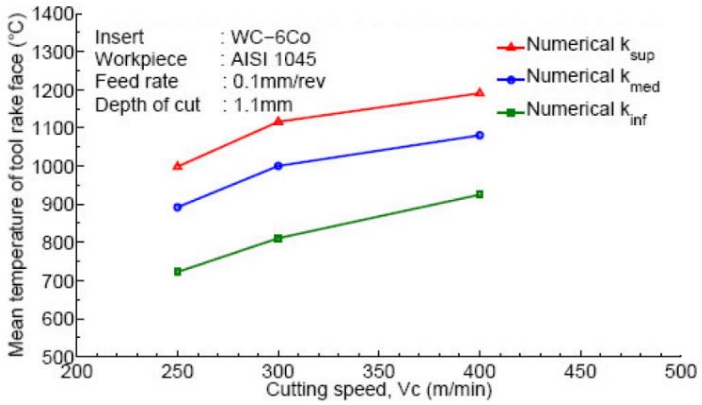

(b)

Figure 2.31: Numerical experiment of turning operation (a) Simulated temperature distribution of the toot insert and (b) Mean temperature of the rake face vs cutting speed [176]

Haddag and Nouari [125] conducted numerical analyse for dry machining which was based on multi-steps heat transfer modelling. The authors considered non-uniform heat flux on the rake face of the tool for their numerical analysis. Figure 2.32 shows the heat flux magnitudes and the tool temperatures based on their numerical analysis.

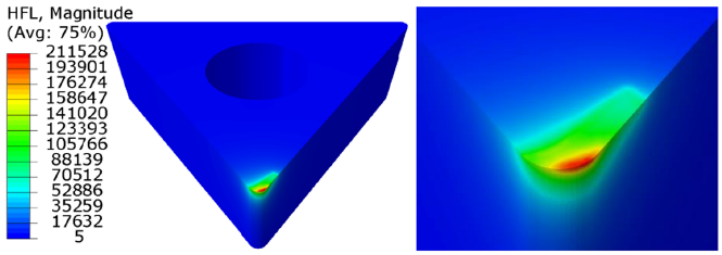

(a)

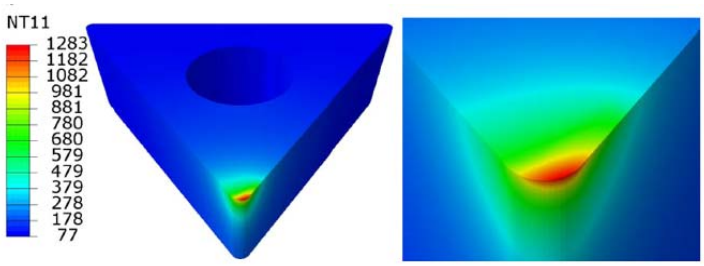

(b)

Figure 2.32: Numerical analysis of the tool insert (a) Heat flux magnitude and (b) Tool temperature distributions [125]

Ozel [177] calculated 3D computational modelling of turning process for varying shape of cutting tool inserts. The study revealed the effects of the variable edge micro-geometry design from the temperature and stress distributions contours. Kwon et al. [178] experimentally measured the machining temperature with infrared camera and numerically compared the results. The authors compared the results for machining gray cast iron (GCI) and AISI 1045 against the prediction of Cook method, as shown in Figure 2.33.

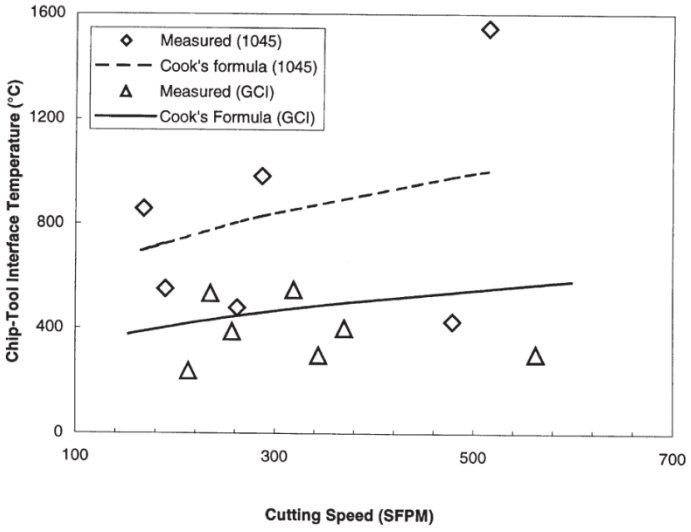

Figure 2.33: Graphical evaluation of measured temperature against the prediction by Cook, obtain from [178]

Movahhedy [179] found that both the Lagrangian and the Eulerian finite element approaches have some limitations and inefficient although these are enormously used for the orthogonal metal cutting modelling. The authors claimed that the arbitrary Lagrangian Eulerian method can be used to combine the advantages of these two methods and eliminate the limitations.

Olovsson et al. [180] used Arbitrary Lagrangian-Eulerian approach but emphasised on the mesh generation. Pantale et al. [181] used Arbitrary Lagrangian-Eulerian approach and added the damage constitutive law with the machining model but did not obtain the temperature contours for the tool insert.

Ceretti et al. [182] numerically allied Arbitrary Lagrangian-Eulerian approach in finite element method and experimentally obtained by embedded thermocouple method to obtain tool temperature. Considering the contact pressure and temperature, the authors proposed a model for heat transfer coefficient. Pusavec et al. [183] employed ABAQUS Explicit software, which is based on an Arbitrary-Lagrangian-Eulerian approach in finite element method. The authors simulated the machining temperature and heat transfer coefficient but used liquid nitrogen as cutting fluid by developing a novel optical nitrogen phase status sensor.

Abdelkrim et al. [184] used finite element based COMSOL Multiphysics for modelling the tool temperature and experimentally validated the model by obtaining the tool temperature with K type thermocouple, but the experiment was conducted under dry condition without any cutting fluid.

Fratila [185] used the DEFORM 2D software to numerically obtain the temperature distributions during machining operations but the simulation was limited for dry cutting condition only. Numerical code is also used to develop tool wear models with successful validation [186]. Artificial neural network based models can predict the surface roughness for varying metal cutting conditions [187].

Jiang et al. [188] used ABAQUS software to emphasis on the cooling processes of turning operations and experimentally validated the model by obtaining the temperature with infrared camera, but their research was not involved with flood cooling process.

Shen [189] developed a transient three-dimensional thermal model using ANSYS® and validated through experiments. The heat generation process related to the machining was considered in the finite element analysis study. Koyama [190]

conducted computational fluid dynamics based study with ANSYS CFX® and demonstrated the application of ANSYS CFX® for heat transfer and fluid flow based analysis. The application of the ANSYS CFX® is also found in the study of water jet and abrasion as well [191]. ANSYS CFX® software was used to simulate and analyse the turning objects but there was no validation of the model [192], [193]. In the industry, generally the commercial CFD code is used for numerical analysis rather than developing own code for the research [194]. It is very time consuming to develop complex geometry without the commercial code. Therefore, commercial CFD code will be used in this study to for the numerical analysis.

2.4 Limitation of Previous Research

With the availability of powerful computer, it is possible to perform numerical analysis which was previously technically unaffordable. A few finite element analysis based studies were found to obtain the tool temperature, but the number of element of the mesh is very low [195]. As the number of element of the mesh is low, the accuracy of the analysis will not be high as well. Computer based fluid dynamics analysis for machining with flood cooling is rarely found, although few analysis for spraying of oil mist [196, 197] or air cooling [198, 199] exist. Therefore, the application of multiphase computational fluid dynamics based modelling technique in the present study is a new approach for obtaining the tool temperature for flood cooling.

In other words, the tool cooling process during flood machining operations was rarely investigated by applying computational fluid dynamics analysis. If any research exists, lack of accuracy and validation of the models provided an opportunity to develop a new methodology and validate against experimental data.

2.5 Conclusion

Based on the literature review, it can be concluded that the analytical methods have some limitations and most of the experimental techniques are not suitable to apply for the present study. The radiation pyrometer technique is difficult to apply where liquid cutting fluids are used. The presence of fluids can block the view to the tool chip interface. During the flood turning operations, the infra-red pyrometer method is not suitable as the coolant prevents the sight of the cutting zone from the camera. On the other hand, although the tool-work thermocouple method is easy to implement [120], but it may not be possible to capture the flash or high local temperature which is

generated during machining. The tool-work thermocouple method provides average temperature of contact area [122]. In addition, this method is not suitable for the present study as the tool and workpiece should be isolated from machine tool electrically. The coolant used for the turning operation can prevent maintaining the insulation which is the crucial requirement for this method.

Arndt and Brown [89] found that the thermosensitive painting technique had a tendency to provide inaccurate data as the temperature gradients was very high. Similarly, the thermo-colours is not sensitive enough to provide accurate machining temperature. Among the experimental methods, the embedded thermocouple method was selected to apply to obtain tool temperature considering the suitability of the objective of the study. One of the objectives of the present study is to understand the effect of cutting fluid on tool temperature. The embedded thermocouple technique has limitations as well but these limitations can be resolved. Although, it is difficult to place a standard thermocouple exactly at the tool-chip interface, but a hole can be made in the tool insert as near as possible to the tool-chip interface with the help of spark eroding process. Literature review [200] revealed that the high local temperature that occurs for relatively short period of time and cannot be captured property by regular thermocouple. But real time temperature measurement with thermocouple can express the transient type temperature. In addition, thermocouple has a response lagging time during the recording of the temperature [114]. Real time temperature measurement with thermocouple can address this issue as well.

The combination of an experimental method and the numerical methods can be used as an effective approach to obtain tool temperatures. The finite element analysis is applied in many areas such as the fluid flow analysis; lubrication and seepage analysis; understanding of the electromagnetic fields; the heat transfer process study; biomechanics etc. [201]. By developing a numerical model, the temperature distribution of the tool insert can be simulated in fine points. Numerical methods have been applied for modelling machining operations. Many researchers applied numerical methods to obtain the tool, chip or workpiece temperature distributions. The application of the numerical methods to predict the tool temperature is rapid, on the other hand, experimental investigations are problematic [202].

In the present study, the numerical analysis will be conducted with the help of Modelling Software, ANSYS CFX® as it is capable of performing numerical analysis

of cutting fluid during the machining operations [203]. The present study will demonstrate the effectiveness of the numerical method to obtain the tool temperature for flood turning operations.

Chapter 3

Temperature Determination at the Chip-Tool Interface

3.1 Introduction

There are several methods to obtain the tool temperature for machining but most of them are not easy to implement for flood cooling. A viable method to obtain tool temperature for the flood cooling may be the computer modelling. To evaluate the effects of the cutting fluid on the tool temperature, a computer model will be developed and validated against experimental data sets available from literature. This chapter presents the development process of the methodology for obtaining the tool temperature distributions during flood turning operations. The numerical analysis will be performed using the computational fluid dynamics modelling technique. This chapter presents an alternative approach based on computational fluid dynamics for determining the effect of the cooling media on the tool temperature distributions using conjugate heat transfer approach. A heat source will be assigned on the tool, due to the heat generation based on the cutting conditions during metal cutting, following the conjugate heat transfer approach. A solid-fluid interface will be developed between the cutting tool and cutting fluid by employing Ansys CFX software package.

The application of cutting fluids in machining operations is under review in recent years. The cutting fluid has confrontational effects on the health of the worker and also on the environment. Researchers around the world are trying to reduce the use of cutting fluids for machining operations. The present study is an initiative to find a solution for the framework of traditional forms of machining by determining the amount of cutting fluid necessary for machining operations. The cost of manufacturing can be reduced if less amount of cutting fluid is used for machining operations. Application of the reduced amount of cutting fluid can decrease the environmental effects. Reduction of usage of cutting fluid also minimises the need for disposal of contaminated fluid.

Experimental investigations of metal cutting is an expensive process, in addition this process consumes a lot of time. The results of the experiments are only useful for specific cutting conditions. The experimental results can fluctuate depending on the accuracy of experimental equipment. The calibration process of equipment for some

experimental methods also plays a role on the results. The finite element method is becoming more popular although there are several numerical methods to study metal cutting process. The finite element method already used in predicting the stresses, temperatures, cutting force and the chip formation [204]. On the other hand, using numerical analysis is identified as low cost, less time consuming process for obtaining tool temperature and finding the amount of cutting fluids necessary to reduce the tool temperature for the turning operations. Nowadays, researchers have reduced the number of actual tests and moved towards the computer simulations due to less cost and time involvement.

The difficulty of measuring the tool temperature using thermocouples is employing a regular thermocouple at the cutting zone. Literature review, in the Chapter 2, revealed that there are few ways to investigate the tool temperature during metal cutting. Analytical methods are limited in their usefulness as these methods are heavily based on some assumptions. The application of infra-red pyrometers is not suitable for flood cooling, due to the presence of the cutting fluids in the line of view from camera. Therefore, an appropriate method is needed for successfully obtain the tool temperature for flood cooling, so that it will be possible to identify the influence of flow rate for a specified cutting conditions. Reducing the amount of cutting fluid is a step toward achieving sustainable manufacturing by minimising environmental effects. Identifying the influence of flow rate of cutting fluid is one of the main objectives of the present research project. The computational fluid dynamics based 3D model will be developed to predict the tool interface temperature and identify the effects of cutting fluid on the tool temperatures.

3.2 Proposed Methodology

The development process of the proposed methodology has been described in a systematic way by means of five steps. At the beginning of these five steps, the heat generating inputs for the machining operations have been considered, which include the material properties, depth of cut, feed, cutting speed etc. As a part of the development process of the methodology, the heat generation and distributions during the turning operations have been analysed. The heat distributions during turning operations among the cutting tool insert, workpiece and chip are considered. In the next step, the 3D geometry development and mesh employment processes have been described. The properties of the cutting fluid and fluid flow velocity are considered as

well. Various parameters of the cutting fluids were assigned in the software after reviewing the characteristics of the cutting fluids. The properties of tungsten carbide were assigned for the numerical analysis as the cutting tool insert material of the model.

Followed by, computational fluid dynamics related issues were accomplished which are boundary condition declaration, initialisation, analysis type selection etc. Tool temperatures were obtained by varying the quantity of the cutting fluid. The success of the model will be demonstrated by the ability to capture the effect of cutting fluid on the tool temperatures. Finally, the validation of the model was performed by comparing numerically obtained interface temperature against experimentally measured temperature taken from three sources available in the literature. Finally, this chapter is concluded by highlighting the significant findings. The proposed methodology is illustrated in the Figure 3.1.

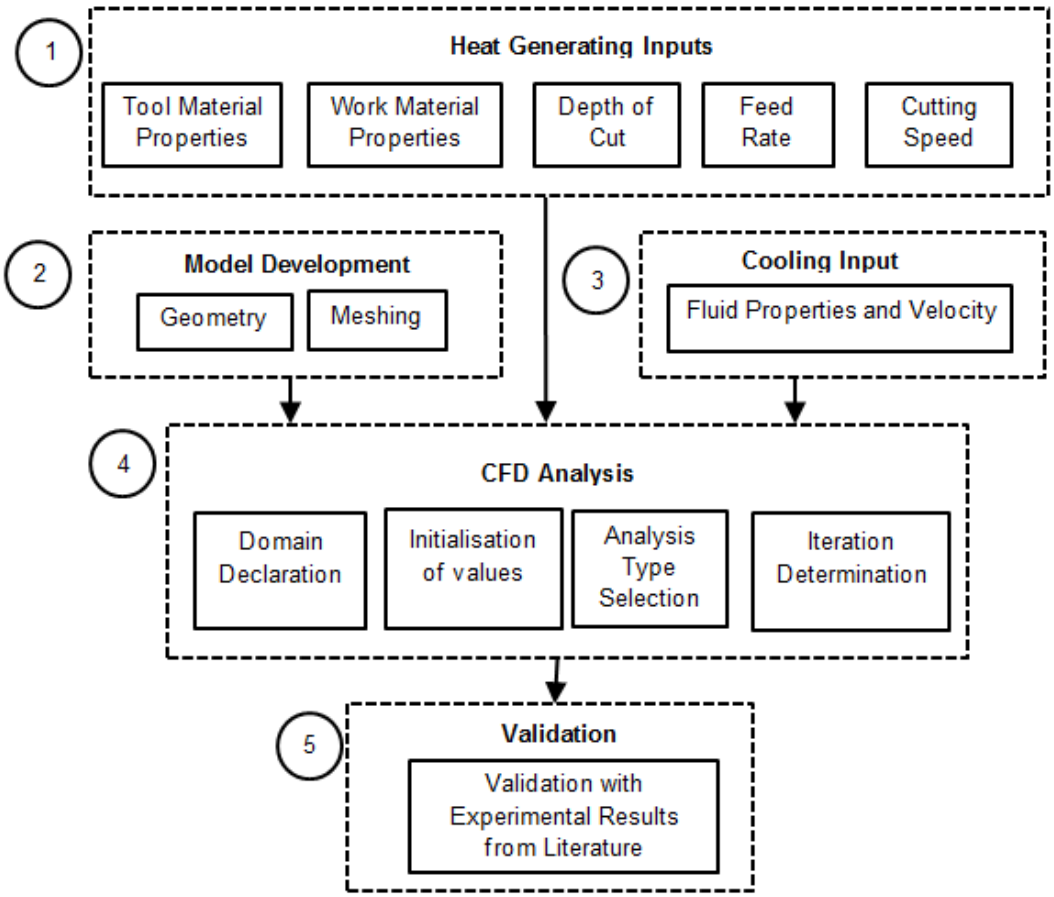

Figure 3.1: The proposed methodology for predicting the tool temperature distributions

3.3 Heat Generation

The proposed methodology begins with considering the heat generating parameters during the cutting process ①. The heat distribution fluctuates significantly depending on the machining process. Oxley [205] proposed a method by which the shear angle can be calculated allowing the normal stress along the shear plane in orthogonal metal cutting. In addition, Oxley and Hatton [206] solved the tool-chip interface problem based on realistic stress distributions. Al-Odat [53] identified that the power consumed in machining operations is largely converted into heat. The conversion happens mainly through plastic deformation particularly near the cutting edge of the tool.

Merchant [207] calculated the force components, stresses and the coefficient of friction of cutting tool and chip. The author also calculated the total work completed for shearing the workpiece and friction which are as following as shown in Figure 3.2.

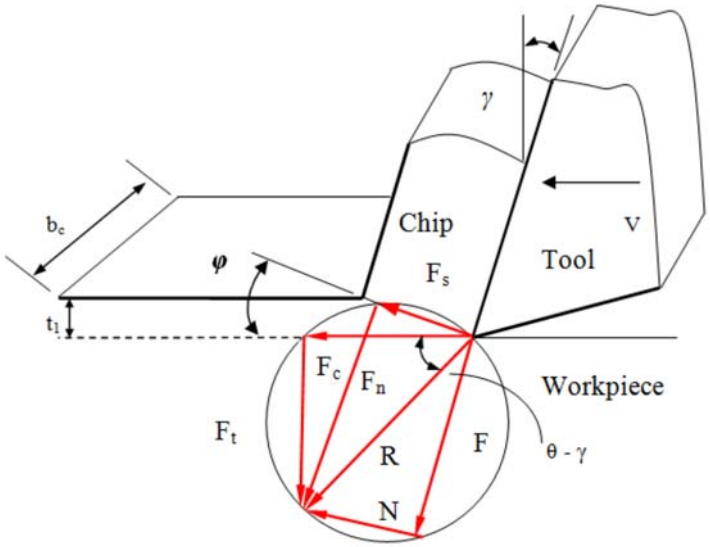

Figure 3.2: Single shear plane model as calculated by Merchant

F and *N* are the forces along and perpendicular to the rake face, *R* represents the sum of the normal and forces shear, F_c is the cutting force, F_t is the trust force, F_n is the normal force and F_s is the shearing force. Merchant calculated the shearing force as Equation 3.1:

$$F_s = \frac{\tau_y A_c}{sin\varphi} \tag{3.1}$$

where, A_c is chip cross-sectional area, A_c = t_1 . b_c and τ_y represents the shear strength of the work material. It was assumed that the flow shear stress not governed by normal stress on the shear plane.

$$F_c = \frac{F_s \cos(\theta-\gamma)}{\cos(\varphi+\theta-\gamma)} \quad (3.2)$$

The combination of the Equation 3.1 and 3.2 can be written as Equation 3.3:

$$F_c = \frac{\tau_y A_c \cos(\theta-\gamma)}{sin\varphi \cos(\varphi+\theta-\gamma)} \quad (3.3)$$

The total heat generation during the turning operations can be expressed by the following Equation 3.4:

$$P_{total} = F_c \, . \, V_c \quad (3.4)$$

where, V_C is the cutting velocity. Research groups like, Davim et al. [208], Abhang and Hameedullah [209] and etc. employed the Equation 3.4 for calculation of the cutting power. Koenigsberger and Sabberwal [210] conducted research on the variations of the chip section and the cutting force. Based on the forces measured, the authors developed mechanistic models for forces to chip area. The model developed by Waldorf et al. [211] was able to predict the total force for cutting with large edge radii and small uncut chip thicknesses. Ehmann et al. [212] summarised the modelling of the metal cutting process. The authors evaluated four modelling approaches (a) analytical modelling methods (b) experimental approaches (c) mechanistic modelling methods and (d) numerical modelling methods. Their study of dynamic cutting has emphasised on the modelling of the dynamic cutting forces.

Based on the research of Koenigsberger and Sabberwal [210], Waldorf et al. [211] and Ehmann et al. [212], Coelho et al. [213] concluded that the first models that proposed a direct relation between forces and the chip cross sectional area can be expressed by the Equation 3.5:

$$F_c = K_s \, . \, A_c \quad (3.5)$$

where, K_s is the specific cutting force. Davim et al. [208] employed the Equation 3.5 for calculation of the cutting force and explained that the value of K_s depends on the work materials. Specific cutting force can be obtained by dividing the cutting force with the cutting area [214]. It can be found machining handbook data or tool manufacturers data [215]. It is noteworthy that the value of specific cutting force is selected based on the tensile strength and hardness of the material. The reason for this selection is that the amount of heat generation during machining of a material with the same designation, for example AISI 4140, would differ significantly based on the heat

treatment process of the material. In addition, the value of specific cutting force is also selected based on feed rates which ensure that the depth of cut and feed rates do not the same effect on the cutting force.

In a machining process, several parameters can contribute the heat generation and thus influence the requirement of cutting fluid amount for the tool cooling. Silva and Wallbank [91] concluded that the cutting zone temperature depends on the metal cutting parameters and emphasised that the following parameters should be considered for the heat related calculation: (a) the depth of cut, (b) the feed rate, (c) the cutting speed and (d) material properties for the workpiece, tool insert and cutting fluid. Therefore, for the proposed methodology, the input parameters for the generation are: tool material propertied, work material properties, depth of the cut, feed rate and machining speed. Among these cutting parameters, the most important parameters are the cutting velocity, the feed rate and the depth of cut; as the tool temperature increases with the increase of these conditions as more heat generates [91]. Sun et al. [216] found that the amount of heat generation is higher with higher feed rate and cutting speed. For the present study, one of the assumptions is that all mechanical work performed during the machining is transformed to the same quantity of heat. It is also assumed that the specific cutting energy is not effected by other parameters of the machining regime such as tool design or geometry. The effect of the edge radius is ignored as Ivester et al. [217] established that the effect of the edge radius on the tool temperatures is small and inconsistent with classical theory. In addition, any variation of cutting power or produced heat, due to the influence of cutting fluid on the friction of tool-chip interface, is assumed negligible. It is understood that cutting fluid is not able to penetrate the tool-chip interface effectively due to occurrence of high pressure. On the other hand, the application of the cutting fluid attracts some heat from the cutting zone, and this absorption of heat converts the workpiece a little rigid and counter balance the reduction of cutting force due to friction. The total heat produced P_{total} can be estimated [215] from the Equation 3.6:

$$P_{total} = K_s \,.\, d \,.\, f \,.\, V_c \tag{3.6}$$

where, d is the depth of cut, f is the feed rate and V_c is the cutting velocity. After extensive literary research, Fleischer et al. [218] concluded that the values of the heat distribution varied depending on the source used and estimated that the heat goes in

the cutting tool is 2.1-18% of the total heat, during turning operations. In Table 3.1, a summarisation of the cutting energy distribution is presented.

Table 3.1: The Cutting Energy Distribution [218]

	Drilling	Turning	Milling
Tool	5-15 %	2.1-18 %	5.3-10 %
Workpiece	10-35 %	1.1-20 %	1.3-25 %
Chip	55-75 %	74.6-96.3 %	65-74.6%

Shaw [219] calculated that the dissipation of heat during cutting is approximately 5% to tool, 5% to work and 90% to the chips. More precisely, Fleischer et al. [218] identified that the Vieregge heat distribution model is the most standard model and this model concluded that 3.3% of the total heat passes in the cutting tool insert. In this conjugate heat transfer approach, a heat source is assigned on the tool due the heat generation for metal cutting based on this heat partition model. To justify the heat partition model, other partition values were assigned in the methodology, but the validation process has shown acceptable results for this heat partition model. The heat distribution during the machining operation is shown in Figure 3.3.

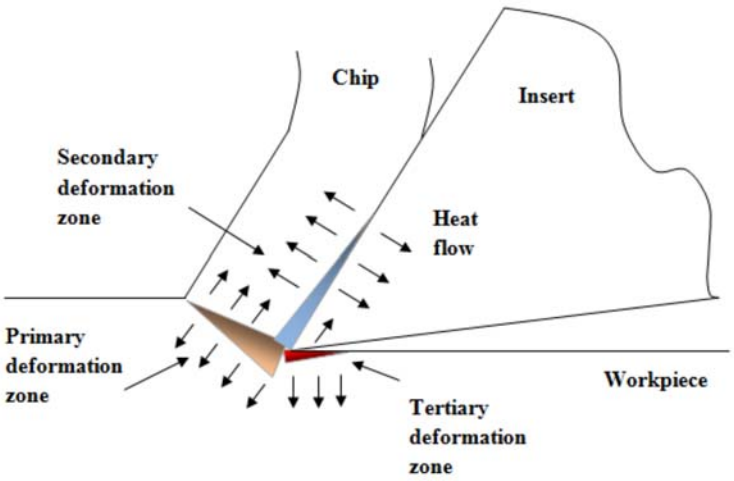

Figure 3.3: Heat distribution in the cutting zone during turning operations, adopted from [114]

Cutting fluid removes the heat from the tool by forced convection during turning operations. The heat transfer process for cutting fluid was analysed by conjugate heat transfer. A computational fluid dynamics based conjugate heat transfer analysis was conducted for the cutting tool in the present study. Conjugate Heat Transfer is

applicable for two adjacent domains and the heat transfer between these domains can be analysed. Conduction of heat through the cutting tool is combined with convective heat transfer of the cutting fluid in this conjugate heat transfer analysis. A point heat source was assign on the cutting tool. Heat conduction at the surface in the selected direction is equal to the heat convection at the surface in the same direction.

3.4 Model development

The next step of the proposed methodology is the model development process ② which include geometrical representation of the metal cutting process and mesh development. At first, the geometrical representation of the turning operation was developed by ANSYS Design Modeler®. Subsequently, the mesh was employed for the domains by the ANSYS® Meshing technology. Meshing is the process to decompose the domain into number of locations for the analysis. The basic building-blocks for a 3D mesh are shown in Figure 3.4 which are (a) Tetrahedron, (b) Hexahedron, (c) Prism and (d) Pyramid.

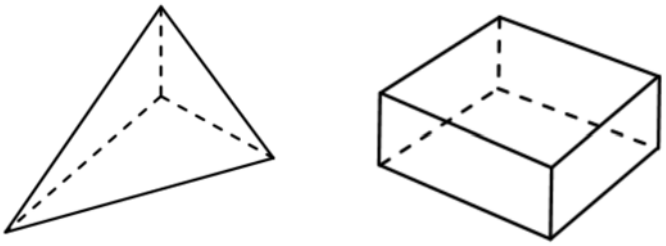

(a) Tetrahedrons (b) Hexahedrons

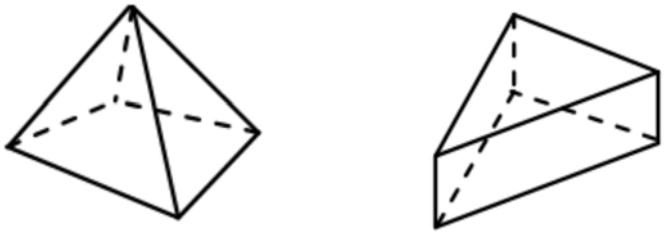

(c) Pyramids (d) Prisms

Figure 3.4: The basic building-blocks for a 3D mesh

Tetrahedrons are usually unstructured. On the other hand, hexahedrons are usually structured. Prisms formed when a tetrahedron mesh is extruded. Pyramids formed where tetrahedron and hexahedron cells are meet [203]. The number of elements and nodes for the domains are presented in Table 3.2.

Table 3.2.: The Number of Elements and Nodes for the Domains

Domain	Number of elements (Appx.)	Number of nodes (Appx)
Fluid domain	192000	36000
Workpiece domain	192000	32000
Tool holder domain	6000	1200
Tool insert domain	14000	3000

Total number of elements is more than 800 thousands and the number of nodes is more than 180 thousands. The employed mesh on the fluid domain for numerical analysis is depicted in Figure 3.5.

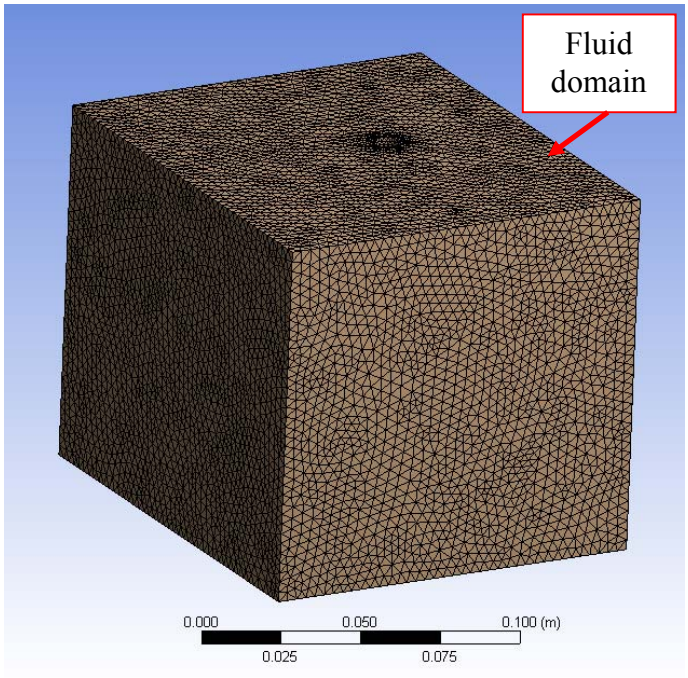

Figure 3.5: Employed mesh on the fluid domain for numerical analysis

The number of elements of the mesh was kept reasonably high to achieve acceptable output from the simulations. It is worth pointing out that the success of the simulation process greatly depends on mesh generation. When the number of nodes or the number of elements of the model is less, the achieved accuracy from the numerical study is less as well. Figure 3.6 illustrates the mesh wireframe view of all the domains. The fluid domain is located inside the en-closer along with the workpiece, tool holder and tool insert. Therefore, there are interfaces between the fluid and solid domains. The nodes of the fluid domain and the solid domains are connected. Heat can be

transferred between these fluid- solid interfaces if there is a temperature difference. The employed mesh for workpiece, tool insert and tool holder for the analysis is depicted in Figure 3.7.

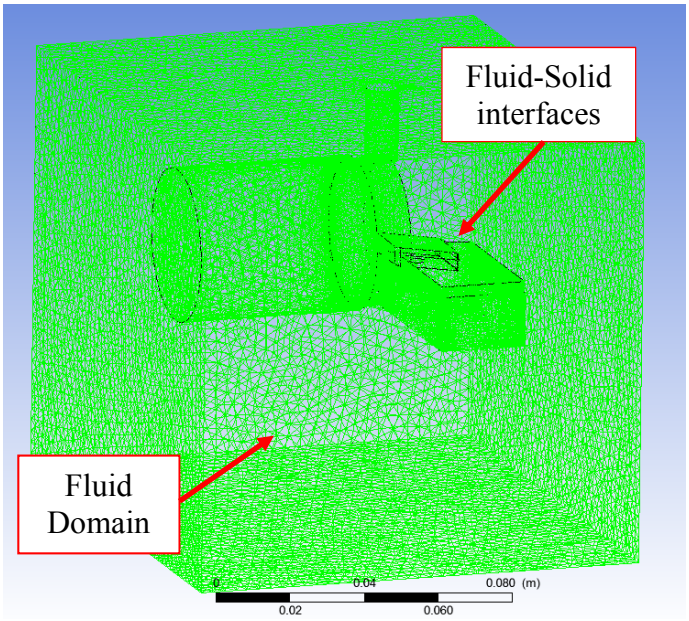

Figure 3.6: Mesh wireframe view showing all the domains

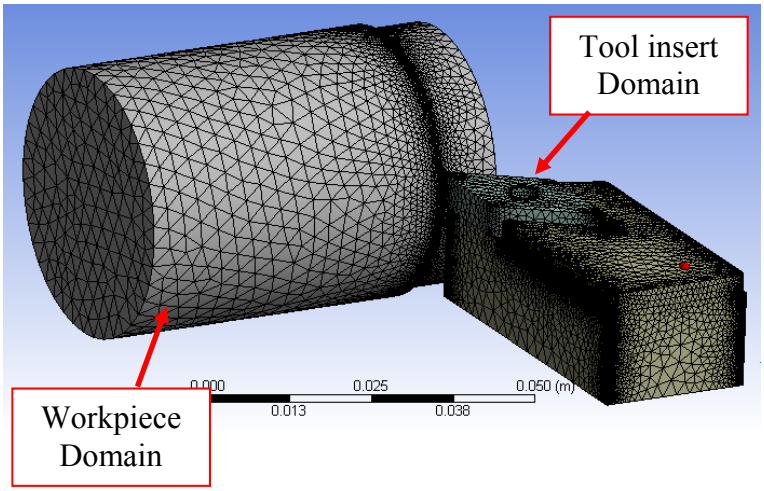

Figure 3.7: Employed mesh on tool insert, tool holder and workpiece domain for numerical analysis

If the number of elements is too high the simulation takes unrealistically long time for a desktop computer. A balance is required between accuracy and the run time. Therefore, coarse mesh was generated at initial stage and the mesh was refined by increasing the number of mesh at the later stage. Figure 3.8 illustrates the mesh wireframe view of tool insert, tool holder and workpiece domains.

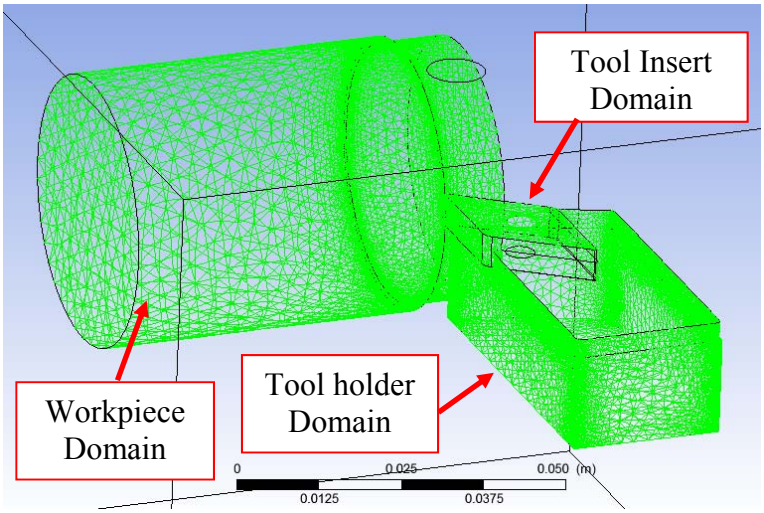

Figure 3.8: Mesh wireframe view showing tool insert, tool holder and workpiece domains

If the quality of the mesh elements is not good, the results from the analysis will not be good as well. Even, the analysis may be unable to provide a result if the quality is too low. The mesh elements can become distorted if geometric is too complex. Distortions of an element compared to its ideal shape are shown in Figure 3.9, where the ideal shape of the element is shown in Figure 3.9a; and distorted shapes are shown in Figure 3.9b and Figure 3.9c. Mesh metrics indicate the quality of the mesh.

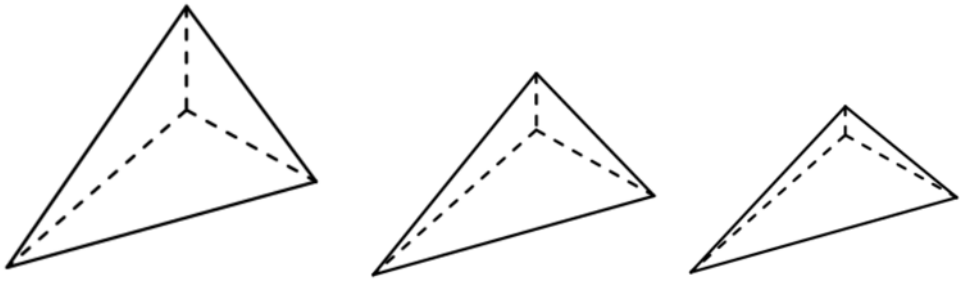

(a) (b) (c)

Figure 3.9: Distortions of an element against the ideal shape, obtained [203]

Skewness is one of the metrics for measuring the quality of the mesh. The skewness is relative measure of an element against the ideal shape. The skewness measured from 0.0 to 1.0, where 0.0 indicates excellent quality and 1.0 indicates unacceptable quality. In the proposed model the skewness is 0.24, which is in the range of Excellent. Table 3.3 represents the mesh metrics of skewness.

Table 3.3: Mesh Metrics – Skewness [203]

Cell quality	Inacceptable	Bad	Acceptable	Good	Very good	Excellent
Skewness	0.98-1.00	0.95-0.98	0.80-0.95	0.50-0.80	0.25-0.50	0-0.25

The boundary conditions are crucial for the numerical analysis. The boundary and domain conditions applied for the model are presented in Table 3.4. Figure 3.10 shows the inlet, outlet and symmetry boundary conditions of the model. The fluid-solid interfaces for the numerical analysis is presented in Figure 3.11.

Table 3.4: Boundary Conditions applied for the Model

Boundary / Domain	Status /Condition
Inlet Boundary	Velocity (Temperature 25°C)
Outlet Boundary	Pressure outlet (1 atm)
Workpiece domain	Rotating (Temperature 25°C)
Tool Insert domain	Stationary (Temperature 25°C)

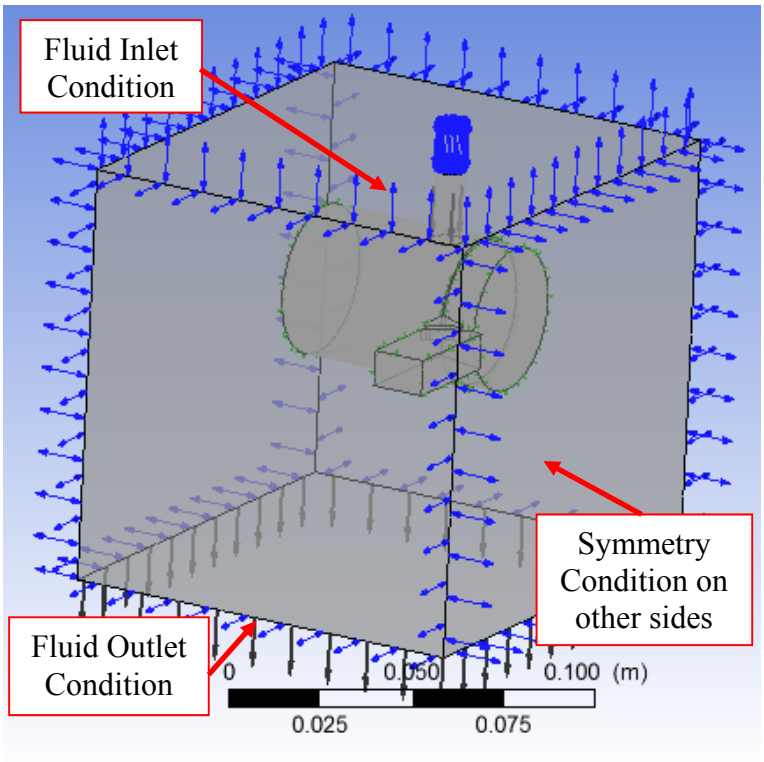

Figure 3.10: Illustration of the inlet, outlet and symmetry boundary conditions

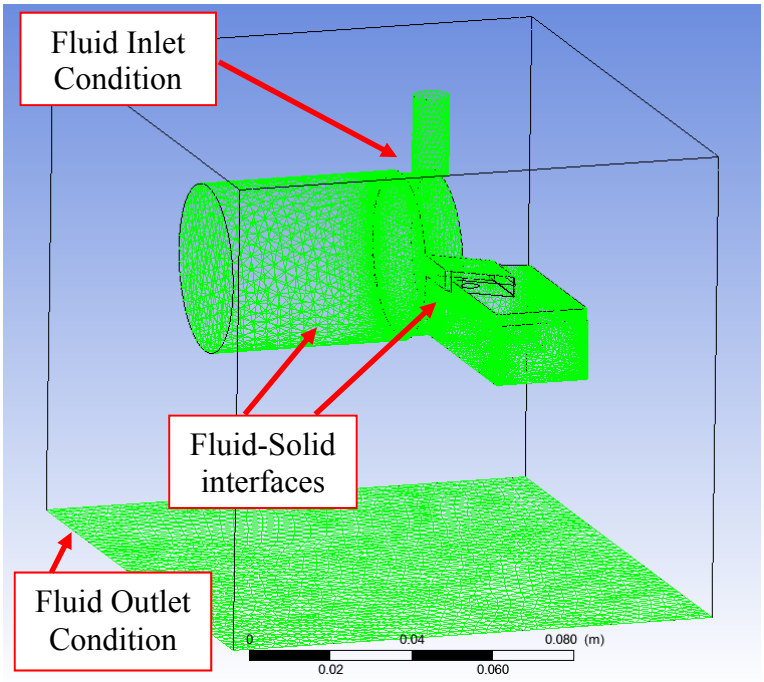

Figure 3.11: The fluid-solid interfaces for the numerical analysis

3.5 Cooling Input

The physical and chemical properties of the cutting fluids were defined and the initial boundary conditions such as the velocity and temperature of the cutting fluid were declared ③. The initial temperature for the simulation was considered 25ºC. The properties of the cutting fluid used and cutting tool for the analysis are presented in Table 3.5 and Table 3.6.

Table 3.5: Properties of the Cutting Fluid used for the analysis [44]

Soluble Oil Properties 10% Chrysan C225	Value
Dynamic Viscosity	1061 x 10^{-6} N s /m^2
Density	981 kg/m^3
Specific heat capacity	4006 J/kg K
Thermal Conductivity	0.2 W/m/K
Molar Mass	18.02 kg/ kmol
Temperature	25ºC

Carbides are able to operate under high temperature and pressure. Therefore, carbide are used in manufacturing of tool materials. Tungsten Carbide is very hard and wear resistance [220]. It is very refractory compound as its melting point is above 2800^{o}C [221].

Table 3.6: Properties of the Tungsten Carbide used for the analysis [222, 223]

Tungsten Carbide Properties	Value
Molar Mass	195.851 kg/ kmol
Density	15800 kg/m^3
Specific heat capacity	210.0 J/kg K
Thermal Conductivity	84.02 W/m/K

The simulation was achieved by applying the Computational Fluid Dynamics software package ANSYS CFX®, which is special for fluid dynamics study [203]. In general, the basic steps for computational fluid dynamics based simulation are: (a) Pre-processing (b) processing or calculation and (c) Post-processing i.e. visualisation of the results. The Pre-processing has some steps as well: (i) geometry creation (ii) mesh employment (iii) equations defining (iv) boundary condition declaration etc. [224].

3.5.1 Governing Equations

The mass of a fluid is conserved. The derivation of the Navier–Stokes equations starts through the use of Newton's second law. The Newton's second law, which is known as conservation of momentum, established that the momentum changing rate is equals to the total forces of fluid particle. The general form of Navier–Stokes equations can be written as following[225]:

$$\rho\left(\frac{\partial \mathrm{v}}{\partial t} + \mathrm{v}.\nabla \mathrm{v}\right) = -\nabla p + \nabla.\mathrm{T} + \mathrm{f}. \qquad (3.7)$$

where, flow velocity is v, ρ represents the density of fluid, p represents pressure, T represents total stress, f is force and ∇ represents operator. Similarly, the Navier–Stokes equations for incompressible flow:

$$\rho\left(\frac{\partial \mathrm{v}}{\partial t} + \mathrm{v}.\nabla \mathrm{v}\right) = -\nabla p + \mu\boldsymbol{\nabla}^2\mathrm{v} + \mathrm{f}. \qquad (3.8)$$

The vector equation can be written explicitly as V = (u, v, w):

$$\rho\left(\frac{\partial u}{\partial t}+\ u\frac{\partial u}{\partial x}+v\frac{\partial u}{\partial y}+w\frac{\partial u}{\partial z}\right)=\rho\,\mathcal{G}x-\frac{\partial p}{\partial x}+\mu(\frac{\partial^2 u}{\partial x^2}+\frac{\partial^2 u}{\partial y^2}+\frac{\partial^2 u}{\partial z^2})$$

$$\rho\left(\frac{\partial v}{\partial t}+\ u\frac{\partial v}{\partial x}+v\frac{\partial v}{\partial y}+w\frac{\partial v}{\partial z}\right)=\rho\,\mathcal{G}y-\frac{\partial p}{\partial y}+\mu(\frac{\partial^2 v}{\partial x^2}+\frac{\partial^2 v}{\partial y^2}+\frac{\partial^2 v}{\partial z^2}) \quad (3.9)$$

$$\rho\left(\frac{\partial w}{\partial t}+\ u\frac{\partial w}{\partial x}+v\frac{\partial w}{\partial y}+w\frac{\partial w}{\partial z}\right)=\rho\,\mathcal{G}x-\frac{\partial p}{\partial x}+\mu(\frac{\partial^2 w}{\partial x^2}+\frac{\partial^2 w}{\partial y^2}+\frac{\partial^2 w}{\partial z^2})$$

The continuity equation can be written as:

$$\left(\frac{\partial \rho}{\partial t}+\ \frac{\partial(\rho u)}{\partial x}+\frac{\partial(\rho v)}{\partial y}+\frac{\partial(\rho w)}{\partial z}\right)=0 \quad (3.10)$$

Similarly, the continuity equation can be written as following if the flow is incompressible and ρ is unchanged:

$$\frac{\partial u}{\partial x}+\frac{\partial v}{\partial y}+\frac{\partial w}{\partial z}=0 \quad (3.11)$$

The basic form of the energy equation can be written as following:

$$u\frac{\partial T}{\partial x}+\ v\frac{\partial T}{\partial y}=K(\frac{\partial^2 T}{\partial x^2}+\frac{\partial^2 T}{\partial y^2}) \quad (3.12)$$

where, *K* is the thermal conductivity. The ANSYS® CFX software is based on these equations.

3.5.2 Turbulence Modelling

In the present study, a compressible turbulence analysis of the cutting fluid was conducted using a finite volume method for turning operations. In turbulent flow, the fluid properties change chaotically. The pressure and velocity of fluid change rapidly in space and time. It is likely that the reason for the turbulence is inertia. Many researchers conducted research on turbulence modelling. As a result, there are several turbulence models available in the literature. The popular turbulence models were categorised by Zhai et al. [226] which are presented in Figure 3.12.

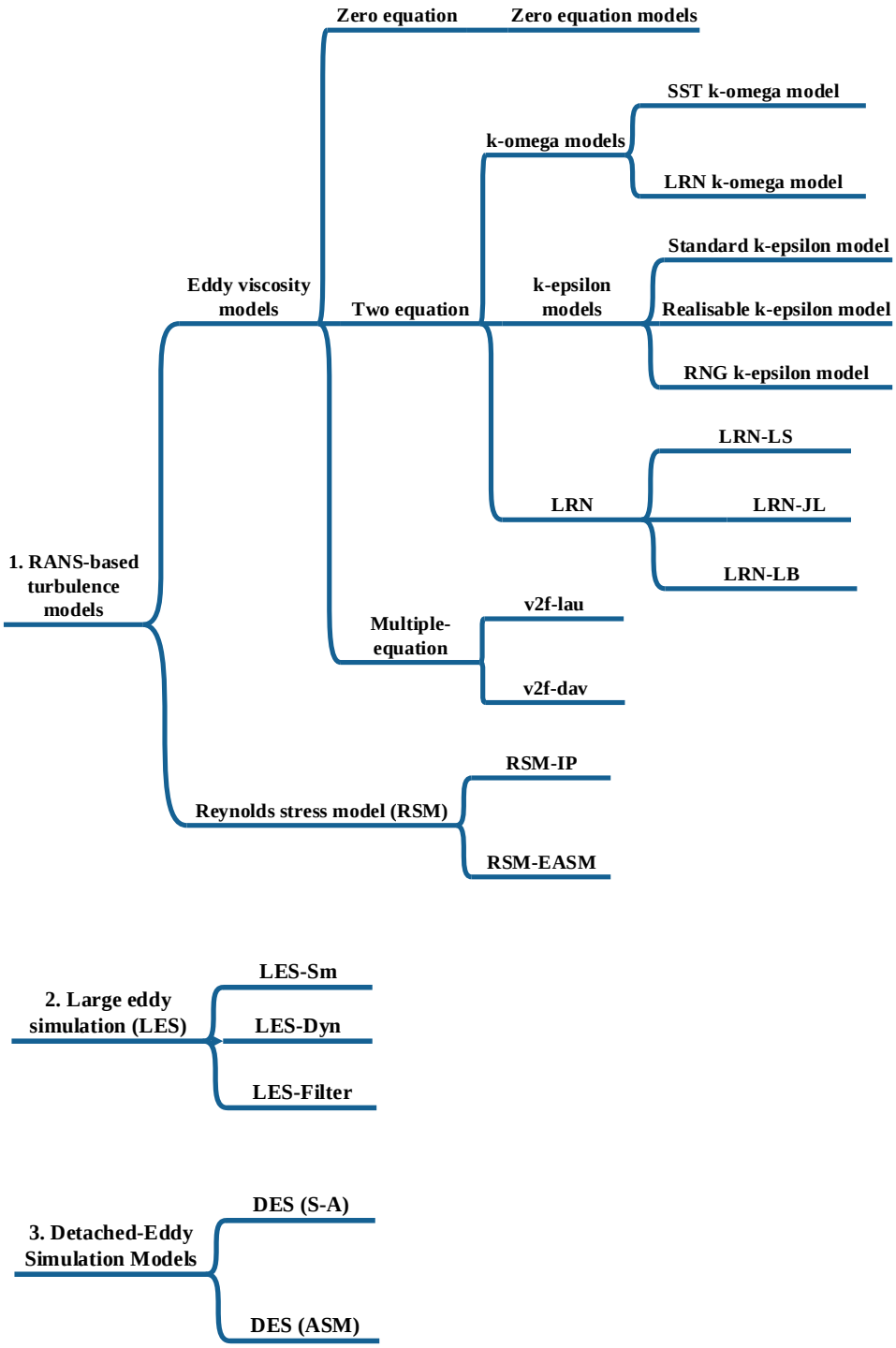

Figure 3.12: Category of the turbulence models, adopted from [226]

Reynolds number (Re) is a dimensionless number is used to predict the pattern of the flow. For the laminar flow the Reynolds number is low. On the other hand, for the turbulence flow the Reynolds number is high. For turbulence flow modelling, time-averaged equations, for example, the Reynolds-averaged Navier-Stokes equations

(RANS) are used with other models like the Spalart-Allmaras, k-ω (k-omega), k-ε (k-epsilon), Shear Stress Transport (SST) models etc.

A single model is unable to reliably ANSYS® predict all practical turbulent flows with sufficient accuracy. The standard k-epsilon model was selected for the simulation. The nominal turbulence intensities range is from 1% to 5%. The default turbulence intensity value in the CFX® is 3.7% which can be used if the experimental value is unknown. If the turbulence is generated due to wall friction, the upstream domain should be extended to allow the flow to develop completely.

3.5.3 Robust Simulation

Designing a robust simulation is another challenge. The following recommendations are helpful for achieving the robust simulation as emphasised by ANSYS® [203]:

- The most robust simulation can be achieved by considering the velocity or mass flow at the inlet; and considering static pressure at the outlet, if the number of inlet is one and outlet is also one. The analysis will generate inlet total pressure as a part of the solution.
- Robust simulation can be also achieved by considering total pressure at the inlet and velocity or mass flow at the outlet, if the number of inlet is one and outlet is also one. The analysis will generate inlet velocity as a part of the solution. In a similar situation, the simulation will not be robust and be sensitive to initial assumptions by considering total pressure at inlet boundary and static pressure at outlet boundary. The analysis will generate mass flow as a part of the solution.
- Very unreliable simulation will be produced by considering static pressure both at inlet and outlet boundaries. The combination of this boundary condition is very weak as the inlet total pressure and the mass flow both will be generated by the simulation.
- In an open system, at least one boundary should be specified as pressure (either total or static). The simulation will be unstable if the total pressure is set at an outlet. Generally, the static pressure is considered as zero for the outlets that vent to the atmosphere.

3.6 Computational Fluid Dynamics Analysis

The next step of the methodology is the computational fluid dynamics analysis ④. The computational fluid dynamics based packages, for example ANSYS CFX®, usually have the following parts: (1) Pre-processor, (2) Solver and (3) Post processor. ANSYS CFX® is gaining popularity for solving a wide range of fluid flow problems. The steps used for the computational fluid dynamics analysis is depicted in Figure 3.13.

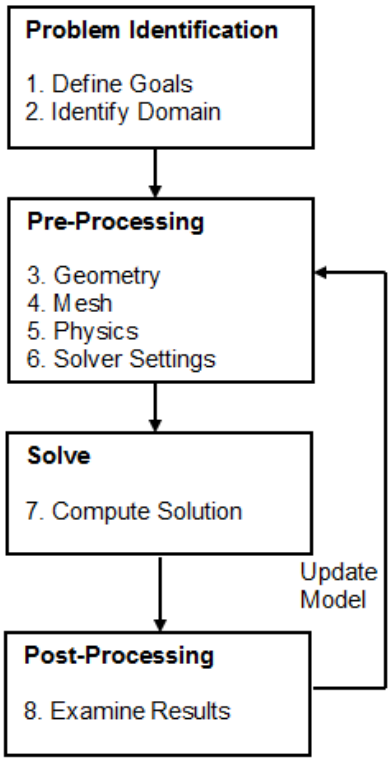

Figure 3.13: Steps for computational fluid dynamics based analysis, adopted from [203]

The flow direction as well as distance between the nozzle and the tool are considered for the analysis. The direction of the flow was perpendicular to the rake surface of the tool insert and the nozzle diameter was 9 mm. There are parameters related to nozzle which can influence the effectiveness of the cooling process. The parameters that influence the cooling process are: (a) distance between the nozzle tip and the tool surface (b) the angle by which the nozzle is inclined (c) the location of the nozzle i.e. top or side. In the present analysis, the workpiece is rotating and the turbulence intensity is considered as 5%.

First the domains and subdomains of the methodology were declared in the ANSYS® pre-processor. Based on the heat generating parameters, the calculated heat on the tool interface was applied. The CFD software vendor, Ansys, has two separate CFD programs, ANSYS® CFX and ANSYS® FLUENT. The solver, used in both the CFX and FLUENT, is prepared on finite volume method [227], where discretising of the volume results a number of control volumes. The difference between the cell centered control volumes and node-centered control volumes is presented in Figure 3.14.

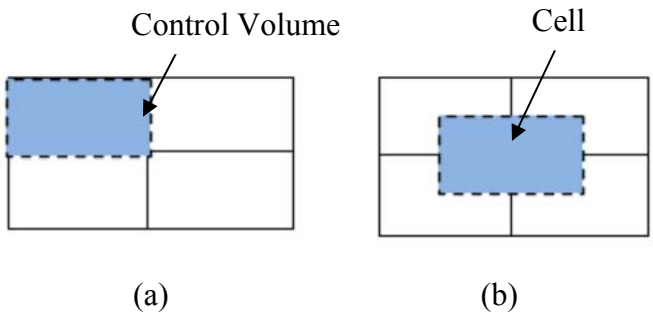

Figure 3.14: The control volumes (a) cell centered control volumes and (b) node-centered control volumes , simplified from [228]

The ANSYS CFX® allows selection of the analysis type as steady or transient state type. The steady state analysis results are added as initial values for the analysis as shown in Figure 3.15. Transient state type analysis is more appropriate for unsteady heat transfer. The convergence of steady state analysis can be achieved easily as steady state analysis ignores many higher order terms dealing with time. Therefore, one of the advantages of the steady state analysis is that less cost is associated with this analysis. In addition, generated results from the steady state analysis can be used for the initialisation of the transient analysis as initialisation plays an important part for the numerical analysis. In the present analysis, steady state analysis type was selected for first 100 iterations. The generated results from the steady state analysis were used as initialisation data for the transient analysis. In the Solver, the convergence criteria i.e. residual type and target were selected so that the simulation could finish at an expected point.

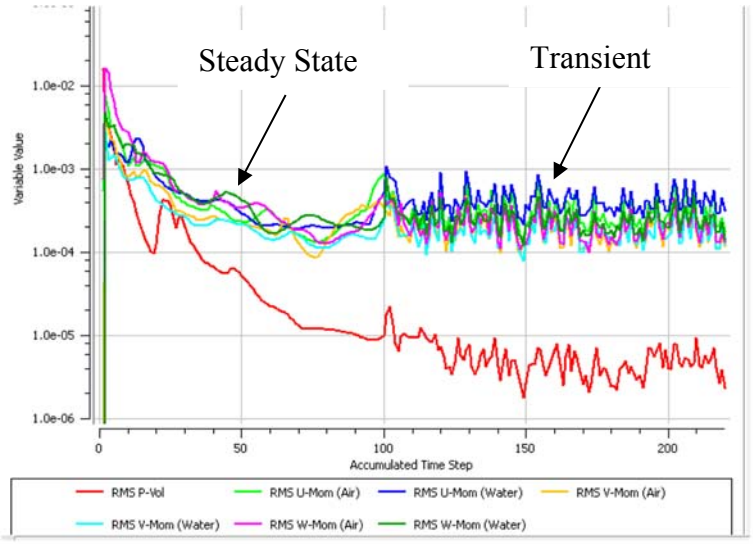

Figure 3.15: Steady state analysis up to 100 time steps and transient analysis from 101 time step to rest

The development of fast computers are allowing the researchers to contribute advance knowledge to the science [229]. ANSYS CFX® Solver Manager allows executing the analysis in local parallel and distributed parallel platform. Subject to availability, the other option is to run in High Performance Computers i.e. Supercomputers to save computation time. The analysis converged more rapidly if higher number of computer processors was used in the Supercomputer. The average run time for one analysis was more than 12 hours on a 4 core PC.

In modern supercomputers, the use of Linux based operating system is noticeable [230]. Therefore, the program was submitted in Linux environment to the Supercomputer. To achieve a better convergence for transient simulation, initial data from a previously run analysis was used as input in the ANSYS CFX®. The availability of required number of licences is essential for a supercomputer to run a program. The following issues were observed during the use the super computer:

- The average run time for an analysis was depended on the number of processors was allocated for the analysis. The requested number of processors can be allocated for the analysis if sufficient number of licenses is available at the time when the analysis will started.
- The number of available licenses at the run time is depended on the number of licenses not already allocated to the other running programs.

- In reality, the number of purchased licenses is limited. The actual number of available licenses at the run time is unknown because the start time of the run is unknown as super computers use batch scheduling method to run the programs. A program will run if the requested number of licences are available.
- Theoretically, if there is no bottleneck in the program and the number processes is doubled to run a program in the super computer, the run time should reduce to half.
- It is anticipated that the run time will be less in super computer compared to a desktop computer as the processors are better in a super computer. For example, a program will take less than six hours in super computer using eight processors instead of taking 12 hours using four processors in a desktop computer.

After the completion of the computation, post processor was used for the visualisation which allows displaying vectors, plots and animation for dynamic result display of the analysis. Figure 3.16 depicts the simulation of the flood cooling process during a turning machining operations. Figure 3.17 depicts the streamlines of the cutting fluid flow during machining in turning metal cutting operations.

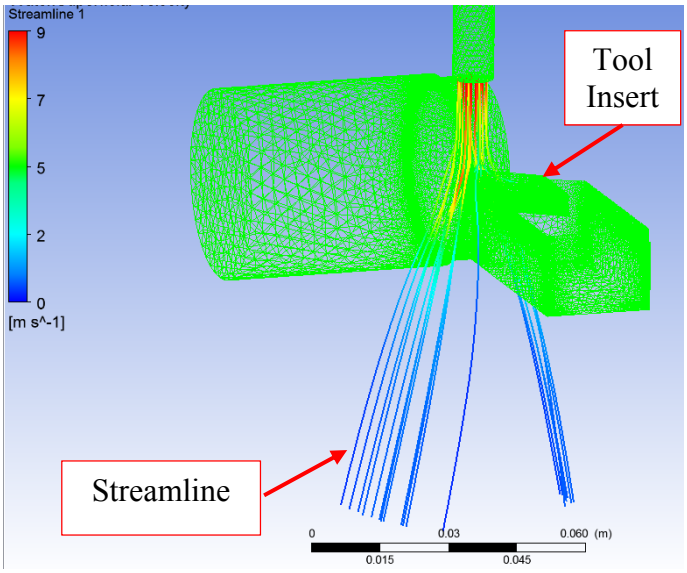

Figure 3.16: Mesh view simulation of the cutting fluid flow during machining

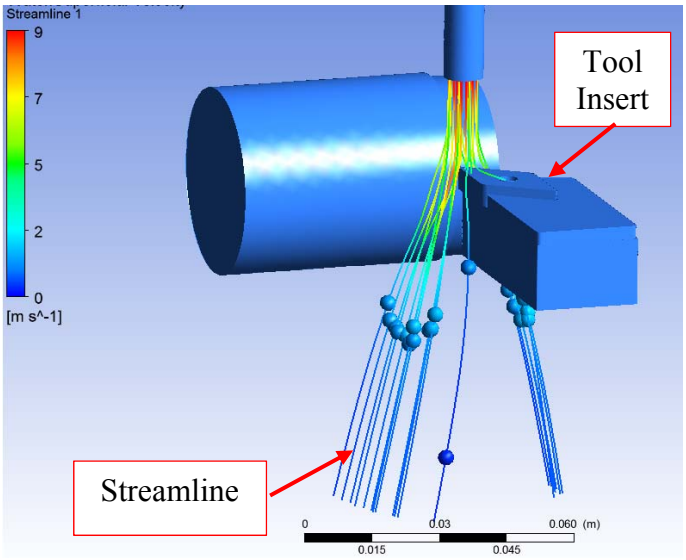

(b)

Figure 3.17: Streamlines of the cutting fluid flow during machining

3.6.1 Tool Temperature Distributions

The tool temperature distributions during the cooling process were analysed after the numerical experiments. The analysis was conducted under dry and flood conditions. The numerical experiments were performed according to the parameters of Table 3.7.

Table 3.7: Cutting Parameters for the Numerical Experiments

Parameters	Condition 1	Condition 2
Feed Rate, *f* (mm/rev)	0.11	0.33
Cutting Velocity, V_c (m/min)	87	87
Depth of Cut, *d* (mm)	1.0	1.0
Coolant Flow Rate, C_F (l/min)	Dry and 1.0	Dry and 1.5
Workpiece Material	AISI4140	AISI4140
Tool Insert Material	Tungsten Carbide	Tungsten Carbide

The generated heat due to the turning operation transmits to the tool holder from the tool insert and increase the tool holder temperature. The proposed methodology is capable of reflecting the temperature increase in the tool insert and holder as well. The surface temperature distributions of the tool insert and the tool holder obtained by numerical analysis are shown in Figure 3.18 according to the Condition 1 of Table 3.7

under dry condition. Figure 3.18a shows the tool holder and tool insert under the same temperature contours. On the other hand, Figure 3.18b shows the temperature contours of the tool holder only. To distinguish the contours, local temperature contours are shown in this figure.

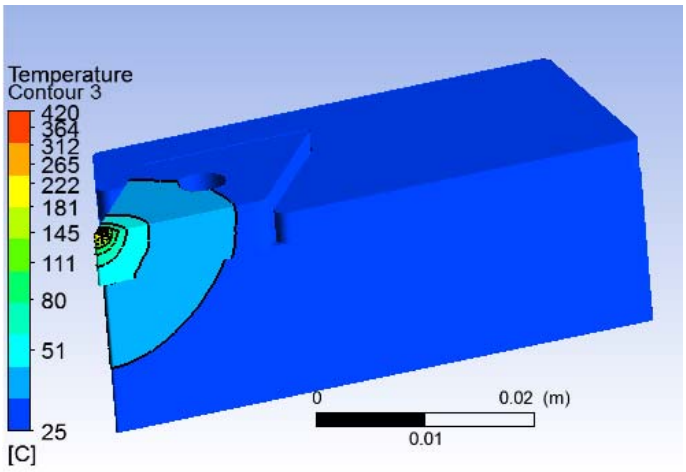

(a)

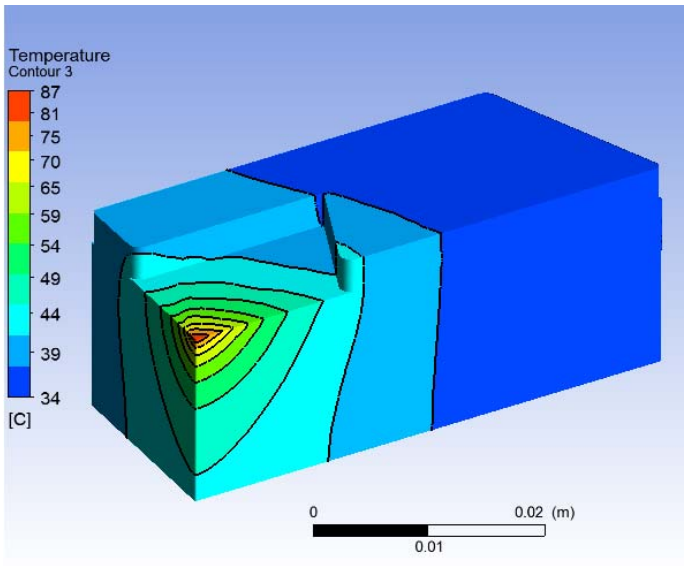

(b)

Cutting Parameters are according to the Condition 1 of Table 3.7

Figure 3.18: Numerically obtained temperature distribution under dry condition (a) temperature distribution (global) of the tool holder and tool insert and (b) temperature distribution (local) of the tool holder only

Figure 3.19a shows a close view of the tool holder and tool insert under the same temperature contours. On the other hand, Figure 3.19b shows the temperature contours of the tool only. The temperature contours shown in Figure 3.19a and Figure 3.19b are according to the Condition 1 of Table 3.7 under dry condition.

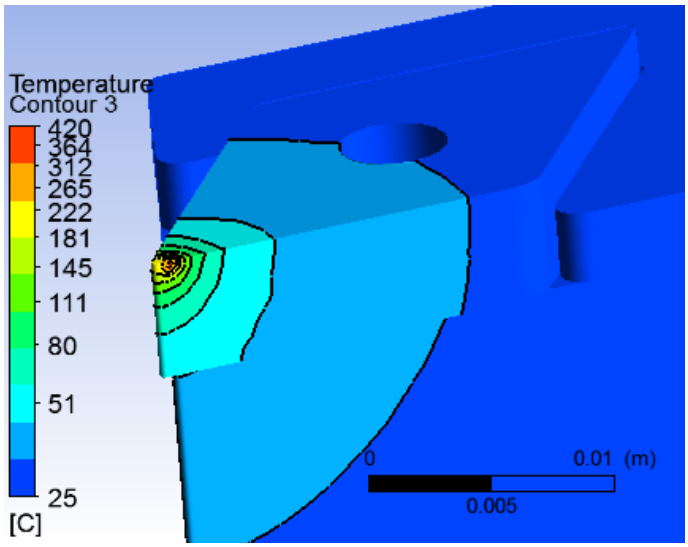

(a)

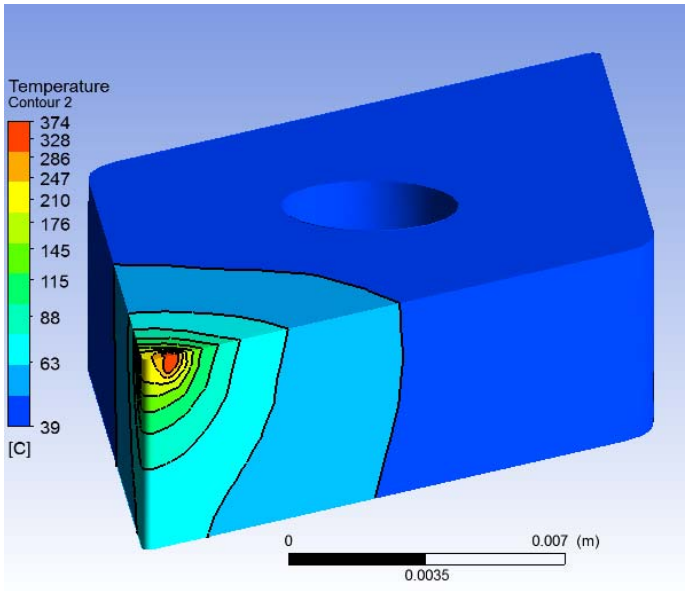

(b)

Cutting Parameters are according to the Condition 1 of Table 3.7

Figure 3.19: Numerically obtained temperature distribution under dry condition (a) Close view of the temperature contours (global) of the tool holder and tool insert and (b) Temperature distribution (local) of the tool insert only

The tool insert surface temperature distributions are depicted in Figure 3.20 where (a) under dry condition and (b) under flood cooling condition at 1.0 l/min flow rate of the cutting fluid obtained by numerical analysis according to the Condition 1 of Table 3.7.

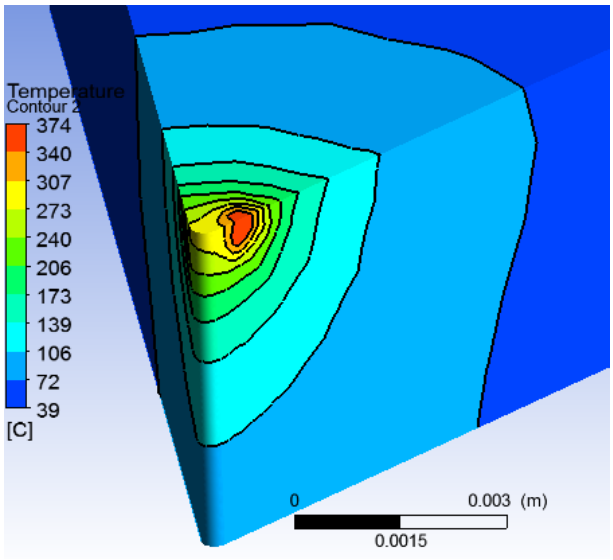

(a)

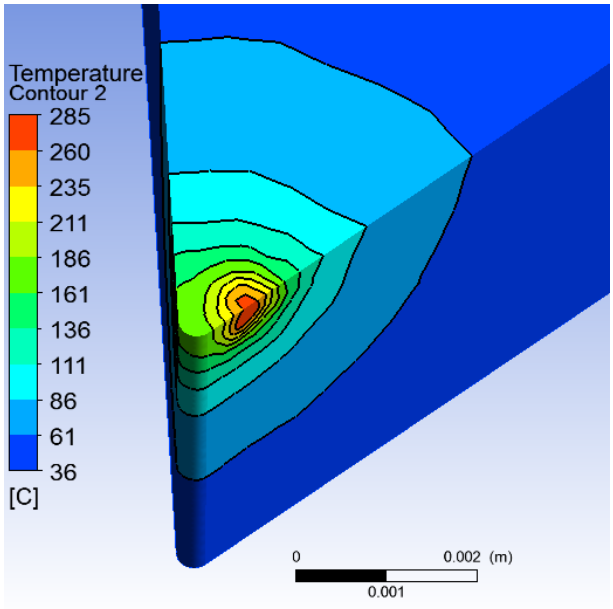

(b)

Cutting Parameters are according to the Condition 1 of Table 3.7

Figure 3.20: Tool insert surface temperature distributions obtained by numerical analysis (a) Machining under dry condition and (b) Flood machining at 1.0 l/min flow rate of the cutting fluid

The tool insert surface temperature distributions in the dry and flood machining are depicted in Figure 3.21a and Figure 3.21b according to the Condition 2 of Table 3.7. Figure 3.21a shows temperature distribution under dry condition. On the other hand, Figure 3.21b shows temperature distribution under flood cooling with 1.5 l/min flow rate of cutting fluid.

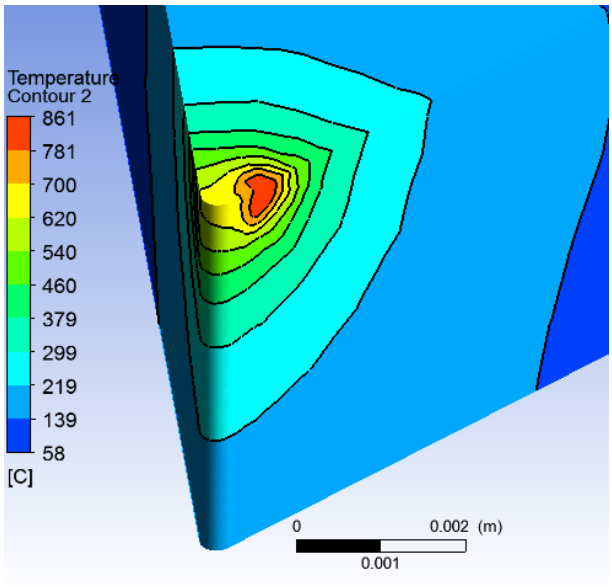

(a)

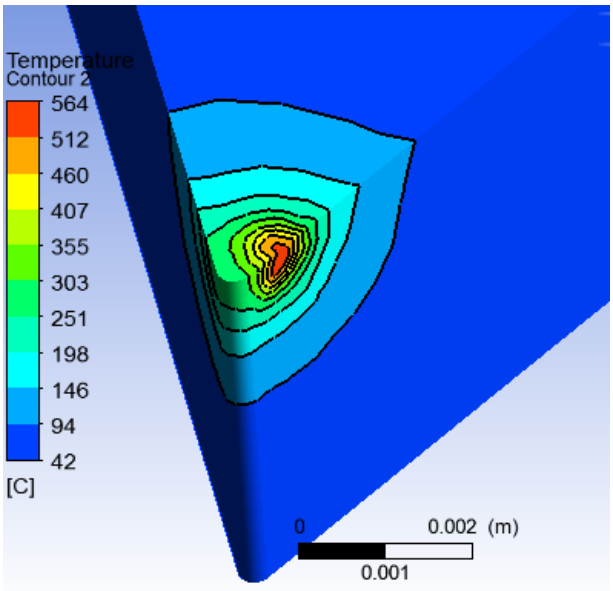

(b)

Cutting Parameters are according to the Condition 2 of Table 3.7

Figure 3.21: Tool insert surface temperature distributions obtained by numerical analysis (a) Machining under dry condition and (b) Flood machining at 1.5 l/min flow rate of the cutting fluid

3.7 Validation of the Model against data from Literature

The validation of the simulated results against experimental results are necessary to provide additional support to the numerical analysis. The developed methodology was validated ⑤ against three different experimental data sets available in the literature for comparison under a wide range of cutting conditions. Although, there is a lack of availability of the literature based on flood cooling tool temperature distribution, but for validation purpose, three experimental data sets were selected from literature. There are publications where experimental data sets from literature were used for validation of numerical results in the several cases, for example [231].

For the validation, three selected experimental data sets form literature are summarised on Table 3.8. One by one, the conditions of each experiment according to the literature were applied in the methodology to identify the accuracy of the methodology for each of the experimental conditions. By comparing the output results against the experimental data sets from the literature, percentage of deviation were calculated. The experimental conditions and percentage of deviations of the outputs are also presented in Table 3.8. The validation of the numerically obtained tool temperature against the experimentally obtained temperature from literature are presented in Figure 3.22, according to the conditions of: (a) Carvalho et al. [162], (b) Chen et al. [165] and (c) Li et al. [174].

Table 3.8: Validation of the Proposed Methodology comparing the Experimental Results from literature

		Experimental conditions		
		Carvalho et al. [162]	Chen et al. [165]	Li et al. [174]
Cutting Parameters	Cutting Velocity, V_c (m/min)	217	129	215
	Feed Rate, f (mm/rev)	0.138	0.112	0.03
	Depth of Cut, d (mm)	1.5	0.76	0.5
Workpiece material		Gray cast iron	AISI 1020	AISI 1045
Experimental and Numerical Temp Deviation (%)		4.50	-12.18	14.66

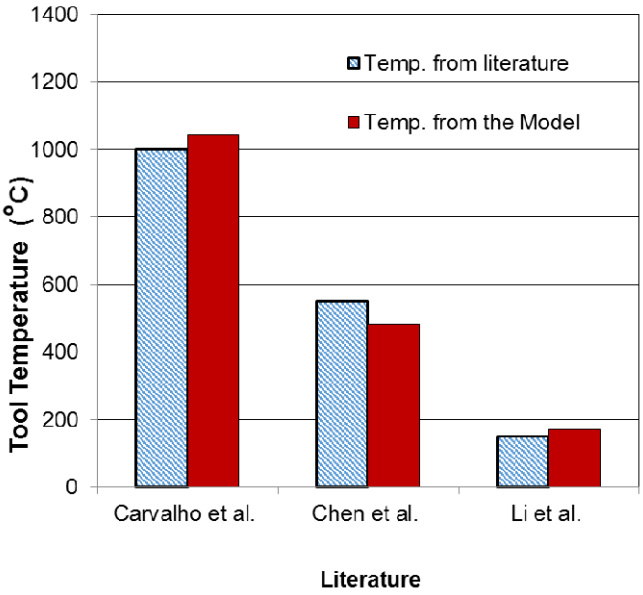

Figure 3.22: Comparisons of the tool temperatures (°C) obtained by the experimental and proposed methodology, following to the cutting conditions of: (a) Carvalho et al. [162], (b) Chen et al. [165] and (c) Li et al. [174]

The tool interface temperature distribution applying to the conditions of Carvalho et al. [162] is illustrated in Figure 3.23. Similarly, Figure 3.24 and Figure 3.25 depict the simulated tool interface temperature distributions applying to the conditions of Chen et al. [165] and Li et al. [174].

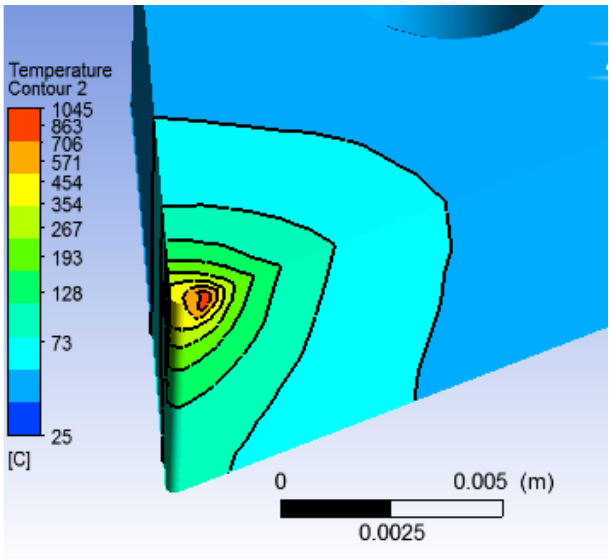

Figure 3.23: Validation of the developed model against Carvalho et al.

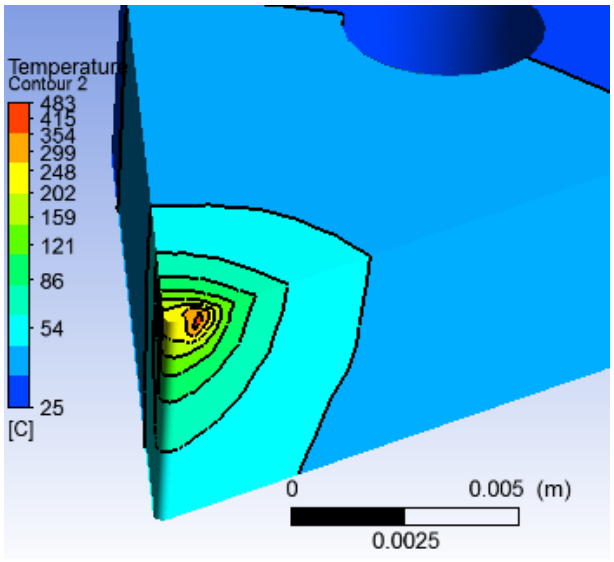

Figure 3.24: Validation of the developed model against Chen et al.

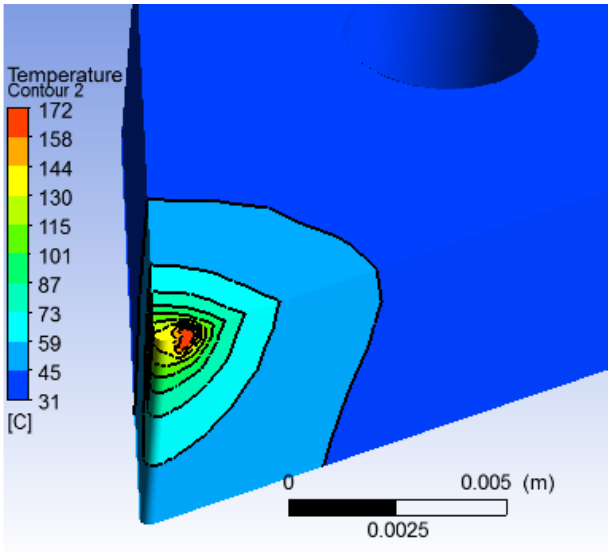

Figure 3.25: Validation of the developed model against Li et al.

Carvalho et al., [162] experimentally measured the tool temperature in turning operation of gray cast iron with tungsten carbide inserts using a tool-work thermocouple technique. The parameters were as following: feed rate was 0.138 mm/rev, the cutting speed was 217 m/min and the depth of cut was 1.5mm. The model was calibrated and validated comparing with the above experimental investigations.

The agreement obtained between the experimental data sets available in the literature and numerical results from the proposed methodology indicate that the proposed methodology is suitable for studying the cooling process of turning

operations. Wanigarathne [200] concluded that the tool-chip interface temperature increases with increasing cutting speed which is also reflected in the results of the methodology.

The proposed methodology points in the direction that it is possible to analyse the tool temperature distribution by using computational fluid dynamics based analysis. The numerical methodology presented in this chapter demonstrated that it is possible to illustration the tool cooling process for varying cutting parameters. It is anticipated that the tool temperature will be the highest for the machining without any cutting fluid. This expectation is reflected by Figure 3.21a, as the tool temperature is highest for the dry condition. The tool temperature drops with the application of cutting fluid, as shown in Figure 3.21b. Therefore, the model is capable of simulating the flood cooling process and reflecting the cutting fluid flow rate variation. It is experimentally found that the measured temperatures increased with the increase of cutting velocity and the feed rate. The temperatures predicted by the developed methodology are in line with the experiment of Wang et al. [232] as the authors found that the increases of cutting velocity and feed rate generate additional heat. These prediction of the tool temperatures are also in line with the Equation 3.6.

The results of the validation are in close range and presented graphically which were performed by comparing numerically obtained interface temperature against experimentally measured temperature taken from three sources available in the literature. It is worth pointing out that the success of the simulation process greatly depends on mesh generation. When the number of nodes or the number of elements of the model is less, then the achieved accuracy from the numerical study is less as well. On the other hand, if the number of elements is too high, the simulation takes unrealistically long computation time. A balance is required between accuracy and the run time. After the development of CFD model, solution step was initiated. The CFD solvers apply an iterative approach to compute the multiphase fluid dynamics based problems. To start the iterative solving process, initial conditions for the fluid velocity, pressure, temperature and transport properties are necessary. The selection of these initial conditions is significant for outcome of the iterative procedure. If initial conditions are selected accurately, the computational outcome would be more accurate.

3.8 Concluding Remarks

It is demonstrated that the effects of cutting fluids on the tool temperatures can be obtained by following the propose methodology for specified cutting conditions. As a result of conducting the present study, it is revealed that using computational fluid dynamics based simulation is an effective method to analyse tool temperature distributions and obtain the effect of cutting fluids on tool temperatures during machining operations. The major observations from the work are as following:

- The proposed methodology provided an alternative approach based on computational fluid dynamics for determining the effect of the cooling media on the tool temperature distributions using conjugate heat transfer process. In this approach, a heat source was assigned on the tool based on the amount of heat generated during metal cutting process. A solid-fluid interface was developed between the tool and cutting fluid by employing Ansys CFX software package. A compressible turbulence analysis of the cutting fluid was conducted using the finite volume method for turning operations.
- The proposed methodology was tested for two sets of cutting conditions. The results obtained from these tests revealed that the methodology is capable of capturing the effects of cutting conditions on the tool temperature distributions.
- The proposed methodology was also verified under dry and flood cooling conditions. The results demonstrated that the model is capable of reflecting the effect due to cutting fluid flow on the tool temperature distributions.
- The validation of the model was performed by comparing numerically obtained tool temperatures against experimentally measured temperatures taken from three sources available in the literature and the results demonstrated that the methodology fulfilled the accuracy requirement.
- The proposed methodology can be applied to identify the influence of flow rates on tool temperature distributions. This advanced multiphase computational fluid dynamics modelling techniques can be deployed to study heat transfer under different types of cooling environments including the minimum quantity lubrication techniques.

Chapter 4

Experimental Validation of the Proposed Methodology

4.1 Introduction

In numerical research, experimental validation provides an additional level confirmation. Therefore, experimental investigation procedures are necessary to compare the numerical results against the experimental findings. Previously in Chapter 3, a computational fluid dynamics based 3D model for the turning operations was developed to comprehend the effects of the cutting fluid on the tool temperature distributions. Cutting tool temperature data during machining with cutting fluid is rarely found. In this chapter, experimental validation of the proposed model is presented. The objective of this experiment is to validate the proposed methodology by obtaining the tool temperatures with embedded thermocouple. As result of the experiment, it will be possible to understand the phenomenon of the tool temperature elevation and cooling during turning operations. The experimental procedure to obtain the tool temperatures has been described in details. The comparisons of numerical and experimental tool temperatures are presented to demonstrate the effectiveness of the proposed methodology.

Various experimental procedures have been developed by the researchers to obtain the tool temperatures during metal cutting. Komanduri and Hou [233] emphasised that the appropriate technique to measure machining temperature is the one which is the most suitable for the experimental situation and easily accessible. To identify the most suitable experimental procedure, an extensive literature review was conducted to identify the available experimental methods for tool temperature measurement. The literature review revealed that the tool-work thermocouple method, embedded thermocouple method and thermal radiation method are widely used methods to measure the tool chip temperature for turning operations. In addition, the thin film thermocouples are also used by the researchers for turning temperature measurement.

Based on the literature review, it was identified that the embedded thermocouple method would be the most suitable experimental method for the flood cooling process.

Hoyne at el. [234] preferred the embedded thermocouple technique to understand the tool cooling process as it allows the measurement of cutting temperature at different locations of the tool, after employing both the embedded thermocouple and tool–work thermocouple technique for tool temperature measurement experiment. The embedded thermocouple method is widely used for the tool temperature estimation [200]. It is comprehensible from the literature review that the embedded thermocouple method is the most effective method for the tool temperature measurement with flood cooling technique if a comparison is conducted among the tool-work thermocouple, embedded thermocouple and thermographic methods. On the other hand, the infra-red pyrometers have some limitations as well, as the chips block the view to the cutting zone. In addition, dust or smoke developed during machining also prevents the view from the camera. Similarly, the strength of thin film thermocouples against the friction of the chips produced during the machining is low.

After the experiment, the results are compared with the numerical tool temperatures and presented graphically. These graphs demonstrate the validation of the proposed methodology. Finally, this chapter is concluded by presenting the significant findings.

4.2 Experimental Work

4.2.1 Machine Tool Setup

A Harrison Lathe Alpha was used for the experimental investigations which was located in the machining laboratory of the Curtin University. This machine was chosen for the experiment because of the easy of assembly of various measuring instruments. A three-phase electric power motor was attached with the lathe. This machine offers optimum combination of capacity and performance. With the advanced control and software systems, this machine is capable of providing high level of accuracy.

The schematic of the experimental setup for the tests is presented in Figure 4.1. In this experiment, the tool temperatures of the turning operations were measured by a thermocouple which was connected to computer through a data logger. The details of the machine tool used for the experimental investigation are presented in Table 4.1.

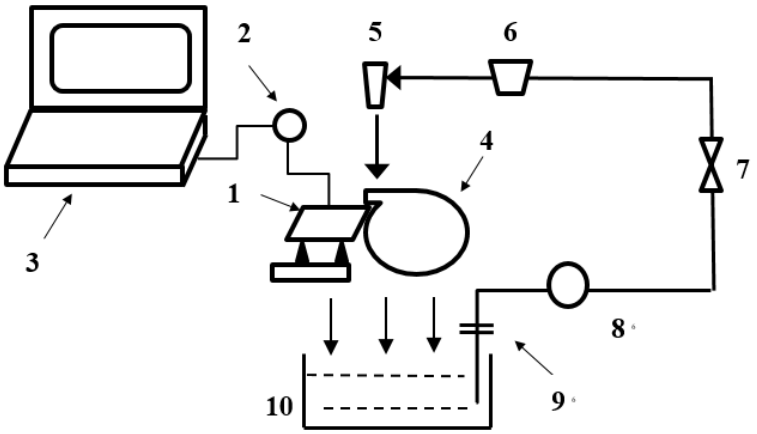

1. Tool insert, 2. Thermocouple, 3. Computer, 4. Workpiece, 5. Nozzle, 6. Flowmeter, 7. Control valve, 8. Pump, 9. Filter and 10. Coolant tank.

Figure 4.1: Schematic of experimental setup to obtain tool temperature

Table 4.1: The Specification of the Experimental Equipment

Tool	Specification
Machine tool	Harrison Lathe Alpha I400XS 600
Work specimen	
Materials	AISI 4140 Steel
Size	Cylindrical Dia. 60 X 600 mm
Cutting Tool	Carbide Turning Insert Rhombic 55
Insert	DNMG 150404 PM 4215
Chip-Breaker	PM
Coating	MTCVD
Nose radius	4 mm
Tool holder	PDJNR 2525M 15HP
Working tool geometry	Angle of inclination: -7
	Rake angle (valid with flat insert): -6
	Entering angle: 93
	clearance angle: 0

The present study involves turning of AISI4140 alloy steel as a workpiece under a set of cutting conditions. The AISI 4140 is a low-allow steel containing Cr, Mn, C and Mo. The chemical composition of AISI 4140 in percentages is presented in Table 4.2.

Table 4.2: Chemical Composition of AISI 4140 [235, 236]

Element	Percentage
Carbon	0.40
Silicon	0.23
Manganese	0.82
Chromium	0.80
Molybdenum	0.15
Iron	97.00

The machinability of the hardened and tempered AISI 4140 is easy in supplied condition. Manufacturing processes of AISI 4140 can be suitably performed. In general, during the selection of the cutting parameters the recommendation of manufacturer should be followed. A rhombic carbide tool insert was used for the experiments which is suitable for medium type application for steel workpiece material. The mounting style of this insert is “top and hole” clamping; and the insert was attached to a right handed sandvik coromant tool holder. Figure 4.2 shows that the machine tool that was used for the experimental validation.

Figure 4.2: The machine tool used for the experiment

The cutting fluid used for this experiment was Rocol Ultracut Long Life. This commercially available oil based cutting fluid was used with varying flow rates. The cutting fluid has long sump life and suitable for medium to severe cutting applications. In addition, the cutting fluid is able to provide good tool life and the cutting performance is good. The cutting fluid provides residual corrosion protection, suitable for use with most metals and foaming formation is low.

4.2.2 Measuring Instrument

In these experiments, the temperature and fluid flow rate were measured by embedded thermocouple and flow meter accordingly. The specifications of the measurement instruments used for the experimental investigation are presented in Table 4.3.

Table 4.3: The Measurement Instruments

Tool	Specifications
Thermocouple	K Type Ni Cr+ Ni Al-
	Control Unit: Pico TC 08
Parker Flow Meter	0.2–2.0 l/min

The application of thermocouples is very popular as many researchers used these temperature measuring transducers for their experiments. The tool temperatures were measured by a K-type thermocouple which was placed inside the cutting tool insert by making a hole. This type thermocouple are readily available from the vendors and can be supplied with different dimensions of diameters. Tungsten carbide is known as hard material and making a hole in a tungsten carbide tool is a challenging process. By applying the spark eroding process a narrow hole was created to place the thermocouple into the tool insert. Initiative has taken to keep the location of the hole as close as possible to the tool cutting edge. The diameter of the hole was 1.0 mm which was located 2.0 mm away from the tool tip. Only one side of the hole was open to place the thermocouple. There was a 1.0 mm thin wall at the other end of the hole to protect the thermocouple from frictional wear. It is possible to achieve high level of accuracy by the electrical discharge machine applying the spark eroding process. The thermocouple should be inserted completely inside the hole to obtain the tool temperature. A proper thermo-conductivity contact should achieved between the thermocouple and the tool for complete and uninterrupted heat flow during the

machining. The location of the hole to insert thermocouple is illustrated in Figure 4.3. The experimental set up displaying the workpiece, tool inset, holder and thermocouple is presented in Figure 4.4. Figure 4.5 illustrates the tool insert with thermocouple in the hole.

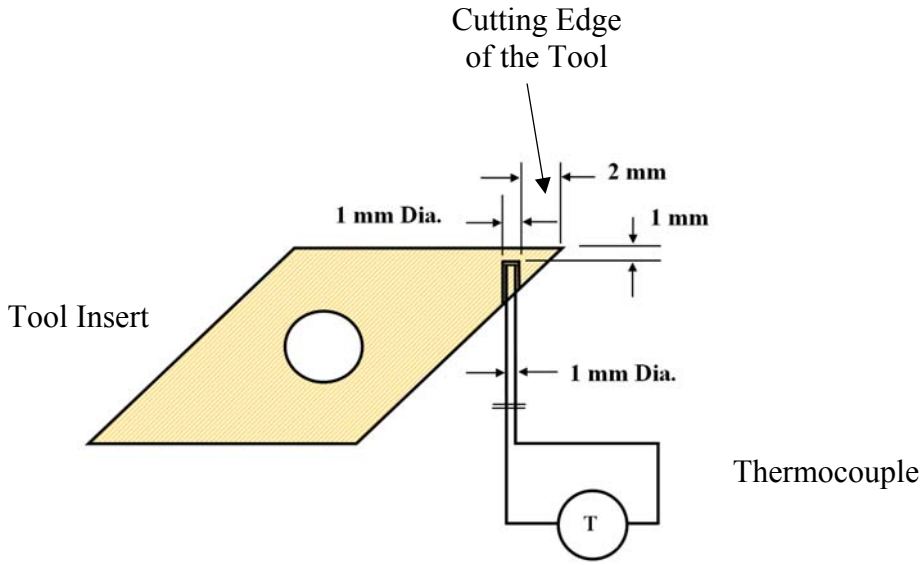

Figure 4.3: Schematic of the thermocouple embedded tool insert

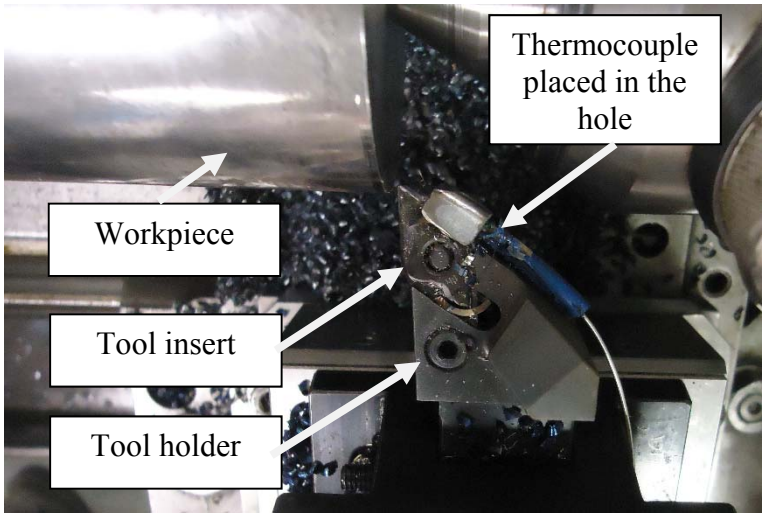

Figure 4.4: The experimental set up showing the workpiece, tool inset, holder and thermocouple

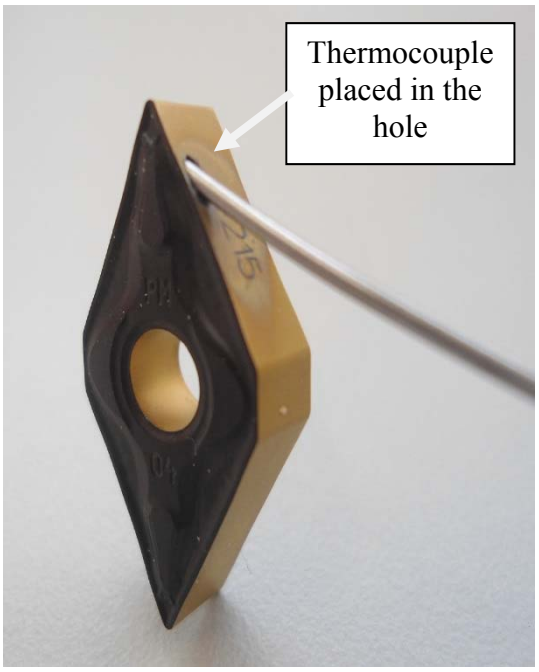

Figure 4.5: Photograph of the tool insert with the thermocouple in the hole

The experimental process should be able to detect temperature rise up to 1000°C. The material 310 stainless steel has low corrosion properties and it is oxidation resistance. This material is used for many manufacturing processes. The specifications of the thermocouple is as following[237]:

- Probe diameter 1.0 mm
- Probe length 1000 mm
- Probe material Stainless Steel
- K type thermocouple
- 310 stainless steel sheath
- Flexible is high for bending
- The hot junction is insulated
- Can measure -40°C up to +1100°C
- Miniature plug termination (200°C)
- Conforms to IEC 584 specification

The temperature measurement process consists of a data acquisition system which is attached to a thermocouple to acquire temperature from the tool insert and send data to the computer [238]. The real time tool temperatures were displayed on a computer monitor with the help of the data logger. The transient type temperature can be expressed only by the real time temperature measurement thermocouple when the high

local temperature exists for relatively short period of time and cannot be properly captured by thermocouple [200]. Therefore, the temperature was measured in real time. The calibration of the thermocouple was performed and the results found from the calibration process were in a close range. A review was conducted on commercially available data loggers and associated software. It was found that the Pico TC 08 is suitable for the experiment. The thermocouple data logger used for the experiment is shown in Figure 4.6. Figure 4.7 shows the real time temperature measurement with thermocouple software.

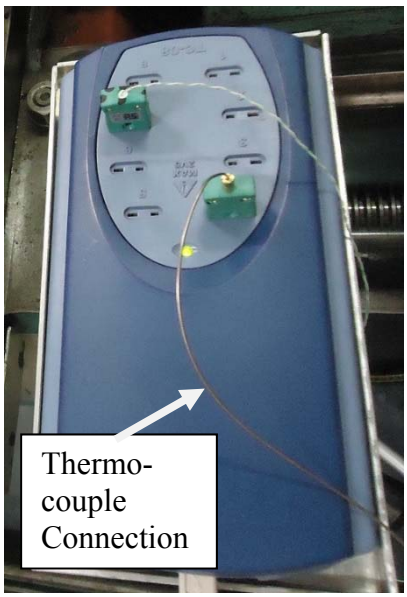

Figure 4.6: The thermocouple data logger used for the experimental

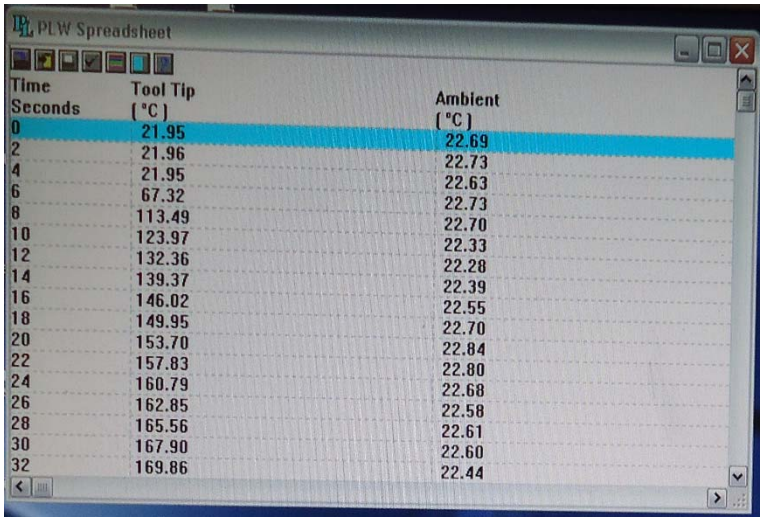

Time Seconds	Tool Tip (°C)	Ambient (°C)
0	21.95	22.69
2	21.96	22.73
4	21.95	22.63
6	67.32	22.73
8	113.49	22.70
10	123.97	22.33
12	132.36	22.28
14	139.37	22.39
16	146.02	22.55
18	149.95	22.70
20	153.70	22.84
22	157.83	22.80
24	160.79	22.68
26	162.85	22.58
28	165.56	22.61
30	167.90	22.60
32	169.86	22.44

Figure 4.7: The real time temperature measurement with thermocouple software

The machine tools manufacturers usually do not provide the flow meters with the machine. Therefore, a Parker flow meter with variable area technology was procured which was made of brass, suitable for industrial use, non-reactive with the cutting fluid and calibrated between 0.2–2.0 l/min. The flow meter was attached with the cutting fluid supply system of the machine tool to read the flow rate during the turning operations. The flow meter that was used to measure the cutting fluid during the experimental is shown in Figure 4.8.

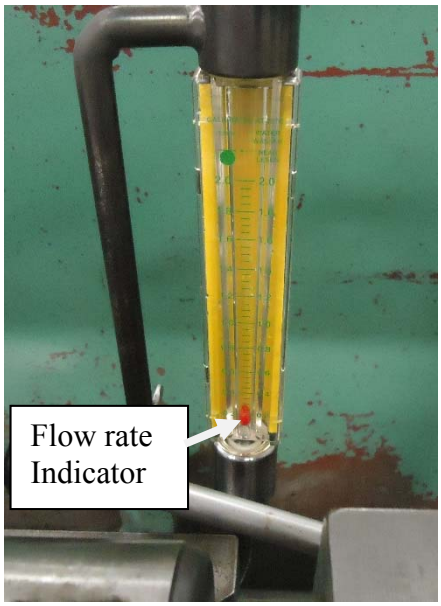

Figure 4.8: The Parker flow meter used for the experimental

4.2.3 Experimental Procedure

To validate the proposed methodology, the experiments were conducted for varying cutting conditions. A number of experiments were conducted by varying the cutting speed, feed rate and flow rate of the cutting fluid; and the tool temperatures were recorded during machining. After each of the experiment the tool wear was evaluated and if necessary, the tool was replaced. The evaluation of the tool insert was necessary because the tool wear effects the tool temperature during the machining.

To keep a constant cutting speed, a workpiece bar with same diameter was attached to the machine tool at the end of machining of each bar. As workpiece material, a 6 meter long bar was procured and cut into 10 pieces in the laboratory. Therefore, the length of each bar was 600mm with a diameter of 60mm. The cutting velocity for the first experiment was 87 m/min and the depth of cut was selected as 1.0 mm for the experiments.

During turning experiments, the cutting fluid flow rate reading was taken from the flow meter. For the flood turning experiments, the amount of cutting fluid was controlled with the valve. Although, it is generally anticipated that a hole, in the tool insert, limits the strength of the insert significantly but none of the insert was broken during the machining operation. Keeping the thermocouple in the position during machining was a challenge. The opening of the hole on the tool insert was from the opposite side of the cutting edge to make sure that the moving chips cannot displace the thermocouple from the position. In addition, thermal glue was applied to achieve and maintain contact between thermocouple and tool insert. No tool insert failure was observed in relation to making the hole in the insert.

The workpiece material for the experiment was similar to the material used in the proposed methodology. Similarly, the cutting tool material and shape of the tool were selected according to the material and shape which were used for the numerical analysis.

4.3 Obtaining Numerical Temperature

After obtaining the tool temperatures by the experimental investigation, the tool temperatures were also obtained by numerical method to make comparisons between results. The numerical temperatures were obtained from the proposed methodology for the similar cutting conditions. A point heat source was applied on the cutting tool based on the cutting conditions due the heat generation for metal cutting following the conjugate heat transfer approach. To compare the numerical and experimental results, a probe was assigned in the developed model. In numerical method, the location of the probe was the same as the location of the thermocouple that was used to obtain the temperature from the tool insert by experimental method. The effects of cutting fluid on the tool temperatures were captured by applying this advanced multiphase computational fluid dynamics based methodology. The solid-fluid interfaces were developed between the cutting tool and cutting fluid by employing Ansys CFX software package. The detail process of obtaining temperature is described in the Chapter 3. Three numerical experiments were conducted to establish the relationships between the numerical and experimental tool temperature with varying cutting conditions. The location of the probe in the cutting tool insert is shown in Figure 4.9 which is the intersection of the three yellow lines.

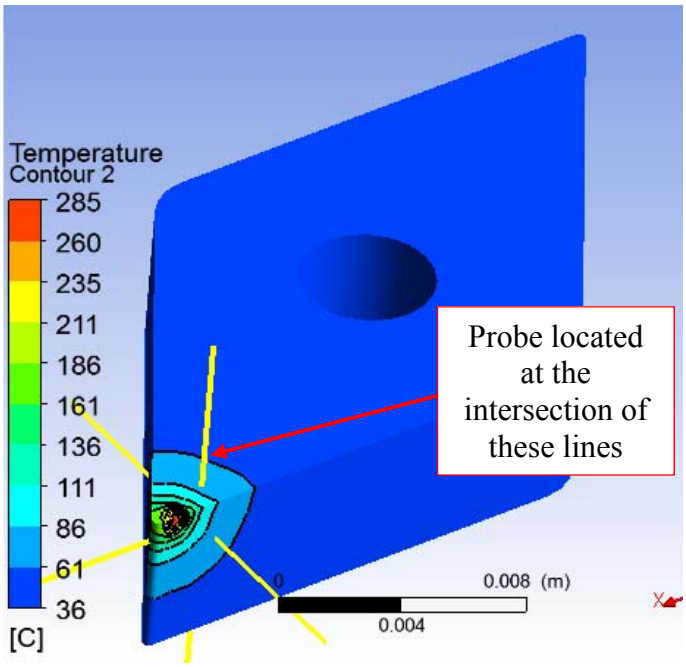

(a)

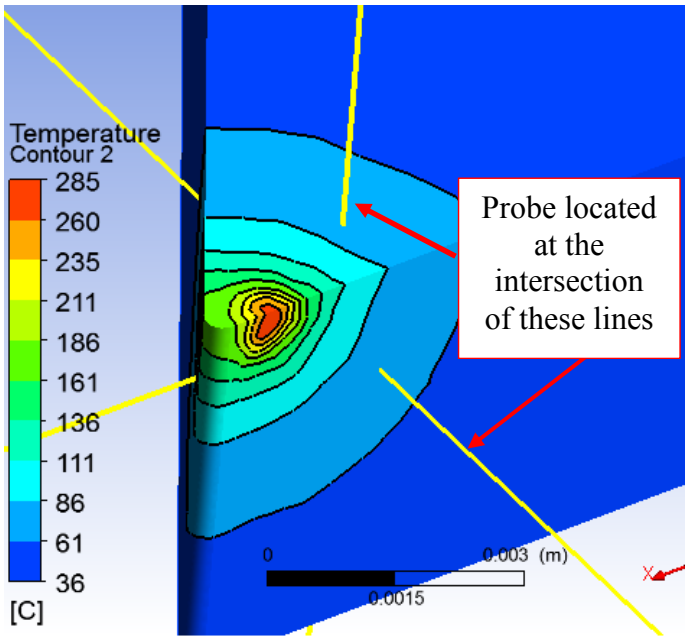

(b)

Figure 4.9: The assigned probe on the thermocouple (a) the location of the probe on the tool insert and (b) a close view of the location of the probe

4.4 Comparison of Numerical and Experimental Results

In this section, the comparisons are presented between the numerical and experimental results to find the accuracy of the proposed methodology. To compare the temperature, the same cutting conditions were applied for the numerical and experimental method.

In Table 4.4, the temperatures obtained from the proposed methodology are compared against the experimentally measured temperatures applying the similar machining conditions. The graphical comparisons of the tool temperatures obtained by the experimental and proposed methodology for the Condition 1, 2 and 3 are presented in Figure 4.10.

Table 4.4: Comparison of Experimentally Measured Temperature and Numerical Temperature from the Proposed Methodology

		Experimental conditions		
		Comparison 1	Comparison 2	Comparison 3
Cutting Parameters	Cutting Velocity, V_c (m/min)	87	87	178
	Feed Rate, f (mm/rev)	0.11	0.22	0.11
	Depth of Cut, d (mm)	1	1	1
Cutting Fluid Flow Rate, C_F (l/min)		2	1.5	Dry
Experimental and Numerical Temp Deviation (%)		5.4	-14.5	7.8

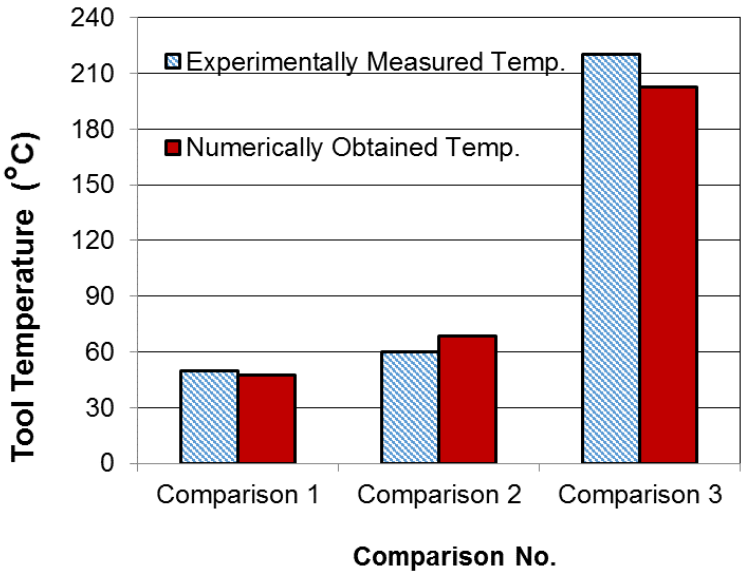

Figure 4.10: Comparisons of the tool temperatures obtained by the experimental and proposed methodology for the Condition 1, 2 and 3

The tool temperature is obtained from the developed model by assigning a probe at the thermocouple location. As shown in Figure 4.11, the temperatures of the thermocouple location were obtained by the Probe Tool which is a part of the Ansys CFX. The thermocouple location is the intersection of the three lines. Both the location of the probe and the obtained temperature are visible in the figures. The tool temperature distribution obtained from the developed model for Comparison 1 of Table 4.4 is shown in Figure 4.11, including the probe temperature at the thermocouple location. The probe temperature is 320.44K (47°C) with the cutting fluid flow rate to 2.0 l/min.

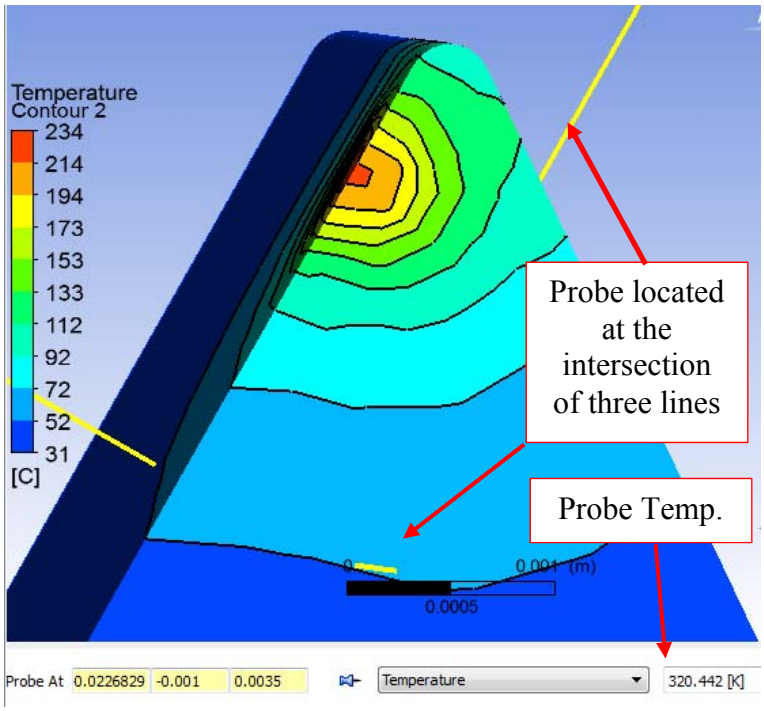

Figure 4.11: The tool temperature distribution for Comparison 1, including the probe temperature at the thermocouple location

The tool temperature distributions obtained from the proposed methodology for Comparison 2 of Table 4.4 is shown in Figure 4.12, including the probe temperature at the thermocouple location. The probe temperature is 341.85K (69°C) with 1.5 l/min cutting fluid flow rate. Similarly, the tool temperature distribution obtained from the developed model for Comparison 3, of Table 4.4, is shown in Figure 4.13, including the probe temperature at the thermocouple location. The probe temperature is 475.87K (203°C) for dry cutting condition.

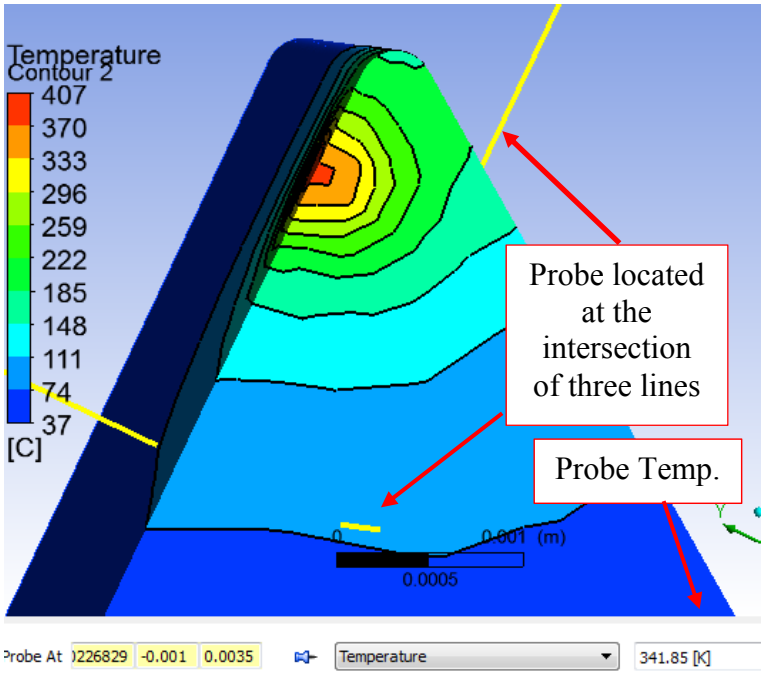

Figure 4.12: The tool temperature distribution for Comparison 2, including the probe temperature at the thermocouple location

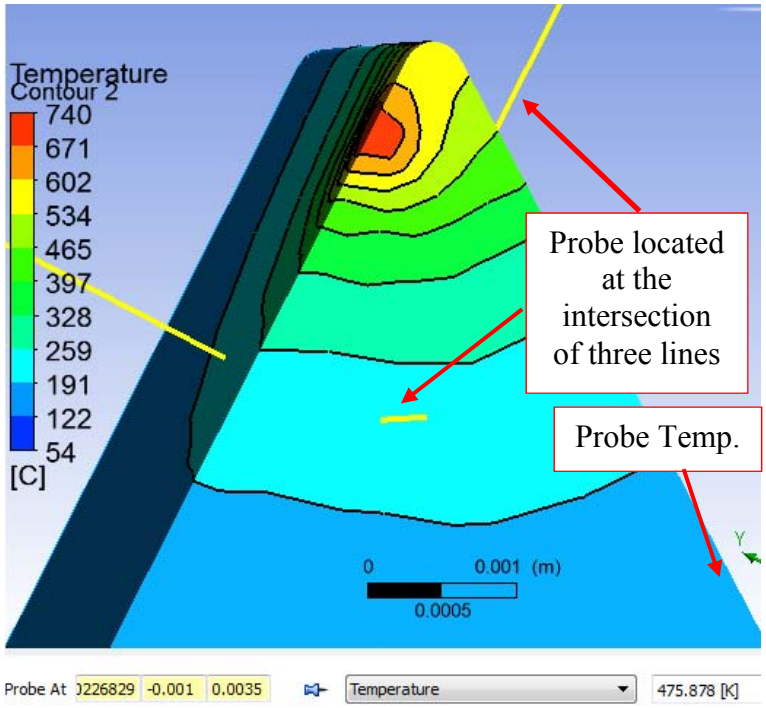

Figure 4.13: The tool temperature distribution for Comparison 3, including the probe temperature at the thermocouple location

4.5 Discussion and Justification

An extensive literature review was conducted to identify the available experimental methods for tool temperature measurement before starting the experimental procedure. Each of the methods has been distinguishable characteristics to obtain tool temperature. The advantages and disadvantages associated with each of the methods have been analysed bearing in mind the following criteria:

- The chosen experimental method should be able to provide tool temperature under flood cooling condition.
- The chosen experimental method should have the capability of measuring tool temperature much higher than the measured temperature.
- The chosen experimental method should not obstruct the machining process.

It was concluded that the embedded thermocouple method is the most suitable experimental method for the flood cooling process. The location of the hole should be as close as to the tool cutting edge. The location of the hole chosen should not interfere with the heat flow of the tool due to machining process. The dimensional accuracy of the hole was high which was achieved by the electrical discharge machine applying the spark eroding process. The application of the thermal glue was helpful to keep thermocouple inside the hole during the tool temperature measurement due to machining. The thermal glue maintained a thermo-conductivity contact between the thermocouple and the tool for heat flow from the high temperature area.

Based on the experimental data sets and numerical results from the proposed methodology, it is demonstrated that there is a correlation between the experimentally measured temperature and the numerically obtained temperatures. In general, the experimental tool temperatures were higher for the dry cutting condition and the proposed methodology was capable of providing comparable temperatures for dry conditions. The generated results from the model are within a close range of the experimental results and the accuracy of the numerically obtained results depends on cutting parameters. The results also provided the effects of the cutting fluid on the tool temperature for varying flow rates of the cutting fluid.

Applying the proposed methodology, it is possible to predict the temperature for any location of the cutting tool. The experimental method provided the temperature at the location of the thermocouple. Therefore, a probe was assigned at the same position of the thermocouple that was used in the experimental investigation to obtain the

temperature. Consequently, the temperature shown by the probe is the temperature of the same location of the tool insert obtained by the thermocouple. From the numerical analysis, it is found that the tool chip interface temperature is much higher than the probe temperature. After conducting similar experiments, researchers also reported temperature difference between the tool chip interface and thermocouple location temperature. Boswell [239] conducted research to obtain tool interface temperature by embedded thermocouple methods and obtained the tool temperature distributions, as shown in Figure 4.14. To obtain the tool interface temperature, the thermocouple should be placed as close as possible to the cutting edge. But it is not possible to place the thermocouple on the cutting edge due to aggressive wear. As a solution, Boswell [239] calculated the interface temperature based on recording of the experimental temperatures at different positions on the tool insert and in conjunction with the measured power consumption during machining operations.

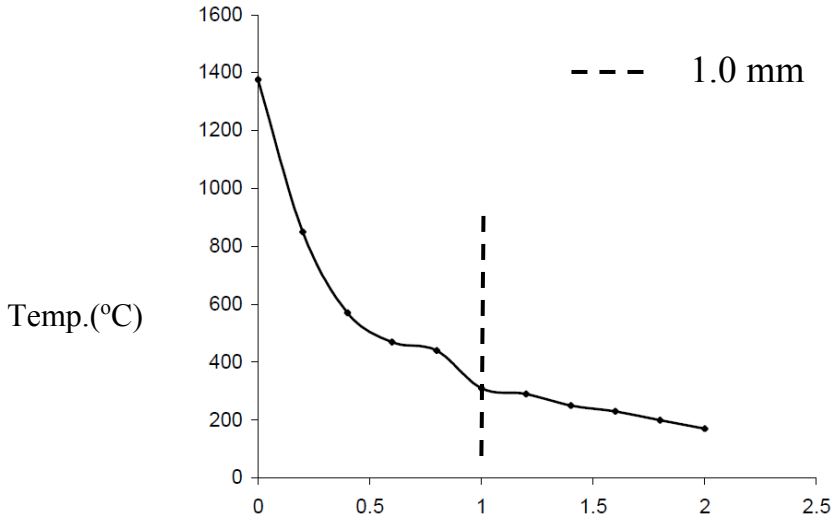

Figure 4.14: The temperature distribution over the tool tip rake face [239]

As shown in Figure 4.14, although the temperature is around 350°C at 1.0 mm distance from the cutting edge, but the temperature at the interface is 1400°C for a cutting speed of 175 m/min and feed rate of 0.23 mm/rev. Therefore, there is a large temperature difference around 1000°C within just 1.0 mm distance of the rake side of the tool. Similarly, according to Figure 4.15, although the temperature is more than 400°C at 1.0 mm distance from the cutting edge, but the temperature at the interface is

1000ºC for cutting conditions of feed rate 0.138 mm/rev, cutting speed 217 m/min and depth of cut 1.5mm. It is shown that there is a temperature difference of around 600 ºC within just 1.0 mm distance of the rake side of the tool.

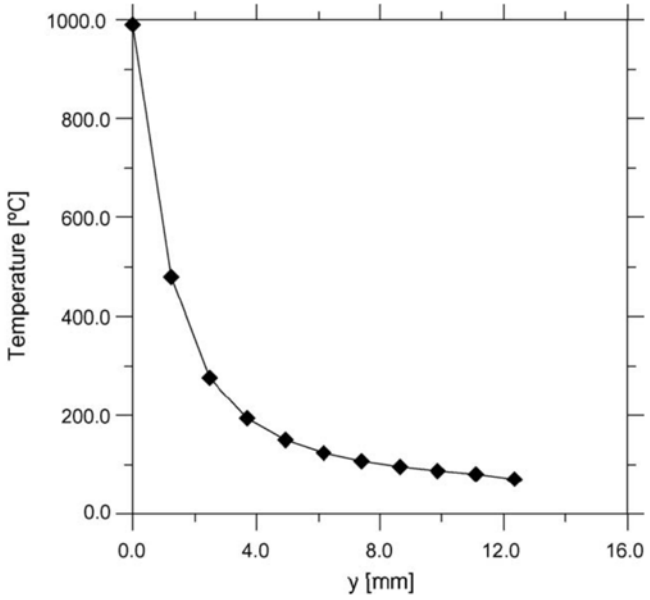

Cutting conditions of feed rate 0.138 mm/rev, cutting speed 217 m/min and depth of cut 1.5mm

Figure 4.15: The chip–tool interface temperature in the y-direction [162]

Similarly, according El-Wardany et al. [195] as shown in Figure 4.16, although the temperature is around 400ºC at 1.0 mm distance from the cutting edge, but the temperature at the interface is 1000ºC. Therefore, the numerical and experimental temperatures obtained by the present study can be justified by the investigation of these researchers.

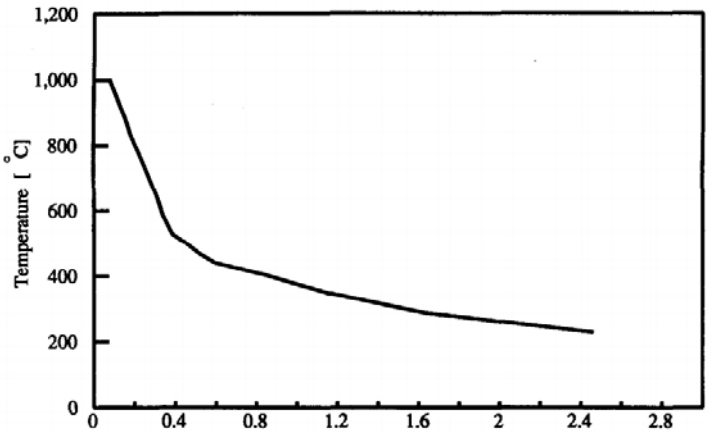

Figure 4.16: The change in the value of the thermal gradient on the tool rake face [195]

4.6 Concluding Remarks

In conclusion of this chapter, the proposed methodology has been experimentally validated by obtaining tool temperatures. After the validation of the proposed methodology, it is possible to predict the tool temperature for particular cutting conditions accurately. The major observations from this chapter are as following:

- For flood turning operations, the embedded thermocouple method is found as a suitable experimental method for obtaining tool temperatures. Due to the location of the thermocouple, the temperature obtained during the machining was different from the temperature of the tool interface.
- The validation of the model was performed by comparing numerically obtained tool temperatures against experimentally measured tool temperatures by placing thermocouple inside a narrow hole which was created through spark eroding process. The location of the hole chosen did not significantly interfere with the heat flow of the tool due to machining process.
- The proposed methodology was verified under dry and flood cooling conditions and the results demonstrated that the methodology is capable of predicting the tool temperatures in both dry and flood cooling environments.
- The experimental method provided higher cutting tool temperatures for higher cutting speeds. This is because of the higher volume of material removal rate of the metal generates more heat. For the same reason, the cutting tool temperatures was higher for the higher feed rates. The proposed methodology also provided higher cutting tool temperature for higher cutting speeds and feed rates.
- Based on the experimental validation, it is concluded that the proposed methodology provided a reasonable agreement between the numerical and experimental results. After the validation, the proposed methodology is capable of predicting tool temperatures for particular cutting conditions without conducting the experiments in the laboratory.

Chapter 5

Application of the Methodology to obtain the Tool Temperature

5.1 Introduction

A numerical model, validated by experiment method, is capable of simulating the tool temperature distribution in details, on the other hand, the tool temperature distributions cannot be presented only by means of experimentation. The proposed methodology can be applied to identify the effects of the cutting fluid on the tool temperature distributions. Previously in Chapter 4, the proposed computational fluid dynamics based methodology was validated for turning operations with varying cutting conditions. The experimental validation process was performed by obtaining tool temperatures with embedded thermocouple. The objective of this chapter is to demonstrate the application of the proposed methodology to identify the effects of the amount of cutting fluid on tool temperature distributions for flood turning operations. In other words, this chapter presents numerically obtained tool temperature distributions for turning operations under flood cooling.

The flow rate of the cutting fluid widely fluctuate machine to machine and there is no scientific guideline for selecting the flow rate. The amount of the cutting fluid currently used in the industry for some turning operations is as high as 19 l/min [240]. To understand the effect of the cutting fluid on the tool insert, a line was assigned along the cutting edge and temperature was obtained from this line. A number of numerical experiments were conducted to understand the effect of the cutting fluid on the tool along this line for varying cutting fluid flow rates. The results from the numerical experiments were able to provide the effects of varying flow rates of the cutting fluid. Applying the proposed methodology, the amount of cutting fluid required to adequately reduce the tool temperature for turning operations has been identified. The amount of cutting fluid can be reduced by selecting the flow rate from the curve obtained by the numerical results. For the numerical experiments, the properties of the workpiece material were selected as similar to the properties of the experimental workpiece material. Similarly, the properties of the tungsten carbide were assigned as the properties of the tool insert.

5.2 Obtaining the Tool Temperature Distribution

The effect of the cutting fluid on the tool temperature was obtained with the help of a reference line. A 10 mm long reference line was assigned along the cutting edge. The location of the reference line along the cutting edge is shown in Figure 5.1. The relative location of the probe and the reference line is also shown in Figure 5.1b.

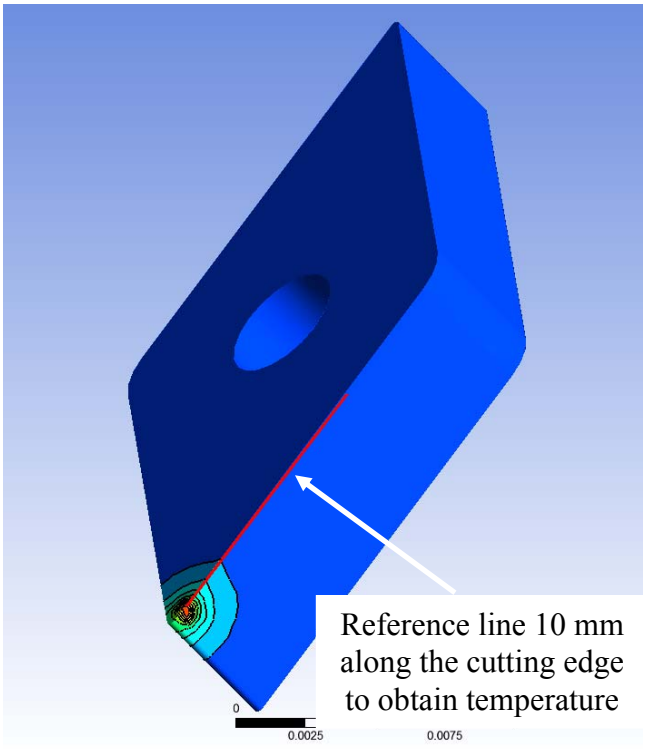

(a)

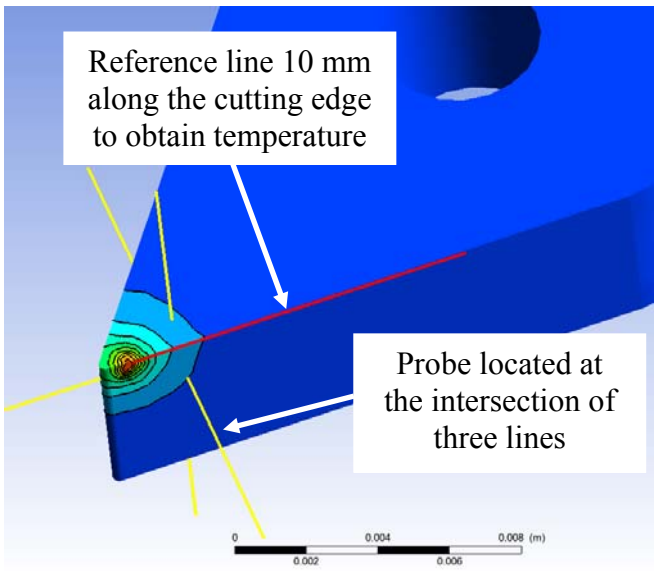

(b)

Figure 5.1: The 10 mm long reference line on the cutting edge used to obtain temperature drop (a) location of the line and (b) location of the line and the probe

5.2.1 Case Study 1

Numerical approach can provide the tool temperature distribution along the cutting edge because of the difficulty of employing the thermocouple at the cutting edge for direct measurement of cutting temperature. The effect of varying cutting fluid flow rates on the tool temperature has been analysed by using the proposed methodology and presented in this chapter.

To understand the effectiveness of the cutting fluid, numerical experiments were conducted considering case by case for varying cutting conditions. The major difference between of these cases is the workpiece materials. The workpiece material for the Case 1 was alloy steel AISI4140. Similarly, the workpiece material for the Case 2 and Case 3 are aluminium alloy and alloy steel AISI 1030 respectively. The first numerical experiment was conducted for dry condition without any coolant. The effects of cutting fluid on the tool temperatures were captured by applying the proposed multiphase computational fluid dynamics based methodology. Flood cooling process was applied for the rest of the experiments. The flow rates of the cutting fluid were selected as 0.5, 1.0, 1.5 and 2.0 l/min. The temperatures from the reference line were obtained and presented graphically. The cutting parameters for the numerical analysis are presented in Table 5.1. In dry condition, without any cutting fluid, the tool temperature is near 350^{o}C at the maximum temperature area as shown in Figure 5.2. Initially, the reduction of the temperature is rapid along the cutting edge and reaches around 160^{o}C at 1.0 mm distance from the maximum temperature. Finally, the temperature comes down to approximately 60^{o}C. A little difference between the maximum temperatures in the tool temperature contours and in the graph is due to the location of the reference line which is not accurately at the maximum temperature of the tool.

Table 5.1: Cutting Parameters for the Numerical Analysis

Parameters	Condition
Feed Rate, *f (*mm/rev*)*	0.11
Cutting Velocity, V_c (m/min)	87
Depth of Cut, *d* (mm)	1.0
Coolant Flow Rate, C_F (l/min)	0.5, 1.0, 1.5 and 2.0
Workpiece Material	AISI4140
Tool Insert Material	Tungsten Carbide

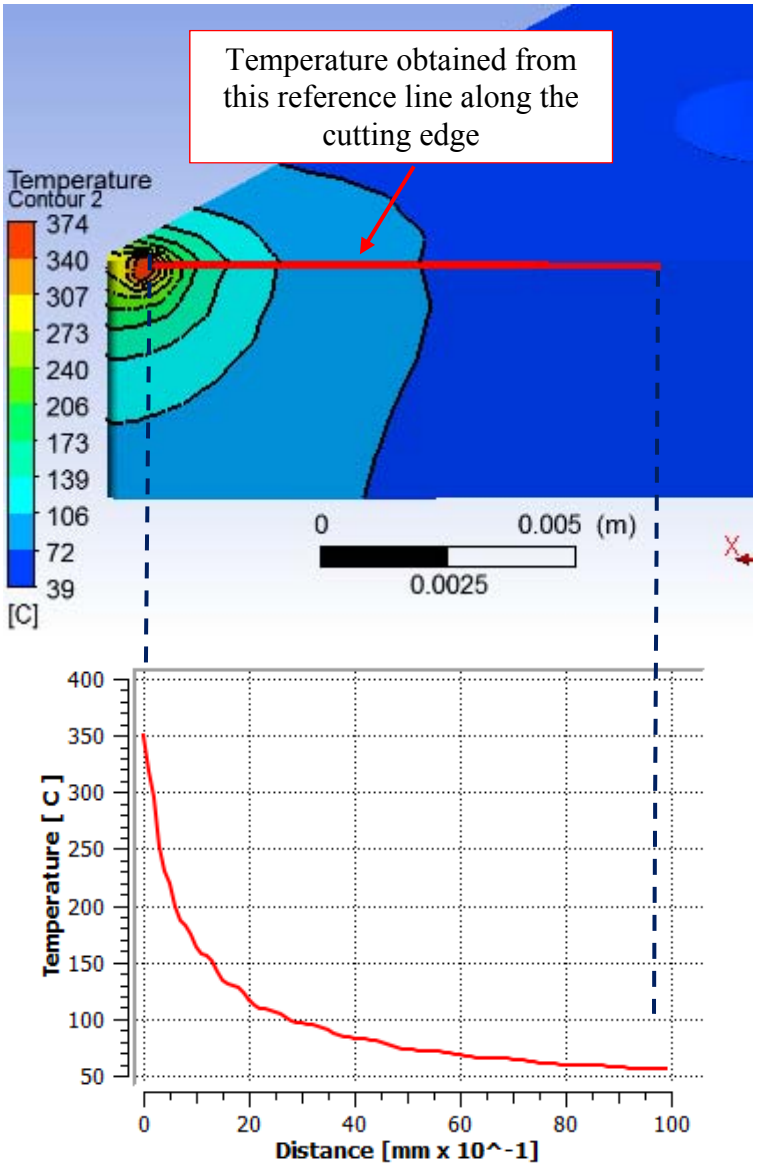

Cutting parameters according to the of Table 5.1

Figure 5.2: For dry condition with AISI4140 workpiece, numerically obtained temperature drop of the reference line along the cutting edge

A significant temperature reduction of the tool has been observed with the application of cutting fluid at 1.0 l/min flow rate. As shown in Figure 5.3, the tool temperature is near 270^{o}C at the maximum temperature area. Initially, the reduction of the temperature is rapid along the cutting edge and reaches around 100^{o}C at 1.0 mm distance from the maximum temperature. Finally, the temperature becomes relatively stable at the last part of the line and comes down close to 50^{o}C.

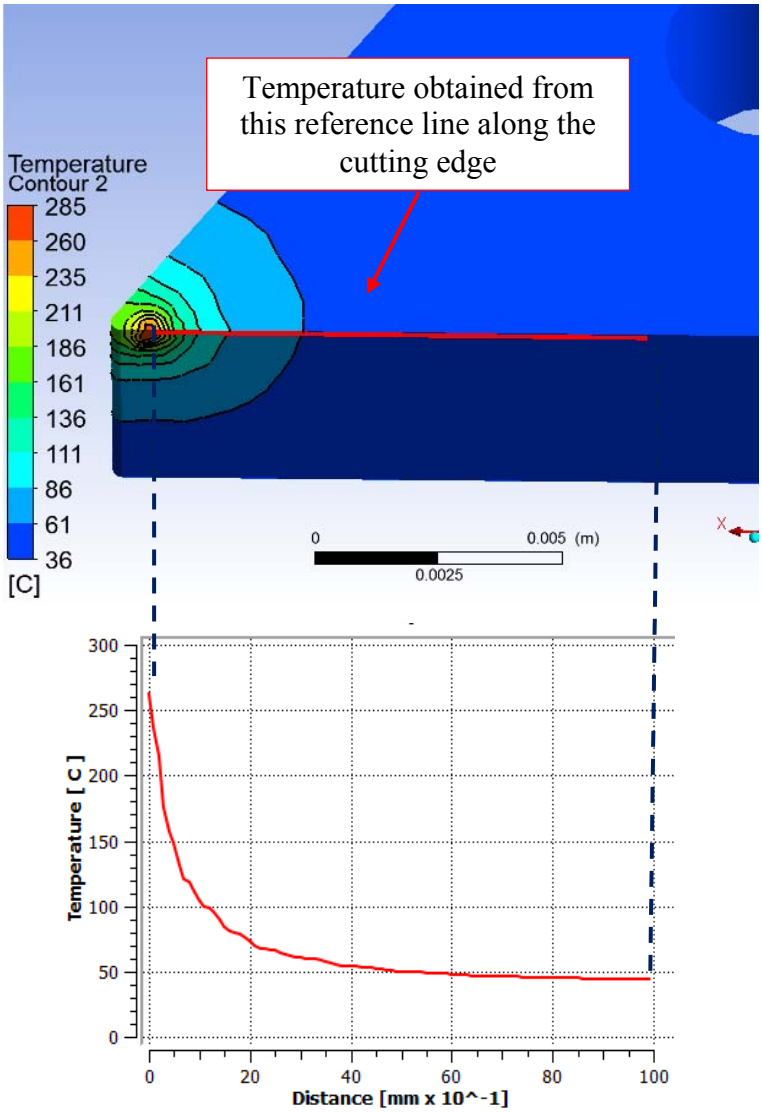

Cutting parameters according to Table 5.1

Figure 5.3: For 1.0 l/min flow rate with AISI4140 workpiece, numerically obtained temperature drop of the reference line along the cutting edge

With the application of cutting fluid at 1.5 l/min flow rate, as shown in Figure 5.4, the tool temperature is around 220°C at the maximum temperature area. The temperature reduction of the tool is not enormous with the application of cutting fluid at 1.5 l/min flow rate, compared with the flow rate of 1.0 l/min. Initially, the reduction of the temperature is rapid along the cutting edge and reaches around 70°C at 1.0 mm distance from the maximum temperature. Finally, the temperature becomes relatively stable at the last part of the line and comes down to 40°C.

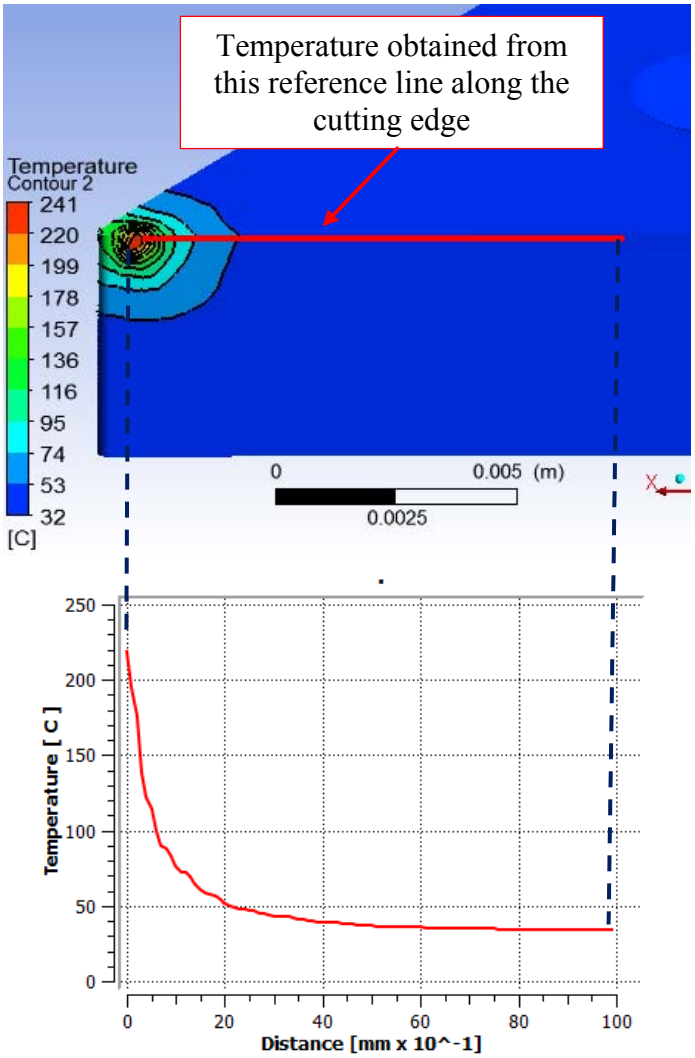

Cutting parameters according to Table 5.1

Figure 5.4: For 1.5 l/min flow rate with AISI4140 workpiece, numerically obtained temperature drop of the reference line along the cutting edge

By increasing the cutting fluid up to 2.0 l/min flow rate, as shown in Figure 5.5, there is no significant change at the maximum temperature area. The reduction of temperature along the reference line is not significantly different compared with the reduction of the temperature for the flow rate of cutting fluid at 1.5 l/min as well. Therefore, it is logical to maintain a much lower flow rate than 2.0 l/min from the point of view of reduction of cutting fluid which is the interest of many researchers around the world. A significant amount of cutting fluid can be saved by not increase the flow rate higher than the required level.

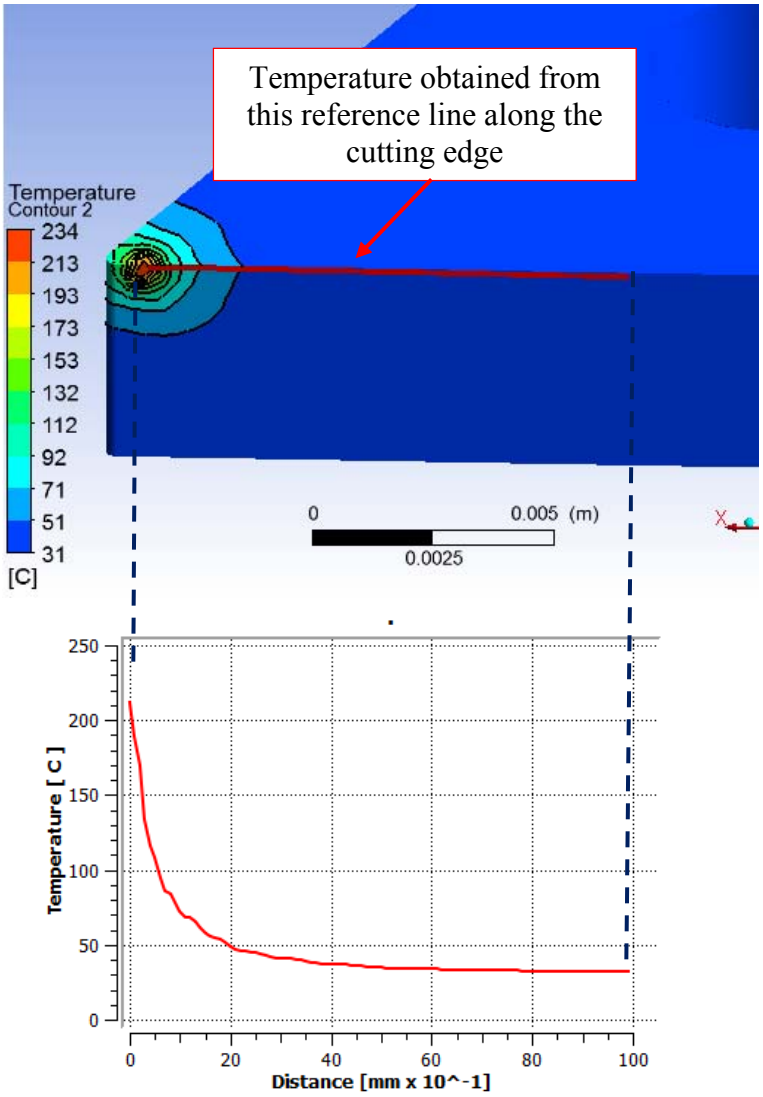

Cutting parameters according to Table 5.1

Figure 5.5: For 2.0 l/min flow rate with AISI4140 workpiece, numerically obtained temperature drop of the reference line along the cutting edge

A combination of tool temperature data collected for varying flow rates along the reference line is presented in Figure 5.6. This reference line is the same line as shown in Figure 5.1. Similarly, the temperatures are obtained by the numerical analysis considering the parameters of Table 5.1. This figure depicts the reduction of the tool insert temperature against the cutting fluid flow rate from dry condition to 2.0 l/min. The reduction of the tool insert temperature is substantial when compared between dry condition and with the flow rate of 1.0 l/min of cutting fluid.

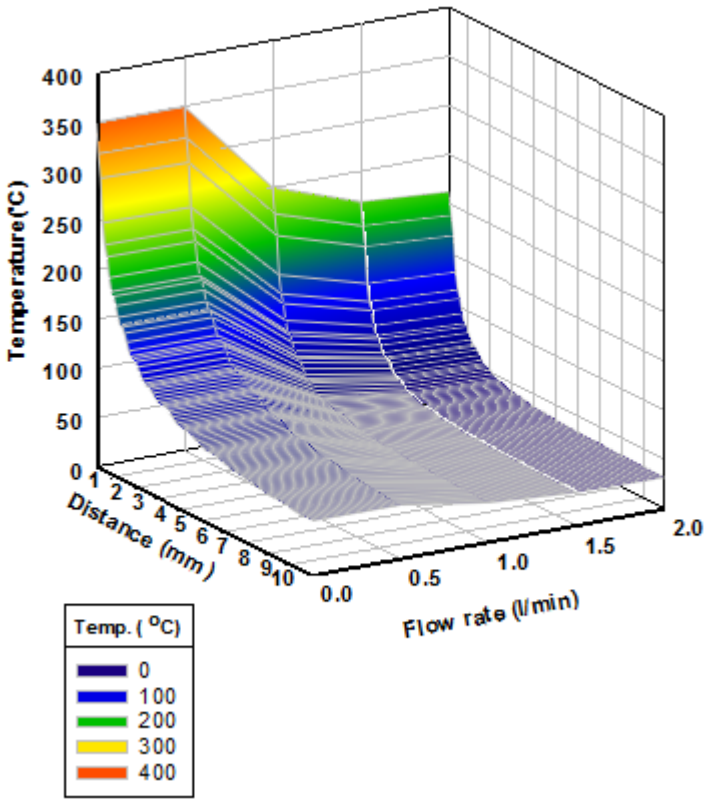

Numerically obtained temperature from the reference line along the cutting edge, considering the parameters of Table 5.1

Figure 5.6: The effect of cutting fluid on the tool insert temperature for varying flow rates with AISI4140 workpiece

It is depicted that the reduction of the tool insert temperature is not much significant between the flow rate of 1.0 and 2.0 l/min of cutting fluid. According to numerical analysis, cutting fluid is able to significantly reduce the insert temperature with the flow rate of 1.0 l/min of cutting fluid. The temperature reduction along the reference line is not significant after the flow rate of 1.0 l/min of cutting fluid.

Further numerical experiments were conducted to gain insight of the heat elimination of cutting tool under the influence of cutting fluid where the workpiece material for the numerical experiment is AISI4140 bar and the cutting tool insert material is tungsten carbide. The cutting parameters for the numerical experiments are presented in Table 5.2. The selection of the cutting parameters are based on the usual cutting parameters which are followed during the machining of AISI4140.

Table 5.2: Cutting Parameters for the Numerical Experiments with AISI4140 Workpiece and Tungsten Carbide Insert

Parameters	Expt. 1	Expt. 2	Expt. 3
Feed Rate, *f* (mm/rev)	0.11	0.33	0.22
Cutting Velocity, V_c (m/min)	87	87	178
Depth of Cut, *d* (mm)	1.0	1.0	1.0

The effects of cutting fluid on the tool insert temperatures are presented in Figure 5.7. This figure depicts the change of the tool insert temperatures due to the variation of cutting fluid flow rates. In all three experiments, Numerical Expt. 1, 2 and 3, it is revealed that there are significant reductions of tool insert temperatures with the flow rate of 1.0 l/min of cutting fluid compared with dry conditions. Although, the flow rate is increased further up to 2.0 l/min, but the temperature reduction is not significant after the flow rate of 1.0 l/min of cutting fluid, unless the material removal rate is high.

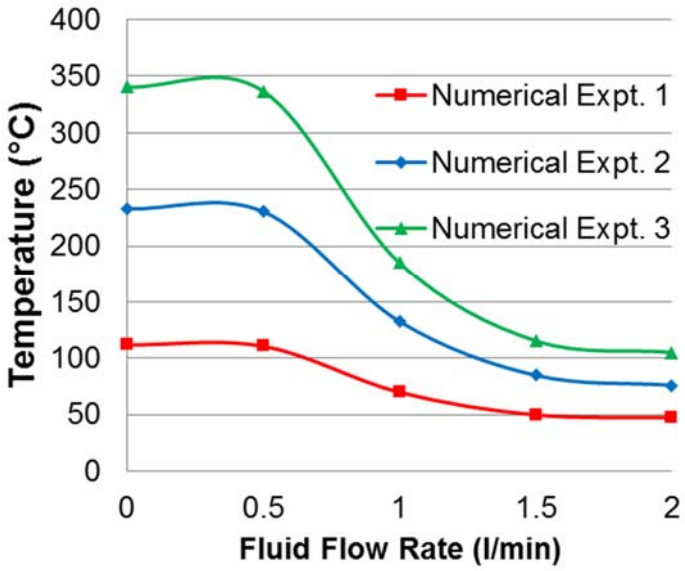

Cutting parameters according to Table 5.2

Figure 5.7: The effect of cutting fluid on the tool temperature for AISI4140 workpiece by numerical analysis

5.2.2 Case Study 2

To understand the effectiveness of the cutting fluid, further numerical experiments were conducted with aluminium alloy workpiece and tungsten carbide insert considering varying cutting conditions. The aluminium alloy can be machined easily but the strength and melting temperature are lower than the steel. Therefore, the cutting parameters for the numerical analysis were selected to keep similarity with practical machining conditions which are presented in Table 5.3. Sreejith [241] investigated the role of cutting fluid on aluminium machining and concluded that cutting fluid has a significant influence to the adhesion of material on the cutting tool. Aluminium has a tendency to weld on the cutting edge during machining and cutting fluid hinders the welding of particles on the tool. Therefore, application of cutting fluid during machining of aluminium is necessary to keep the cutting tool temperature low and reduce the adhesion of material on it.

Table 5.3: Cutting Parameters for the Numerical Experiments with Aluminium Alloy Workpiece and Tungsten Carbide Insert

Parameters	Expt. 4	Expt. 5	Expt. 6
Feed Rate, *f* (mm/rev)	0.06	0.08	0.10
Cutting Velocity, V_c (m/min)	60	85	90
Depth of Cut, *d* (mm)	0.80	1.0	1.2

The first numerical experiment was conducted considering dry condition without any coolant. Flood cooling process was applied for the rest of the experiments. The flow rate of the cutting fluid were selected as 0.5, 1.0, 1.5 and 2.0 l/min. The temperatures from the reference line were obtained and presented in the graphs.

In dry condition, without any cutting fluid, as shown in Figure 5.8, the tool temperature is near 100^{o}C at the maximum temperature area. As the material removal rate of the workpiece was not very high, the amount of generated heat was not very high as well; and consequently the tool temperature rise was not significant. Initially, the reduction of the temperature is rapid along the cutting edge and reaches to 55^{o}C at 1.0 mm distance from the maximum temperature. Finally, the temperature comes down close to 30^{o}C.

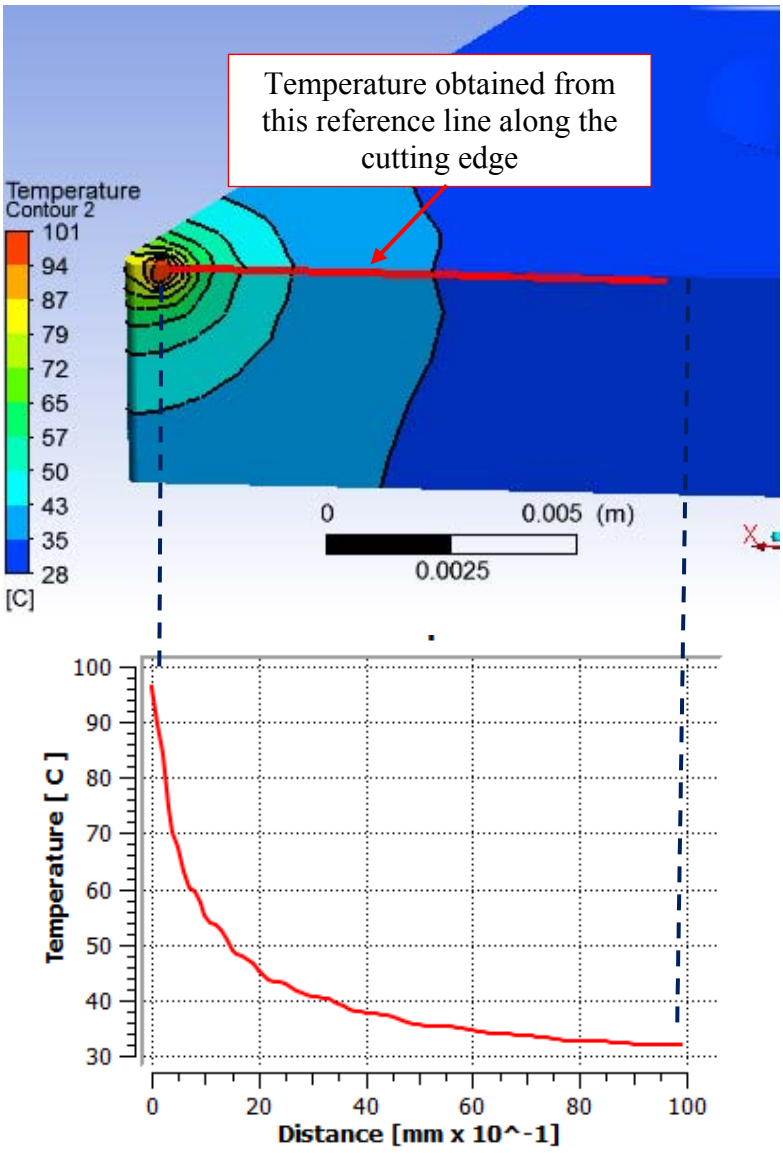

Cutting parameters according to the Expt. 6 of Table 5.3

Figure 5.8: For dry cutting condition with aluminium workpiece, numerically obtained temperature reduction of the reference line along the cutting edge

A significant temperature reduction of the tool has been observed with the application of cutting fluid at 1.0 l/min flow rate. As shown in Figure 5.9, the tool temperature is near 80^{o}C at the maximum temperature area. Initially, the reduction of the temperature is rapid along the cutting edge and reaches around 40^{o}C at 1.0 mm distance from the maximum temperature. Finally, the temperature becomes relatively stable at the last part of the line and comes down to 30^{o}C.

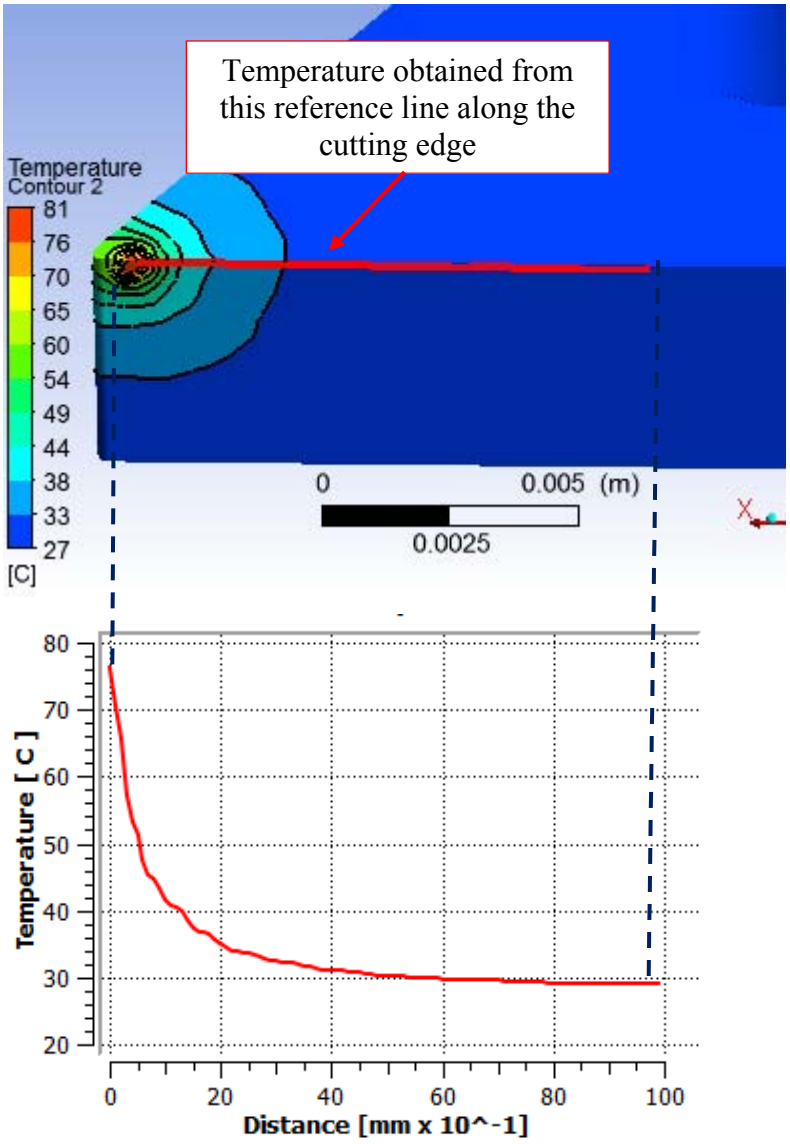

Cutting parameters according to the Expt. 6 of Table 5.3

Figure 5.9: For 1.0 l/min flow rate with aluminium workpiece, numerically obtained temperature reduction of the reference line along the cutting edge

With the application of cutting fluid at 1.5 l/min flow rate, as shown in Figure 5.10, the tool temperature is near 70°C at the maximum temperature area. The temperature reduction of the tool is not huge with the application of cutting fluid at 1.5 l/min flow rate, compared with the flow rate of 1.0 l/min. The temperature keeps dropping rapidly along the cutting edge and reaches around 35°C at 1.0 mm distance from the maximum temperature. Finally, the temperature along the line becomes relatively stable at the last part of the line and comes to below 30°C.

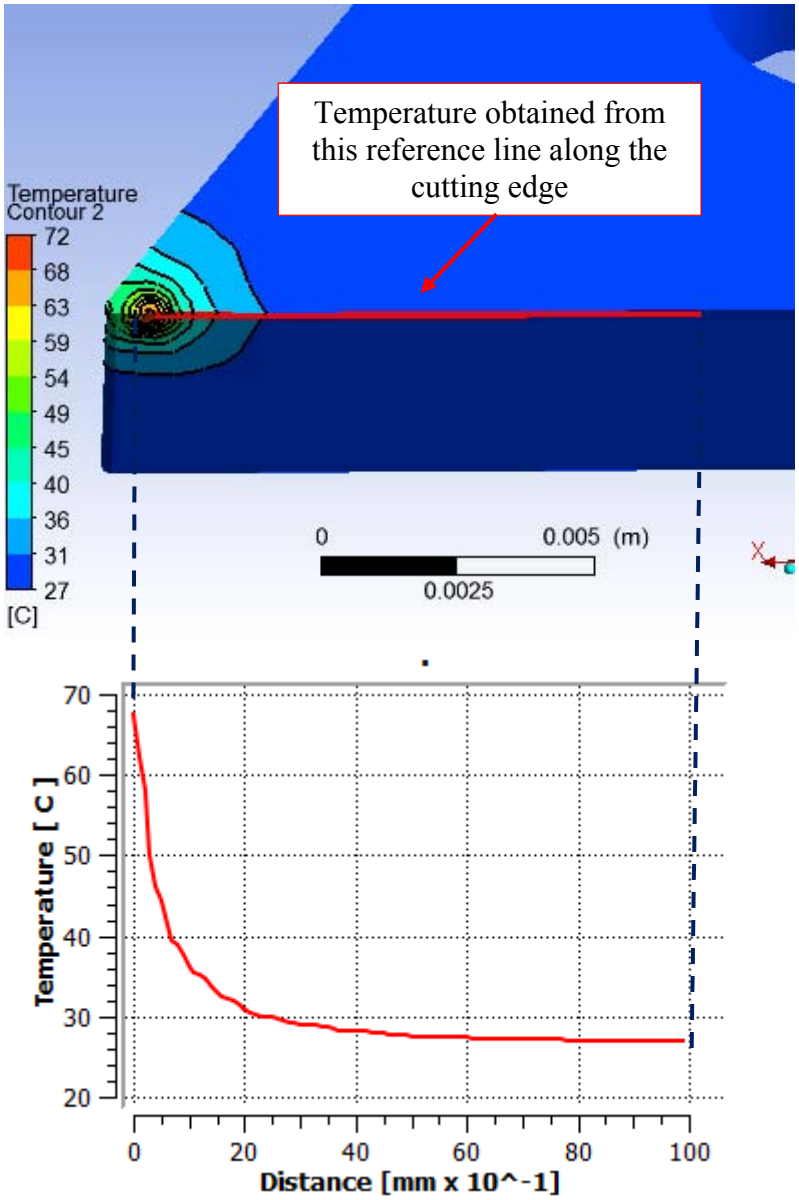

Cutting parameters according to the Expt. 6 of Table 5.3

Figure 5.10: For 1.5 l/min flow rate with aluminium workpiece, numerically obtained temperature reduction of the reference line along the cutting edge

By increasing the cutting fluid up to 2.0 l/min flow rate, as shown in Figure 5.11, there is no significant change at the maximum temperature area. The temperature reduction along the reference line is not significantly different when compared with the temperature reduction with the cutting fluid at 1.5 l/min flow rate as well. Therefore, from the heat eliminating point of view, there is not much advantage of increasing the flow rate higher than 1.0 l/min.

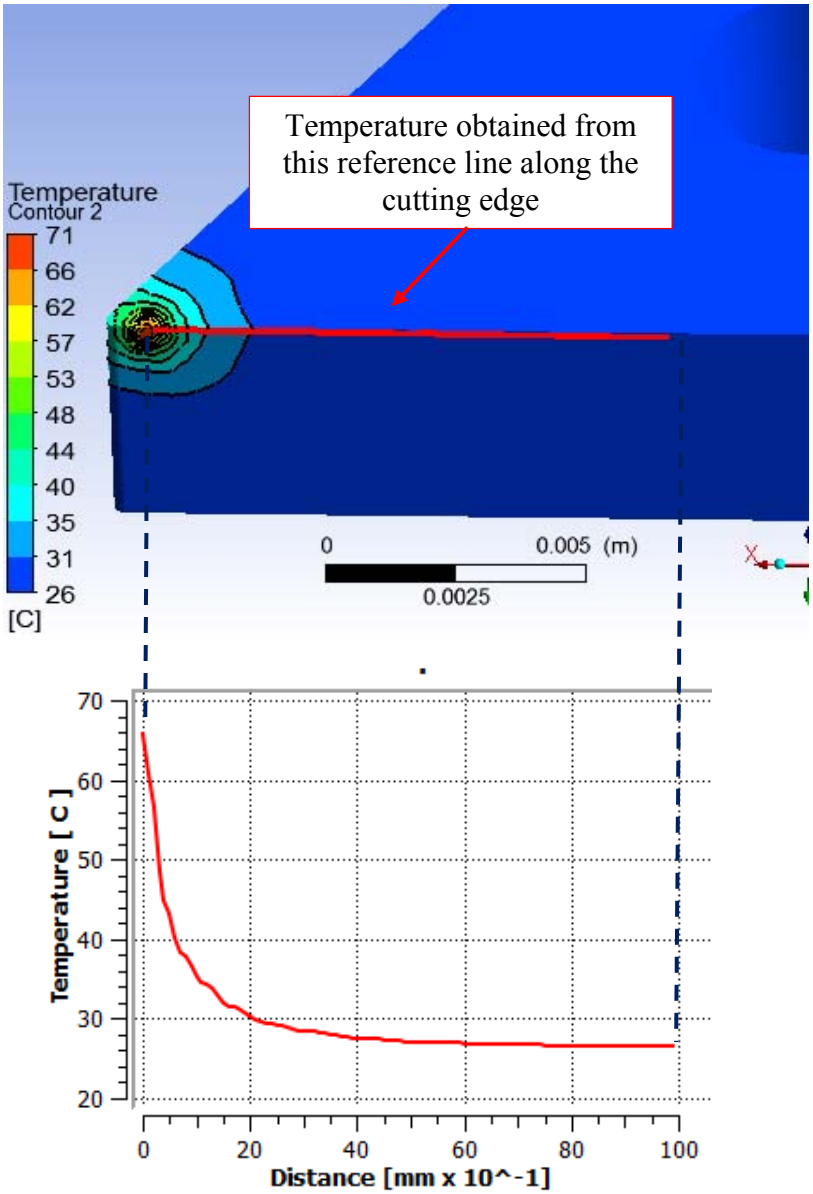

Cutting parameters according to the Expt. 6 of Table 5.3

Figure 5.11: For 2.0 l/min flow rate with aluminium workpiece, numerically obtained temperature reduction of the reference line along the cutting edge

A combination of tool temperature data collected for varying flow rates along the reference line is presented in Figure 5.12. This reference line is the same line as shown in Figure 5.1. Similarly, the temperatures are obtained by the numerical analysis considering the parameters of Table 5.3. This figure depicts the reduction of the tool insert temperature against the cutting fluid flow rate from dry condition to 2.0 l/min. The cutting fluid is capable of reducing the tool insert temperature significantly with

the flow rate of 1.0 l/min. It is shown that the reduction of the tool insert temperature is not significant between the flow rate of 1.0 and 2.0 l/min of cutting fluid.

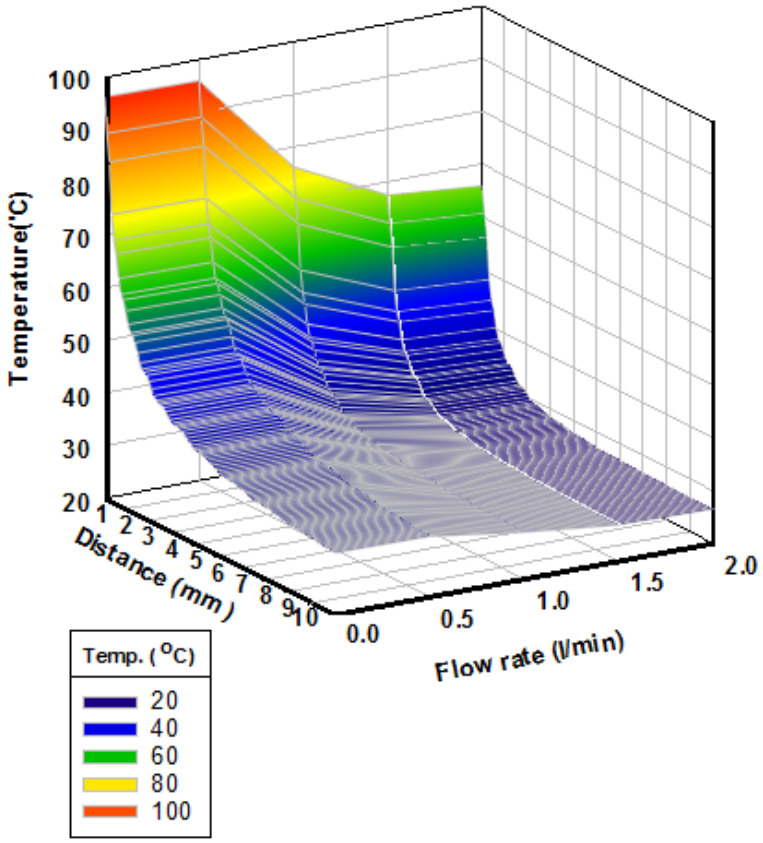

Numerically obtained temperature from the reference line along the cutting edge, considering the parameters of the Expt. 6 of Table 5.3

Figure 5.12: The effect of cutting fluid on the tool insert temperature for varying flow rates with aluminium workpiece

The effect of cutting fluid on the tool insert temperature is presented in Figure 5.13. This figure depicts the change of the tool insert temperature due to the variation of cutting fluid flow rate. In all three experiments, Numerical Expt. 4, 5 and 6, there are significant drops of tool insert temperatures with the flow rate of 1.0 l/min of cutting fluid. Although, the flow rate is increased further up to 2.0 l/min, but the temperature reduction is not significant after the flow rate of 1.0 l/min of cutting fluid.

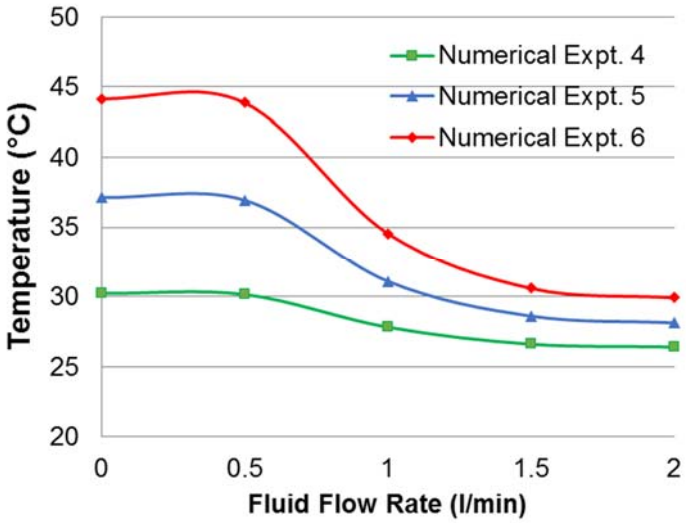

Cutting parameters according to Table 5.3

Figure 5.13: The effect of cutting fluid on the tool temperature for Aluminium workpiece by numerical analysis

5.2.3 Case Study 3

The workpiece material for the Numerical Expt. 7, 8 and 9 is AISI1030 bar and the cutting tool insert material is tungsten carbide. The cutting parameters for the numerical analysis are presented in Table 5.4.

Table 5.4: Cutting Parameters for the Numerical Experiments with AISI 1030 Workpiece and Tungsten Carbide Insert

Parameters	Expt. 7	Expt. 8	Expt. 9
Feed Rate, *f* (mm/rev)	0.2	0.3	0.4
Cutting Velocity, V_c (m/min)	18	22	24
Depth of Cut, *d* (mm)	0.80	1.0	1.2

The first numerical experiment was conducted considering dry condition without any coolant. Flood cooling process was applied for the rest of the experiments. The flow rate of the cutting fluid were selected as 0.5, 1.0, 1.5 and 2.0 l/min. The temperature of the reference line was obtained and presented in the graph. In dry condition, without any cutting fluid, as shown in Figure 5.14, the tool temperature is near 190°C at the maximum temperature area. Initially, the reduction of the

temperature is rapid along the cutting edge and reaches below 90°C at 1.0 mm distance from the maximum temperature. Finally, the temperature comes down to 40°C.

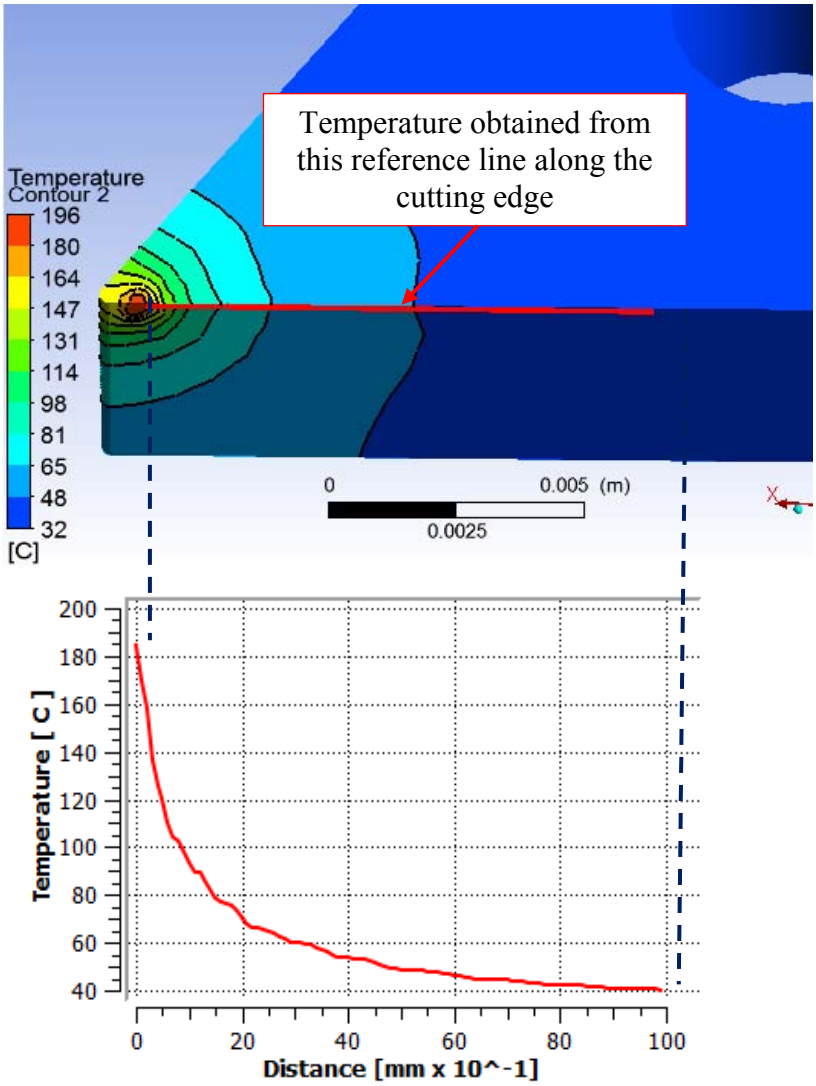

Cutting parameters according to the Expt. 8 of Table 5.4

Figure 5.14: For dry cutting condition with AISI1030 workpiece, numerically obtained temperature reduction of the reference line along the cutting edge

A significant temperature reduction of the tool has been observed with the application of cutting fluid at 1.0 l/min flow rate. As shown in Figure 5.15, the tool temperature is approximately 140°C at the maximum temperature area. Initially, the temperature keeps dropping rapidly along the cutting edge and reaches around 60°C at 1.0 mm distance from the maximum temperature. Finally, the temperature becomes relatively stable at the last part of the line and comes to below 40°C.

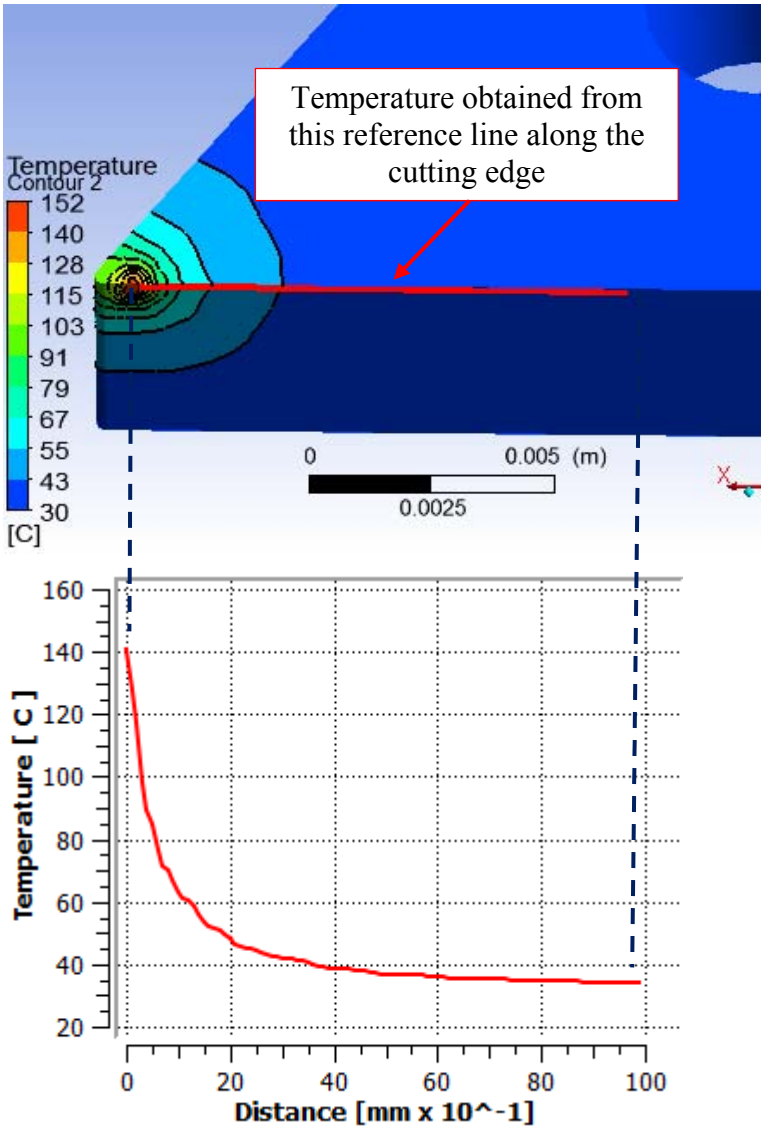

Cutting parameters according to the Expt. 8 of Table 5.4

Figure 5.15: For 1.0 l/min flow rate with AISI1030 workpiece, numerically obtained temperature reduction of the reference line along the cutting edge

With the application of cutting fluid at 1.5 l/min flow rate, as shown in Figure 5.16, the tool temperature is near 120°C at the maximum temperature area. The temperature reduction of the tool is not huge with the application of cutting fluid at 1.5 l/min flow rate, compared with the flow rate of 1.0 l/min. The reduction of the temperature is rapid along the cutting edge at the beginning and reaches around 50°C at 1.0 mm distance from the maximum temperature. Finally, the temperature becomes relatively stable at the last part of the line and comes down to approximately 30°C.

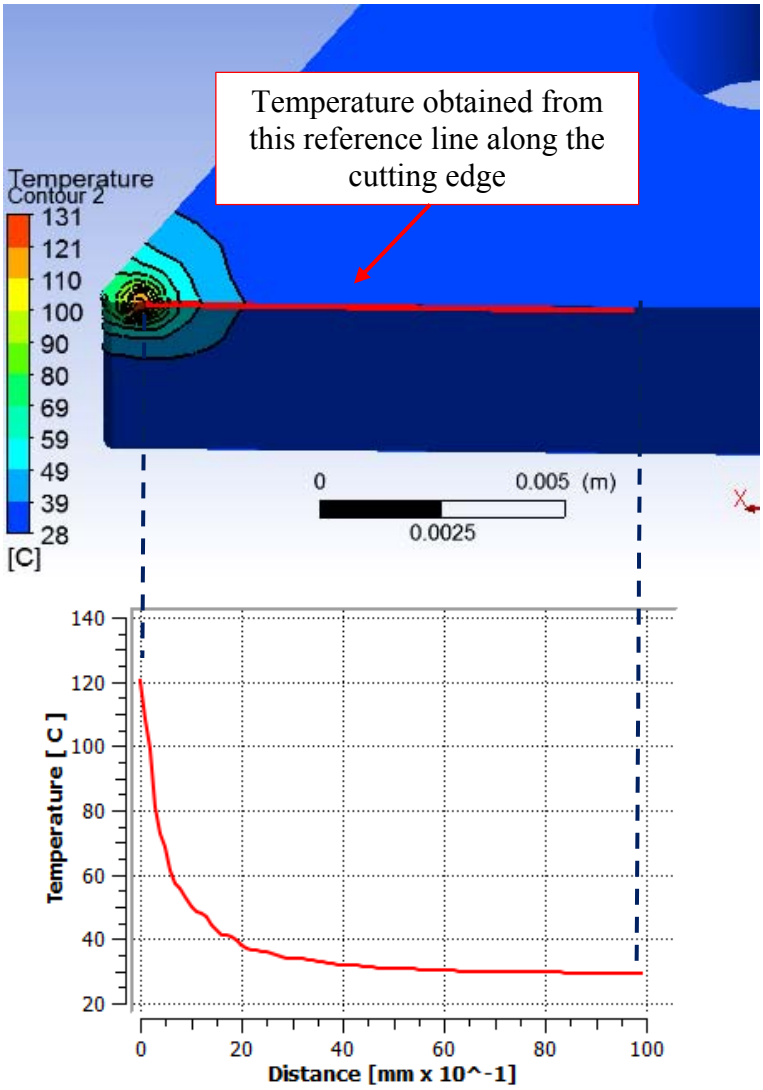

Cutting parameters according to the Expt. 8 of Table 5.4

Figure 5.16: For 1.5 l/min flow rate with AISI1030 workpiece, numerically obtained temperature reduction of the reference line along the cutting edge

By increasing the cutting fluid up to 2.0 l/min flow rate, as shown in Figure 5.17, there is no significant change at the maximum temperature area. The temperature reduction along the reference line is not significantly different compared with the temperature reduction with the cutting fluid at 1.5 l/min flow rate as well. Therefore, it is revealed that the application of cutting fluid at a flow rate higher than 1.0 l/min is not providing much advantage from the heat eliminating point of view. This finding provides the indication of the possibility of reduction of the amount of cutting fluid.

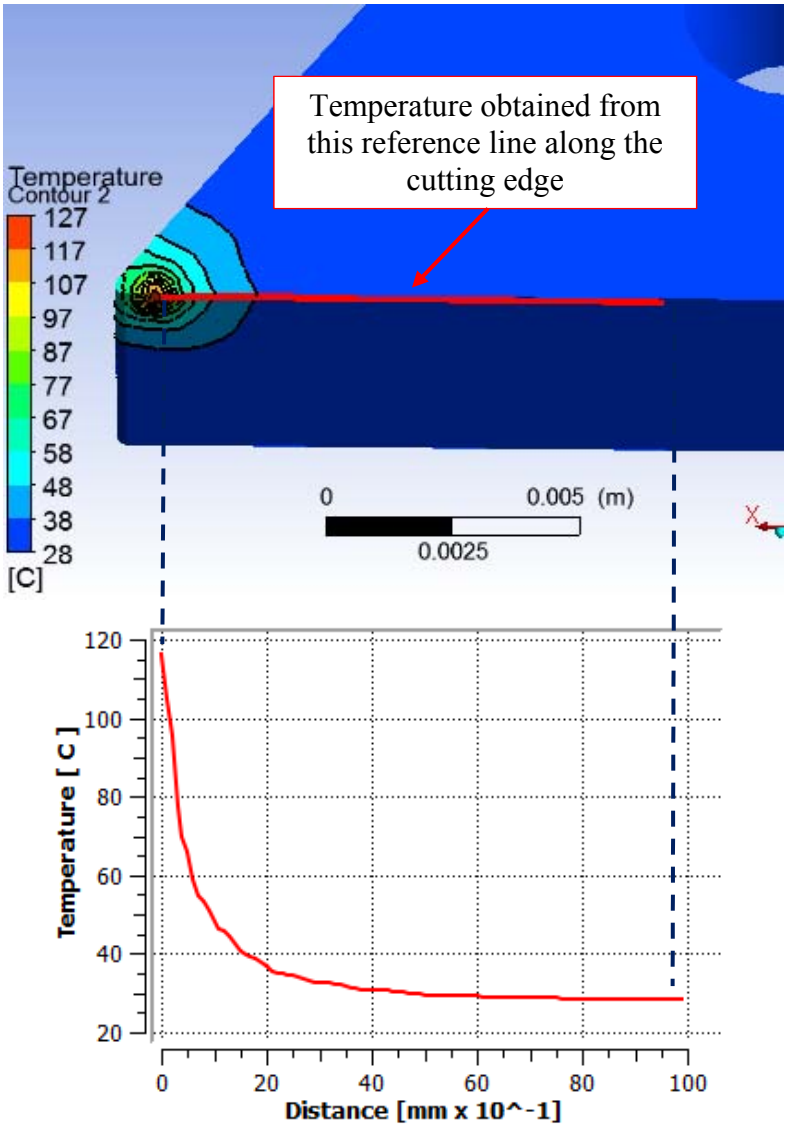

Cutting parameters according to the Expt. 8 of Table 5.4

Figure 5.17: For 2.0 l/min flow rate with AISI1030 workpiece, numerically obtained temperature reduction of the reference line along the cutting edge

A combination of tool temperature data collected for varying flow rates along the reference line is presented in Figure 5.18. This reference line is the same line as shown in Figure 5.1. Similarly, the temperatures are obtained by the numerical analysis considering the parameters of Table 5.4. This figure depicts the reduction of the tool insert temperature against the cutting fluid flow rate from dry condition to 2.0 l/min. The cutting fluid tool is capable of reducing the tool insert temperature significantly with the flow rate of 1.0 l/min.

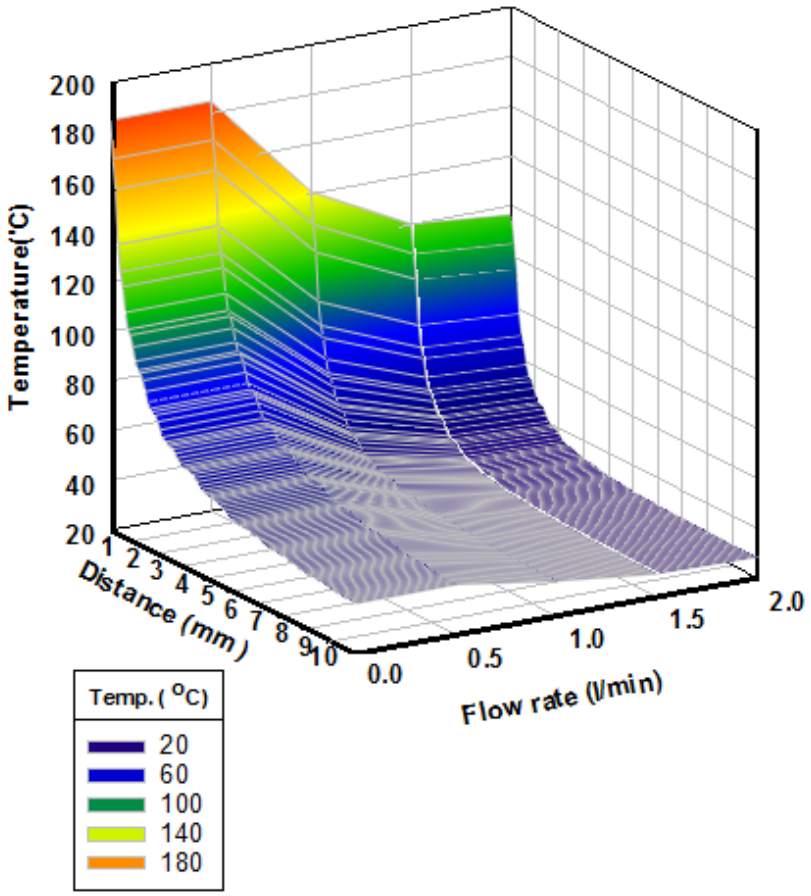

Numerically obtained temperature from the reference line along the cutting edge, considering the parameters of the Expt. 8 of Table 5.4

Figure 5.18: The effect of cutting fluid on the tool insert temperature for varying flow rates with AISI1030 workpiece

The effect of cutting fluid on the tool insert temperature is presented in Figure 5.19. This figure depicts the change of the tool insert temperature due to the variation of cutting fluid flow rate. In all three experiments, Numerical Expt. 7, 8 and 9, there are significant drops of tool insert temperature with the flow rate of 1.0 l/min of cutting fluid. Although, the flow rate increased further up to 2.0 l/min, but the temperature reduction is not significant after the flow rate of 1.0 l/min of cutting fluid. It is revealed that the reduction of the tool insert temperature is not significant between the flow rate of 1.0 and 2.0 l/min of cutting fluid, unless the material removal rate during the machining is very high.

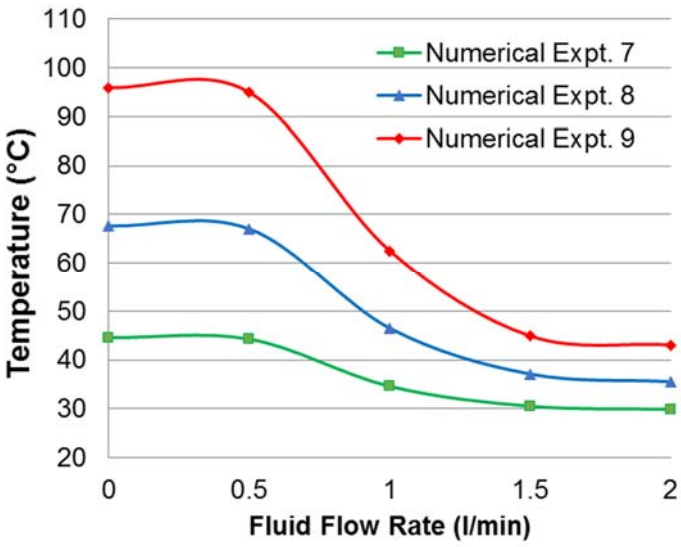

Cutting parameters according to Table 5.4

Figure 5.19: The effect of cutting fluid on the tool temperature for AISI1030 workpiece by numerical analysis

One of the important observations from this study is that, despite the increase of the amount of cutting fluids, the reduction of tool insert domain maximum temperature is not significant after a certain of flow rate. The reason for this phenomenon can be explained as the contact pressure is so high at the tool chip interface that cutting fluids is unable to penetrate and reduce the temperature significantly. The temperatures of the areas away from the cutting zone are reduced by the cutting fluids. From the numerical experiments, it is noticeable that tool temperatures decrease with the distance from the tool-chip interface and the far-regions of the tool become cooler.

Based on this study, it is found that the cutting fluid can reduce the tool temperature by certain percentage. This phenomenon provides the indication regarding the reduction of usage of the amount of cutting fluids. Based on this findings, it is scientifically possible to identify the optimal amount of cutting fluid required for specified cutting condition. The conventional cutting fluids have lower than 350°C of film boiling temperature [242]. Therefore, cutting fluids vaporised at high temperature and this vapour creates a blanket which reduces the heat transfer capability of the cutting fluids. Therefore, it is unlikely to reduce the interface enormously with the application of the cutting fluids. A summary of cutting fluid flow rates used for the

turning operations are presented in Table 5.5. This summary indicates that the flow rates of the cutting fluid significantly fluctuate in the machining industry.

Table 5.5: Summary of Cutting Fluid Flow Rates for Turning Operations

Researchers	Flow type	Fluid Flow Rate
Drozda and Wick [240]	Flood	19.0 l/min
Ginting et al. [243]	Flood	12.0 l/min
Diniz and Micaroni [244]	Flood	11.0 l/min
Kamata and Toshiyuki [245]	Flood	3.7 l/min
Ezugwu et al. [246]	Flood	2.7 l/min

For instance, the recommended cutting fluid flow rate for turning operations by SME handbook on Machining [240] is 19.0 l/min. Therefore, a large quantities of cutting fluid would be wasted if these recommendations are followed through. The obtained results from the numerical experiments have demonstrated that the proposed methodology is capable of reflecting the effect of the cutting fluid on the tool temperature. In addition, the methodology also capable of identifying the optimal flow rate. According to this analysis, the cutting tool temperature is highest for the dry condition and the tool temperature starts to decrease with the application of the cutting fluid. After a point, the reduction of tool temperature is marginal in spite of increasing the cutting fluid flow rate further.

5.3 Pareto ANOVA analysis

By applying the proposed methodology, it is also possible to obtain the temperatures of the tool insert for variety of cutting conditions. The Pareto ANOVA analysis is presented using the temperatures obtained from the model for varying cutting conditions. Taguchi method is a kind of statistical technique which is known as Design of Experiments (DOE), in addition, with Taguchi method, it possible to identify the effect of the factors and this method reduces the number of experiments [247]. Pareto ANOVA is known as a simplified analysis of variance method that uses Pareto principles and this method is a quick and easy way to analyse the results of the parameter design [247]. Pareto ANOVA analysis is presented for varying cutting conditions, and the use of the Taguchi method and Pareto ANOVA analysis is noticeable in the literature [248-250]. Alagumurthi et al. [251] evaluated that factorial

design of experiment and orthogonal array design are used in the design of experiments for process optimisation. Factorial designs are broadly applied in the experiments with several factors for identifying the main factor and the interaction [252]. Taguchi method is suitable for the metal cutting problems [253], [254]. Taguchi method with orthogonal arrays provides the best results with less number of experiments and save time and cost of experimentation [255]. The analysis is designed by following the Taguchi's orthogonal array. The orthogonal array selected for the experiment has two levels and three parameters. The values of the control parameters and levels are presented in Table 5.6.

Table 5.6: Control Parameters and their Levels for Cutting Fluid Flow Rate for 0.0 to 1.0 l/min

Control Parameters		Levels		
	Unit	Symbol	Level 0	Level 1
Fluid Flow Rate, C_F	l/min	A	0.0	1.0
Cutting Velocity, V_c	m/min	B	87	178
Feed Rate, f	mm/rev	C	0.11	0.22

The analysis is divided into two parts. The first part of the analysis is conducted considering machining under dry condition and for 1.0 l/min flow rate of cutting fluid. The second part of the analysis is conducted considering the flow rate 1.0 and 1.5 l/min flow rate of cutting fluid. The reason of selecting 1.5 l/min of flow rate was narrowing down the flow rate from 2.0 l/min. In each of the analysis, the contributions from the cutting fluid toward the tool temperatures are identified. At the end, the contributions from each analysis are compared to understand the variation of the contribution of the cutting fluid based on flow rates.

The proposed methodology is used to obtain the temperature at the same position where the thermocouple was inserted for the tool temperature measurement experiment in the machining laboratory. The input values for the model were calculated according to the cutting parameters and the tool cooling condition i.e. dry or fluid flow rate were selected accordingly. The numerically obtained temperatures for the particular cutting conditions are presented in Table 5.7.

Table 5.7: Numerical Temperature for Dry Condition and 1.0 l/min Flow Rate of Cutting Fluid

	Control Parameters			Numerical Tool Temp (°C) at Thermocouple Location
	Fluid Flow Rate, C_F	Cutting Velocity, V_c	Feed Rate, f	
	A	B	C	
1	0.0	87	0.11	112
2	0.0	87	0.22	179
3	0.0	178	0.11	203
4	0.0	178	0.22	340
5	1.0	87	0.11	63
6	1.0	87	0.22	92
7	1.0	178	0.11	105
8	1.0	178	0.22	169

Pareto ANOVA analysis for dry condition and 1.0 l/min flow rate of cutting fluid is presented in Table 5.8. According to the analysis, cutting fluid, (A), has most significant contribution (42.9%) on the tool temperature. Subsequently, cutting speed, (B), has 35.2%; and feed rate, (C), has 21.5% contribution.

Table 5.8 Pareto ANOVA Analysis for Dry Condition and 1.0 l/min Flow Rate of Cutting Fluid by Numerically Obtained Temperature

Sum at factor level	A	B	C	AxB	AxC	BxC
0	-182.82	-161.30	-163.54	-172.04	-172.10	-170.91
1	-160.24	-181.76	-179.52	-171.02	-170.97	-172.16
Sum of squares of difference (S)	509.71	418.49	255.21	1.04	1.28	1.57
Contribution ratio (%)	42.93	35.25	21.49	0.09	0.11	0.13
	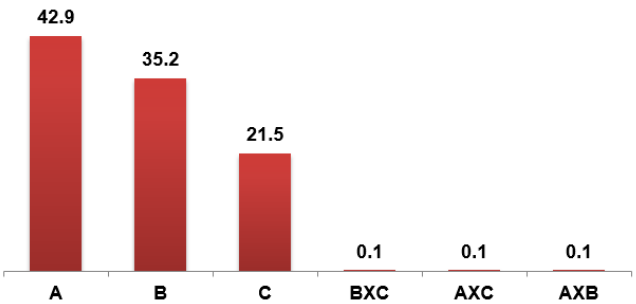					
Cumulative contribution	42.93	78.18	99.67	99.80	99.91	100.00

The second part of the analysis is conducted considering the flow rate 1.0 and 1.5 l/min flow rate of cutting fluid. The two-level three-parameter orthogonal array is selected for the experiment. The control parameters and levels are selected accordingly. The values of the control parameters and levels are presented in Table 5.9.

Table 5.9: Control Parameters and their Levels for Cutting Fluid Flow Rate of 1.0 to 1.5 l/min

Control parameters	Unit	Levels		
		Symbol	Level 0	Level 1
Fluid Flow Rate, C_F	l/min	A	1.0	1.5
Cutting Velocity, V_c	m/min	B	87	178
Feed Rate, f	mm/rev	C	0.11	0.22

Similarly, the proposed methodology is used to obtain the temperature from the same position where the thermocouple was inserted for the tool temperature measurement experiment in the machining laboratory. The input values for the model were calculated according to the cutting parameters; and the flow rates were selected accordingly. The obtained temperatures for the particular cutting conditions are presented in Table 5.10.

Table 5.10: Numerical Temperature for Cutting Fluid Flow Rate of 1.0 to 1.5 l/min

	Control Parameters			Numerical Tool Temp (°C) at Thermocouple Location
	Fluid Flow Rate, C_F	Cutting Velocity, V_c	Feed Rate, f	
	A	B	C	
1	1.0	87	0.11	63
2	1.0	87	0.22	92
3	1.0	178	0.11	105
4	1.0	178	0.22	169
5	1.5	87	0.11	58
6	1.5	87	0.22	79
7	1.5	178	0.11	82
8	1.5	178	0.22	141

Pareto ANOVA analysis for 1.0 and 1.5 l/min flow rate of cutting fluid is presented in Table 5.11. According to the analysis, cutting speed, (B), has most significant contribution (54.5%) on the tool temperature. Subsequently, feed rate, (C), has 37.9% contribution. But cutting fluid, (A), has less significant contribution, only 5.7%. It is revealed that the contribution of the cutting fluid is significantly low when the flow rate is between 1.0 and 1.5 l/min compared with the machining condition when the flow rate is between 0.0 and 1.0 l/min.

Table 5.11: Pareto ANOVA analysis for Cutting Fluid Flow Rate of 1.0 to 1.5 l/min for Numerical Temperature

Sum at factor level	A	B	C	AxB	AxC	BxC
0	-160.24	-148.48	-149.96	-158.20	-157.38	-155.93
1	-154.48	-166.24	-164.77	-156.52	-157.35	-158.80
Sum of squares of difference (S)	33.20	315.36	219.48	2.82	0.00	8.23
Contribution ratio (%)	5.73	54.46	37.90	0.49	0.00	1.42
	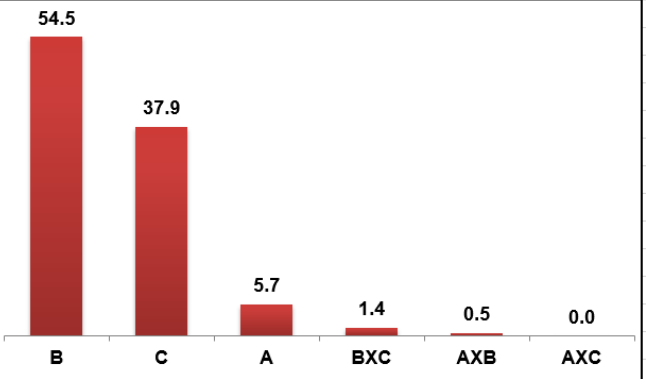					
Cumulative contribution	54.46	92.36	98.09	99.51	100.00	100.00

5.4 Concluding Remarks

This chapter demonstrated an application of the proposed methodology to understand the effect of the cutting fluid on the tool temperature distributions. A reference line was considered on the cutting edge and temperatures were obtained alone this line for varying cutting fluid flow rates. The variation of the temperatures along the reference line demonstrated the effect of the cutting fluid flow rate on the tool temperatures. From the analysis, it is established that reduction of the amount of cutting fluid is possible for machining operations. There are several significant findings from this chapter which are:

- The proposed methodology is a new way of predicting the tool temperature distributions for both dry and flood conditions. It is demonstrated that the temperature variation for any location of the tool is predictable by applying the proposed methodology.
- The reduction of tool temperature along the reference line is initially high, but with the increase of the amount of cutting fluid, the reduction of tool temperature is not significant after a specific flow rate. Therefore, this flow rate is sufficient to decrease the tool temperature and application of cutting fluid can be reduced by not exceeding the flow rate over this specific limit.
- For a clear understanding, the numerical investigations were conducted case by case and the effect of the fluid flow rate on tool temperatures was identified for particular machining parameters. In all the cases, the similar trend is found which confirms the consistency of result of the proposed methodology.
- By applying the methodology, the tool temperatures were obtained for variety of cutting conditions and analysed with the Pareto ANOVA. It is revealed that the contribution of the cutting fluid toward the tool temperature is significantly low for the flow rate between 1.0 and 1.5 l/min compared with the contribution of the flow rate between nil (dry condition) and 1.0 l/min.
- The amount of cutting fluid currently used in the industry for some turning operations is as high as 19.0 l/min. The numerical experiments with the proposed methodology indicated that a significant reduction of the cutting fluid is possible by selecting the optimal flow rate. The optimal flow rate is identified close to 1.0 l/min by the numerical analysis in most of the cases.

Chapter 6

Machining Performance Test with Reduced Amount of Cutting Fluid

6.1 Introduction

Applying the proposed methodology, it was revealed that the amount of cutting fluid used in the industry for turning operations is higher than the amount required to reduce the tool temperature. In Chapter 5, it was demonstrated that reduced amount of cutting fluid is capable of decreasing the tool temperature to a satisfactory level. However, it is essential to know the effects of the reduced amount of cutting fluid on the machining performance. In other words, additional knowledge is necessary to understand the effects of the reduced amount of cutting fluid on the machining performance. Therefore, in this chapter, experimental investigations are presented to demonstrate the effects of reduced amount of cutting fluid on the machining performance. More specifically, the objective of the experimental investigations is to identify the effects of the reduced amount of cutting fluid on tool wear, surface roughness, cutting forces, cutting power etc.

In the present experimental study, cutting force and cutting power consumption were measured to identify the effects of cutting fluid flow rates during the metal cutting. In addition, tool wear and surface roughness were measured to identify the effects of the reduced amount of cutting fluid on the machining quality. The experimental procedure to measure the machining performance is presented in details. The results of the experiments have been analysed and comparisons are graphically presented for cutting force requirement, tool wear, surface roughness and power consumptions under dry and with reduced amount of cutting fluid. Finally, the significant findings are highlighted in the conclusion section of this chapter.

6.2 Tool Life

There are a number of factors that influence the tool life but in most cases tool wear is used for the determination of the tool-life. Zhao et al. [256] accentuated that tool life predominantly depends on the tool wear. Tool life is the period of time when a tool is able to machine work material by maintaining the desired machining qualities of the

operations. It is noteworthy that a high level of productivity and quality is highly desirable for the manufacture parts [257]. Therefore, a tool can become unusable due to lack of delivering desired machining qualities, although it is capable to continue machining. As a result, a tool should be removed from the machining operation before it is unable to remove work material. Thus, "total time to failure" or "volume of work material removed to failure" is not much meaningful without these conditions. Similarly, "total length of tool path to failure" or "the number of components produced to failure" is more significant for machine tool operators rather than tool researchers. The tool life depends on the work material, tool material, tool geometry, cutting condition i.e. cutting speed, feed rate and depth of cut, condition of the machine etc. In addition, it is worth mentioning that cutting fluid has an important role on tool life [258].

The most primitive tool life equation was proposed by Taylor which is as following Equation 6.1:

$$V_c \, T^n = C \tag{6.1}$$

where, cutting speed is represented by V_c , T is the tool life, the letter n and C represent constants which can be found by experiment or from published data for specific workpiece and tool material. Despite the number of variables in the equation is limited and heavily dependent on the constants, Taylor's equation was used in some cases, but one of the limitations of the Taylor's formula is that the constants are specific workpiece and tool material. Kronenberg [259] highlighted that the Taylor formula does not always represent tool life for newer metal such as high temperature alloys. Therefore, lack of essential variables provided the opportunity for other researchers to improve the Taylor's equation.

Many researchers developed tool wear/tool life model based on Taylor's equation. Wang and Wysk [260] proposed the use of empirical approaches for the expanded Taylor tool-life equations and quoted the following Equation 6.2 for their expert system for machining data section research:

$$V = C_1 / T^m \, . \, D^x \, . \, F^y \, . \, (BHN/200)^n \tag{6.2}$$

where, V is the cutting speed in mm per minute; T is the tool life in minute; F is the feed rate, mm per revolution; BHN is the material hardness, bhn; D is the depth of cut in mm; and m, x, y, n, C_1 are equation constants. Therefore, the empirical approach for the expanded Taylor tool-life equations studied by Wang and Wysk [260] is also consist of several equation constants.

Nagasaka and Hashimoto [261] proposed the tool life equation where the cutting parameters and the tool wear amount are independent variables. Their model is able to fit in three stages of tool wear (a) initial rapid wear (b) little wear at the middle and (c) rapid final wear and catastrophic wear. For validation, the authors compared against multiplication and polynomial models and the applied for optimum cutting process. As shown in Figure 6.1b, the authors assumed that $t = T_o$, where T_o represents critical cutting time and expressed the relationship between V_B and t by the following Equation 6.3:

$$t = T_o \exp [-\exp (b)\ V_B{}^n] \tag{6.3}$$

where, n and b represent constants and expressed T_o as following Equation 6.4:

$$T_o = a\ V^{n_1}\ f^{n_2} \tag{6.4}$$

where, a, n_1 and n_2 represent constants, the cutting velocity represented by V and feed rate represented by f. The authors also ignored the role of depth of cut considering that it has negligible effect on tool life.

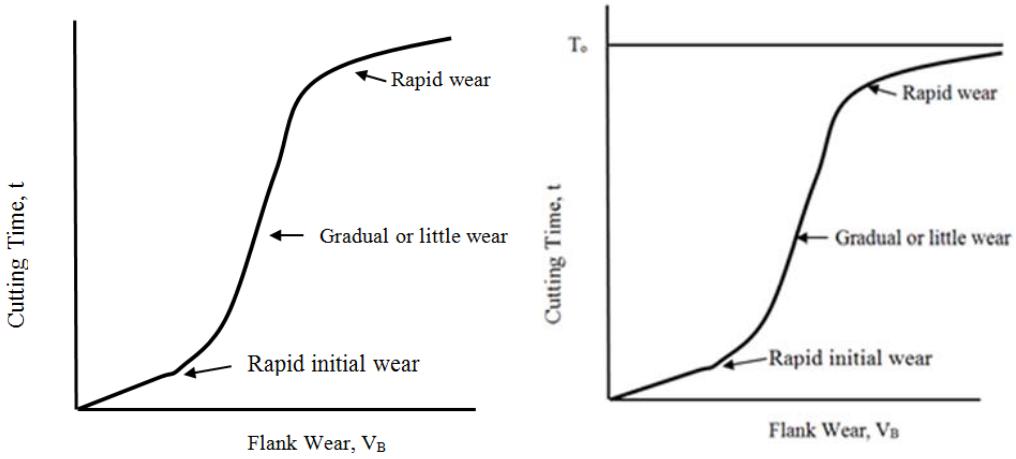

(a) (b)

Figure 6.1: The tool wear process curve, (a) Ordinary curve and (b) Approximate curve, adopted from [261]

Jawahir et al. [262] developed a tool-life equation for the groove including the tool coating effect that is expressed as following Equation 6.5:

$$T = T_R\ W_g\ (V_R / V)^{Wc\ .\ 1/n} \tag{6.5}$$

where, T represents the tool life; T_R represents the reference tool life; V represents cutting velocity; V_R represents the reference cutting velocity; W_c represents the factor for tool coating and can be expressed as Equation 6.6:

$$W_c = n / n_c \tag{6.6}$$

n_c represents the coating effect factor and W_g represents the chip grove effect factor and can be expressed as following Equation 6.7:

$$W_g = km / f^{n1} d^{n2} \quad (6.7)$$

where, f represents the feed; d represents the depth of cut; m represents machining type, for turning operation, m=1; and k, n_1 ,n_2 are empirical constants. Likewise, the tool-life equation developed by Jawahir et al. [262], for the groove including the tool coating effect, is based on several empirical constants as well. Therefore, the tool life equations are either heavily dependent on the constants or the equations are applicable only for very specific conditions. As a consequence, Dolinšek et al. [263] emphasised that making a reliable prediction of the tool life is difficult in spite of having a lot of information and experiences available. These aspects make necessary measuring tool wear by experimental procedure and identify the real tool life.

6.3 Tool Wear

Tool wear can be described as an erosion or deformation of the tool due to friction from its original shape performed by machining operations. A tool becomes unusable due to wear. Researchers are constantly trying to improve the tribological condition of the metal cutting. Astakhov [110] concluded that the methods of improvement can be divided into two categories (a) component methods and (b) systemic methods. The component methods can be further divided into (a) cutting tool and (b) workpiece. The examples of the cutting tool improvements are coating of the cutting tools, polishing of the rake and flank surface and improving the micro geometry of the cutting edge. The most of the tools used for the machining are coated, although there is an additional cost involve to put the coating on the cutting tool [264]. The composition of the coating may vary enormously. The coating can comprise with 1-2 nm thick few thousands of layers [265]. Multiple layers of thin coats, rather than on thick coat, provide more stable tool [266] and multi-layer provides better resistance against crack growth [267]. A coating behaves like a thermal barrier as it has low thermal conductivity. The performance against wear is not the same for all coatings, some are better than other [268].

The examples of the workpiece improvements are altering the properties of the workpiece by heat treatment, reducing the strain to fracture the workpiece by sulphur, lead etc. and changing mechanical properties by changing chemical composition. The systemic methods can be further divided into (a) application of the cutting media (b)

alternation of the properties of the layer being removed by preheating and plastic deformation before machining, and (c) introducing forced vibration for better penetration of the cutting fluid. However, cutting fluid is the most widely used method for the improvement of the tribological condition in the metal cutting [110].

Tool wear increases the possibility of chatter and low dimensional accuracy [269]. Cutting fluid reduces the vibrations of the machine tool [270]. Hence, tool wear is so important that monitoring the cutting tool wear is crucial for the automation of the manufacturing process [271]. Tool deterioration in the form of wear is used for determine the tool-life. The ISO 3685 [272] highlighted that tool life is the cutting time required to reach a tool-life criterion, where tool-life criterion is a predetermined threshold value of a tool wear measure or the occurrence of a phenomenon.

The flank wear progression and flank wear zones on turning inserts are shown in Figure 6.2 and Figure 6.3 accordingly. In general, the flank wear land has uniform width at the Zone B. It is relatively easy to measure the width of the flank wear. This is one of the reasons why flank wear is widely used in determining tool wear. The development of the flank wear also depends on the tool materials. The rate of development also varies with time as the flank wear rate is higher at the initial stage. For sintered carbide tools, if the flank land wear is regular in the Zone B, average width of the wear land VB_B should be less than 0.3 mm. If the flank wear is not regular in the Zone B, maximum width of the wear land VB_B should be less than 0.6 mm [272]. Tool temperature is also influenced by the tool wear as it is experimentally established that there is relationship between the tool wear and embedded thermocouple reading located in the cutting tool insert [175]. There are several procedure to measure the tool wear. The classifications [273] of tool wear sensing methods are presented in Figure 6.4 and Figure 6.5.

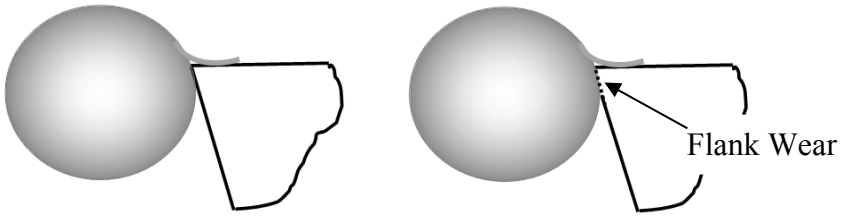

(a) Before (b) After

Figure 6.2: The flank wear progression during turning operations

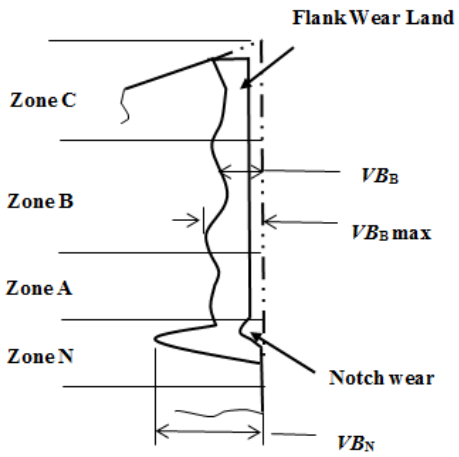

Figure 6.3: The flank wear and notch wear on turning inserts, adopted from [272].

The surface finish of the machined part may be effected due to wear and the accuracy of finished part can be decreased. Tool wear may influence the machining cutting forces and cutting temperatures. In some cases, the cutting edge of the tool insert may break as well. In materials science, wear can be measured as material volume loss. The weight loss of the material can be another method for the expression of wear but may not be applicable across the industry due to different densities of materials.

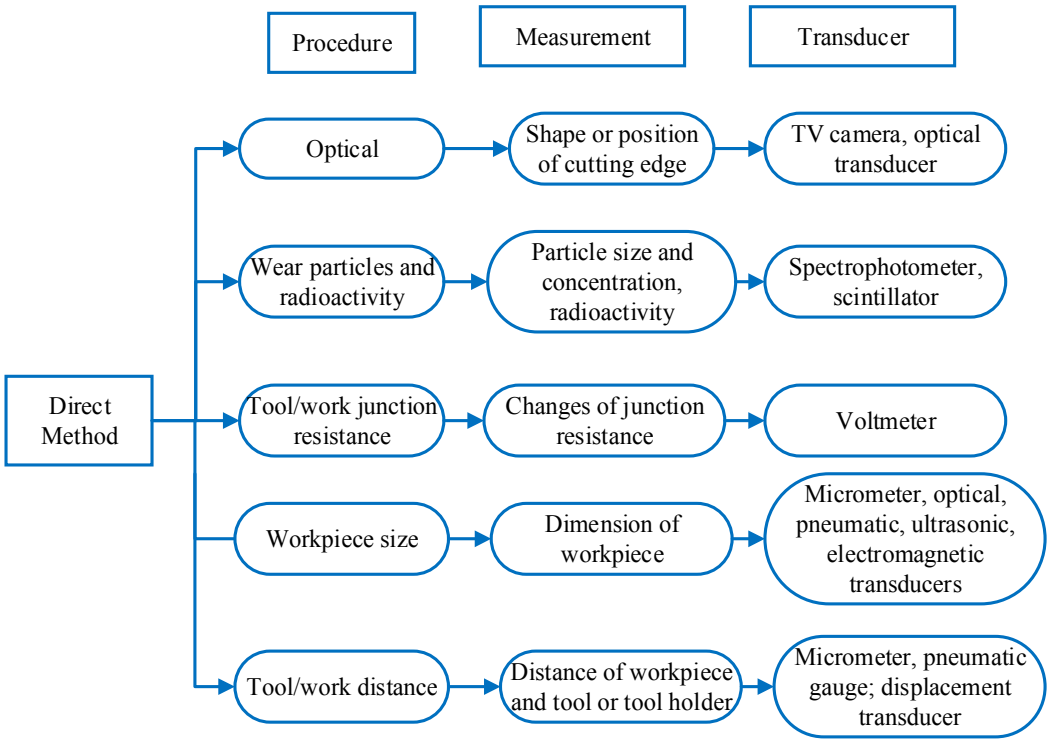

Figure 6.4: Tool wear sensing by direct methods, adopted from [273]

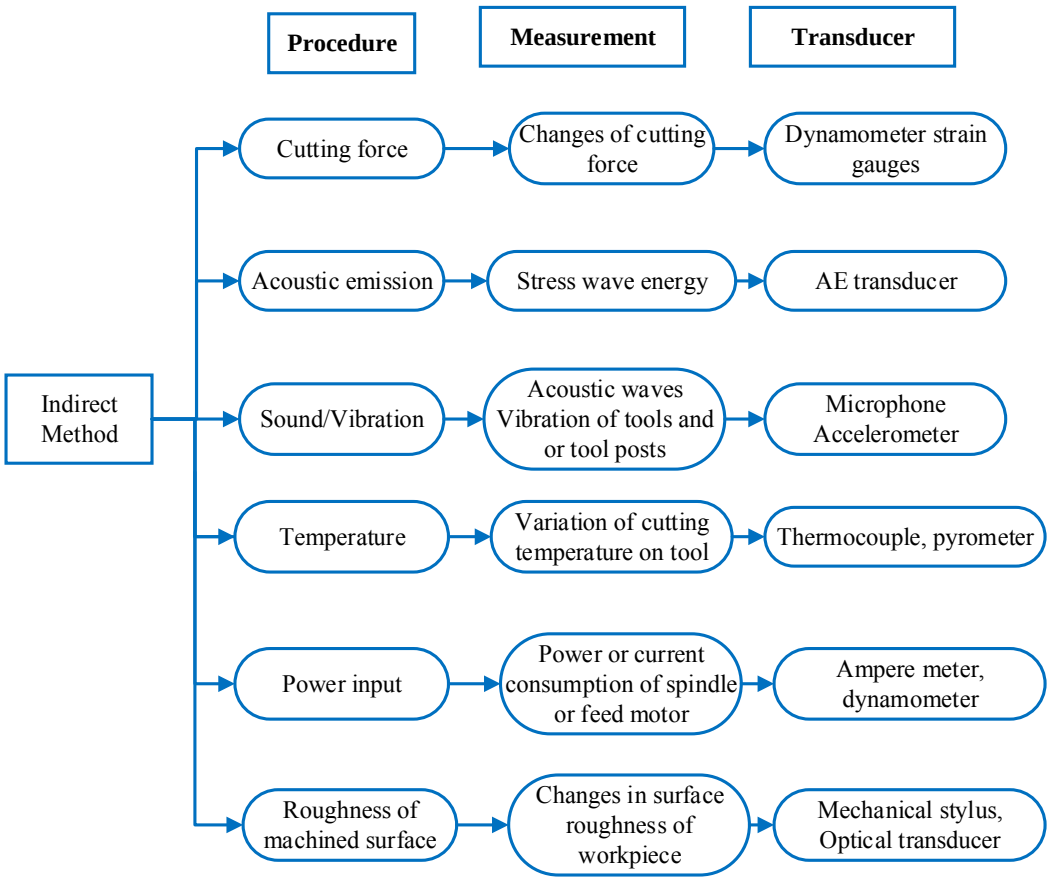

Figure 6.5: Tool wear sensing by indirect methods, adopted from [273]

6.4 Surface Roughness

One of the important machining qualities is surface finish or surface roughness as the quality of the machined product is expressed by the surface finish. Although, for some products require grinding or polishing but the surface defects and cost can be minimised by keeping the surface roughness as low as possible. There is a relationship between the surface roughness and the feed rate. A better surface finish can be achieved from the lower feed rate [274]. Dhar et al. [70] emphasised that one of the major reasons of the surface roughness is the feed marks left by the tool tip on the finished surface of the workpiece. Another reason is the deformation of the auxiliary cutting edge due to wear, chipping or fracturing.

More elaborately, Arbizu and Perez [275] emphasised that the obtained surface finish from a manufacturing process is the combination of (a) the ideal surface finish

due to the marks during manufacturing process on the surface of the product and (b) the surface finish due to the irregularities or deficiencies that usually appear during the process. The authors also concluded that obtaining the theoretical surface roughness for manufacturing processes is not allowed as the defects, appearing on machined surfaces, depend on deficiencies and imbalances in the process. Similarly, Wang and Feng [276] emphasised that the investigators were divided on their opinion with the role of cutting speed on surface roughness. Some of the investigators concluded that the effect of cutting speed on surface roughness is insignificant. On the other hand, some investigators demonstrated that cutting speed has a significant impact. Therefore, in the present study surface roughness was measured by experimental method to understand the effect of the reduced amount of cutting fluid on the surface roughness. The other reasons behind surface roughness are vibration of the machining system, build up edge formation etc.

There are several roughness parameters. The most widely used roughness parameter is R_a which is the arithmetic average of the absolute values. According to ISO 4287 [277], the arithmetic average can be estimated from the following Equation 6.8:

$$R_a = \frac{1}{L}\int_0^L |Y(x)|\, dx \qquad (6.8)$$

where, R_a represents roughness (the arithmetic average), Y represents the vertical deviation and L represents the measured distance.

6.5 Experimental Work

The experimental investigations were conducted to identify the effects of the reduced amount of cutting fluid on cutting forces, tool wear, surface roughness, cutting power etc. The details of the experimental work is described in the following sections.

6.5.1 Machine Tool Setup

For this experiment a Harrison Lathe Alpha I400XS 600 group and a three-phase electric power motor was installed with the lathe. The cutting tool was a tungsten carbide turning insert which was attached with a tool holder for machining. The schematic diagram of the experimental setup is shown in Figure 6.6. The specifications of the machine tool for machining time experiments are presented in Table 6.1.

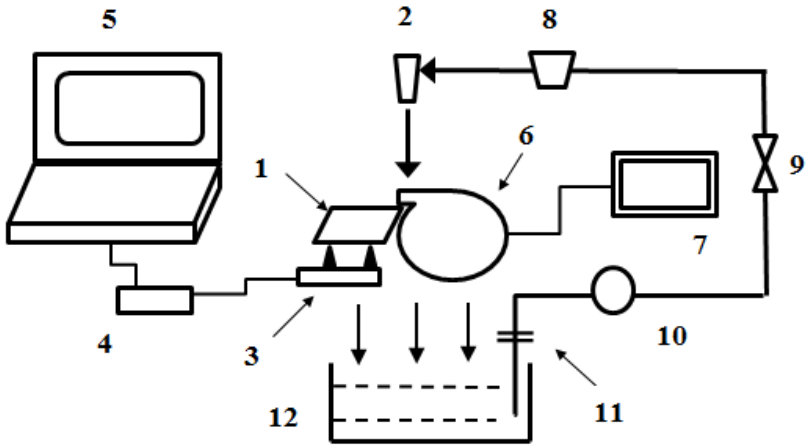

1. Tool insert, 2. Nozzle, 3. Dynamometer, 4. Control Unit for Dynamometer, 5.Computer, 6. Workpiece, 7. Power analyser, 8. Flowmeter, 9. Control valve, 10.Pump, 11. Filter and 12. Coolant tank

Figure 6.6: The schematic of experimental setup for machining performance

The present study involves turning of AISI 4140 alloy steel as a workpiece under a selected cutting condition. The basis composition of AISI 4140 is Cr, Mn, C and Mo at 0.80 %, 0.82 %, 0.40 % and 0.15 % by weight. The length of the bar was 600 mm with a diameter of 60 mm. The tool cooling environments were dry and conventional flood cooling. A commercially available oil based cutting fluid was used for flood cooling process. The flow meter to measure the cutting fluid flow rate was attached with the Harrison Lathe Alpha I400XS 600 is shown in Figure 6.7.

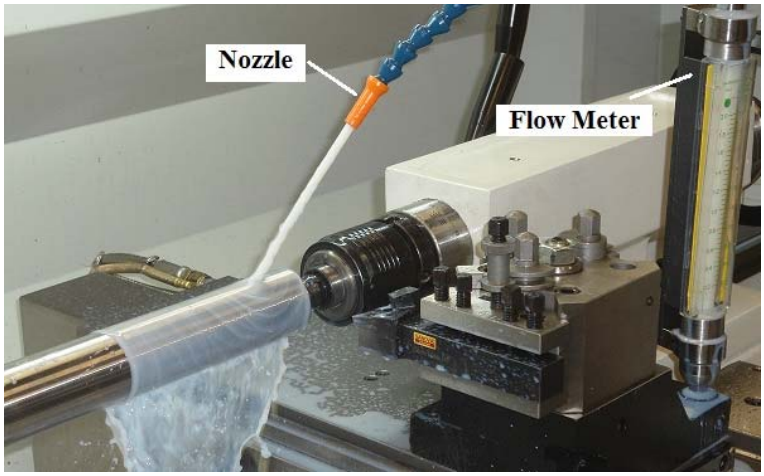

Figure 6.7: The flow meter to measure the cutting fluid flow rate

Table 6.1: Specifications of the Machine Tool

Machine tool	Harrison Lathe Alpha I400XS 600
Work specimen	Steel Alloy
Materials	AISI 4140 Steel
Size	Cylindrical Dia. 60 X 600 mm
Cutting Tool	Carbide Turning Insert
Insert	SNMA 432A SC 1519
Coating	CVD
Nose radius	0.8 mm
Tool holder	PSDNN 2525 M12
Working tool geometry	Angle of inclination: -6
	Rake angle (valid with flat insert): -6
	Entering angle: 45
	clearance angle: 0
Cutting Direction	Neutral
Chip-Breaker	KR
Application	Roughing

6.5.2 Measuring Instrument

The details of the experimental equipment are presented in Table 6.2 and shown in Figure 6.8.

Table 6.2: Experimental Equipment and Cooling Environment

Dynamometer	Kistler 9257BA and Control Unit: 5233A
Optical Microscope	Olympus BX51M
Surface roughness tester	Mitutoyo SJ201
Power Analyser	Yokogawa CW40
Cooling Environment	Dry and Flood

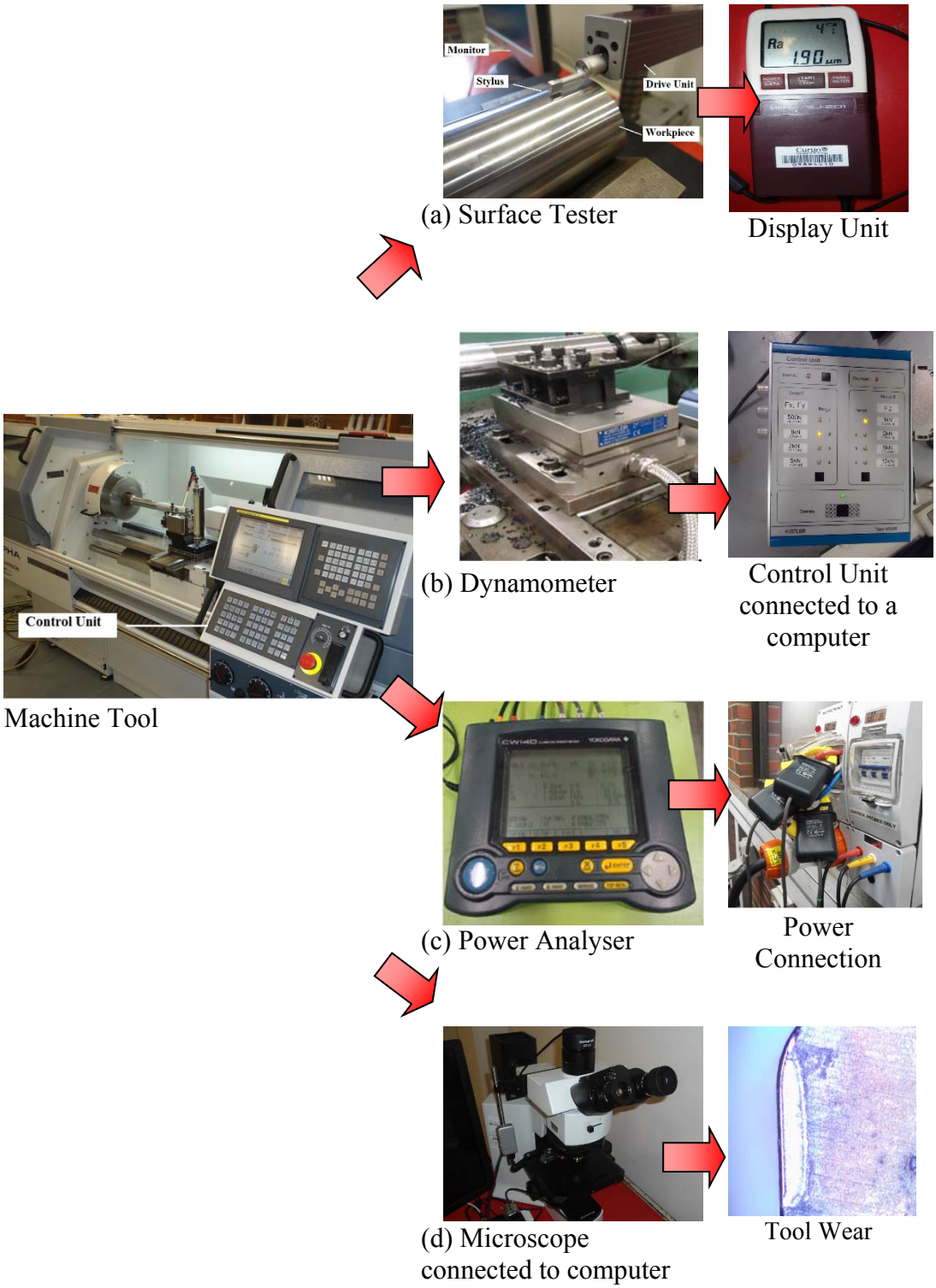

Figure 6.8: The equipment used for machining performance experiments

The surface roughness of the workpiece was measured by a Mitutoyo SJ201 portable surface roughness tester as shown in Figure 6.8a. The cutting force components were measured by a Kistler 9257BA dynamometer which has a high natural frequency and provides precise measurement. The Dynoware software is capable of providing real-time data in numerical and graphical form for the cutting forces. The Dynoware software was installed in a desktop computer which was connected with the control unit. With the help of the control unit, the Dynoware software was used to capture, display and evaluate the forces during machining. The dynamometer measures the three components of cutting force for turning operations. The three components of cutting force were added to obtain the total cutting force. The dynamometer and the control unit which were used for the experiment are shown in Figure 6.8b.

The cutting power consumptions were measured by a Yokogawa CW40 power analyser. Figure 6.8c shows power analyser and the connection of power analyser with the electric motor of the machine tool. The Olympus BX51M optical microscope connected with image capturing software was used to record the tool wear progress in dry and flood with reduced amount of cutting fluid machining conditions. Figure 6.8d shows the optical microscope, Olympus BX51M.

6.6 Results and Discussion

The knowledge of the performance of cutting fluids during machining is highly significant with the purpose of improving the efficiency of the machining process [278]. Sokovic and Mijanović [17] highlighted that the most important characteristics to evaluate a cutting fluid are the tool wear, surface quality, cutting forces, energy consumption etc. Therefore, in the present study, investigations were conducted to identify the influence of cutting fluids on the machining performance such as cutting forces, tool wear, surface quality and power consumption. After conducting the experimental investigations, the effects of reduced amount of cutting fluids on machining performance were analysed. The results from the experiment provided comparisons of cutting force requirement, tool wear, surface roughness and power consumptions for the machining in dry and flood turning operations with reduced amount of cutting fluid.

6.6.1 Effect on Cutting Force

In turning operations, cutting force is one of the important factors that has relation with other parameters such as tool wear or surface finish [279]. Cutting force is correlated with the power consumption of the machining operations. The cutting force depends on cutting speed, feed rate, depth of cut, tool wear and cutting tool material and geometry [280], [281]. In this study, the first set of experiments was in dry condition. The flow rate of the cutting fluid was gradually increased to observe the effect of cutting fluid on the cutting force. The components of the total cutting force for metal cutting in the turning operations are shown in Figure 6.9, which are cutting force F_c; thrust of feed force, *Ft;* and radial force, *Fr.* These components were added to calculate the total cutting force, F_{total}.

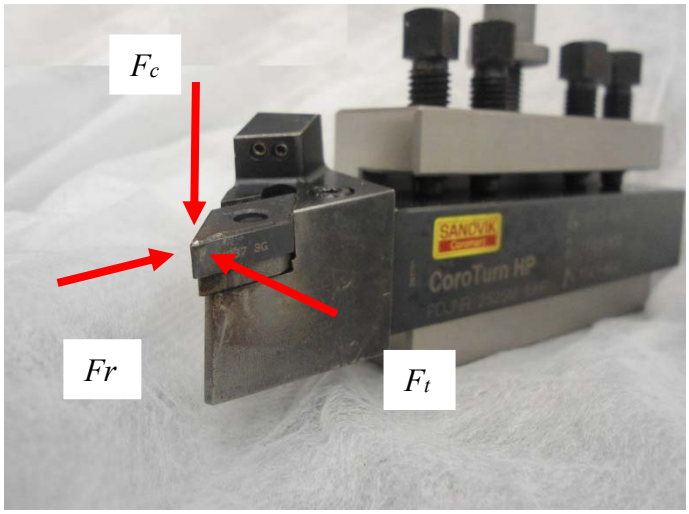

Figure 6.9: The components of the cutting force in the turning operations

Figure 6.10a, b and c show the total cutting force against coolant flow rate at varying cutting speeds. The cutting velocities were 87, 178 and 273 m/min. The feed rates were 0.11 mm/rev, 0.22 mm/rev and 0.33 mm/rev in Figure 6.10a, b and c respectively, where the depth of cut was 1 mm. Although, it may be assumed that cutting fluid always decreases the cutting forces, but this assumption was not upheld by the results of the experiments. In general, the cutting forces initially increased with the application of the cutting fluid at the flow rate of 0.5 l/min; although later decreased at the flow rate of 1.0 l/min in all cases. In addition, it was observed that the cutting forces again marginally increased with further higher flow rates, especially at the flow rate of 2.0 l/min.

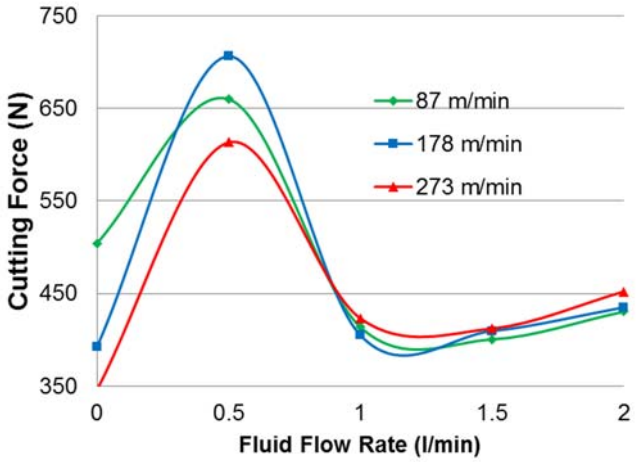

(a)

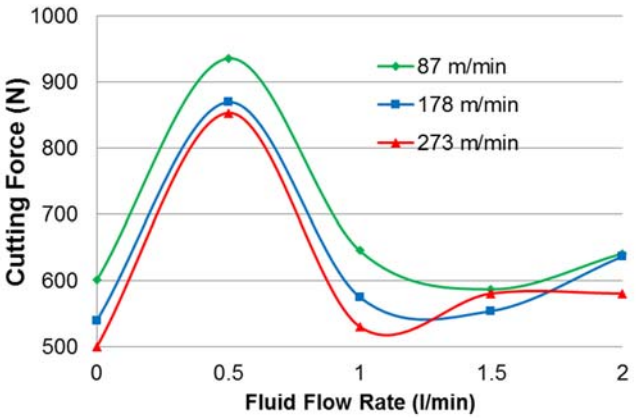

(b)

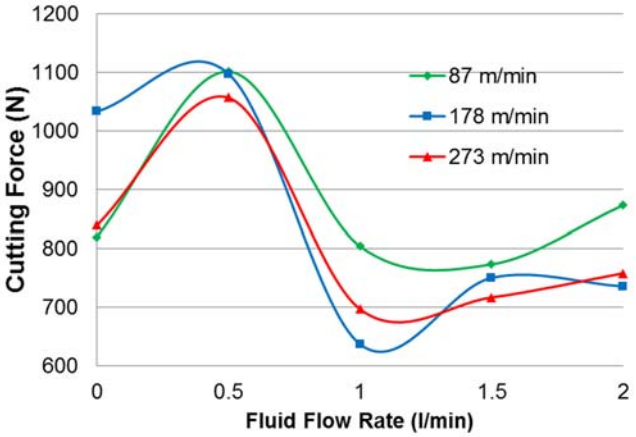

(c)

Figure 6.10: Experientially measured total cutting force against coolant flow rate at varying cutting speeds with 1mm depth of cut and (a) 0.11 mm/rev feed (b) 0.22 mm/rev feed and (c) 0.33 mm/rev feed

Figure 6.11a, b and c show the total cutting force against coolant flow rate with cutting speeds 87 m/min, 178 m/min and 273 m/min respectively. The feed rates were 0.11 mm/rev, 0.22 mm/rev and 0.33 mm/rev and depth of cut was 1 mm. In all the experiments, cutting forces increased with the increase of the feed rates, due to higher volume of material removal rates. In general, the cutting forces initially increased with the application of the cutting fluid at the flow rate of 0.5 l/min. The reason for increase of cutting fluid is that the application of the cutting fluid absorbed some of the heat and made the workpiece little rigid. The cutting forces requirement decreased at the flow rate of 1.0 l/min in all cases. Finally, the cutting forces again marginally increased at the flow rate of 2.0 l/min. It is experimentally found that lubrication property of the cutting fluid does not contribute significantly to reduce the cutting forces during machining as the advantage of lubrication is neutralised by the increase of rigidity of the workpiece. Therefore, it is experimentally established that 1.0 l/min flow rate of cutting fluid is the optimal flow rate in term of cutting forces for these cases.

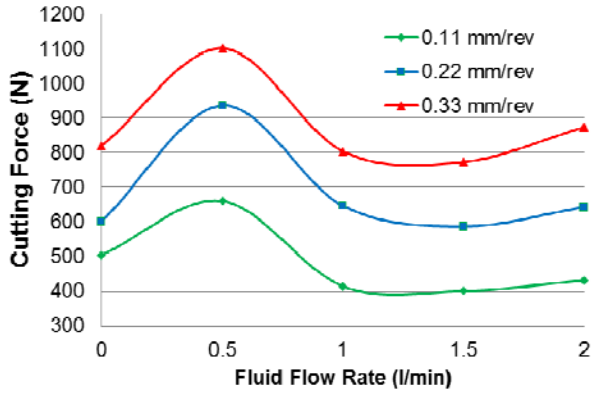

(a)

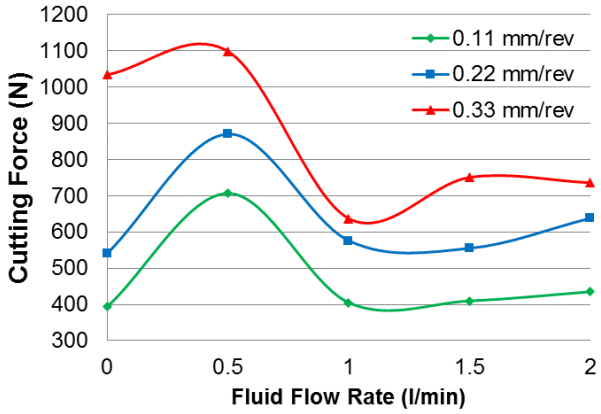

(b)

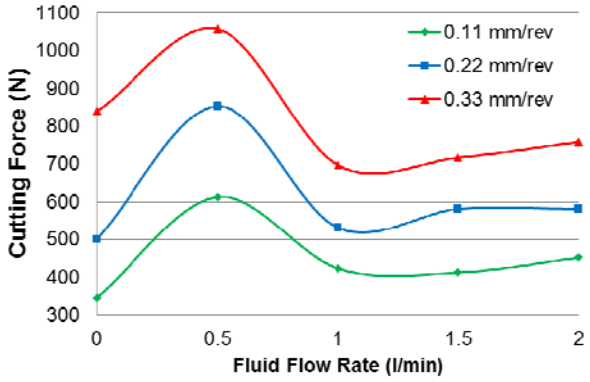

(c)

Figure 6.11: Experimentally measured total cutting force against coolant flow rate at varying feed rates with 1mm depth of cut and (a) 87 m/min cutting speed (b) 178 m/min cutting speed and (c) 273 m/min cutting speed

Further, cutting forces were measured against the machining time with 1.0 l/min flow rate, after establishing that 1.0 l/min flow rate of cutting fluid is the optimal flow rate. Figure 6.12 shows the trend of the experimentally measured cutting force versus machining time in dry and flood with reduced amount of cutting fluid, i.e. flow rate of 1.0 l/min, for turning operations.

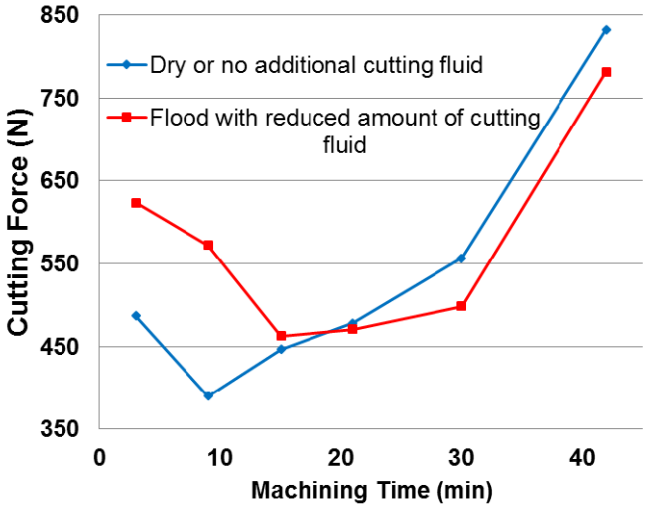

For cutting velocity 226 m/min, depth of cut 1mm and 0.11 mm/rev feed rate

Figure 6.12: The experimentally measured total cutting force versus machining time under dry and flood with reduced amount of cutting fluid

Initially, the requirement of the cutting force was lower in dry turning operations. Likewise, the reason for the cutting force increase is that the cutting fluid removes heat from the cutting zone and makes the work material a little rigid and as a consequence more force is required for flood turning. It was found that cutting force increased with the progression of tool wear which is in line with the study of literature [282].

As the machining time increased, the cutting force increased more rapidly in dry condition compared with the flood turning operations. This is because of the higher tool wear under dry condition requires more force for the turning operation. In both cases, the increasing trend indicates higher cutting force requirement with the progression of the flank wear as the number of cracks on the tool surface increases with the machining time. At the last part of machining, the tool required higher cutting forces to overcome the resistance from the workpieces due to higher tool wear. As the tool wear was higher in dry condition, the cutting force increased rapidly for dry machining at the last part of the machining time.

6.6.2 Effect on Tool Wear

Improving the machining accuracy is one of the optimisation strategies to increase productivity, improve quality and cost reduction [283]. On the other hand, tool wear can reduce the machining accuracy. Several types of cutting tool wear are observed during turning operations such as abrasion, adhesion, diffusion, chemical erosion, galvanic action etc. Out of these, flank wear, crater wear and notch wear are the major types of wear and, particularly, flank wear is used as an indicator of the tool life because flank wear develops uniformly and the measure is more reliable compared to the other types of wear.

In the present study, flank wear was measured to understand the effect of the reduced amount of cutting fluid on the tool wear. As the flank wear progresses with the machining time. The most important type of wear that has drawn constant attention is flank wear [284]. On the other hand, the crater wear based tool-life criterion is the crater front distance and the other criterion is the crater break through at the minor cutting edge. The position of the crater is significant as a narrow crater wear, close to that cutting edge, can reduce the tool-life more aggressively than a distant deep and wide crater. Therefore, the values of the crater centre distance and the crater width are not used as tool-life criteria. Although, minor notch wear was observed along the major cutting edge but the location of the notch wear was outside of the physical contact area

of the tool and work piece. Therefore, the notch wear was not considered as a tool-life criterion. The profile and length of the notch wear depend on the accuracy of the repeated depth settings and the reasons for notch wear occurrence is the work piece hardening due to previous pass of the tool.

The tool life tests are basically tool wear measurements [66]. To understand the influence of reduced amount of cutting fluid on tool wear, the flank wear was measured under dry and flood with reduced amount of cutting fluid condition. Flank wear has been used as an indicator for the tool life in the many tool wear related studies. Therefore, in the present study, flank wear was measured for the tool wear experiment. The flank wear, after 9 minutes of machining, is shown in Figure 6.13 with magnification 50 times. The flank land wear is much higher in dry condition compared with flank land wear in flood machining with 1.0 l/min flow rate.

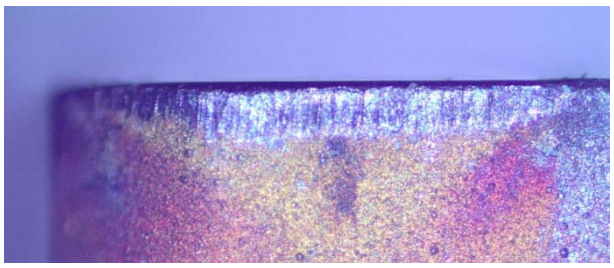

(a)

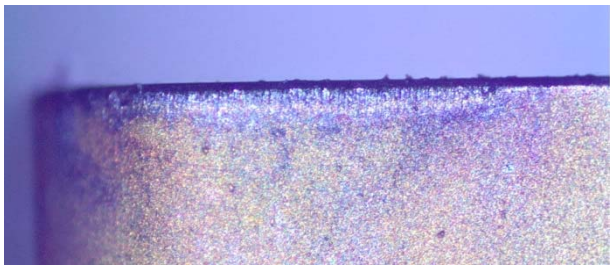

(b)

Magnification 50 times

Figure 6.13: Flank wear of the tool inserts by microscope after 9 minutes of machining (a) Flank wear in dry condition and (b) Flank wear in flood 1.0 l/min flow rate

The progression of the flank wear after 42 minutes of machining with 50 times magnification is shown in Figure 6.14. The flank land wear is clearly higher in dry condition compared with flank land wear in flood turning with reduced amount of cutting fluid. The reason for this is that the cutting fluid provides tribological benefits

during the machining process [278]. The cutting fluid removed the generated heat [285] from the cutting zone and thus reduced the tool wear [81].

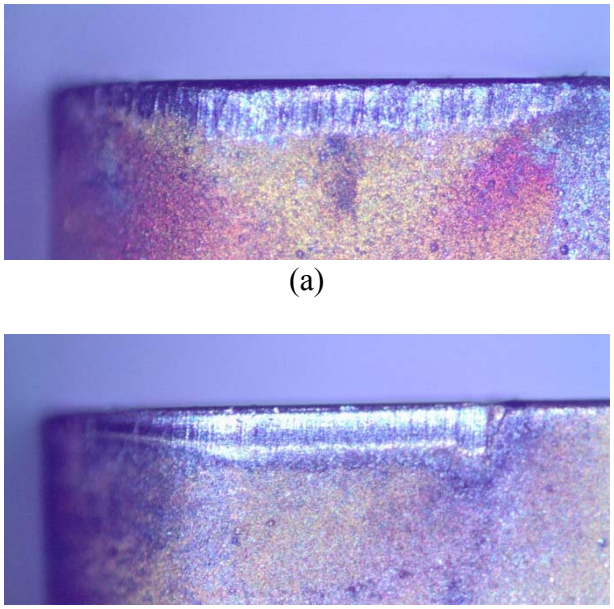

(a)

(b)

Magnification 50 times

Figure 6.14: Flank wear of the tool inserts by microscope after 42 minutes of machining (a) Flank wear in dry condition and (b) Flank wear in flood with 1.0 l/min flow rate

Figure 6.15 shows flank wear under dry and flood with reduced amount of cutting fluid, i.e. flow rate of 1.0 l/min. In both cases, an increasing trend of flank wear is observed over the period of time, but the increasing trend is higher in dry condition due to the higher progression of the flank wear with machining time. A higher rate of flank wear was observed at the beginning of the cutting process. This higher wear rate is known as break-in wear which is caused by attrition and microchipping at the sharp cutting edges [286].

The flank wear is clearly lower with the reduced amount of cutting fluid compared with the dry turning operations. In other words, the reduced amount of cutting fluid was sufficient to decrease the growth of the flank wear on the cutting insert. It is noteworthy that the generated heat is the reason for the formation of the white layer which can generate micro-cracks and micro-hardness variations [287]. Formation of micro cracks due to the high temperature decreases the cohesive bond strength of tool

material. As a consequence, small bits of cutting tool material between the micro cracks are pulled out of the cutting tool. Micro chipping and abrasion are the main reasons of occurring the flank wear during machining. It was observed that the performance of the reduced amount of cutting fluid was sufficient in term of providing lower tool wear than that of in dry condition. The reason for lower tool wear under flood cooling is that the reduced amount of cutting fluid was capable to reduce the high temperatures at the tool interface, thus the thermally induced tool wear was reduced. Because of lower rate of growth of flank wear with reduced amount of cutting fluid, the tool life would be higher as a consequence.

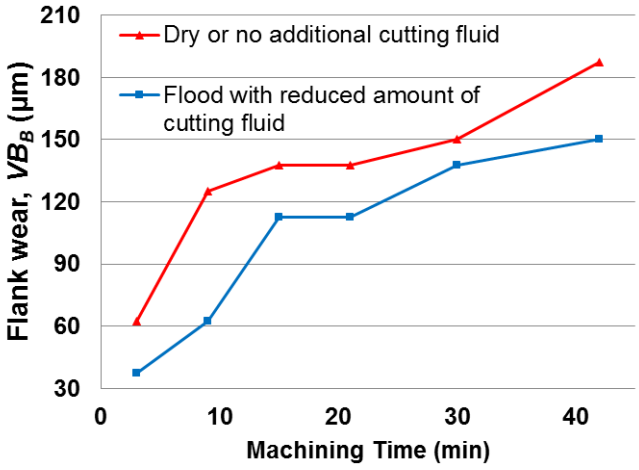

For cutting velocity 226 m/min, depth of cut 1mm and 0.11 mm/rev feed rate

Figure 6.15: Flank wear under dry and flood with reduced amount of cutting fluid

6.6.3 Effect on Surface Roughness

The surface roughness was found lower during flood turning operations with reduced amount of cutting fluid compared to the dry turning operations. Figure 6.16 shows surface roughness of the workpiece versus machining time. In general, an increasing trend is observed over the period of time in both cases. A better surface finish was achieved with reduced amount of cutting fluid, i.e. flow rate of 1.0 l/min, than dry turning operation until 20 minutes of turning. Therefore, the reduced amount of cutting fluid is capable of providing better surface finish than dry condition until this period of time. Cutting fluid can provide better surface finish and increase tool life [208].

Dudzinski et al. [288] reviewed the developments towards dry and high speed machining and highlighted that the generated heat may change the microstructure and create residual stresses. The residual stress can reduce the machined surface quality. In addition, tool wear influences the geometrical, surface and subsurface qualities of the workpiece [289].

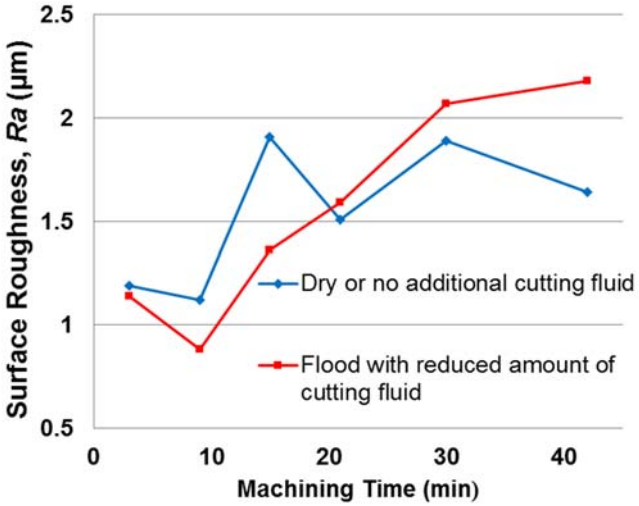

For cutting velocity 226 m/min, depth of cut 1mm and 0.11 mm/rev feed rate

Figure 6.16: Surface roughness of the workpiece versus machining time under dry and flood with reduced amount (1 l/min) of cutting fluid

The surface roughness was marginally higher at the last part due to some irregularities. During the machining operations, the adhesion of the chip material on the cutting tool is the reason of formation of build-up edge. Elevated temperature with the close contact between the tool and the workpiece influence in favour for diffusion of tool material atoms across the tool-workpiece interface [285]. The build-up edge on the cutting tool reduces the machined surface quality. If the chips are hot enough and do not move away from the workpiece before seizing onto the tool, the possibility of formation of build-up edge on the cutting tool is high. For this reason, it is experimentally found that lower cutting speeds provide lower surface quality [290]. The formation of build-up edge may be the reason for marginally higher surface roughness at the last part of the machining with flood cooling. Minor cutting edge and tool corner form the machined surface in the turning operations. The groves on the minor flank effects the roughness of the machined surface. Oxidation of the minor flank can suddenly increase the roughness on the machined surface. This sudden

deterioration of the work piece surface can be used as a tool-life criterion. Therefore, the roughness of the machined surface can be observed to replace the tool as an effect as the groves on the minor flank are difficult to measure. At the last part of the dry machining, surface roughness did not increased significantly. The similar behaviour was observed by Pavel et al. [291] as they found that the value of R_a starts to decrease approximately 15 minutes of machining. They found that while flank wear increases, the values of R_a decreases. Therefore, in continued machining, the surface roughness increased in flood turning operations more rapidly compared with the dry turning operations as the flank wear was higher during dry turning.

Machining experiments were also conducted for turning operations with varying amount of cutting fluid to compare surface roughness. Figure 6.17 shows surface roughness of the workpiece versus cooling environment after 5 min of turning operations. In general, better surface roughness was observed for both flood operations comparted to dry turning operation. Surface roughness was marginally lower with reduced amount of cutting fluid, i.e. flow rate of 1.0 l/min, than 2.0 l/min flood turning operation, although the difference was not substantial. Therefore, the reduced amount of cutting fluid is at least capable of providing similar surface finish compared to higher amount of cutting fluid.

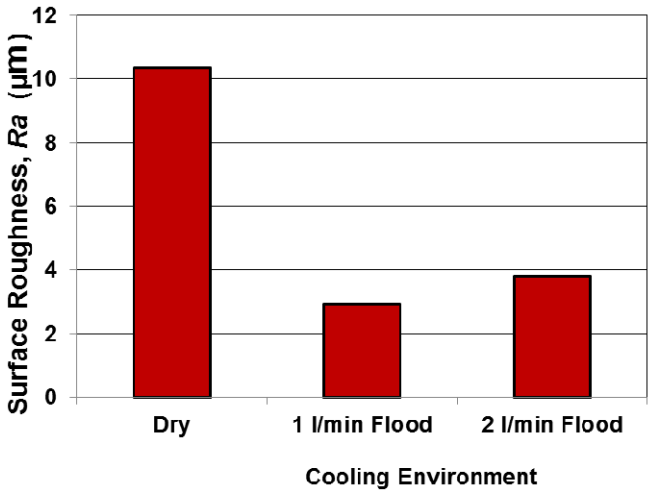

For cutting velocity 273 m/min, depth of cut 1mm and 0.22 mm/rev feed rate

Figure 6.17: Surface roughness of the workpiece versus cooling environment after 5 min of turning operations

6.6.4 Effect on Cutting Power

Power consumption is one of the important factors in machining operations. A higher power consumption naturally attracts higher cost for the machining operations. The initial experiment was performed in dry, i.e. without any coolant. The flow rate of the cutting fluid was gradually increased to observe the effect of cutting fluid on the cutting power. Figure 6.18a, b and c show the total cutting power against coolant flow rate at varying cutting speeds 87 m/min, 178 m/min and 273 m/min. The feed rates were 0.11 mm/rev, 0.22 mm/rev and 0.33 mm/rev in Figure 6.18a, b and c respectively; and the depth of cut was 1 mm. In general, the cutting power did not change much with the increase of flow rate of the cutting fluid. The power consumptions increased with the increase of the cutting speeds as the volume of material removal rates increased.

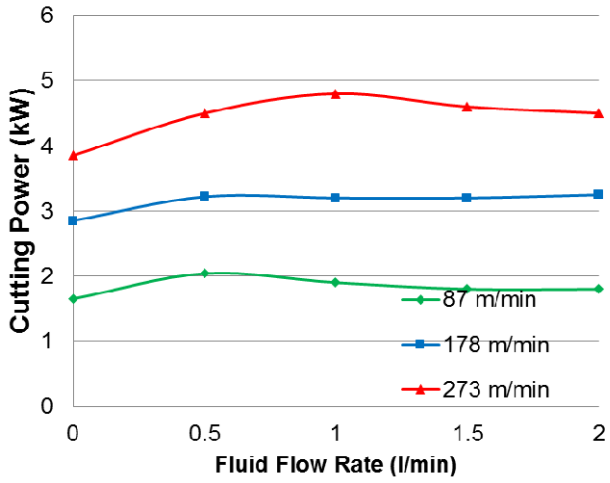

(a)

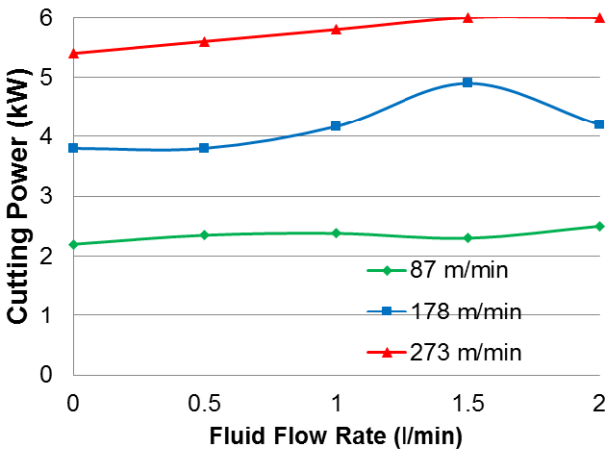

(b)

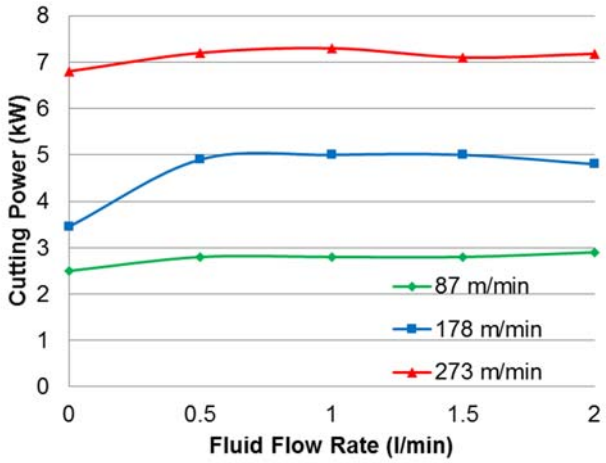

(c)

Figure 6.18: Experimentally measured cutting power against coolant flow rate at varying cutting speeds with 1mm depth of cut and (a) 0.11 mm/rev (b) 0.22 mm/rev and (c) 0.33 mm/rev feed rate

In general, the cutting power consumptions are lower in dry machining operations. Figure 6.19 shows the experimentally measured cutting power consumption versus machining time for dry and flood with reduced amount of cutting fluid, i.e. flow rate of 1.0 l/min. The power consumption is marginally higher for flood condition due to the cutting fluid pump. In flood cooling condition, the cutting power increases at the last part of the machining. At this stage, due to tool wear, the tool requires higher cutting forces to overcome the resistance from the workpieces. An increasing trend is observed over the period of time which indicates that more power is consumed with the progression of the tool wear. This increasing trend of the cutting power was also found in accordance with literature [292]. In dry condition, cutting power is higher at the beginning of the machining time as the machining quality and cutting performance varies with a number of variables. Therefore, the cutting power may be used as an indirect method of tool wear measurement but the reliability is not as high as optical tool wear measurement method.

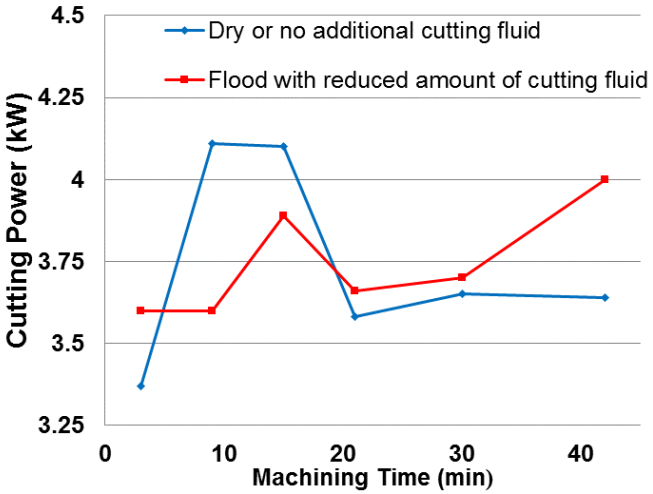

For cutting velocity 226 m/min, depth of cut 1mm and 0.11 mm/rev feed rate

Figure 6.19: Experimentally measured cutting power versus machining time under dry and flood with reduced amount of cutting fluid

6.6.5 Temperature vs Flow rate with variable cutting speeds

In order to substantiate the conclusion regarding the effect of the cutting fluid volume, tests with different flow rates should be carried out to demonstrate the effect on the tool temperature. A number of tests were conducted and results are presented graphically in details. Test No. 1, 2 and 3 were conducted according to the machining conditions of Table 6.3. The cutting velocities for these tests were 87, 178 and 273 m/min. The feed rate was 0.11 and depth of cut was 1 mm. Initially, there was no additional cooling method for the test. Conventional cutting fluid was used for the flood cooling experiments. Commercially available oil based cutting fluid was used with varying flow rate of 0.5, 1.0, 1.5 and 2.0 l/min.

Figure 6.20a shows experimentally measured temperature of the tool at varying cutting speeds with 0.11 mm/rev feed and 1mm depth of cut. Figure 6.20b shows tool temperature drop against coolant flow rate. According to Figure 6.20a, dry tool temperature was highest for the 273 m/min cutting speed. In all tests, the dry cutting tool temperatures dramatically dropped with the application of cutting fluid at the flow rate of 0.5 l/min. There was no significant change of tool temperatures although the flow rate of the cutting fluid was further increased.

Table 6.3: Machining conditions for the Test No. 1, 2 and 3

Test No.	Feed Rate (mm/rev)	Cutting Speed (m/min)	Fluid Flow Rate (l/min)
1	0.11	87	0.0 0.5 1.0 1.5 2.0
2	0.11	178	0.0 0.5 1.0 1.5 2.0
3	0.11	273	0.0 0.5 1.0 1.5 2.0

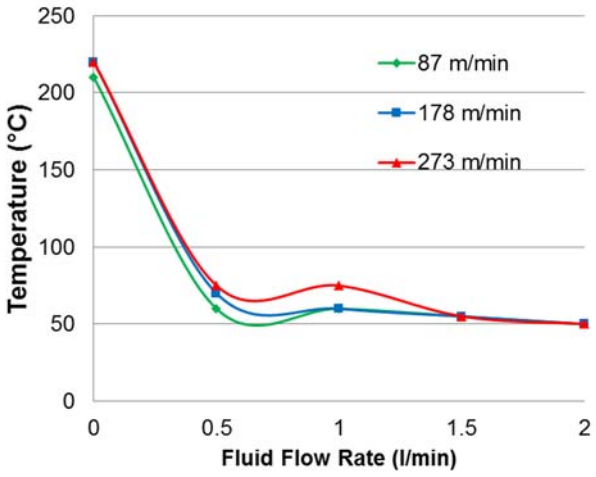

(a)

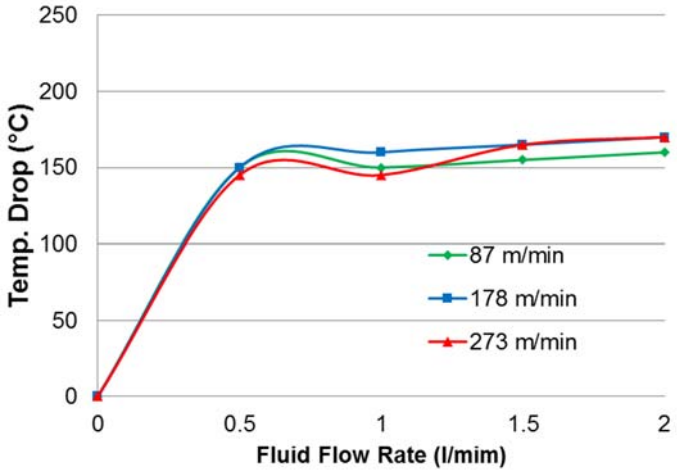

(b)

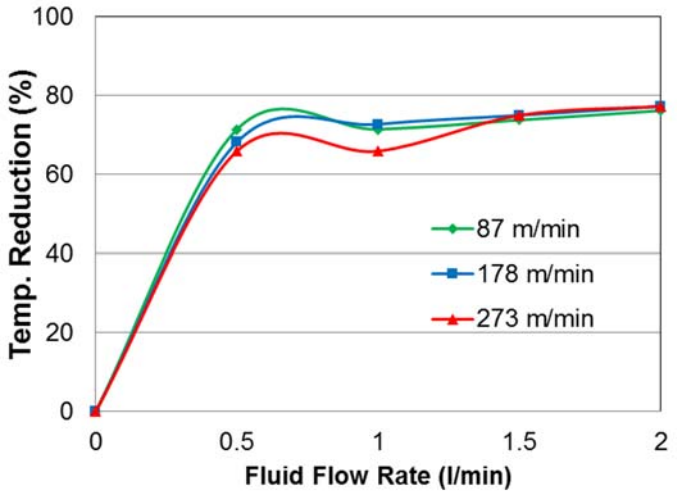

(c)

Figure 6.20: Temperature against coolant flow rate at varying cutting speeds with 0.11 mm/rev feed and 1mm depth of cut for Test No. 1, 2 and 3, (a) experimentally measured tool temperature, (b) experimentally measured tool temperature drop, (c) experimentally measured tool temperature reduction as percentage.

Test No. 4, 5 and 6 were conducted according to the machining conditions of Table 6.4. The feed rate was 0.22 and depth of cut was 1 mm. Figure 6.21a shows the experimentally measured temperature of the tool, at varying cutting speeds, with 0.22 mm/rev feed and 1mm depth of cut. Figure 6.21b shows the tool temperature drop against coolant flow rate. According to Figure 6.21, the tool temperatures dropped with the application of cutting fluid at the flow rate of 0.5 l/min. Although the flow rate of

the cutting fluid was increased, the tool temperatures was not changed significantly. As expected, the dry cutting tool temperature was highest for the cutting velocity of 273 m/min.

Table 6.4: Machining conditions for the Test No. 4, 5 and 6

Test No.	Feed Rate (mm/rev)	Cutting Speed (m/min)	Fluid Flow Rate (l/min)
4	0.22	87	0.0 0.5 1.0 1.5 2.0
5	0.22	178	0.0 0.5 1.0 1.5 2.0
6	0.22	273	0.0 0.5 1.0 1.5 2.0

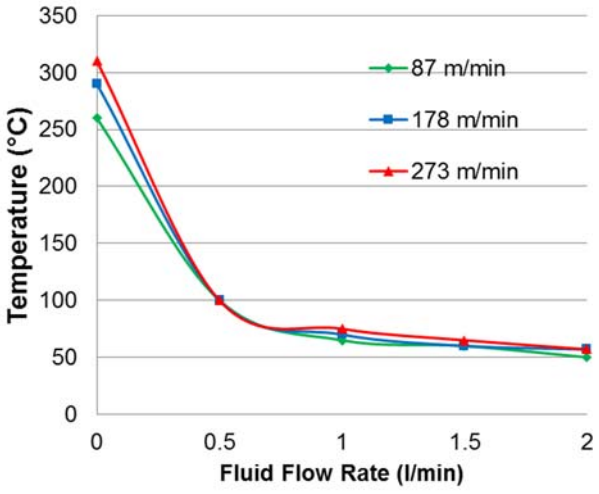

(a)

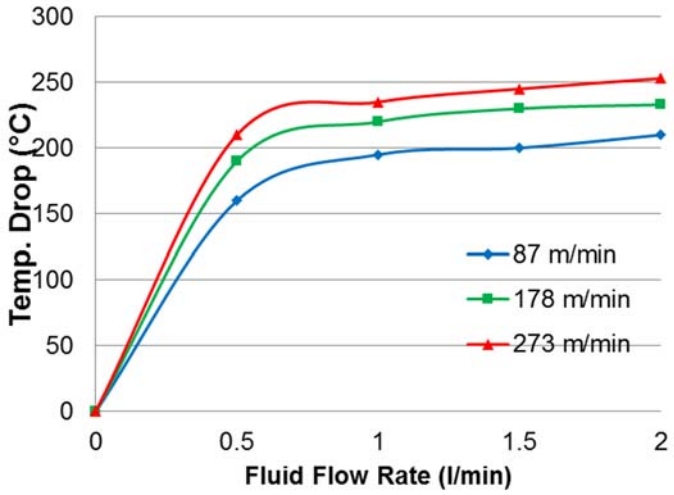

(b)

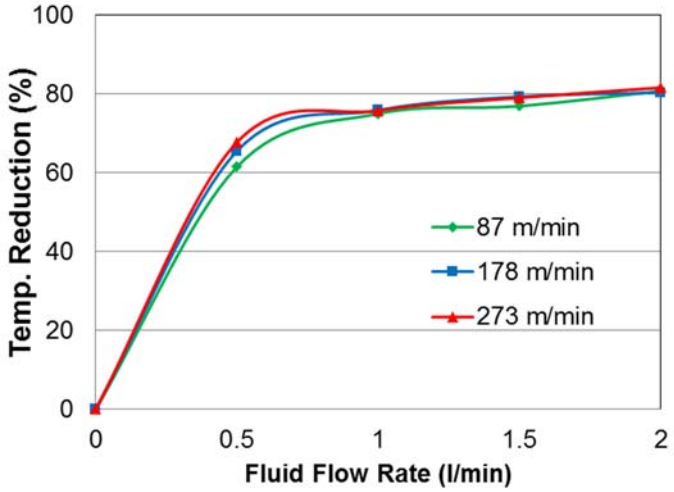

(c)

Figure 6.21: Temperature against coolant flow rate at varying cutting speeds with 0.22 mm/rev feed and 1 mm depth of cut for Test No. 4, 5 and 6, (a) experimentally measured tool temperature, (b) experimentally measured tool temperature drop, (c) experimentally measured tool temperature reduction as percentage.

Test No. 7, 8 and 9 were conducted according to the machining conditions of Table 6.5. The feed rate was 0.33 mm/ rev and depth of cut was 1 mm. Figure 6.22a shows the experimentally measured temperature of the tool for varying cutting speed with 0.33 mm/rev feed and 1 mm depth of cut. Figure 6.22b shows the tool temperature drop against coolant flow rate. According to Figure 6.22, with the application of cutting fluid at the flow rate of 0.5 l/min, the tool temperatures started to drop rapidly.

Although the flow rate of the cutting fluid was increase up to 2.0 l/min, the tool temperatures did not drop significantly.

Table 6.5: Machining conditions for the Test No. 7, 8 and 9

Test No.	Feed Rate (mm/rev)	Cutting Speed (m/min)	Fluid Flow Rate (l/min)
7	0.33	87	0.0 0.5 1.0 1.5 2.0
8	0.33	178	0.0 0.5 1.0 1.5 2.0
9	0.33	273	0.0 0.5 1.0 1.5 2.0

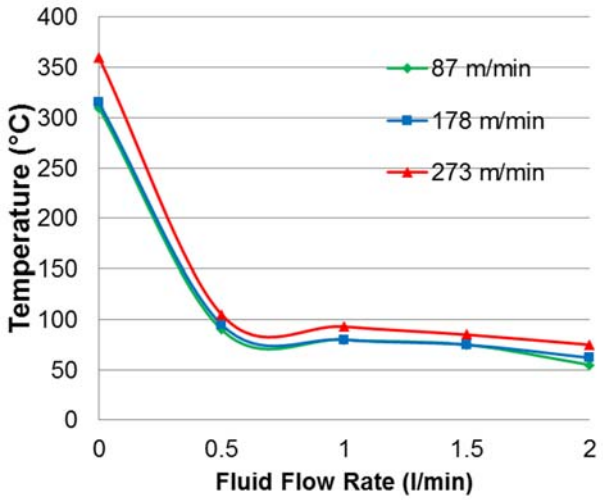

(a)

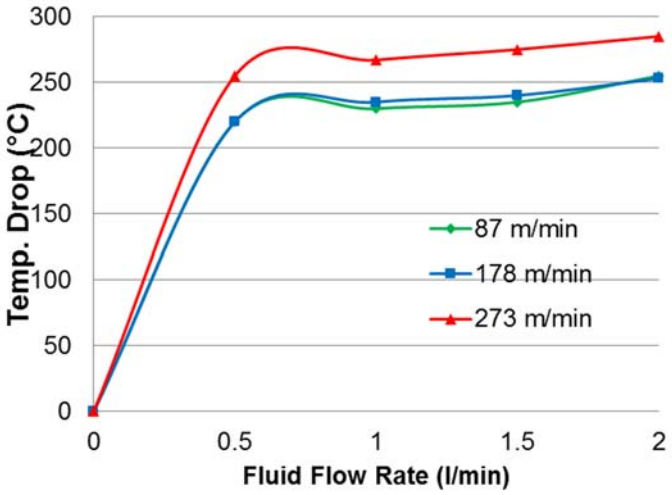

(b)

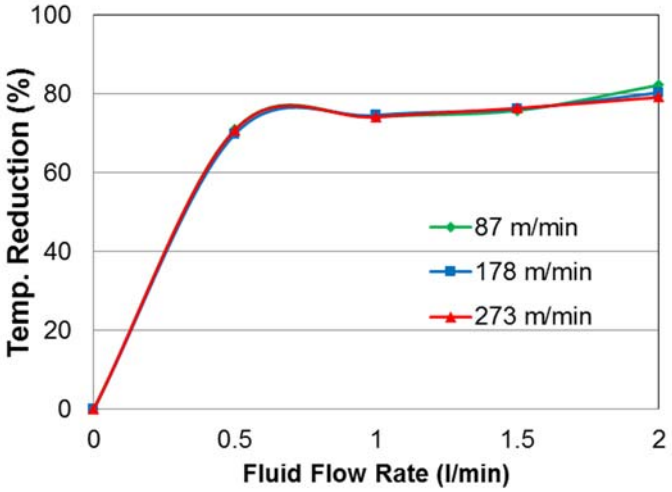

(c)

Figure 6.22: Temperature against coolant flow rate at varying cutting speeds with 0.33 mm/rev feed and 1mm depth of cut for Test No. 7, 8 and 9, (a) experimentally measured tool temperature, (b) experimentally measured tool temperature drop, (c) experimentally measured temperature reduction as percentage.

6.6.6 Temperature vs Flow rate with variable feed rates

In order to further clarification of the results, temperature vs flow rate graphs are presented for variable feed rates. Figure 6.23(a), (b) and (c) show the change of tool temperature against cutting fluid flow rate, for depth of cut 1mm and at the cutting speeds of (a) 87 m/min (b) 178 m/min and (c) 273 m/min. According to Figure 6.23(a),

(b) and (c) the dry cutting tool temperatures were slightly higher for the cutting feed of 0.33 mm/rev. With the application of cutting fluid, the tool temperatures dropped rapidly. Although the flow rate of the cutting fluid was further increased, there was no significant reduction of tool temperature.

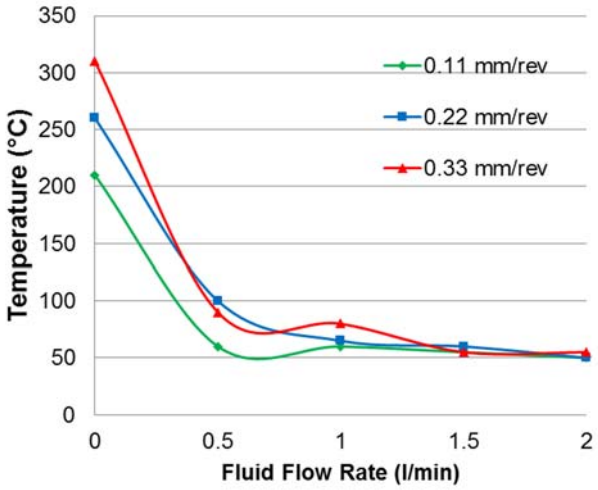

(a)

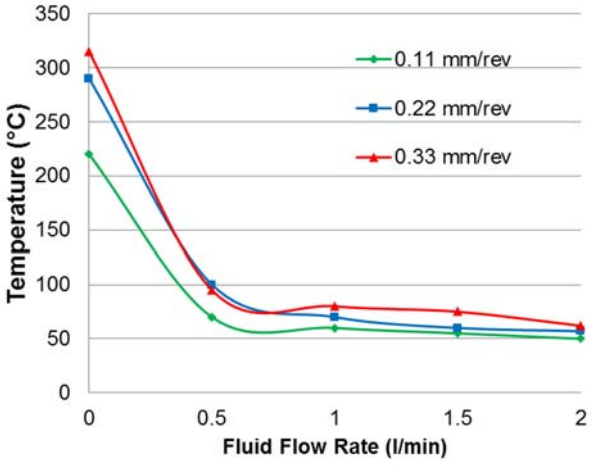

(b)

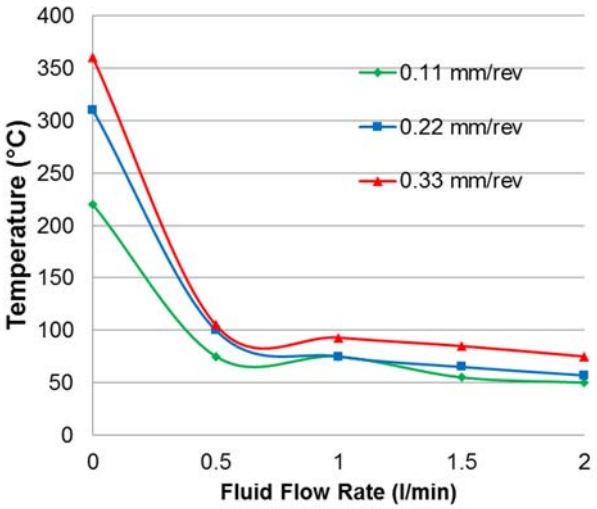

(c)

Figure 6.23: Tool temperature versus flow rate with varying feed rates and 1 mm depth of cut at: (a) 87 m/min cutting speed, (b) 178 m/min and cutting speed (c) 273 m/min cutting speed

6.6.7 Chip Observations

One of the reasons for use of cutting fluids is chip control. In flood cooling, cutting fluid is used to remove the heat from the tool, at the same time it removes the chips from cutting areas away. The flood cooling method is more popular as a liquid coolant removes the heat better than air cooling method. Flood cooling method also has an advantage over the dry and minimum quantity of lubrication method which is that the flood coolant flushes the chips away. As a part of this study, chips were collected during machining experiments for analysis. Figure 6.24 shows collected chips after 7 min of uninterrupted turning operations under dry condition. Most of the produced chips were Connected Arc Chips in term of shape. Although, a distinguishable pattern was observed among the collected chips, as shown in Figure 6.24b, but the tool wear was so high that the insert became unusable after 7 min of turning operation. Lack of additional coolant resulted significant high tool-chip interface temperature as the turning operation was continuous i.e. uninterrupted. This failure of tool emphasises the necessity of cutting fluid during machining operations. Figure 6.25a and b show the weighty tool wear after 7 min of uninterrupted turning operations under dry condition, for rake side and flank side accordingly.

(a) (b)

For cutting velocity 273 m/min, depth of cut 1mm and 0.22 mm/rev feed rate

Figure 6.24: Collected chips after 7 min of uninterrupted turning operations under dry condition (a) connected arc chips, (b) a distinguishable pattern

(a) (b)

For cutting velocity 273 m/min, depth of cut 1mm and 0.22 mm/rev feed rate

Figure 6.25: Tool wear after 7 min of uninterrupted turning operations under dry condition, (a) rake wear (b) flank wear

Chips were collected under flood cooling environment to compare with collected chips under dry condition. Figure 6.26a and b illustrate collected chips after 15 min of interrupted turning operations under (a) dry condition and (b) flood with reduced amount of cutting fluid accordingly. Most of the produced chips were Snarled Ribbon or Tabular Chips in term of shape, but the colours of the chips were significantly different. The dark blue colour of the chips indicates the development of high temperature during dry turning operations, as shown in Figure 6.26a. On the other

hand, the silver and gold colours of the chips indicate that reduced amount of cutting fluid was able to decrease the tool- chip interface temperature to a lower level.

(a) (b)

For cutting velocity 226 m/min, depth of cut 1mm and 0.11 mm/rev feed rate

Figure 6.26: Collected chips after 15 min of interrupted turning operations for (a) under dry condition and (b) flood with reduced amount of cutting fluid

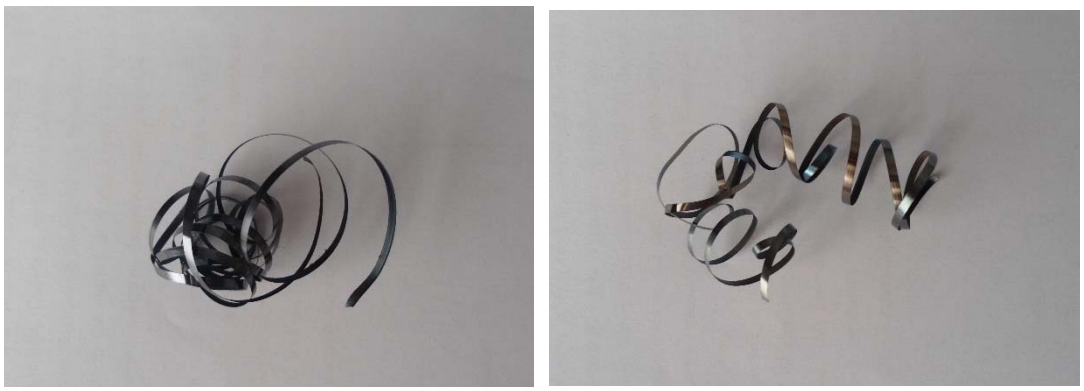

(a) (b)

For cutting velocity 226 m/min, depth of cut 1mm and 0.11 mm/rev feed rate

Figure 6.27: Collected chips after 30 min of interrupted turning operations for (a) under dry condition and (b) flood with reduced amount of cutting fluid

Similar results were observed as more chips were collected after 30 min of interrupted turning operations. Figure 6.27a and b illustrate collected chips after 30 min of interrupted turning operations under (a) dry condition and (b) flood with reduced amount of cutting fluid accordingly. The dark blue colour of the chips

confirms the development of high temperature during dry turning operations, as shown in Figure 6.27a. On the other hand, the silver and gold colours of the chips confirm that reduced amount of cutting fluid was able to decrease the tool- chip interface temperature to a lower level.

6.7 Concluding Remarks

In the present study, experimental investigations were conducted to understand the effects of the reduced amount of cutting fluids on the machining performance. The results provided comparisons of the tool wear, surface roughness, power consumptions and cutting force required for the machining in dry and flood with reduced amount of cutting fluid conditions. It has been demonstrated that the reduced amount of cutting fluid is sufficient to provide better machining performance than dry condition. The major observations from the study are as following:

- The cutting forces initially increased with the application of the cutting fluid at the flow rate of 0.5 l/min but decreased at the flow rate of 1.0 l/min in all cases. On the other hand, the cutting forces again marginally increased at the flow rate of 2.0 l/min. The results demonstrated that the cutting force difference between dry and flood with 1.0 l/min flow rate of cutting fluid is not high for most of the cases.
- It is experimentally found that lubrication property of the cutting fluid not always able to reduce the cutting forces during machining. The advantage of lubrication is neutralised as a result of the increase of strength of the workpiece due to heat absorption by the cutting fluid.
- Another observation is that the cutting forces increased with higher feed rates as the volumes of removed metal were increased. For the same reason, the cutting forces were higher for the lower cutting speeds. Similarly, the power consumptions increased with higher the cutting speeds. These findings are also in line with the Equation 3.6.
- The cutting force varies with cutting speed due to thermal softening and strain rate hardening which may result in increase or decrease in cutting forces depending on which one is more dominant.
- Flank wear is clearly lower with the reduced amount of cutting fluid compared with the dry turning operations. Therefore, the reduced amount of cutting fluid

is sufficient to hinder the flank wear progression and provide lower tool wear than dry condition.

- The reduced amount of cutting fluid is capable of providing better surface finish than dry condition at the first part of the machining time.
- In the tool wear experiment, the cutting force was lower in dry turning operations but, with the application of the cutting fluid, the cutting force increased. This is because of the removing of heat by the cutting fluid from the cutting zone that makes the workpiece a little rigid. The cutting force increased more rapidly in dry condition compared to the reduced amount of cutting fluid. This is because of the fact that the reduced amount of cutting fluid was sufficient to hinder the tool wear progression compared to the tool wear in the dry condition.
- In general, the cutting power consumptions are lower in dry machining operations. This is because of the removing of heat by the fluid from the cutting zone makes the workpiece a little rigid.
- According to the tool temperature tests, there was no significant change of tool temperatures although the flow rate of the cutting fluid was further increased.
- Based on this experiment, it is established that the reduced amount of cutting fluid is sufficient to provide acceptable machining performance and the machining quality and cutting performance vary due to a number of variables.

Chapter 7

Application of the Methodology to Compare the Cooling Environments

7.1 Introduction

The tool temperature distributions under different types of cooling environments have rarely been compared. Previously in Chapter 5, an application of the proposed methodology was presented and it was revealed that the amount of cutting fluid, used in the industry for the turning operations, is higher than the amount required to reduce the tool temperature. In this chapter, another application of the proposed methodology is presented by comparing the tool temperature distributions under different types of cooling environments. By applying the proposed methodology, the effect of cooling environments on the tool temperatures can be identified and additional knowledge regarding the tool cooling process under different types of cooling environments can be acquired. This chapter presents the application of the proposed methodology more elaborately in a perspective of the MQL cooling environment. The obtained knowledge can be helpful to understand the effectiveness of the MQL process by comparing against the conventional flood cooling process. To compare the role of the cutting environments during tool cooling, the proposed methodology was applied under the three cooling environments (a) dry or no additional cutting fluid (b) conventional flood with liquid cutting fluid and (c) minimal quantity lubrication (MQL).

Air contains little moisture and by itself is not sufficient to effectively cool the cutting tool, especially for continuous machining operations, but this limitation can be resolved by adding liquid coolant in the form of minimal quantity of lubrication. Assigning the correct boundary conditions is crucial for achieving accurate results from the numerical analysis. To identify the correct boundary conditions, an experiment was conducted in the MQL system. The mist temperature from the MQL supply system was obtained by an experiment and the result was used to declare the boundary conditions for the computational fluid dynamics model. The results from the experiment provided more accurate data to declare the boundary conditions for the proposed methodology. Subsequently, the tool temperature distributions were predicted from the proposed methodology based on the input mist temperature. The

results of the numerical experiments provided comparison of tool temperatures according to the cooling environments. Finally, this chapter is concluded by highlighting the significant findings.

7.2 MQL

MQL cooling process has drawn a lot of interest as an alternative to the conventional flood cooling method. The MQL shows a strong influence on the cutting temperature over a wide range of speeds; and the application of the MQL can effectively reduce the tangential cutting force, especially at low cutting speeds [293]. MQL cooling method can also provide better tool life than dry turning operations [294], [295]. López de Lacalle et al. [296] injected a high speed air jet with micro-drops of biodegradable oil in suspension in the cutting zone and studied the tool wear. They found that smaller wear with the MQL oil than with the conventional emulsion. Kim et al. [297] manufactured a compressed chilly-air system and investigated the effectiveness based on the tool life. The authors found lower flank wear using compressed chilly-air than a dry environment.

Astakhov [110] explained the heat removal process of the mist in two steps. Initially, the thermal energy entering the droplets heats it up to the saturation point. The cutting fluid droplets in the mist provide effective heat transfer due to the high velocity. In the next stage, the heat causes evaporation and temperature drops. Therefore, the cooling occurs due to convective and evaporative mode of heat transfer [296]. Figure 7.1 shows the movement of the droplets to the hot surface.

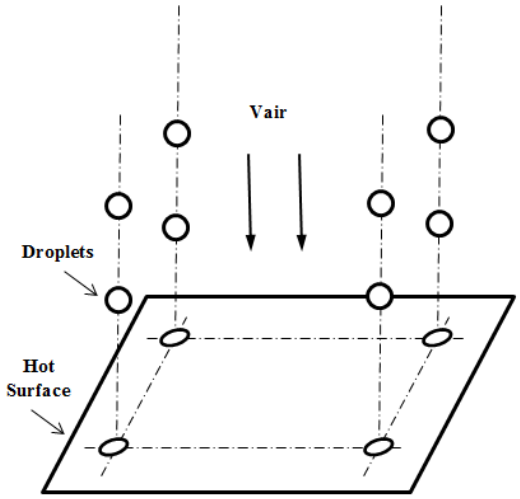

Figure 7.1: Graphical representation of droplets moving towards the hot surface, adopted from [110]

Vegetable oil is mainly used for the MQL, but the lubrication performance of the vegetable oil is relatively low. The preference of vegetable oil for the MQL indicates that lubrication is not the crucial function for the application of the cutting fluids rather the environmental concern. The use of vegetable oil for the MQL can provide an environmental machining solution. In addition, the amount of liquid used in the MQL is relatively lower than the flood cooling method. The classification of the MQL or Near Dry machining is presented in Figure 7.2.

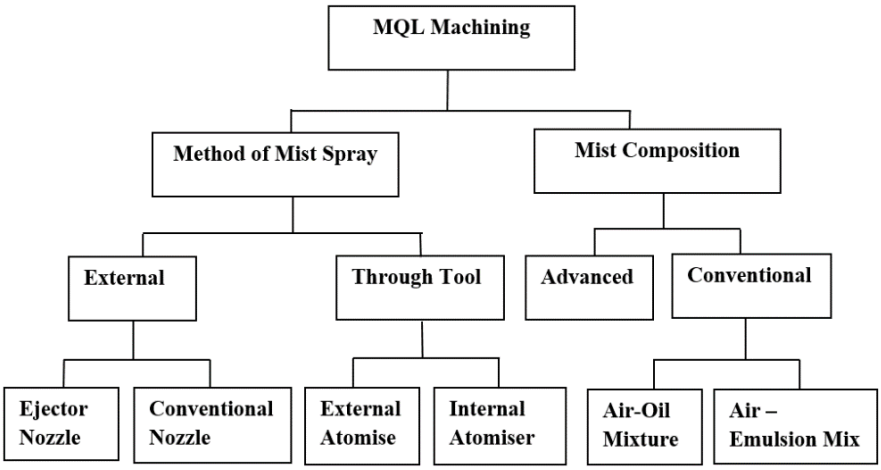

Figure 7.2: Classification of Near Dry machining, adopted from [298], [299]

7.3 Experimental Procedure

The experimental investigation was conducted to obtain the MQL mist temperature and the obtained temperature was used as boundary conditions for the numerical experiments. To obtain the MQL mist temperature, the vortex tube was attached with a machine tool in the laboratory by combining the MQL supply unit [300], [301]. The MQL supply system is shown in Figure 7.3. Figure 7.4 represents the schematic of the MQL system arrangement.

(a)

(b)

Figure 7.3: The MQL supply system components (a) full view of the MQL supply unit and (b) a close view of the air filter

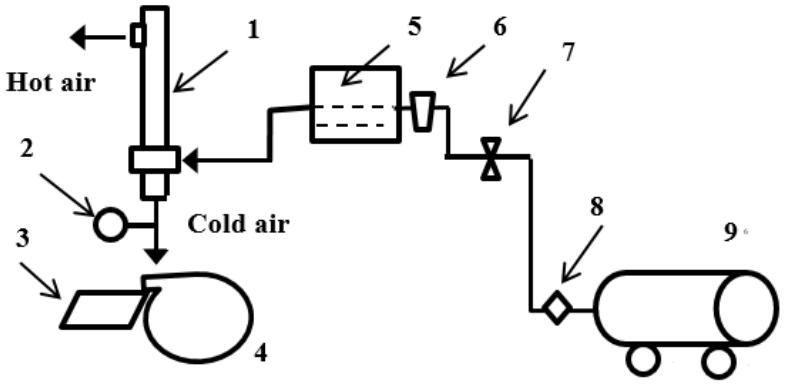

1. Vortex tube, 2. Thermocouple, 3. Tool insert, 4. Workpiece, 5. Fluid chamber, 6. Air filter, 7. Control vale, 8. Dry air filter and 9. Compressor

Figure 7.4: Schematic of the combined of cold air with MQL system

From the experiment, the MQL was delivered from a Uni-max cutting tool lubrication system which distributed atomised coolube lubricant to the cutting zone. This system operates on the same principle as a Serv-O-Spray allowing the lubricant to be sprayed from a single air source, which allows adjustment to the amount of lubricant delivered to the cutting zone. The flow rate for the MQL was 80 ml per hour. In industrial applications, the flow rate for the MQL is in a range of approximately 10-100 ml per hour [77]. Photographs of the vortex tube to supply the cold air is shown in Figure 7.5.

Figure 7.5: The vortex tube used to supply the cold air

The temperature of the air should be as cool as economically possible to maximise heat transfer. A vortex tube was attached with the MQL supply unit to generate the mist by combining the cold air with the MQL. The mist temperature was measured at approximately 25 mm from the nozzles. The vortex tube was set at 90 psi compressed air giving a volumetric flow rate of 10 SCFM and the lowest temperature recorded for these conditions was -11^{o}C. By increasing the input air pressure further, it is possible to obtain lower temperature from the same vortex tube. Ranque-Hilsch vortex tube is in use to supply the cold air in the industry for a long time. The use of an air jet to increase the heat dissipating effects is a sustainable approach as there are no environmental concerns directly related with air jet. One of the advantages of the vortex tube is that compressed air is readily available in most of the machine shops and this air can be used from the vortex tube. There are several advantages if cold compressed air is used as a coolant in machining. The air is safe to use, inexpensive and environmentally suitable [302]. Another noteworthy point is that vortex tube is a low maintenance tool as is capable of separating compressed air into two streams, one is hot and the other is cold, without any moving parts in it. The design of the nozzles can be converging or diverging or converging-diverging type. A better designed nozzle provides higher velocity, higher mass flow and lower losses. The variation of the length and diameter of the tube have significant effects on its performance. The diameter of the diaphragm has an effect on its performance as well. Recently improved Ranque-Hilsch vortex tube, with convergent nozzle, is an effective device and used in the industrial [303]. The different parts of a vortex tube is shown in Figure 7.6.

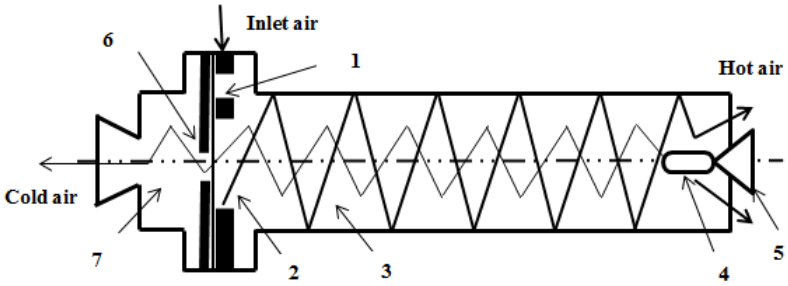

1. Nozzle, 2. Vortex chamber, 3. Hot gas side, 4. Diffuser, 5. Valve, 6. Diaphragm and 7. Cold gas side

Figure 7.6: Schematic diagram of the vortex tube showing hot and cold air separation

There are parameters related to nozzle and air mist which can influence the effectiveness of the MQL. The nozzle related parameters are (a) nozzle tip distance from tool tip (b) nozzle inclination angles (c) nozzle location; and the air mist related parameters are (a) air pressure (b) oil concentration (c) coolant flow rate [298]. It is worth mentioning that control of oil mist flow and shortening of the distance from the nozzle to the tool tip are more important for the performance of the MQL machining [304]. The cutting conditions for the numerical experiment are presented in Table 7.1. Experimentally measured temperature was used as boundary condition for the numerical experiments. The numerical experiments were carried out using three cooling environments: dry, conventional flood, and the MQL. Some of the boundary conditions or inputs for this computational fluid dynamics analysis were as following:

- MQL mist flow rate was 10 SCFM
- MQL temperature was 20 ºC
- Flood temperature was 25ºC

Table 7.1 Cutting Conditions for Numerical Experiments

Cutting Conditions	Value
Process Parameter	
Cutting Velocity, V_c	87 m/min
Feed Rate, f	0.33 mm/rev
Depth of Cut, d	1 mm
Cooling Environment	Dry, Flood and MQL

A fishbone diagram of the variables used for the MQL machining analysis is presented in Figure 7.7 for clarification.

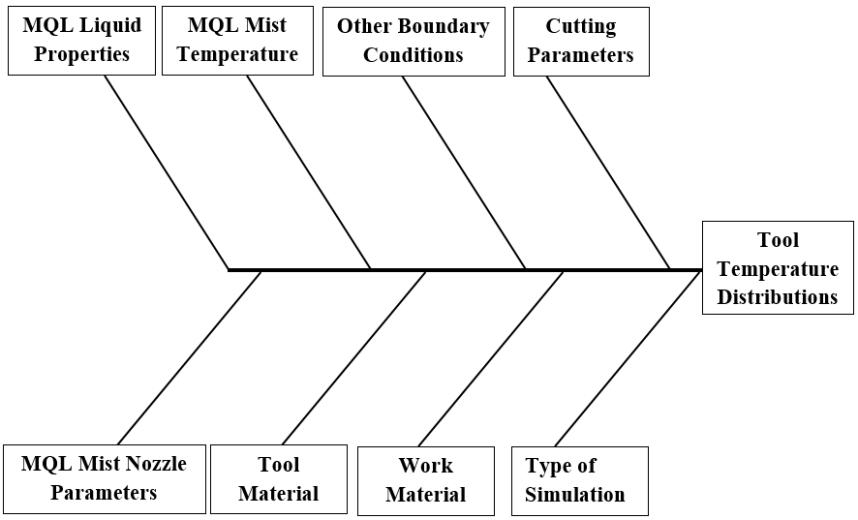

Figure 7.7: Fishbone diagram of the variables used for the MQL tool temperature distributions

7.4 Results and Discussion

Removal of the generated heat from the cutting tool during machining is the primary concern in cutting fluids. Eliminating the liquid cutting fluid during the machining possess several constrains. Gaseous cutting fluids are considered for the better penetration at the cutting zone but the gaseous cutting fluids are not much common due to the high cost of purchase. Although, the application of the air can be achieved at a low cost but it is noteworthy that air cooling has some limitations. Removal of heat from the cutting tool with air cooling during machining requires special attention compared to the heat removal process of the liquid cutting fluid. The workpiece starts to increase in temperature after several minutes of machining and some additional cooling method with air cooling may be required [83]. On the other hand, one of the advantages of the conventional flood cooling is that the liquid coolants cover the tool and workpiece and reduce the heat build-up during machining. The air cooling by itself is not gaining popularity to reduce the tool temperature due to the limitation of the heat removing capability during continued machining operations. To make the air cooling process popular to the manufacturers, the tool life and the machining quality should be satisfactory. Therefore, a high velocity jet of cold air can be added with the MQL supply system to reduce the cutting tool temperature. The heat removing performance

of the air cooling can be enhanced by adding the MQL supply unit with cold air. A combination of cold air with the MQL can be an initiative to reduce the heat build-up.

The proposed methodology provided the tool temperature distribution for the turning operations for a variety of machining parameters. To emphasise on the cooling methods, the same heat generating parameters were considered for the numerical experiments in each of the three cases. There is a relation between the tool life and the tool interface temperature. To achieve sustainable machining, the tool life is one of the important factors. The tool life can be severely shortened due to elevated temperature. Therefore, the tool temperature obtained from the proposed methodology can be used for the prediction of the tool life for three different cases.

The proposed methodology provided the effects of the cooling environments on the tool temperatures for dry, conventional flood cooling and the MQL cooling machining, as shown in Figure 7.8, Figure 7.9 and Figure 7.10 accordingly. In addition, by applying the proposed methodology, the tool interface temperature distributions are also obtained for the combination of the MQL and cold air environment, as shown in Figure 7.11. Based on the computational fluid dynamics simulation, the tool-chip interface temperature is found to be the lowest when liquid cutting fluid was used for conventional flood cooling environment, as shown in Figure 7.10. In conventional flood machining, the initial coolant temperature was considered to be 25^{o}C, and the flow rate was 1.5 l/min as boundary conditions.

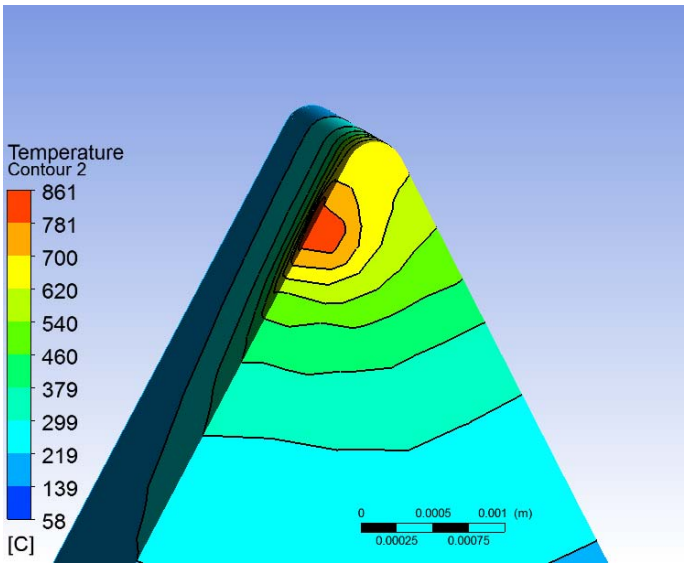

Cutting parameters according to Table 7.1

Figure 7.8: Tool chip interface temperature simulation dry machining

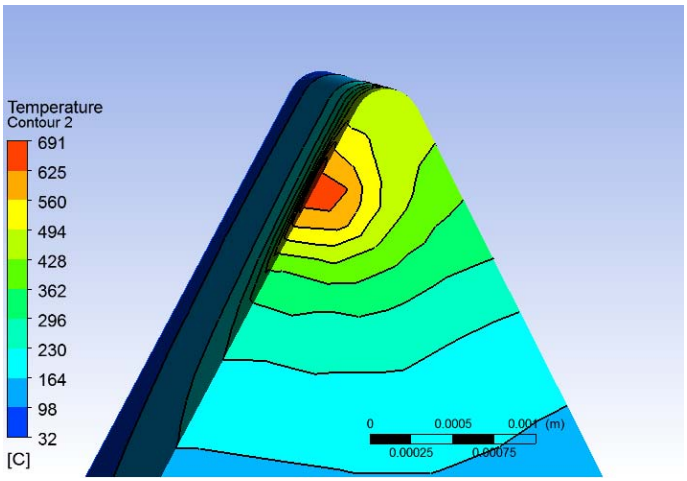

Cutting parameters according to Table 7.1

Figure 7.9: Tool chip interface temperature simulation for the regular MQL machining

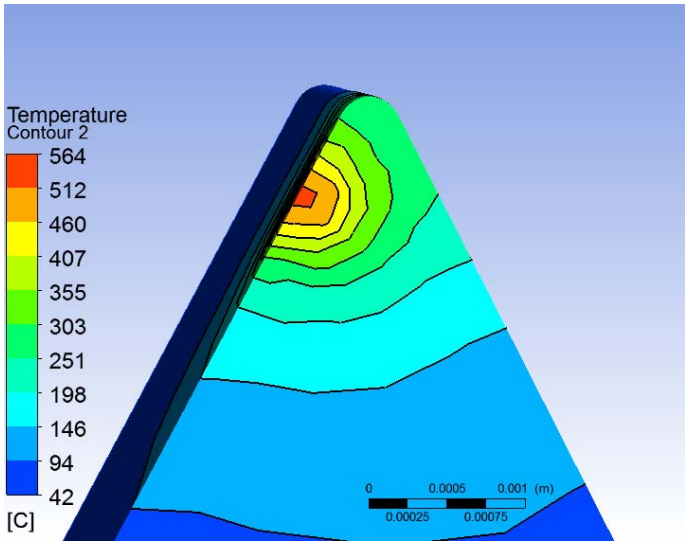

Cutting parameters according to Table 7.1

Figure 7.10: Tool chip interface temperature simulation for conventional flood cooling environment

The proposed methodology also provided tool temperature distributions for the MQL with variety of mist temperatures. The tool temperature distribution for the mist temperature -10ºC is shown in Figure 7.11a. Tool temperature distributions near this temperature has especial significance as the MQL with -15 °C cooling air condition provides better machining performance [305]. The tool insert temperature comes down further, if the cold air mist temperature is reduced to -40ºC, as that shown in Figure 7.11b.

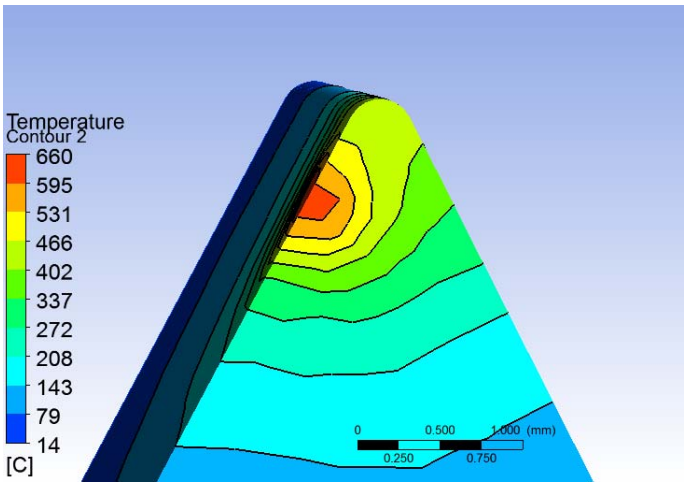

(a)

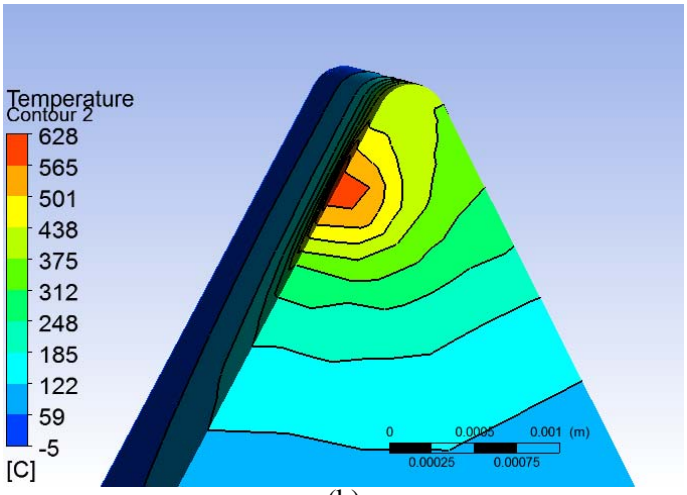

(b)

Cutting parameters according to Table 7.1 in both (a) and (b)

Figure 7.11: Tool chip interface temperature distributions (a) by combining -10 ^{o}C air with the MQL (b) by combining -40 ^{o}C air with MQL

The effectiveness of the coolants can be identified from the tool temperature distributions. Based on the numerical experiments, the maximum interface temperatures are 861^{o}C for the dry machining and 564^{o}C for the flood cooling. On the other hand, the maximum interface temperature for -40^{o}C cold air with MQL cooling is 628^{o}C. A comparision of the tool temperatures is presented in Figure 7.12, based on the cooling environments. The effect of the MQL mist air temperature on the tool chip interface temperature in combined cold air with the MQL is illustrated by Figure 7.13.

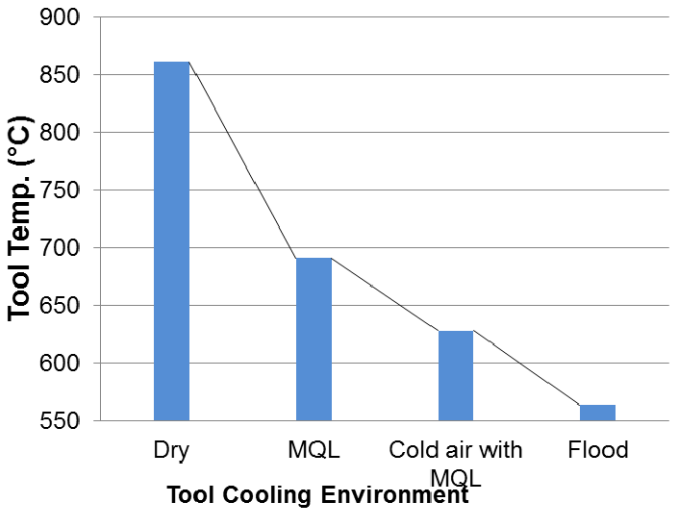

Figure 7.12: Comparision of the tool temperatures based on tool cooling environments

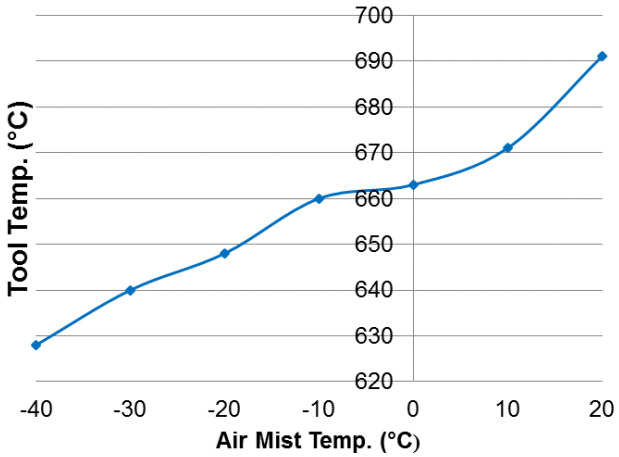

Cutting parameters according to Table 7.1

Figure 7.13: The effect of mist air temperature on the tool chip interface temperature in the MQL

Obtaining tool interface temperature is relatively easier by applying numerical method for a variety of cutting parameters. A tool chip interface temperature based equation for the effectiveness of the MQL was applied by Obikawa et al. [304] which can be modified as the following Equation 7.1:

$$\eta = \frac{T_{Dry} - T_{MQL}}{T_{Dry} - T_{Flood}} \qquad (7.1)$$

where η is the effectiveness of combined of cold air with MQL, T_{Dry} is the dry machining interface temperature, T_{MQL} is the MQL machining interface temperature and T_{Flood} is flood machining interface temperature. Applying the Equation 7.1, it is found that, if the mist temperature is -10°C, the effectiveness of combined of cold air with MQL is 67%. The effectiveness can be further increased to 79% by reducing the mist temperature to -40°C. On the other hand, the effectiveness is only 57% in case of regular MQL machining, if no vortex tube is combined with the MQL system i.e. the mist temperature is 20°C. Therefore, these findings demonstrated the significance of combining vortex tube with the MQL system and the influence of the mist temperature on the tool chip interface.

The study in this chapter has shown the beneficial sides of using cold air with the MQL in metal cutting. The application of cold air with the MQL can reduce the tool temperature to an effective level during turning operations. The tool temperature difference between a regular MQL and flood cooling can be further minimised by adding cold air with the MQL System. The study in this chapter also revealed that the tool interface temperature difference between the combination of cold air with MQL and flood cooling is not enormous. Sreejith [241] compared the role of cutting fluid during the MQL, flood and dry machining and concluded that cutting fluid has little influence on flank tool wear. Therefore, the possibility of tool failure due to high temperature in combined cold air with the MQL would not be significantly higher compared with the tool failure during flood cooling as the tool interface temperature difference is not very significant. This finding will be helpful to motivate the machining industry to implement this environment friendly approach for metal cutting. Even though, a trend of using liquid nitrogen for machining is observed in literature, but the cost to effectiveness of using liquid nitrogen is the main constraint to be an acceptable alternative cooling method that can outperform the flood cooling. However, the application of the MQL with cooled air is appeared to be an effective method in terms of tool temperature reduction compared with flood machining. Although, the machining performance needs to be further investigated for the MQL cooling approach.

7.5 Concluding Remarks

In conclusion, it is possible to determine the effectiveness of the cooling environments using the proposed methodology, without performing the turning operations. The

proposed methodology can significantly reduce the amount of physical prototyping or actual machining testing requirement to determine the effectiveness of the tool cooling environments. The major observations from this study are as following:

- The proposed methodology was further enhanced and applied to study heat transfer under different types of cooling environments and it is demonstrated that the proposed methodology is a new multiphase approach of simulating the effectiveness of the MQL cooling of the cutting tool.
- This study provided an insight of the heat removal of different types of cooling environments. By applying the proposed methodology, the effects of the MQL mist temperature on the cutting tool temperature distributions were shown for variety of cutting parameters.
- Based on the results obtained from the proposed methodology, the combination of cold air with MQL cooling environment turned out as a recommendable alternative of flood cooling, considering the environmental benefits by adopting the combined MQL and cold air cooling. It has been demonstrated that the tool temperature is marginally higher for the combined MQL and cold air cooling than the tool temperature for the flood cooling.
- By applying the proposed methodology, it is possible to compare the effectiveness of different types of cooling environments, which would be otherwise difficult to achieve by other tool temperature obtaining methods.

Chapter 8

Conclusions and Future Research

8.1 Introduction

There are effects on the health and environment due to the application of cutting fluid during machining operations. Any reduction of cutting fluid can lead to economic benefits by decreasing the cost of the cutting fluid. In addition to the cost, the reduction of the amount of cutting fluid is crucial to minimise the environmental effects. The cost of purchase and disposal of the used coolant are contributors toward the total machining cost. The tool cooling cost during the metal cutting operations can contribute up to 17% of the total manufacturing cost. Besides, in the machining industry, the machinists use the cutting fluid without knowing the accurate amount required for the machining operations. The amount of cutting fluid used in the turning operations is not directed by any guidelines. The flood cooling method is the most widely used method in the machining industry. Therefore, reducing the amount of the cutting fluid during the flood turning will be beneficial for a large number of stakeholders related to the manufacturing industry. Enormous amount of cutting fluid will be saved worldwide by reducing its application during machining process. The cost of purchase of the cutting fluid will be less to keep the edge of the cutting tool active for metal removing and maintaining the machining performance.

This chapter concludes the achievement of the present study by completing the research objectives. In addition, the possible improvements of the proposed methodology and the future research interests on this area are also outlined. One of the main objectives of the present study is to identify the effects of the cutting fluids on the tool temperature during the turning operations by developing a computational fluid dynamics based 3D model. In the present study, a methodology to obtain tool temperature is proposed and tool temperatures are predicted for variety of cutting parameters during dry and flood conditions. The methodology was experimentally validated by obtaining temperature with an embedded thermocouple during the turning operations. In addition, the validation of the proposed methodology was conducted against data available from the literature. The correlation obtained between the

experimental and numerical results indicated that the proposed methodology can predict the tool temperature during turning operations for varying flow rates. Furthermore, the proposed methodology was applied to study the heat transfer under different types of cooling environments.

8.2 Achievement

The proposed methodology was applied to obtain cutting tool temperatures and identify the effects of the cutting fluid on the tool temperature distributions. A series of numerical experiments were conducted to analyse the effects of the cutting fluid on the tool temperatures after the validation of the model. The cutting tool cooling processes during turning operations against variety of machining parameters were observed. The numerical results from the computational fluid dynamics based model were analysed and the optimal flow rate of cutting fluid was identified. Applying less amount of cutting fluid for machining operations enables the cost of manufacturing to be reduced. The obtained results from the proposed methodology identified that the amount of cutting fluid used for the turning is more than the amount required for the tool cooling to an acceptable level. Therefore, it is possible to perform the turning operations by using reduced amount of cutting fluid. To analyse the machining performance with the reduced amount of cutting fluid, experimental investigations were conducted. It is found that the reduced amount of cutting fluid can perform machining operations without sacrificing the machining performance. Finally, in Chapter 7, the methodology was applied to obtain tool temperatures under different tool cooling environments. The present study demonstrated that a computational fluid dynamics based approach can identify the effectiveness of the cooling method, without performing the metal cutting. The computer-generated prototyping with simulation software can make the manufacturing process more efficient. The significant findings from the modelling and the experiments are described as following:

- One of the achievements of the present study was the development of a computational fluid dynamics based methodology for flood turning operations. The developed model is capable of predicting the tool temperature distributions during the turning operations. The proposed methodology revealed the effect of cutting fluid during tool cooling process for variety of cutting parameters. From the outputs of the proposed methodology, it is possible to understand the role of cutting fluid in the tool cooling process during the turning operations.

The present study provided a direction to analyse the tool cooling process by using computational fluid dynamics analysis. The proposed methodology was also verified under dry and flood cooling conditions. The output results demonstrated that the proposed methodology is capable of reflecting the effects of cutting fluid flow rates on the tool temperatures under flood cooling conditions. One of the validations of the proposed methodology was performed by comparing numerically obtained tool temperature against experimentally measured temperature taken from three sources available in the literature. It has been demonstrated that the proposed methodology fulfilled the accuracy requirement (Chapter 3).

- The proposed methodology was experimentally validated by obtaining tool temperature with an embedded thermocouple. By applying the spark eroding process a narrow hole was created to place the thermocouple into the tool inserts. The validation of the methodology was performed by comparing numerically obtained tool temperature against experimentally measured tool temperature. The proposed methodology was verified under dry and flood cooling conditions. The results of the validation demonstrated that the methodology is capable of predicting the tool temperature in both dry and flood cooling environments. The experimental validation results were found within acceptable ranges and it was concluded that the proposed methodology is capable of performing numerical analysis. After the validation, it is possible to predict the tool temperature for a particular cutting conditions with a level of assurance. (Chapter 4).
- The data obtained from the numerical experiments was analysed to identify the effectiveness of the cutting fluid during machining. Tool temperatures were obtained by assigning a reference line alone the cutting edge of the tool insert to illustrate the distribution of the tool temperatures. The knowledge obtained from this analysis is helpful to reduce the amount of cutting fluid during the turning operations. The amount of cutting fluid used during the machining can be reduced by not increasing the flow rate after a specified flow rate. By applying proposed methodology, the optimal flow rate of the cutting fluid for the turning operations was revealed. Therefore, it has been demonstrated that computational fluid dynamics based simulation is an effective method to identify the optimal flow rate of the cutting fluids (Chapter 5).

- The results from the proposed methodology revealed that a less amount of cutting fluid can reduce the tool temperature to an acceptable level. Therefore, an experimental investigations were performed to identify the effects of the reduced amount of cutting fluid on the machining performance. It was found that the reduced amount of cutting fluid was sufficient to provide a better machining performance than dry machining. The experimental results provided comparisons of the tool wear, surface roughness, cutting force and power consumptions for the machining in dry and flood conditions. It has been demonstrated that the reduced amount of cutting fluid is able to keep flank wear lower compared to the dry turning operations. Surface roughness is lower with reduced amount of cutting fluid compared with the dry turning operations at the first part of the machining. Initially, the cutting force requirements are lower in dry turning operations, although increased more rapidly compared with the flood turning operations. Based on experimental data, it has been shown that the reduced amount of cutting fluid is sufficient to hinder the tool wear and extend the tool life (Chapter 6).
- The proposed methodology provided an alternative approach to determine the effectiveness of the cooling environments, without performing the turning operations. By applying the proposed methodology, additional knowledge regarding the cooling process was obtained for different types of tool cooling environments, which would be otherwise difficult to achieve by experimental methods. In addition, the proposed methodology can be an effective tool for identifying the effect of the MQL mist temperatures on the cutting tool temperatures for variety of cutting parameters (Chapter 7).

8.3 Suggested Improvements and Future Research Interests

All the objectives of the present study were achieved, nonetheless, there are always opportunities for further development. The following recommendations can be helpful for future work in related field:

- In general, the life of the coated tools is higher than an uncoated tool. The major tool parameters are tool coating types, coating thickness, tool geometry parameters i.e. edge radius etc. The effect of the tool coating on the tool temperature distribution has rarely been investigated by experimental method. It is difficult to measure the temperature variation due to the coatings. There is

an opportunity for future work as the model developed during the present study can be modified by adding layer of coatings [306-308].

- The temperature distribution simulation can be achieved by another method which is based on heat flux. For the heat flux based models, the influence of the cutting parameters i.e. speed, feed and depth of cut etc. are indirectly reflected. In addition, the heat calculation for the present study can be further modified by including additional parameters i.e. nose radius etc. Moreover, there is role of tool wear on the tool temperature [309] which can be added as well.
- In the present study, a hole was made in the tool insert by EDM process to obtain the tool temperature. To obtain the tool temperatures at the different locations of the tool, multiple holes can be made in the tool insert. Multiple holes will allow producing a temperature gradient based on the temperature of the different locations of the tool insert. But multiple holes will make the tool insert structurally weak and can cause the tool insert to break during the machining operations. Keeping the diameter of the holes as low as possible and preparing a sufficient number of tool inserts to replace the broken inserts can be the resolutions for these issues.
- It is shown that the numerical model is able to provide tool interface temperature for the flood and MQL with cold air cooling method. Similarly, it will be possible to obtain tool temperature distributions for liquid nitrogen as well. The resulting data from the liquid nitrogen can be compared with other cooling method. By applying the proposed methodology, it will be possible to obtain detail temperature information about the cutting zone with liquid nitrogen machining. The obtained knowledge regarding the tool temperature can be helpful for the research with liquid nitrogen which would be otherwise expensive to accomplish by traditional experimental methods.

8.4 Conclusion

To achieve high productivity and low machining cost, the edge cutting tool should be active for metal removing without sacrificing the machining performance such as tool life, surface finish etc. The disposal cost of the cutting fluid was not significant few decade ago. With tighten up of environmental protection law and regulations for handling and disposal of cutting fluids, the total cost of the cutting fluid for machining

is increasing to an ever high level. Any reduction of the amount of the cutting fluid will relief the manufacturer from the stress of higher cost. This research has shown that the reduction of the amount of the cutting fluid is possible without sacrificing the machining performance.

References

[1] R. R. Srikant, N. D. Rao, and P. N. Rao, "Influence of emulsifier content in cutting fluids on cutting forces, cutting temperatures, tool wear, and surface roughness," *Proceedings of the Institution of Mechanical Engineers, Part J: Journal of Engineering Tribology,* vol. 223, pp. 203-209, 2009.

[2] R. F. Avila and A. M. Abrao, "The effect of cutting fluids on the machining of hardened AISI 4340 steel," *Journal of Materials Processing Technology,* vol. 119, pp. 21-26, 2001.

[3] Z. M. Bi and L. Wang, "Optimization of machining processes from the perspective of energy consumption: A case study," *Journal of manufacturing systems,* vol. 31, pp. 420-428, 2012.

[4] E. O. Ezugwu, "Key improvements in the machining of difficult-to-cut aerospace superalloys," *International Journal of Machine Tools and Manufacture,* vol. 45, pp. 1353-1367, 2005.

[5] F. Pusavec, D. Kramar, P. Krajnik, and J. Kopac, "Transitioning to sustainable production–part II: evaluation of sustainable machining technologies," *Journal of Cleaner Production,* vol. 18, pp. 1211-1221, 2010.

[6] S. Ekinović, E. Begović, and A. Lušija, "MQL Machining–Oil on Water Droplet System," *space,* vol. 6, p. 6, 2013.

[7] S. Y. Hong and Z. Zhao, "Thermal aspects, material considerations and cooling strategies in cryogenic machining," *Clean Products and Processes,* vol. 1, pp. 107-116, 1999.

[8] S. Y. Hong and M. Broomer, "Economical and ecological cryogenic machining of AISI 304 austenitic stainless steel," *Clean Products and Processes,* vol. 2, pp. 157-166, 2000.

[9] I. H. Tschätsch and D. I. A. Reichelt, "Cutting fluids (coolants and lubricants)," in *Applied Machining Technology,* ed: Springer, 2009, pp. 349-352.

[10] M. N. Islam, N. H. Rafai, and B. C. Heng, "Effect of cutting fluid supply strategies on surface finish of turned parts," in *Advanced Materials Research,* 2011, pp. 4576-4584.

[11] M. N. Islam and D.-W. Cho, "A New Strategy for End Milling Optimization," *International Journal of Management-Theory and Applications (IREMAN),* vol. 2, pp. 64-69, 2014.

[12] M. N. Islam, H. U. Lee, and D.-W. Cho, "Prediction and analysis of size tolerances achievable in peripheral end milling," *The International Journal of Advanced Manufacturing Technology,* vol. 39, pp. 129-141, 2008.

[13] M. N. Islam, H. U. Lee, and D.-W. Cho, "Selection of Optimum Cutting Conditions using Size Tolerance Prediction Model for Peripheral End Milling," in *Proceedings of the International Conference on Mechanical Engineering,* Dhaka 2007.

[14] F. Pusavec, P. Krajnik, and J. Kopac, "Transitioning to sustainable production–Part I: application on machining technologies," *Journal of Cleaner Production,* vol. 18, pp. 174-184, 2010.

[15] M. J. Sheehan and D. Hands, "Metalworking fluid mist—strategies to reduce exposure: a comparison of new and old transmission case transfer lines," *Journal of occupational and environmental hygiene,* vol. 4, pp. 288-300, 2007.

[16] W. Zhao, N. He, and L. Li, "High speed milling of Ti6Al4V alloy with minimal quantity lubrication," in *Key engineering materials*, 2007, pp. 663-668.

[17] M. Soković and K. Mijanović, "Ecological aspects of the cutting fluids and its influence on quantifiable parameters of the cutting processes," *Journal of Materials Processing Technology,* vol. 109, pp. 181-189, 2001.

[18] F. Li, M. V. Hanson, and R. C. Larock, "Soybean oil–divinylbenzene thermosetting polymers: synthesis, structure, properties and their relationships," *Polymer,* vol. 42, pp. 1567-1579, 2001.

[19] M. Sayuti, A. A. Sarhan, and F. Salem, "Novel uses of SiO 2 nano-lubrication system in hard turning process of hardened steel AISI4140 for less tool wear, surface roughness and oil consumption," *Journal of Cleaner Production,* vol. 67, pp. 265-276, 2014.

[20] D. D. Bell, J. Chou, L. Nowag, and S. Y. Liang, "Modeling of the Environmental Effect of Cutting Fluid©," *Tribology transactions,* vol. 42, pp. 168-173, 1999.

[21] M. A. El Baradie, "Cutting fluids: Part II. Recycling and clean machining," *Journal of materials processing technology,* vol. 56, pp. 798-806, 1996.

[22] D. J. Michalek, W. W.-S. Hii, J. Sun, K. L. Gunter, and J. W. Sutherland, "Experimental and analytical efforts to characterize cutting fluid mist formation and behavior in machining," *Applied occupational and environmental hygiene,* vol. 18, pp. 842-854, 2003.

[23] OSHA, "Metalworking Fluids: Safety and Health Best Practices Manual," Salt Lake City1999.

[24] J. Fuchs, J. Burg, J. G. Hengstler, U. Bolm-Audorff, and F. Oesch, "DNA damage in mononuclear blood cells of metal workers exposed to N-nitrosodiethanolamine in synthetic cutting fluids," *Mutation Research/Genetic Toxicology,* vol. 342, pp. 95-102, 1995.

[25] I. S. Foulds, "Cutting fluids," in *Kanerva's Occupational Dermatology*, ed: Springer, 2012, pp. 715-725.

[26] Y. Yue, Y. Zheng, S. Basu, and J. Sutherland, "'Cutting Fluids: Performance Measures and Health Related Characteristics," in *Proceedings of the Japan—USA Symposium on Flexible Automation*, 1998, pp. 199-208.

[27] S. Zhang, J. Li, and Y. Wang, "Tool life and cutting forces in end milling Inconel 718 under dry and minimum quantity cooling lubrication cutting conditions," *Journal of Cleaner Production,* vol. 32, pp. 81-87, 2012.

[28] S. Y. Hong, "Lubrication mechanisms of LN2 in ecological cryogenic machining," *Machining science and technology,* vol. 10, pp. 133-155, 2006.

[29] "Rocol Ultracut Long Life, Chemwatch Material Safety Data Sheet," C. 4908-63, Ed., Version No:2.0 ed: ITW POLYMERS & FLUIDS, 2011.

[30] D. P. Adler, W.-S. Hii, D. J. Michalek, and J. W. Sutherland, "Examining the role of cutting fluids in machining and efforts to address associated environmental/health concerns," *Machining science and technology,* vol. 10, pp. 23-58, 2006.

[31] S. S. Kinare, C. Ju, D. J. Michalek, and J. W. Sutherland, "An experimental investigation of cutting fluid mist removal via a novel atomizer system," SAE Technical Paper 0148-7191, 2004.

[32] F. S. Rosenthal and B. L. Yeagy, "Characterization of metalworking fluid aerosols in bearing grinding operations," *AIHAJ-American Industrial Hygiene Association,* vol. 62, pp. 379-382, 2001.

[33] Z. Bi, "Revisiting system paradigms from the viewpoint of manufacturing sustainability," *Sustainability,* vol. 3, pp. 1323-1340, 2011.

[34] P. J. Ross, "Taguchi techniques for quality engineering, 1996," *Mcgraw-hil International editions*.

[35] S. H. Park and S. H. Park, *Robust design and analysis for quality engineering*: Chapman & Hall London, 1996.

[36] Z. G. Wang, M. Rahman, Y. S. Wong, K. S. Neo, J. Sun, C. H. Tan*, et al.*, "Study on orthogonal turning of titanium alloys with different coolant supply strategies," *The International Journal of Advanced Manufacturing Technology,* vol. 42, pp. 621-632, 2009.

[37] E. Vazquez, J. Gomar, J. Ciurana, and C. A. Rodríguez, "Analyzing effects of cooling and lubrication conditions in micromilling of Ti6Al4V," *Journal of Cleaner Production,* vol. 87, pp. 906-913, 2015.

[38] A. D. Jayal, A. Balaji, R. Sesek, A. Gaul, and D. R. Lillquist, "Machining Performance and Health Effects of Cutting Fluid Application in Drilling of A390. 0 Cast Aluminum Alloy," *Journal of Manufacturing Processes,* vol. 9, pp. 137-146, 2007.

[39] S. K. Choudhury and P. Srinivas, "Tool wear prediction in turning," *Journal of Materials Processing Technology,* vol. 153, pp. 276-280, 2004.

[40] H. Martin, "Heat and mass transfer between impinging gas jets and solid surfaces," *Advances in heat transfer,* vol. 13, pp. 1-60, 1977.

[41] R. Viskanta, "Heat transfer to impinging isothermal gas and flame jets," *Experimental Thermal and Fluid Science,* vol. 6, pp. 111-134, 1993.

[42] X. Li, "Study of the jet-flow rate of cooling in machining Part 1. Theoretical analysis," *Journal of Materials Processing Technology,* vol. 62, pp. 149-156, 1996.

[43] X. Li, "Study of the jet-flow rate of cooling in machining Part 2. Simulation study," *Journal of Materials Processing Technology,* vol. 62, pp. 157-165, 1996.

[44] C. M. Daniel, K. Rao, W. W. Olson, and J. W. Sutherland, "Effect of cutting fluid properties and application variables on heat transfer in turning and boring operations," in *Proceedings of the Japan—USA Symposium on Flexible Automation*, 1996, pp. 1119-1126.

[45] S. A. Lawal, I. A. Choudhury, and Y. Nukman, "A critical assessment of lubrication techniques in machining processes: a case for minimum quantity lubrication using vegetable oil-based lubricant," *Journal of Cleaner Production,* vol. 41, pp. 210-221, 2013.

[46] I. Lazoglu and Y. Altintas, "Prediction of tool and chip temperature in continuous and interrupted machining," *International Journal of Machine Tools and Manufacture,* vol. 42, pp. 1011-1022, 2002.

[47] M. N. Islam, "Effect of Amount of Cutting Fluid on Surface Finish of Turned Parts," *Applied Mechanics and Materials,* vol. 87, pp. 170-177, 2011.

[48] J. Liu and Y. K. Chou, "On temperatures and tool wear in machining hypereutectic Al–Si alloys with vortex-tube cooling," *International Journal of Machine Tools and Manufacture,* vol. 47, pp. 635-645, 2007.

[49] M. Bachraty, M. Tolnay, P. Kovač, and V. Pucovsky, "Influence of Various Cutting Fluids on Energy Consumption during Turning," in *Key Engineering Materials*, 2016, pp. 252-256.

[50] S. Debnath, M. M. Reddy, and Q. S. Yi, "Influence of cutting fluid conditions and cutting parameters on surface roughness and tool wear in turning process using Taguchi method," *Measurement,* vol. 78, pp. 111-119, 2016.

[51] E. Brinksmeier, M. Garbrecht, C. Heinzel, T. Koch, and J. Eckebrecht, "Current approaches in design and supply of metalworking fluids," *Tribology Transactions,* vol. 52, pp. 591-601, 2009.

[52] J. Hodowany, G. Ravichandran, A. Rosakis, and P. Rosakis, "Partition of plastic work into heat and stored energy in metals," *Experimental mechanics,* vol. 40, pp. 113-123, 2000.

[53] M. Al-Odat, "Numerical analysis of cutting tool temperature in dry machining processes with embedded heat pipe," *Engineering Computations,* vol. 27, pp. 658-673, 2010.

[54] NIOSH, "Health hazard evaluation and technical assistance report: HETA. ," National Institute for Occupational Safety and Health, Indianapolis, Indiana. 2007.

[55] M. El Baradie, "Cutting fluids: Part I. characterisation," *Journal of materials processing technology,* vol. 56, pp. 786-797, 1996.

[56] G. Shen, "Modeling the Effect of Cutting Fluids in Peripheral Milling, PhD Thesis," Mechanical Engineering and Engineering Mechanics Michigan Technological University, USA, 2003.

[57] S. Debnath, M. M. Reddy, and Q. S. Yi, "Environmental friendly cutting fluids and cooling techniques in machining: a review," *Journal of Cleaner Production,* vol. 83, pp. 33-47, 2014.

[58] C. Kajdas, "Additives for metalworking lubricants-a review," *Lubrication Science,* vol. 1, pp. 385-409, 1989.

[59] B. Ozcelik, E. Kuram, M. H. Cetin, and E. Demirbas, "Experimental investigations of vegetable based cutting fluids with extreme pressure during turning of AISI 304L," *Tribology International,* vol. 44, pp. 1864-1871, 2011.

[60] R. Irani, R. Bauer, and A. Warkentin, "A review of cutting fluid application in the grinding process," *International Journal of Machine Tools and Manufacture,* vol. 45, pp. 1696-1705, 2005.

[61] E. Kuram, B. Ozcelik, and E. Demirbas, "Environmentally friendly machining: vegetable based cutting fluids," in *Green Manufacturing Processes and Systems,* ed: Springer, 2013, pp. 23-47.

[62] J. J. Eppert, K. L. Gunter, and J. W. Sutherland, "Development of cutting fluid classification system using cluster analysis," *Tribology transactions,* vol. 44, pp. 375-382, 2001.

[63] J. John, M. Bhattacharya, and P. C. Raynor, "Emulsions containing vegetable oils for cutting fluid application," *Colloids and Surfaces A: Physicochemical and Engineering Aspects,* vol. 237, pp. 141-150, 2004.

[64] J. Vieira, A. Machado, and E. Ezugwu, "Performance of cutting fluids during face milling of steels," *Journal of Materials Processing Technology,* vol. 116, pp. 244-251, 2001.

[65] K. Abou-El-Hossein, "Cutting fluid efficiency in end milling of AISI 304 stainless steel," *Industrial Lubrication and Tribology,* vol. 60, pp. 115-120, 2008.

[66] L. De Chiffre and W. Belluco, "Comparison of methods for cutting fluid performance testing," *CIRP Annals-Manufacturing Technology,* vol. 49, pp. 57-60, 2000.

[67] R. V. Rao, "Cutting Fluid Selection for a Given Machining Application," *Decision Making in the Manufacturing Environment: Using Graph Theory and Fuzzy Multiple Attribute Decision Making Methods*, pp. 97-114, 2007.

[68] W. F. Sales, Á. R. Machado, J. Bonney, and E. O. Ezugwu, "Evaluation of cutting fluids using scratch tests and turning process," *Journal of the Brazilian Society of Mechanical Sciences and Engineering*, vol. 29, pp. 372-378, 2007.

[69] B. Davoodi and A. H. Tazehkandi, "Experimental investigation and optimization of cutting parameters in dry and wet machining of aluminum alloy 5083 in order to remove cutting fluid," *Journal of Cleaner Production*, vol. 68, pp. 234-242, 2014.

[70] N. R. Dhar, M. Kamruzzaman, and M. Ahmed, "Effect of minimum quantity lubrication (MQL) on tool wear and surface roughness in turning AISI-4340 steel," *Journal of Materials Processing Technology*, vol. 172, pp. 299-304, 2006.

[71] D. Fratila, "Evaluation of near-dry machining effects on gear milling process efficiency," *Journal of Cleaner Production*, vol. 17, pp. 839-845, 2009.

[72] D. Cozzens, P. Rao, W. Olson, J. Sutherland, and J. M. Panetta, "An experimental investigation into the effect of cutting fluid conditions on the boring of aluminum alloys," *Journal of manufacturing science and engineering*, vol. 121, pp. 434-439, 1999.

[73] D. Haan, S. Batzer, W. Olson, and J. Sutherland, "An experimental study of cutting fluid effects in drilling," *Journal of Materials Processing Technology*, vol. 71, pp. 305-313, 1997.

[74] A. Devillez, F. Schneider, S. Dominiak, D. Dudzinski, and D. Larrouquere, "Cutting forces and wear in dry machining of Inconel 718 with coated carbide tools," *Wear*, vol. 262, pp. 931-942, 2007.

[75] M. Čuma and J. Zajac, "The impact analysis of cutting fluids aerosols on working environment and contamination of reservoirs," *Tehnicki Vjesnik*, vol. 2, pp. 443-446, 2012.

[76] E. G. Lucchesi, S. Y. Eguchi, and Â. M. Moraes, "Influence of a triazine derivative-based biocide on microbial biofilms of cutting fluids in contact with different substrates," *Journal of industrial microbiology & biotechnology*, vol. 39, pp. 743-748, 2012.

[77] V. S. Sharma, M. Dogra, and N. Suri, "Cooling techniques for improved productivity in turning," *International Journal of Machine Tools and Manufacture*, vol. 49, pp. 435-453, 2009.

[78] D. Korn. (2010) The Many Ways Ford Benefits from MQL. *Modern Machine Shop*.

[79] K.-M. Li and S. Y. Liang, "Predictive Modeling of Near Dry Machining," 2006.

[80] N. Boubekri, V. Shaikh, and P. R. Foster, "A technology enabler for green machining: minimum quantity lubrication (MQL)," *Journal of Manufacturing Technology Management*, vol. 21, pp. 556-566, 2010.

[81] M. Rahman and A. S. Kumar, "Evaluation of minimal of lubricant in end milling," *The International Journal of Advanced Manufacturing Technology*, vol. 18, pp. 235-241, 2001.

[82] M. Rahman, A. Senthil Kumar, and M. Salam, "Experimental evaluation on the effect of minimal quantities of lubricant in milling," *International Journal of Machine Tools and Manufacture*, vol. 42, pp. 539-547, 2002.

[83] B. Boswell and T. Chandratilleke, "The introduction of an environmental cooling method is proved by using a reduced tool life cycle time method," *International Journal of Computer Integrated Manufacturing,* vol. 20, pp. 478-485, 2007.

[84] A. A. Khan and M. I. Ahmed, "Improving tool life using cryogenic cooling," *Journal of materials processing technology,* vol. 196, pp. 149-154, 2008.

[85] M. Dhananchezian and M. P. Kumar, "Cryogenic turning of the Ti–6Al–4V alloy with modified cutting tool inserts," *Cryogenics,* vol. 51, pp. 34-40, 2011.

[86] S. Paul, N. Dhar, and A. Chattopadhyay, "Beneficial effects of cryogenic cooling over dry and wet machining on tool wear and surface finish in turning AISI 1060 steel," *Journal of Materials Processing Technology,* vol. 116, pp. 44-48, 2001.

[87] N. Upadhyay, "Environmentally Friendly Machining: Vegetable Based Cutting Fluid," *SAMRIDDHI: A Journal of Physical Sciences, Engineering and Technology,* vol. 7, 2015.

[88] E. Kuram, B. Ozcelik, E. Demirbas, and E. Sik, "Effects of the cutting fluid types and cutting parameters on surface roughness and thrust force," in *Proceedings of the world congress on engineering,* 2010, pp. 978-988.

[89] G. Arndt and R. Brown, "On the temperature distribution in orthogonal machining," *International Journal of Machine Tool Design and Research,* vol. 7, pp. 39-53, 1967.

[90] A. Tay, "A review of methods of calculating machining temperature," *Journal of Materials Processing Technology,* vol. 36, pp. 225-257, 1993.

[91] M. B. da Silva and J. Wallbank, "Cutting temperature: prediction and measurement methods—a review," *Journal of materials processing technology,* vol. 88, pp. 195-202, 1999.

[92] Y. Dogu, E. Aslan, and N. Camuscu, "A numerical model to determine temperature distribution in orthogonal metal cutting," *Journal of Materials Processing Technology,* vol. 171, pp. 1-9, 2006.

[93] R. Dutt and R. Brewer, "On the theoretical determination of the temperature field in orthogonal machining," *International Journal of Production Research,* vol. 4, pp. 91-114, 1965.

[94] B. Chao, H. Li, and K. Trigger, "An experimental investigation of temperature distribution at tool-flank surface," *Journal of Manufacturing Science and Engineering,* vol. 83, pp. 496-503, 1961.

[95] A. Moufki, A. Molinari, and D. Dudzinski, "Modelling of orthogonal cutting with a temperature dependent friction law," *Journal of the Mechanics and Physics of Solids,* vol. 46, pp. 2103-2138, 1998.

[96] R. Komanduri and Z. B. Hou, "Thermal modeling of the metal cutting process: Part I—Temperature rise distribution due to shear plane heat source," *International Journal of Mechanical Sciences,* vol. 42, pp. 1715-1752, 2000.

[97] R. Komanduri and Z. B. Hou, "Thermal modeling of the metal cutting process—Part II: temperature rise distribution due to frictional heat source at the tool–chip interface," *International Journal of Mechanical Sciences,* vol. 43, pp. 57-88, 2001.

[98] R. Komanduri and Z. B. Hou, "Thermal modeling of the metal cutting process—Part III: temperature rise distribution due to the combined effects of shear plane heat source and the tool–chip interface frictional heat source," *International Journal of Mechanical Sciences,* vol. 43, pp. 89-107, 2001.

[99] A. Karas, M. Bouzit, and M. Belarbi, "Development of a thermal model in the metal cutting process for prediction of temperature distributions at the tool-chip-workpiece interface," *Journal of Theoretical and Applied Mechanics,* vol. 51, pp. 553--567, 2013.

[100] K. Huang and W. Yang, "Analytical model of temperature field in workpiece machined surface layer in orthogonal cutting," *Journal of Materials Processing Technology,* vol. 229, pp. 375-389, 2016.

[101] Y. Karpat and T. Özel, "Predictive analytical and thermal modeling of orthogonal cutting process—part I: predictions of tool forces, stresses, and temperature distributions," *Journal of manufacturing science and engineering,* vol. 128, pp. 435-444, 2006.

[102] Y. Karpat and T. Özel, "Predictive analytical and thermal modeling of orthogonal cutting process—part II: effect of tool flank wear on tool forces, stresses, and temperature distributions," *Journal of manufacturing science and engineering,* vol. 128, pp. 445-453, 2006.

[103] R. Radulescu and S. Kapoor, "An analytical model for prediction of tool temperature fields during continuous and interrupted cutting," *Journal of Engineering for Industry,* vol. 116, pp. 135-143, 1994.

[104] P. Dewhurst, "On the non-uniqueness of the machining process," in *Proceedings of the Royal Society of London A: Mathematical, Physical and Engineering Sciences*, 1978, pp. 587-610.

[105] H. Kudo, "Some new slip-line solutions for two-dimensional steady-state machining," *International Journal of Mechanical Sciences,* vol. 7, pp. 43-55, 1965.

[106] T. Shi and S. Ramalingam, "Modeling chip formation with grooved tools," *International Journal of Mechanical Sciences,* vol. 35, pp. 741-756, 1993.

[107] N. Fang, I. Jawahir, and P. Oxley, "A universal slip-line model with non-unique solutions for machining with curled chip formation and a restricted contact tool," *International Journal of Mechanical Sciences,* vol. 43, pp. 557-580, 2001.

[108] N. Fang and I. Jawahir, "An analytical predictive model and experimental validation for machining with grooved tools incorporating the effects of strains, strain-rates, and temperatures," *CIRP Annals-Manufacturing Technology,* vol. 51, pp. 83-86, 2002.

[109] Y. Karpat and T. Özel, "An integrated analytical thermal model for orthogonal cutting with chamfered tools," *Trans. NAMRI/SME,* vol. 34, pp. 9-16, 2006.

[110] V. P. Astakhov, *Tribology of metal cutting* vol. 52: Elsevier, 2006.

[111] A. Amritkar, C. Prakash, and A. Kulkarni, "Development of temperature measurement setup for machining," *World Journal of Science and Technology,* vol. 2, pp. 15-19, 2012.

[112] G. Boothroyd, "Photographic technique for the determination of metal cutting temperatures," *British Journal of Applied Physics,* vol. 12, p. 238, 1961.

[113] G. Boothroyd and ey, "Temperatures in orthogonal metal cutting," *Proceedings of the Institution of Mechanical Engineers,* vol. 177, pp. 789-810, 1963.

[114] N. Abukhshim, P. Mativenga, and M. Sheikh, "Heat generation and temperature prediction in metal cutting: A review and implications for high speed machining," *International Journal of Machine Tools and Manufacture,* vol. 46, pp. 782-800, 2006.

[115] G. Sutter, L. Faure, A. Molinari, N. Ranc, and V. Pina, "An experimental technique for the measurement of temperature fields for the orthogonal cutting

in high speed machining," *International Journal of Machine Tools and Manufacture*, vol. 43, pp. 671-678, 2003.
[116] G. Mulholland and C. Anderson, "Experimental Cutting Tool Temperature Distributions," *Journal of Manufacturing Science and Engineering*, 2003.
[117] M. Kikuchi, "The use of cutting temperature to evaluate the machinability of titanium alloys," *Acta biomaterialia*, vol. 5, pp. 770-775, 2009.
[118] D. Stephenson, "Tool-work thermocouple temperature measurements—theory and implementation issues," *Journal of Manufacturing Science and Engineering*, vol. 115, pp. 432-437, 1993.
[119] C. Leshock and Y. Shin, "Investigation on cutting temperature in turning by a tool-work thermocouple technique," *Journal of manufacturing science and engineering*, vol. 119, pp. 502-508, 1997.
[120] L. Abhang and M. Hameedullah, "Chip-tool interface temperature prediction model for turning process," *International Journal of Engineering Science and Technology*, vol. 2, pp. 382-393, 2010.
[121] L. Li, H. Chang, M. Wang, D. W. Zuo, and L. He, "Temperature measurement in high speed milling Ti6Al4V," in *Key Engineering Materials*, 2003, pp. 804-808.
[122] D. O'sullivan and M. Cotterell, "Temperature measurement in single point turning," *Journal of Materials Processing Technology*, vol. 118, pp. 301-308, 2001.
[123] H. Kishawy, "An experimental evaluation of cutting temperatures during high speed machining of hardened D2 tool steel," 2002.
[124] I. Korkut, M. Boy, I. Karacan, and U. Seker, "Investigation of chip-back temperature during machining depending on cutting parameters," *Materials & design*, vol. 28, pp. 2329-2335, 2007.
[125] B. Haddag and M. Nouari, "Tool wear and heat transfer analyses in dry machining based on multi-steps numerical modelling and experimental validation," *Wear*, vol. 302, pp. 1158-1170, 2013.
[126] L. Filice, D. Umbrello, S. Beccari, and F. Micari, "On the FE codes capability for tool temperature calculation in machining processes," *Journal of materials processing technology*, vol. 174, pp. 286-292, 2006.
[127] A. Tapetado, J. Díaz-Álvarez, M. H. Miguélez, and C. Vázquez, "Two-Color Pyrometer for Process Temperature Measurement During Machining," *Journal of Lightwave Technology*, vol. 34, pp. 1380-1386, 2016.
[128] M. Al Huda, K. Yamada, A. Hosokawa, and T. Ueda, "Investigation of temperature at tool-chip interface in turning using two-color pyrometer," *Journal of manufacturing science and engineering*, vol. 124, pp. 200-207, 2002.
[129] A. M. N. Abang Kamaruddin, A. Hosokawa, T. Ueda, T. Furumoto, and T. Koyano, "Cutting performance of CBN and diamond tools in dry turning of cemented carbide," *Mechanical Engineering Journal*, 2016.
[130] C. Hautamaki, S. Zurn, S. C. Mantell, and D. L. Polla, "Embedded microelectromechanical systems (MEMS) for measuring strain in composites," *Journal of reinforced plastics and composites*, vol. 19, pp. 268-277, 2000.
[131] D. Werschmoeller and X. Li, "Measurement of tool internal temperatures in the tool–chip contact region by embedded micro thin film thermocouples," *Journal of Manufacturing Processes*, vol. 13, pp. 147-152, 2011.

[132] H. Choi, H. Konishi, H. Xu, and X. Li, "Embedding of micro thin film strain sensors in sapphire by diffusion bonding," *Journal of Micromechanics and Microengineering,* vol. 17, p. 2248, 2007.

[133] A. Basti, T. Obikawa, and J. Shinozuka, "Tools with built-in thin film thermocouple sensors for monitoring cutting temperature," *International Journal of Machine Tools and Manufacture,* vol. 47, pp. 793-798, 2007.

[134] J. Shinozuka, "Measurement of the Temperature Distribution at the Tool-Chip Interface by Using a Cutting Tool with Seven Pairs of Built-In Micro Cu/Ni Thermocouples," in *Advanced Materials Research*, 2016, pp. 586-591.

[135] E. Smart and E. Trent, "Temperature distribution in tools used for cutting iron, titanium and nickel," *The International Journal of Production Research,* vol. 13, pp. 265-290, 1975.

[136] S. Kato, K. Yamaguchi, Y. Watanabe, and Y. Hiraiwa, "Measurement of temperature distribution within tool using powders of constant melting point," *Journal of Manufacturing Science and Engineering*, vol. 98, pp. 607-613, 1976.

[137] S. Yeo and S. Ong, "Assessment of the thermal effects on chip surfaces," *Journal of Materials Processing Technology,* vol. 98, pp. 317-321, 2000.

[138] A. H. Tazehkandi, M. Shabgard, and F. Pilehvarian, "On the feasibility of a reduction in cutting fluid consumption via spray of biodegradable vegetable oil with compressed air in machining Inconel 706," *Journal of Cleaner Production,* vol. 104, pp. 422-435, 2015.

[139] A. H. Tazehkandi, M. Shabgard, G. Kiani, and F. Pilehvarian, "Investigation of the influences of PCBN tool on the reduction of cutting fluid consumption and increase of machining parameters range in turning Inconel 783 using spray mode of cutting fluid with compressed air," *Journal of Cleaner Production,* 2016.

[140] B. Shi and H. Attia, "Current status and future direction in the numerical modeling and simulation of machining processes: a critical literature review," *Machining Science and Technology,* vol. 14, pp. 149-188, 2010.

[141] C. Van Luttervelt, T. Childs, I. Jawahir, F. Klocke, P. Venuvinod, Y. Altintas, *et al.*, "Present Situation and Future Trends in Modelling of Machining Operations Progress Report of the CIRP Working Group 'Modelling of Machining Operations'," *Cirp Annals-Manufacturing Technology,* vol. 47, pp. 587-626, 1998.

[142] V. Sukaylo, A. Kaldos, H.-J. Pieper, V. Bana, and M. Sobczyk, "Numerical simulation of thermally induced workpiece deformation in turning when using various cutting fluid applications," *Journal of materials processing technology,* vol. 167, pp. 408-414, 2005.

[143] X. Sui, X. Liu, and D. Wang, "Development and analysis of milling model coupled thermal-mechanical," *Int J Smart Home,* vol. 8, pp. 211-216, 2014.

[144] J. Mayr, M. Ess, S. Weikert, and K. Wegener, "Simulation and prediction of the thermally induced deformations of machine tools caused by moving linear axis using the FDEM simulation approach," in *Proceedings ASPE 2008 Annual Meeting*, 2008.

[145] T. Özel and T. Altan, "Process simulation using finite element method—prediction of cutting forces, tool stresses and temperatures in high-speed flat end milling," *International Journal of Machine Tools and Manufacture,* vol. 40, pp. 713-738, 2000.

[146] A. Tay, M. Stevenson, and G. D. V. Davis, "Using the finite element method to determine temperature distributions in orthogonal machining," *Proceedings of the institution of mechanical engineers,* vol. 188, pp. 627-638, 1974.
[147] J. Mackerle, "Finite element analysis and simulation of machining: an addendum: a bibliography (1996–2002)," *International Journal of Machine Tools and Manufacture,* vol. 43, pp. 103-114, 2003.
[148] A. H.-D. Cheng and D. T. Cheng, "Heritage and early history of the boundary element method," *Engineering Analysis with Boundary Elements,* vol. 29, pp. 268-302, 2005.
[149] D. Ulutan, I. Lazoglu, and C. Dinc, "Three-dimensional temperature predictions in machining processes using finite difference method," *journal of materials processing technology,* vol. 209, pp. 1111-1121, 2009.
[150] I. Lazoglu and C. Islam, "Modeling of 3D temperature fields for oblique machining," *CIRP Annals-Manufacturing Technology,* vol. 61, pp. 127-130, 2012.
[151] C. Islam, I. Lazoglu, and Y. Altintas, "A Three-Dimensional Transient Thermal Model for Machining," *Journal of Manufacturing Science and Engineering,* vol. 138, p. 021003, 2016.
[152] M. Bartoszuk and W. Grzesik, "Numerical prediction of the interface temperature using updated Finite Difference Approach," in *Advanced Materials Research,* 2011, pp. 231-239.
[153] A. Tay, M. Stevenson, G. de Vahl Davis, and P. Oxley, "A numerical method for calculating temperature distributions in machining, from force and shear angle measurements," *International Journal of Machine Tool Design and Research,* vol. 16, pp. 335-349, 1976.
[154] C. L. Chan and A. Chandra, "A BEM approach to thermal aspects of machining processes and their design sensitivities," *Applied mathematical modelling,* vol. 15, pp. 562-575, 1991.
[155] P. Muraka, G. Barrow, and S. Hinduja, "Influence of the process variables on the temperature distribution in orthogonal machining using the finite element method," *International Journal of Mechanical Sciences,* vol. 21, pp. 445-456, 1979.
[156] F. Akbar, P. Mativenga, and M. Sheikh, "An evaluation of heat partition in the high-speed turning of AISI/SAE 4140 steel with uncoated and TiN-coated tools," *Proceedings of the institution of mechanical engineers, Part B: Journal of Engineering Manufacture,* vol. 222, pp. 759-771, 2008.
[157] M. A. Davies, Q. Cao, A. Cooks, and R. Ivester, "On the measurement and prediction of temperature fields in machining AISI 1045 steel," *CIRP Annals-Manufacturing Technology,* vol. 52, pp. 77-80, 2003.
[158] S. Iqbal, P. Mativenga, and M. Sheikh, "An investigative study of the interface heat transfer coefficient for finite element modelling of high-speed machining," *Proceedings of the Institution of Mechanical Engineers, Part B: Journal of Engineering Manufacture,* vol. 222, pp. 1405-1416, 2008.
[159] F. Samadi, F. Kowsary, and A. Sarchami, "Estimation of heat flux imposed on the rake face of a cutting tool: a nonlinear, complex geometry inverse heat conduction case study," *International Communications in Heat and Mass Transfer,* vol. 39, pp. 298-303, 2012.
[160] F. Samadi, F. Kowsary, M. Hamedi, and A. Sarchami, "Estimation of the Heat Generation in a Cutting Tool Using a Sequential Inverse Method," in *ASME*

2010 10th Biennial Conference on Engineering Systems Design and Analysis, 2010, pp. 567-572.

[161] P. Majumdar, R. Jayaramachandran, and S. Ganesan, "Finite element analysis of temperature rise in metal cutting processes," *Applied Thermal Engineering*, vol. 25, pp. 2152-2168, 2005.

[162] S. Carvalho, S. Lima e Silva, A. Machado, and G. Guimarães, "Temperature determination at the chip–tool interface using an inverse thermal model considering the tool and tool holder," *Journal of Materials Processing Technology*, vol. 179, pp. 97-104, 2006.

[163] S. R. De Carvalho, M. R. Dos Santos, P. F. De Souza, G. Guimarães, and S. M. D. L. E. Silva, "Comparison of inverse methods in the determination of heat flux and temperature in cutting tool during a machining process," *High Temperatures-High Pressures*, vol. 38, pp. 119-136, 2009.

[164] A. U. Anagonye and D. A. Stephenson, "Modeling cutting temperatures for turning inserts with various tool geometries and materials," *Journal of Manufacturing Science and Engineering*, vol. 124, pp. 544-552, 2002.

[165] W.-C. Chen, C.-C. Tsao, and P.-W. Liang, "Determination of temperature distributions on the rake face of cutting tools using a remote method," *International communications in heat and mass transfer*, vol. 24, pp. 161-170, 1997.

[166] J. Yvonnet, D. Umbrello, F. Chinesta, and F. Micari, "A simple inverse procedure to determine heat flux on the tool in orthogonal cutting," *International Journal of Machine Tools and Manufacture*, vol. 46, pp. 820-827, 2006.

[167] M. Lazard and P. Corvisier, "Inverse method for transient temperature estimation during machining," in *of the 5th International Conference on Inverse Problems in Engineering: Theory and Practice*, 2005.

[168] M. Bagheri and P. Mottaghizadeh, "Analysis of Tool-Chip Interface Temperature with FEM and Empirical Verification," *World Academy of Science, Engineering and Technology*, vol. 68, pp. 2228-2237, 2012.

[169] L. Liang, H. Xu, and Z. Ke, "An improved three-dimensional inverse heat conduction procedure to determine the tool-chip interface temperature in dry turning," *International Journal of Thermal Sciences*, vol. 64, pp. 152-161, 2013.

[170] L. Wang, Z. L. Sun, X. K. Wang, and S. C. Guo, "Numerical and analytical modeling of temperature rise on the machined stainless steel 316L," in *Mechanic Automation and Control Engineering (MACE), 2010 International Conference on*, 2010, pp. 3250-3253.

[171] R. Li and A. J. Shih, "Finite element modeling of 3D turning of titanium," in *ASME 2004 International Mechanical Engineering Congress and Exposition*, 2004, pp. 825-833.

[172] S. Pervaiz, I. Deiab, A. Rashid, and C. Nicolescu, "Experimental and numerical investigation of TI6AL4V alloy machinability using TiAlN coated tools," *Proceedings of NAMRI/SME*, vol. 42, 2014.

[173] S. Pervaiz, I. Deiab, A. Rashid, and M. Nicolescu, "Prediction of energy consumption and environmental implications for turning operation using finite element analysis," *Proceedings of the Institution of Mechanical Engineers, Part B: Journal of Engineering Manufacture*, vol. 229, pp. 1925-1932, 2015.

[174] K.-M. Li, C. Wang, and W.-Y. Chu, "An improved remote sensing technique for estimating tool–chip interface temperatures in turning," *Journal of Materials Processing Technology,* vol. 213, pp. 1772-1781, 2013.
[175] M. Groover, R. Karpovich, and E. Levy, "A study of the relationship between remote thermocouple temperatures and tool wear in machining," *International Journal of Production Research* vol. 15, pp. 129-141, 1977.
[176] T. Kagnaya, M. Lazard, L. Lambert, C. Boher, and T. Cutard, "Temperature evolution in a WC-6% Co cutting tool during turning machining: experiment and finite element simulations," *Heat Mass Transf-T WSEAS,* vol. 5044, p. 2011, 1790.
[177] T. Özel, "Computational modelling of 3D turning: Influence of edge micro-geometry on forces, stresses, friction and tool wear in PcBN tooling," *Journal of Materials Processing Technology,* vol. 209, pp. 5167-5177, 2009.
[178] P. Kwon, T. Schiemann, and R. Kountanya, "An inverse estimation scheme to measure steady-state tool–chip interface temperatures using an infrared camera," *International Journal of Machine Tools and Manufacture,* vol. 41, pp. 1015-1030, 2001.
[179] M. Movahhedy, M. Gadala, and Y. Altintas, "Simulation of the orthogonal metal cutting process using an arbitrary Lagrangian–Eulerian finite-element method," *Journal of materials processing technology,* vol. 103, pp. 267-275, 2000.
[180] L. Olovsson, L. Nilsson, and K. Simonsson, "An ALE formulation for the solution of two-dimensional metal cutting problems," *Computers & structures,* vol. 72, pp. 497-507, 1999.
[181] O. Pantalé, J.-L. Bacaria, O. Dalverny, R. Rakotomalala, and S. Caperaa, "2D and 3D numerical models of metal cutting with damage effects," *Computer methods in applied mechanics and engineering,* vol. 193, pp. 4383-4399, 2004.
[182] E. Ceretti, L. Filice, D. Umbrello, and F. Micari, "ALE simulation of orthogonal cutting: a new approach to model heat transfer phenomena at the tool-chip interface," *CIRP Annals-Manufacturing Technology,* vol. 56, pp. 69-72, 2007.
[183] F. Pusavec, T. Lu, C. Courbon, J. Rech, U. Aljancic, J. Kopac, *et al.*, "Analysis of the influence of nitrogen phase and surface heat transfer coefficient on cryogenic machining performance," *Journal of Materials Processing Technology,* vol. 233, pp. 19-28, 2016.
[184] M. Abdelkrim, M. Brioua, A. Belloufi, and A. Gherfi, "Experimental and Numerical Study of the Cutting Temperature during the Turning of the C45 Steel," in *Applied Mechanics and Materials*, 2016, pp. 507-512.
[185] D. Fratila, "Numerical and Experimental Approach of Cutting Temperatures to Green Turning of 42CrMo4 Steel," *Materials and Manufacturing Processes,* vol. 31, pp. 657-666, 2016.
[186] D. Umbrello, L. Filice, F. Micari, T. Matsumura, and T. Shirakashi, "Prediction of Tool Wear Progress in Machining of Carbon Steel using different Tool Wear Mechanismsl," *International Journal of Material Forming,* vol. 1, pp. 571-574, 2008.
[187] C. Bruni, L. d'Apolito, A. Forcellese, F. Gabrielli, and M. Simoncini, "Surface roughness modelling in finish face milling under MQL and dry cutting conditions," *International Journal of Material Forming,* vol. 1, pp. 503-506, 2008.

[188] F. Jiang, T. Zhang, and L. Yan, "Estimation of temperature-dependent heat transfer coefficients in near-dry cutting," *The International Journal of Advanced Manufacturing Technology*, pp. 1-12, 2016.
[189] X. Shen, "Numerical modeling and experimental investigation of laser-assisted machining of silicon nitride ceramics," Kansas State University, 2010.
[190] K. Koyama, "CFD simulation on LNG storage tank to improve safety and reduce cost," in *Systems Modeling and Simulation*, ed: Springer, 2007, pp. 39-43.
[191] M. G. Mostofa, K. Y. Kil, and A. J. Hwan, "Computational fluid analysis of abrasive waterjet cutting head," *Journal of mechanical science and technology*, vol. 24, pp. 249-252, 2010.
[192] M. N. Islam, M. Noguchi, S. A. Chowdhury, and B. Boswell, "Reduction of amount of cutting fluid in flood turning by finite element analysis," *International Review of Mechanical Engineering*, vol. 6, pp. 846-854, 2012.
[193] M. Noguchi, "FEA of Cooling Process in Turning Object," M Sc Thesis, Department of Mechanical Engineering, Curtin University, Australia, 2011
[194] M. S. Skjøth-Rasmussen, O. Holm-Christensen, M. Østberg, T. S. Christensen, T. Johannessen, A. Jensen, *et al.*, "Post-processing of detailed chemical kinetic mechanisms onto CFD simulations," *Computers & chemical engineering*, vol. 28, pp. 2351-2361, 2004.
[195] T. El-Wardany, E. Mohammed, and M. Elbestawi, "Cutting temperature of ceramic tools in high speed machining of difficult-to-cut materials," *International Journal of Machine Tools and Manufacture*, vol. 36, pp. 611-634, 1996.
[196] T. Obikawa, Y. Asano, and Y. Kamata, "Computer fluid dynamics analysis for efficient spraying of oil mist in finish-turning of Inconel 718," *International Journal of Machine Tools and Manufacture*, vol. 49, pp. 971-978, 2009.
[197] E. Vazquez, D. T. Kemmoku, P. Y. Noritomi, J. V. da Silva, and J. Ciurana, "Computer Fluid Dynamics Analysis for Efficient Cooling and Lubrication Conditions in Micromilling of Ti6Al4V Alloy," *Materials and Manufacturing Processes*, vol. 29, pp. 1494-1501, 2014.
[198] S. Pervaiz, I. Deiab, E. Wahba, A. Rashid, and C. M. Nicolescu, "A novel numerical modeling approach to determine the temperature distribution in the cutting tool using conjugate heat transfer (CHT) analysis," *The International Journal of Advanced Manufacturing Technology*, vol. 80, pp. 1039-1047, 2015.
[199] S. Pervaiz, I. Deiab, E. M. Wahba, A. Rashid, and M. Nicolescu, "A coupled FE and CFD approach to predict the cutting tool temperature profile in machining," *Procedia CIRP*, vol. 17, pp. 750-754, 2014.
[200] P. C. Wanigarathne, "Experimental and analytical modeling of near-dry turning operations with coated grooved tools for improved sustainability," PhD, ProQuest, 2006.
[201] N. Knowles, "Finite element analysis," *Computer-Aided Design*, vol. 16, pp. 134-140, 1984.
[202] B. A. Khidhir and B. Mohamed, "Study of cutting speed on surface roughness and chip formation when machining nickel-based alloy," *Journal of mechanical science and technology*, vol. 24, pp. 1053-1059, 2010.
[203] "ANSYS CFX Technical Specifications, ANSYS Inc.," ANSYS Inc., Canonsburg, PA 2010.

[204] V. P. Astakhov and J. C. Outeiro, "Metal cutting mechanics, finite element modelling," in *Machining*, ed: Springer, 2008, pp. 1-27.
[205] P. Oxley, "A strain-hardening solution for the “shear angle” in orthogonal metal cutting," *International Journal of Mechanical Sciences*, vol. 3, pp. 68-79, 1961.
[206] P. Oxley and A. Hatton, "Shear angle solution based on experimental shear zone and tool-chip interface stress distributions," *International Journal of Mechanical Sciences*, vol. 5, pp. 41-55, 1963.
[207] M. E. Merchant, "Mechanics of the metal cutting process. I. Orthogonal cutting and a type 2 chip," *Journal of applied physics*, vol. 16, pp. 267-275, 1945.
[208] J. P. Davim, P. Sreejith, and J. Silva, "Turning of brasses using minimum quantity of lubricant (MQL) and flooded lubricant conditions," *Materials and Manufacturing Processes*, vol. 22, pp. 45-50, 2007.
[209] L. Abhang and M. Hameedullah, "Power prediction model for Turning En-31 steel Using Response surface methodology," *Journal of Engineering Science and Technology Review*, vol. 3, pp. 116-122, 2010.
[210] F. Koenigsberger and A. Sabberwal, "An investigation into the cutting force pulsations during milling operations," *International Journal of Machine Tool Design and Research*, vol. 1, pp. 15-33, 1961.
[211] D. J. Waldorf, R. E. DeVor, and S. G. Kapoor, "A slip-line field for ploughing during orthogonal cutting," *Journal of Manufacturing Science and Engineering*, vol. 120, pp. 693-699, 1998.
[212] K. Ehmann, S. Kapoor, R. DeVor, and I. Lazoglu, "Machining process modeling: a review," *Journal of Manufacturing Science and Engineering*, vol. 119, pp. 655-663, 1997.
[213] R. Coelho, A. Braghini Jr, C. Valente, and G. Medalha, "Experimental evaluation of cutting force parameters applying mechanistic model in orthogonal milling," *Journal of the Brazilian Society of Mechanical Sciences and Engineering*, vol. 25, pp. 247-253, 2003.
[214] Z. Lu and T. Yoneyama, "Micro cutting in the micro lathe turning system," *International Journal of Machine Tools and Manufacture*, vol. 39, pp. 1171-1183, 1999.
[215] (8 Nov 2014). *Cutting Power in Turning*. Available: http://www.mitsubishicarbide.net/contents/mhg/ru/html/product/technical_information/information/formula4.html
[216] J. Sun, Y. Wong, M. Rahman, Z. Wang, K. Neo, C. Tan, *et al.*, "Effects of coolant supply methods and cutting conditions on tool life in end milling titanium alloy," *Machining Science and Technology*, vol. 10, pp. 355-370, 2006.
[217] R. Ivester, E. Whitenton, J. Hershman, K. Chou, and Q. Wu, "Analysis of Orthogonal Cutting Experiments Using Diamond-Coated Tools with Force and Temperature Measurements," in *Traditional Machining Processes*, ed: Springer, 2015, pp. 33-48.
[218] J. Fleischer, R. Pabst, and S. Kelemen, "Heat flow simulation for dry machining of power train castings," *Cirp Annals-Manufacturing Technology*, vol. 56, pp. 117-122, 2007.
[219] M. Shaw, "Energy Conversion in Cutting and Grinding*," *CIRP Annals-Manufacturing Technology*, vol. 45, pp. 101-104, 1996.
[220] K. Liu and X. Li, "Ductile cutting of tungsten carbide," *Journal of Materials Processing Technology*, vol. 113, pp. 348-354, 2001.

[221] A. Kurlov and A. Gusev, "Tungsten Carbides," *Springer Ser. Mater. Sci,* vol. 184, pp. 34-6, 2013.
[222] M. A. Lajis, H. Radzi, and A. Amin, "The implementation of Taguchi method on EDM process of tungsten carbide," *European Journal of Scientific Research,* vol. 26, pp. 609-617, 2009.
[223] K. Liu, X. Li, M. Rahman, and X. Liu, "CBN tool wear in ductile cutting of tungsten carbide," *Wear,* vol. 255, pp. 1344-1351, 2003.
[224] B. Xia and D.-W. Sun, "Applications of computational fluid dynamics (CFD) in the food industry: a review," *Computers and electronics in agriculture,* vol. 34, pp. 5-24, 2002.
[225] S. Schneiderbauer and M. Krieger, "What do the Navier–Stokes equations mean?," *European Journal of Physics,* vol. 35, p. 015020, 2013.
[226] Z. J. Zhai, Z. Zhang, W. Zhang, and Q. Y. Chen, "Evaluation of various turbulence models in predicting airflow and turbulence in enclosed environments by CFD: Part 1—Summary of prevalent turbulence models," *Hvac&R Research,* vol. 13, pp. 853-870, 2007.
[227] F. Molina-Aiz, H. Fatnassi, T. Boulard, J. Roy, and D. Valera, "Comparison of finite element and finite volume methods for simulation of natural ventilation in greenhouses," *Computers and Electronics in Agriculture,* vol. 72, pp. 69-86, 2010.
[228] B. Diskin, J. L. Thomas, E. J. Nielsen, H. Nishikawa, and J. A. White, "Comparison of node-centered and cell-centered unstructured finite-volume discretizations: viscous fluxes," *AIAA journal,* vol. 48, pp. 1326-1338, 2010.
[229] W. Gropp, E. Lusk, and A. Skjellum, *Using MPI: portable parallel programming with the message-passing interface* vol. 1: MIT press, 1999.
[230] S. Muraki, M. Ogata, K.-L. Ma, K. Koshizuka, K. Kajihara, X. Liu, *et al.*, "Next-generation visual supercomputing using PC clusters with volume graphics hardware devices," in *Proceedings of the 2001 ACM/IEEE conference on Supercomputing*, 2001, pp. 51-51.
[231] W. Grzesik, "Composite layer-based analytical models for tool–chip interface temperatures in machining medium carbon steels with multi-layer coated cutting tools," *Journal of materials processing technology,* vol. 176, pp. 102-110, 2006.
[232] S. Wang, X. Chen, S. To, X. Ouyang, Q. Liu, J. Liu, *et al.*, "Effect of cutting parameters on heat generation in ultra-precision milling of aluminum alloy 6061," *The International Journal of Advanced Manufacturing Technology,* pp. 1-11, 2015.
[233] R. Komanduri and Z. Hou, "A review of the experimental techniques for the measurement of heat and temperatures generated in some manufacturing processes and tribology," *Tribology International,* vol. 34, pp. 653-682, 2001.
[234] A. C. Hoyne, C. Nath, and S. G. Kapoor, "On Cutting Temperature Measurement During Titanium Machining With an Atomization-Based Cutting Fluid Spray System," *Journal of Manufacturing Science and Engineering,* vol. 137, p. 024502, 2015.
[235] M. P. Reddy, A. A. S. William, M. M. Prashanth, S. S. Kumar, K. D. Ramkumar, N. Arivazhagan, *et al.*, "Assessment of Mechanical Properties of AISI 4140 and AISI 316 Dissimilar Weldments," *Procedia Engineering,* vol. 75, pp. 29-33, 2014.

[236] C. Rubio-González, J. Gallardo-González, G. Mesmacque, and U. Sanchez-Santana, "Dynamic fracture toughness of pre-fatigued materials," *International Journal of Fatigue,* vol. 30, pp. 1056-1064, 2008.

[237] Mineral Insulated Thermocouple with Miniature Plug [Online]. Available: http://docs-asia.electrocomponents.com/webdocs/115e/0900766b8115eb3c.pdf

[238] K. Resendez and R. Bachnak, "LabVIEW programming for internet-based measurements," *Journal of Computing Sciences in Colleges,* vol. 18, pp. 79-85, 2003.

[239] B. Boswell, "Use of air cooling and its effectiveness in dry machining processes," Ph. D., Department of Mechanical Engineering, , Curtin University, , Australia, 2008.

[240] T. J. Drozda and C. Wick, *Tool and Manufacturing Engineers Handbook, Machining.* vol. 1 pp 4–14. Dearborn, Michigan, 1983.

[241] P. Sreejith, "Machining of 6061 aluminium alloy with MQL, dry and flooded lubricant conditions," *Materials letters,* vol. 62, pp. 276-278, 2008.

[242] S. Paul and A. Chattopadhyay, "Effects of cryogenic cooling by liquid nitrogen jet on forces, temperature and surface residual stresses in grinding steels," *Cryogenics,* vol. 35, pp. 515-523, 1995.

[243] Y. R. Ginting, B. Boswell, W. Biswas, and M. N. Islam, "Advancing Environmentally Conscious Machining," *Procedia CIRP,* vol. 26, pp. 391-396, 2015.

[244] A. E. Diniz and R. Micaroni, "Influence of the direction and flow rate of the cutting fluid on tool life in turning process of AISI 1045 steel," *International Journal of Machine Tools and Manufacture,* vol. 47, pp. 247-254, 2007.

[245] Y. Kamata and T. Obikawa, "High speed MQL finish-turning of Inconel 718 with different coated tools," *Journal of Materials Processing Technology,* vol. 192, pp. 281-286, 2007.

[246] E. Ezugwu, R. Da Silva, J. Bonney, and A. Machado, "Evaluation of the performance of CBN tools when turning Ti–6Al–4V alloy with high pressure coolant supplies," *International Journal of Machine Tools and Manufacture,* vol. 45, pp. 1009-1014, 2005.

[247] A. Rajesh and J. Venkatesh, "Taguchi method and Pareto ANOVA: An approach for process parameters optimization in micro-EDM drilling."

[248] I. Hanafi, A. Khamlichi, F. M. Cabrera, E. Almansa, and A. Jabbouri, "Optimization of cutting conditions for sustainable machining of PEEK-CF30 using TiN tools," *Journal of Cleaner Production,* vol. 33, pp. 1-9, 2012.

[249] M. Sarıkaya and A. Güllü, "Taguchi design and response surface methodology based analysis of machining parameters in CNC turning under MQL," *Journal of Cleaner Production,* vol. 65, pp. 604-616, 2014.

[250] C. Camposeco-Negrete, "Optimization of cutting parameters for minimizing energy consumption in turning of AISI 6061 T6 using Taguchi methodology and ANOVA," *Journal of Cleaner Production,* vol. 53, pp. 195-203, 2013.

[251] N. Alagumurthi, K. Palaniradja, and V. Soundararajan, "Optimization of grinding process through design of experiment (DOE)—A comparative study," *Materials and Manufacturing Processes,* vol. 21, pp. 19-21, 2006.

[252] A. Bhattacharya, S. Das, P. Majumder, and A. Batish, "Estimating the effect of cutting parameters on surface finish and power consumption during high speed machining of AISI 1045 steel using Taguchi design and ANOVA," *Production Engineering,* vol. 3, pp. 31-40, 2009.

[253] J. A. Ghani, I. Choudhury, and H. Hassan, "Application of Taguchi method in the optimization of end milling parameters," *Journal of Materials Processing Technology,* vol. 145, pp. 84-92, 2004.
[254] N. H. Rafai, M. H. Othman, S. Hasan, and T. R. A. Sinnasalam, "The Optimization in Machining AISI 1030 Using Taguchi Method for Dry and Flood Cutting Condition," in *Applied Mechanics and Materials*, 2013, pp. 841-845.
[255] D. Fratila and C. Caizar, "Application of Taguchi method to selection of optimal lubrication and cutting conditions in face milling of AlMg 3," *Journal of Cleaner Production,* vol. 19, pp. 640-645, 2011.
[256] H. Zhao, G. Barber, and Q. Zou, "A study of flank wear in orthogonal cutting with internal cooling," *Wear,* vol. 253, pp. 957-962, 2002.
[257] A. Gatto and L. Iuliano, "Advanced coated ceramic tools for machining superalloys," *International Journal of Machine Tools and Manufacture,* vol. 37, pp. 591-605, 1997.
[258] Z. Liu, X. Cai, M. Chen, and Q. An, "Investigation of cutting force and temperature of end-milling Ti–6Al–4V with different minimum quantity lubrication (MQL) parameters," *Proceedings of the Institution of Mechanical Engineers, Part B: Journal of Engineering Manufacture,* vol. 225, pp. 1273-1279, 2011.
[259] M. Kronenberg, "Replacing the Taylor formula by a new tool life equation," *International Journal of Machine Tool Design and Research,* vol. 10, pp. 193-202, 1970.
[260] H.-P. b. Wang and R. A. Wysk, "An expert system for machining data section," *Computers & Industrial Engineering,* vol. 10, pp. 99-107, 1986.
[261] K. Nagasaka and F. Hashimoto, "The establishment of a tool life equation considering the amount of tool wear," *Wear,* vol. 81, pp. 21-31, 1982.
[262] I. Jawahir, P. Li, R. Gosh, and E. Exner, "A new parametric approach for the assessment of comprehensive tool wear in coated grooved tools," *CIRP Annals-Manufacturing Technology,* vol. 44, pp. 49-54, 1995.
[263] S. Dolinšek, B. Šuštaršič, and J. Kopač, "Wear mechanisms of cutting tools in high-speed cutting processes," *Wear,* vol. 250, pp. 349-356, 2001.
[264] I. Ciftci, "Machining of austenitic stainless steels using CVD multi-layer coated cemented carbide tools," *Tribology International,* vol. 39, pp. 565-569, 2006.
[265] A. Sharman, R. C. Dewes, and D. K. Aspinwall, "Tool life when high speed ball nose end milling Inconel 718™," *Journal of Materials Processing Technology,* vol. 118, pp. 29-35, 2001.
[266] E. M. Trent and P. K. Wright, *Metal cutting*: Butterworth-Heinemann, 2000.
[267] K. Weinert, I. Inasaki, J. Sutherland, and T. Wakabayashi, "Dry machining and minimum quantity lubrication," *Cirp Annals-Manufacturing Technology,* vol. 53, pp. 511-537, 2004.
[268] Y. Sahin and G. Sur, "The effect of Al 2 O 3, TiN and Ti (C, N) based CVD coatings on tool wear in machining metal matrix composites," *Surface and Coatings Technology,* vol. 179, pp. 349-355, 2004.
[269] E. Kannatey-Asibu, "A transport-diffusion equation in metal cutting and its application to analysis of the rate of flank wear," *Journal of engineering for industry,* vol. 107, pp. 81-89, 1985.
[270] L. De Chiffre, S. Lassen, K. Pedersen, and S. Skade, "A reaming test for cutting fluid evaluation," *Journal of Synthetic Lubrication,* vol. 11, pp. 17-34, 1994.

[271] P. Tseng and A. Chou, "The intelligent on-line monitoring of end milling," *International Journal of Machine Tools and Manufacture,* vol. 42, pp. 89-97, 2002.
[272] I. S. O. 3685, "Tool-life testing with single-point turning tools," ed, 1993.
[273] L. Dan and J. Mathew, "Tool wear and failure monitoring techniques for turning—a review," *International Journal of Machine Tools and Manufacture,* vol. 30, pp. 579-598, 1990.
[274] M. Noordin, V. Venkatesh, C. Chan, and A. Abdullah, "Performance evaluation of cemented carbide tools in turning AISI 1010 steel," *Journal of Materials Processing Technology,* vol. 116, pp. 16-21, 2001.
[275] I. P. Arbizu and C. L. Perez, "Surface roughness prediction by factorial design of experiments in turning processes," *Journal of Materials Processing Technology,* vol. 143, pp. 390-396, 2003.
[276] X. Wang and C. Feng, "Development of empirical models for surface roughness prediction in finish turning," *The International Journal of Advanced Manufacturing Technology,* vol. 20, pp. 348-356, 2002.
[277] I. S. O. 4287, "Geometrical Product Specifications - Surface Texture: Profile Method - Terms, Definitions and Surface Texture Parameters," ed, 1997.
[278] M. A. Xavior and M. Adithan, "Determining the influence of cutting fluids on tool wear and surface roughness during turning of AISI 304 austenitic stainless steel," *Journal of materials processing technology,* vol. 209, pp. 900-909, 2009.
[279] S. Sulaiman, A. Roshan, and M. Ariffin, "Finite Element Modelling of the effect of tool rake angle on tool temperature and cutting force during high speed machining of AISI 4340 steel," in *IOP Conference Series: Materials Science and Engineering*, 2013, p. 012040.
[280] H. Saglam, F. Unsacar, and S. Yaldiz, "Investigation of the effect of rake angle and approaching angle on main cutting force and tool tip temperature," *International Journal of machine tools and manufacture,* vol. 46, pp. 132-141, 2006.
[281] M. Dogra, V. S. Sharma, and J. Dureja, "Effect of tool geometry variation on finish turning–A Review," *Journal of Engineering Science and Technology Review,* vol. 4, pp. 1-13, 2011.
[282] H. Ravindra, Y. Srinivasa, and R. Krishnamurthy, "Modelling of tool wear based on cutting forces in turning," *Wear,* vol. 169, pp. 25-32, 1993.
[283] G. Poulachon, A. Moisan, and I. Jawahir, "Tool-wear mechanisms in hard turning with polycrystalline cubic boron nitride tools," *Wear,* vol. 250, pp. 576-586, 2001.
[284] S. Rao, "Tool wear monitoring through the dynamics of stable turning," *Journal of Engineering for Industry,* vol. 108, pp. 183-190, 1986.
[285] Y. Su, N. He, L. Li, and X. Li, "An experimental investigation of effects of cooling/lubrication conditions on tool wear in high-speed end milling of Ti-6Al-4V," *Wear,* vol. 261, pp. 760-766, 2006.
[286] N. Dhar and M. Kamruzzaman, "Cutting temperature, tool wear, surface roughness and dimensional deviation in turning AISI-4037 steel under cryogenic condition," *International Journal of Machine Tools and Manufacture,* vol. 47, pp. 754-759, 2007.
[287] A. Shokrani, V. Dhokia, and S. T. Newman, "Environmentally conscious machining of difficult-to-machine materials with regard to cutting fluids,"

International Journal of Machine Tools and Manufacture, vol. 57, pp. 83-101, 2012.

[288] D. Dudzinski, A. Devillez, A. Moufki, D. Larrouquere, V. Zerrouki, and J. Vigneau, "A review of developments towards dry and high speed machining of Inconel 718 alloy," *International Journal of Machine Tools and Manufacture*, vol. 44, pp. 439-456, 2004.

[289] C. Scheffer, H. Kratz, P. Heyns, and F. Klocke, "Development of a tool wear-monitoring system for hard turning," *International Journal of Machine Tools and Manufacture*, vol. 43, pp. 973-985, 2003.

[290] E. Kılıckap, O. Cakır, M. Aksoy, and A. Inan, "Study of tool wear and surface roughness in machining of homogenised SiC-p reinforced aluminium metal matrix composite," *Journal of Materials Processing Technology*, vol. 164, pp. 862-867, 2005.

[291] R. Pavel, I. Marinescu, M. Deis, and J. Pillar, "Effect of tool wear on surface finish for a case of continuous and interrupted hard turning," *Journal of Materials Processing Technology*, vol. 170, pp. 341-349, 2005.

[292] D. Cuppini, G. D'errico, and G. Rutelli, "Tool wear monitoring based on cutting power measurement," *Wear*, vol. 139, pp. 303-311, 1990.

[293] K.-M. Li and S. Y. Liang, "Performance profiling of minimum quantity lubrication in machining," *The International Journal of Advanced Manufacturing Technology*, vol. 35, pp. 226-233, 2007.

[294] A. Attanasio, M. Gelfi, C. Giardini, and C. Remino, "Minimal quantity lubrication in turning: effect on tool wear," *Wear*, vol. 260, pp. 333-338, 2006.

[295] F. Klocke and G. Eisenblätter, "Dry cutting," *CIRP Annals-Manufacturing Technology*, vol. 46, pp. 519-526, 1997.

[296] L. L. De Lacalle, C. Angulo, A. Lamikiz, and J. Sanchez, "Experimental and numerical investigation of the effect of spray cutting fluids in high speed milling," *Journal of Materials Processing Technology*, vol. 172, pp. 11-15, 2006.

[297] S. Kim, D. Lee, M. Kang, and J. Kim, "Evaluation of machinability by cutting environments in high-speed milling of difficult-to-cut materials," *Journal of materials processing technology*, vol. 111, pp. 256-260, 2001.

[298] V. Upadhyay, P. K. Jain, and N. K. Mehta, "Minimum Quantity Lubrication Assisted Turning - An Overview," *DAAAM International Scientific Book*, pp. 463-479, 2012.

[299] V. P. Astakhov, "Ecological machining: near-dry machining," in *Machining*, ed: Springer, 2008, pp. 195-223.

[300] S. A. Chowdhury, M. N. Islam, and B. Boswell, "Effectiveness of Using CFD for Comparing Tool Cooling Methods," in *Proceedings of the World Congress on Engineering*, 2014.

[301] S. A. Chowdhury, M. N. Islam, and B. Boswell, "Predicting the Influence of the Machining Parameters on the Tool Tip Temperature," in *Transactions on Engineering Technologies*, ed: Springer, 2015, pp. 305-316.

[302] S. Jozić, D. Bajić, and L. Celent, "Application of compressed cold air cooling: achieving multiple performance characteristics in end milling process," *Journal of Cleaner Production*, vol. 100, pp. 325-332, 2015.

[303] G. M. Perri, M. Bräunig, G. Di Gironimo, M. Putz, A. Tarallo, and V. Wittstock, "Numerical modelling and analysis of the influence of an air cooling system on a milling machine in virtual environment," *The International Journal of Advanced Manufacturing Technology*, pp. 1-12, 2016.

[304] T. Obikawa, Y. Kamata, Y. Asano, K. Nakayama, and A. W. Otieno, "Micro-liter lubrication machining of Inconel 718," *International Journal of Machine Tools and Manufacture,* vol. 48, pp. 1605-1612, 2008.
[305] S. Yuan, L. Yan, W. Liu, and Q. Liu, "Effects of cooling air temperature on cryogenic machining of Ti–6Al–4V alloy," *Journal of Materials Processing Technology,* vol. 211, pp. 356-362, 2011.
[306] Y.-C. Yen, A. Jain, P. Chigurupati, W.-T. Wu, and T. Altan, "Computer simulation of orthogonal cutting using a tool with multiple coatings," *Machining science and technology,* vol. 8, pp. 305-326, 2004.
[307] J. Rech, A. Kusiak, and J. Battaglia, "Tribological and thermal functions of cutting tool coatings," *Surface and Coatings Technology,* vol. 186, pp. 364-371, 2004.
[308] M. Attia and L. Kops, "A new approach to cutting temperature prediction considering the thermal constriction phenomenon in multi-layer coated tools," *CIRP Annals-Manufacturing Technology,* vol. 53, pp. 47-52, 2004.
[309] Y. Huang and S. Liang, "Modelling of the cutting temperature distribution under the tool flank wear effect," *Proceedings of the Institution of Mechanical Engineers, Part C: Journal of Mechanical Engineering Science,* vol. 217, pp. 1195-1208, 2003.

Appendix

Appendix 1

List of Supporting Papers

1. S. A. Chowdhury, M. N. Islam, and B. Boswell, "Effectiveness of Using CFD for Comparing Tool Cooling Methods," in *Proceedings of the World Congress on Engineering*, 2014.

2. S. A. Chowdhury, M. N. Islam, and B. Boswell, "Predicting the Influence of the Machining Parameters on the Tool Tip Temperature," in *Transactions on Engineering Technologies*, ed: Springer, 2015, pp. 305-316.

3. M. N. Islam, M. Noguchi, S. A. Chowdhury, and B. Boswell, "Reduction of amount of cutting fluid in flood turning by finite element analysis," *International Review of Mechanical Engineering*, vol. 6, pp. 846-854, 2012.

4. S. A. Chowdhury, M. N. Islam, and B. Boswell, "Temperature Determination at the Chip-Tool Interface using a Computational Fluid Dynamics Package," unpublished.

Appendix 2

Code for HPC

```
#!/bin/bash
# job name (qstat)
#PBS -N cfxjob1
#
# The number of nodes.
#PBS -l select=1:ncpus=2:mem=23GB:mpiprocs=6
# Time requested.
#PBS -l walltime=10:00:00
#
# project name
#PBS -W group_list=directorF
#PBS -m ea
```

```
#PBS -M sayem.chowdhury@postgrad.curtin.edu.au
# declaring the queue.
# default.
#PBS -q routequeue

cd $PBS_O_WORKDIR

. /etc/bashrc

# Get the path to CFX
module load CFX/14.0

# declaring the CFX licence server.

export ANSYSLI_SERVERS@x.edu.au
export ANSYSLMD_LICENSE@x.edu.au


#or

# Single node
#cfx5solve -batch -def "filename.def" -part $cpus -start-method "Platform MPI Local
Parallel"
(partial code)
```

Commands

Working with files:

:e filename	(open 'filename' for editing)
:q!	(exit without saving)
:wq	(save and exit)
:w filename	(save as 'filename')
:r !ls	(reads result of ls into the file - replace 'ls' with your choice!)

Inserting/writing text:

i	(insert)
I	(insert at start of line)
a	(append)
A	(append at end of line)
o	(open new line below and insert)
O	(open new line above and insert)
C	(change rest of current line)

Deleting text:

x	(deletes like DELETE key)
X	(deletes like BACKSPACE key)